Synthesis, Characterization, and Catalytic Applications of Metallic Nanoparticles in Tetraalkylphosphonium Ionic Liquids

A Thesis Submitted to the College of
Graduate Studies and Research
In Partial Fulfillment of the Requirements
For the Degree of Doctor of Philosophy
In the Department of Chemistry
University of Saskatchewan
Saskatoon

By

Abhinandan Banerjee

Permission to Use

In presenting this thesis in partial fulfilment of the requirements for a Postgraduate degree from the University of Saskatchewan, I agree that the Libraries of this University may make it freely available for inspection. I further agree that permission for copying of this thesis in any manner, in whole or in part, for scholarly purposes may be granted by the professor or professors who supervised my thesis work or, in their absence, by the Head of the Department or the Dean of the College in which my thesis work was done. It is understood that any copying or publication or use of this thesis or parts thereof for financial gain shall not be allowed without my written permission. It is also understood that due recognition shall be given to me and to the University of Saskatchewan in any scholarly use which may be made of any material in my thesis.

Requests for permission to copy or to make other use of material in this thesis in whole or part should be addressed to:

Head of the Department of Chemistry

University of Saskatchewan

Saskatoon, Saskatchewan S7N 5C9

Canada

ABSTRACT

In recent years, ionic liquids have emerged as one of the most promising alternatives to traditional volatile organic solvents when it comes to catalytic reactions. Stable metal nanoparticles suspended in ionic liquids, are catalytic systems that mimic aspects of nanoparticles on solid supports, as well as traditional metal-ligand complexes used in organometallic catalysis. While alkylimidazolium ionic liquids, with or without appended functionalities, have been earmarked as the media of choice for the dispersal of nanoparticles, the tetraalkylphosphonium family of ionic liquids has largely been overlooked, despite their facile synthesis, commercial availability, chemical resemblance to surfactants traditionally used for nanoparticle stabilization, stability under basic conditions, and wide thermal as well as electrochemical windows. It is only recently that a number of research groups have given this family of novel alternative solvents the recognition it deserves, and used metal NPs dispersed in these ILs as catalysts in reactions such as hydrogenations, oxidations, C-C cross-couplings, hydrodeoxygenations, aminations, etc.

This thesis investigates the synthesis, characterization, and catalytic applications of transition metal nanoparticles in tetraalkylphosphonium ionic liquids. The ionic liquids described in this thesis functioned as the reaction media as well as intrinsic nanoparticle stabilizers during the course of the catalytic processes. Metallic nanoparticles synthesized in these ionic liquids proved to be stable, efficient and recyclable catalytic systems for reactions of industrial significance, such as hydrodeoxygenations, hydrogenations, and oxidations. It was

demonstrated that stability and catalytic activity of these systems were profoundly dependent on the properties of the ionic liquids, such as the nature of the alkyl chains attached to the phosphonium cation, and the coordination ability of the anion. Since heat-induced nanoparticle sintering was a problem, a procedure was devised to redisperse the aggregated and/or sintered nanoparticles so as to restore their initial sizes and catalytic activities. The presence of halides as counter-ions in tetraalkylphosphonium ionic liquids was seen to facilitate the oxidative degradation of agglomerated metal nanoparticles, which was a key step in our redispersion protocol. It was demonstrated that this redispersion protocol, when applied to heat-sintered nanoparticles, produces nanostructures that resemble the freshly made nanoparticles not only in size but also in catalytic activities. The presence of by-products from the borohydride reduction step used to generate the nanoparticles in the ionic liquids actually facilitated multi-step reactions such as hydrodeoxygenation of phenol, where a Lewis Acid was necessary for a dehydration step. Finally, an attempt was made to utilize nanoparticles of an earth-abundant metal (iron) as a hydrogenation catalyst in a variety of alternative solvents (including tetraalkylphosphonium ionic liquids) in order to enhance the “green”ness of the catalyst systems. X-ray absorption spectroscopy (XAS) of the iron- nanoparticles/ionic liquid systems at the Canadian Light Source revealed significant details about the chemical interaction between iron and the ionic liquid matrices, which added to our understanding of this neoteric family of catalysts.

Dedication

To the Earth, who nurtures us all.

To Earth-Mothers, who carry the burden of humanity on their broad shoulders.

To people who nurture and become mothers.

To my mother.

Die Zeit, die ist ein sonderbar Ding.
Wenn man so hinlebt, ist sie rein gar nichts.
Aber dann auf einmal, da spürt man nichts als sie.
Sie ist um uns herum, sie ist auch in uns drinnen.
In den Gesichtern rieselt sie,
im Spiegel da rieselt sie,
in meinen Schläfen fliesst sie.
Und zwischen mir und dir da fliesst sie wieder,
lautlos, wie eine Sanduhr.
(.....) Manchmal hör' ich sie fliessen – unaufhaltsam.
Manchmal steh' ich auf mitten in der Nacht
und lass die Uhren alle, alle stehn.

------ *"**Der Rosenkavalier"**, 1911, Dresden, Germany.*
Music: Richard Strauss
Libretto: Hugo von Hofmannsthal

Translates as:

Time, indeed, is a wondrous thing.
We live and we breathe,
And time means nothing.
But then, come one day,
Time is all we can think of.
Time surrounds us, and it fills us.....
Our faces reflect it,
Our mirrors depict it,
My temples throb with it.
And between us it flows: trickling,
Like sand in an hourglass.
(.....) Often, I sense it flowing - relentlessly.
Sometimes I wake up in the still of the night
And wind the clocks down... one by one.

------ *"**The Knight of the Rose",** 1911, Dresden, Germany.*
Music: Richard Strauss
Libretto: Hugo von Hofmannsthal.

Acknowledgement

Life doesn't present one with opportunities galore for thanking people formally; however, the acknowledgement section of a dissertation can be rightfully considered to be one of those infrequent opportunities. Therefore, I intend to make use of it as comprehensively as I can. In other words, this is going to be a long read.

First of all, I shall thank my graduate advisor, Prof. Robert William James Scott. I have come to appreciate his qualities such as patience, a genuine love for exploring new frontiers of research, willingness to tackle issues ranging from the intricacies of chemistry to the routine woes of graduate school, a keen social conscience, and an interest in the well-being of every person who is a part of the Scott research group. He makes it easy for us to do science, because he leads by example.

I thank Professors Stephen Foley, Jens Mueller, and Ajay Dalai for serving on my advisory committee. I also had the privilege of being a part of Prof. Foley's organometallics class. I have attended lectures on organometallic chemistry in three continents; this was the first time I had actually looked forward to those lectures. I had the remarkable good fortune of being taught chemical kinetics and molecular spectroscopy by Prof. Ronald Steer; I look forward to boasting about that to posterity. Prof. Matthew Paige's class on aspects of surface sciences was another wonderful experience that I enjoyed very much indeed. I have had some very valuable conversations with Professors Foley, Steer, and Paige about my own research, and I remember coming back to my office after those chats with a renewed urge to do more science

and better science.

Chemistry, however, is an experimental science; most of it is done in laboratories. The Department of Chemistry at the University of Saskatchewan has a diverse graduate student population, and it ensures that all its graduate students are well-trained in state-of-the-art, cutting-edge experimental techniques. The person responsible for imparting this knowledge is Dr. Pia Wennek, Inorganic and Senior Organic Chemistry Laboratory Manager, who is well-versed in the quasi-magical arts of air-sensitive chemistry. I feel privileged to have learned many laboratory practices that I use on a daily basis from her. Her encyclopedic knowledge of practical inorganic chemistry has come to my aid many times since then; I sincerely thank her for those occasions. I also had the privilege of serving as a teaching fellow for her in the Inorganic Chemistry 231.3 course; it was truly a memorable experience. Finally, she is my go-to person in the department when I am in the mood for a little opera gossip. Other laboratory managers – Drs. Alexandra Bartole-Scott, Valerie MacKenzie, and Marcelo Sales – have been equally helpful, happy to train me in instrumental usage, willing to listen to grievances about recalcitrant spectrometers and uncooperative gas chromatographs, and ready to offer helpful hints and suggestions. I have also received considerable help from Garth Parry and Ken Thoms, especially during the repair and reinstallation of the GC-FID in our laboratory. I am very grateful to them for their time. Dr. Keith Brown, Research Officer and coordinator of the NMR facilities at the Saskatchewan Structural Science Centre, has also been an invaluable ally. Dr. Guosheng Liu from the Department of Biology was extremely helpful during the TEM analysis of my samples. Dr. Yongfeng Hu at the Canadian Light Source helped us make maximum use of our

beam-times at the CLS; I am obliged to him for his help and support.

During my PhD career at the University of Saskatchewan, I have received scholarships that reduced my teaching load to a minimum and helped me to focus exclusively on my research. I would like to mention the Dean's Scholarship, the Saskatchewan Innovation and Opportunity Scholarship, the Gerhard Herzberg Thesis Acceleration award, and numerous travel grants that made it possible for me to attend conferences and present my research to an international audience. I came across some truly awesome scientists at these meetings; I would especially treasure my interactions with Professors Audrey Moores (McGill University), Francesca Kerton, and Christopher Kozak (both from Memorial University of Newfoundland). I am truly grateful to the funding agencies for making life a little easier for me.

Members of the Scott research group, both past and present, have been wonderful colleagues. I would especially like to thank Atal Shivhare, Yali Yao, Robin Theron, Danielle Penrod, Aimee Maclennan, Jiaqui Liang, Mahesh Gangishetty, Wendy Bai, and Toby Bond. Robin and I collaborated on several projects over a period of years; working with her was truly a great experience. Aimee and Toby, both employed at the Canadian Light Source now, are amazing scientists and wonderful human beings. It was a pleasure to work alongside them. Toby generously shared some of his 'special' tricks and tips for synthesizing ultra-clean ionic liquids with me before he left the group for his own graduate research at Halifax; I would like to thank him for that.

Having friends outside one's own research group can give one a sense of perspective, and occasionally, save one's sanity. Conie Ponce did both; even better, she inspired me (and

many others) to volunteer for “Let's Talk Science”, an award-winning, national charitable organization focused on education and outreach to support youth development. Bidraha, Nora, Lewis, Scott, John, and Neeraj are/were some of the other students from the department that I became (and have remained) friends with. It has been a pleasure to interact with them both socially as well as professionally; I wish them the very best of luck in all their future endeavors.

No research group could thrive in a vacuum; in fact, without the help of our wonderful departmental staff, even day-to-day operations would have been a challenge. I would like to express my heartfelt gratitude towards Leah Hildebrandt, our amazing graduate secretary; Ronda Duke, secretary to the Departmental Head; Bonita Wong, our Finance and Operations Manager; Linda Duxbury and Heather Lynchuk, Keepers of the Keys (to the Chemical Stores!); and other ‘key’ personnel of the Chemistry department. Without their constant help and support, I would never have survived the daily grind of working in a research laboratory. DeDe Dawson, our Science Librarian, introduced me to the mysteries of referencing software and Open Access vouchers. Irene Henriksen, who keeps our laboratory space clean, and takes care of some very unusual messes, is another wonderful person. Virgina Issacs, Cathy Surtees, Dwight Reynolds, and Brenda Weenks, who have since moved on to other departments or to well-deserved retirements, are also to be thanked. The staff-members at the Murray and the Natural Sciences Libraries have been very helpful and approachable. I have also benefited from my use of the Public Library system of Saskatchewan.

Now, I would like to take a look back at several people who I have known before my time in Saskatoon; people who have had a profound influence on my academic interests,

hopes, and dreams. I would like to thank the first two people who introduced me to the magical realms of chemistry way back in high school: Dr. Indrani Bhattacharya, and Dr. Debjani Ghosh. Afterwards, during my undergraduate education at Jadavpur University, I had the good fortune of learning Chemistry from scientists such as Dr. Rupendranath Banerjee, and Dr. Samaresh Bhattacharjee, who are still active in the field of research, producing wonderful results with the limited resources at their disposal. If it were not for their help, support, and encouragement, I would never have had an opportunity to intern at the Tata Institute of Fundamental Research in 2006, and savor my first taste of Big Research.

My graduate studies at the Indian Institute of Technology, Kharagpur, were one of the happiest periods of my life. Working in Professor Panchanan Pramanik's Nanomaterials laboratory infected me with the “nano”-fever that still seems to continue unabated when it comes to my research interests. Working for Professor Pramanik was truly a wonderful experience, and my collaboration with his graduate student Dr. Sudeshna Ray (now a professor herself at AISECT University) led to several publications, which also gave me an opportunity to brush up my scientific writing skills. At IIT Kgp, I had the good fortune of attending courses run by scientists such as Professors Srabani Taraphder and Swagata Dasgupta, leaders in their fields of research. I would like to thank them for believing in me and insisting that I continue in academic research.

Now, I would like to go back to the very beginning, and thank the people without whose unwavering love and support, my existence, let alone my research, would have been impossible. I would like to thank my parents, whose personal sacrifices made it possible for me

to go seek knowledge in a far-away country; my great-aunt, proud possessor of an undergraduate degree in English from Calcutta University (in the 1930s!), who ensured that I grew up bilingual, and instilled in me a love for the Golden Age of Detective Fiction; and my grandmother, who taught me to treasure learning for its own sake. It might seem a little callow to dismiss their contributions with a few sentences; but then, I would never be able to express my immense gratitude towards these people, even if I write another dissertation on the topic!

People have biological families, but they create their 'logical' families, especially Children of the Wind like me, who fly halfway across the world to build their nests. The Becker-Swann-Joss family in Saskatoon took me under their collective wings in 2010, and never let go; during the darkest periods of my life here in the chilly prairies, they provided love, comfort, hope and succor. Again, there are really no words that one can use to thank such friends. They have been gone to great lengths to ensure my continued existence and well-being, and I will remain in their debt for all eternity. I would also like to thank Vikram Johri, Hazen Colbert, Roy Wadia, Marilyn Elliott, and Richard Liberty; their friendships mean a lot to me.

Into all life, proverbial wisdom states, some rain must fall; and often, it is easy to lose hope, become demoralized, and to question one's convictions. One must, however, hold on to the things one believes in, and remember the people one holds dear in one's heart. Like the Bard, 'I can no other answer make, but, thanks, and thanks'.

TABLE OF CONTENTS

PERMISSION TO USE……i

ABSTRACT……ii

DEDICATION……iv

ACKNOWLEDGEMENT……vi

TABLE OF CONTENTS……xii

LIST OF FIGURES……xvi

LIST OF SCHEMES……xxii

LIST OF TABLES……xxiii

LIST OF ABBREVIATIONS……xxiv

CHAPTER 1……**1**

1.0 Introduction 1

1.1 Solvents in Catalysis 1
1.1.1 Volatile Organic Solvents 4
1.1.2 Water 6
1.1.3 Liquid Polymers 8
1.1.4 Ionic Liquids 11
1.1.4.1 Imidazolium Ionic Liquids 12
1.1.4.2 Phosphonium Ionic Liquids 15
1.1.4.3 Other Ionic Liquids 18
1.1.5 Deep Eutectic Solvents 20
1.1.6 Fluorous Solvents 24
1.1.7 Supercritical Fluids 26
1.1.8 Other Solvent Systems 27

1.2 Nanoparticle (NP) Catalysts 29
1.2.1 Classification of Nanoparticle Catalysts 30
1.2.2 Stabilization of Nanoparticle Catalysts in Ionic Liquids 33
1.2.2.1 Extrinsic Stabilization 35

1.2.2.2 Intrinsic Stabilization 44

1.3 Reactions Catalyzed by Metal Nanoparticles in an Ionic Liquid Phase 53

1.3.1 Hydrogenation 54
1.3.2 Oxidation 57
1.3.3 Hydrodeoxygenation 60
1.3.5 Other Reactions 62

1.4 Organization and Scope 65

1.5 References 67

CHAPTER 2……**79**

2. Highly Stable Noble Metal Nanoparticles in Tetraalkylphosphonium Ionic Liquids for *in-situ* Catalysis

2.1 Abstract 80
2.2 Introduction 81
2.3 Experimental 85
2.4 Results and Discussion 89
2.5 Conclusions 105
2.6 References 107

CHAPTER 3……**112**

3. Aerobic Oxidation of α,β-Unsaturated Alcohols Using Sequentially-Grown AuPd Nanoparticles in Water and Tetraalkylphosphonium Ionic Liquids

3.1 Abstract 114
3.2 Introduction 115
3.3 Experimental 119
3.4 Results and Discussion 124
3.5 Conclusions 142
3.6 References 144

CHAPTER 4……**147**

4. Redispersion of Transition Metal Nanoparticle Catalysts in Tetraalkylphosphonium Ionic Liquids

4.1 Abstract 149

4.2 Introduction 150
4.3 Experimental 152
4.4 Results and Discussion 157
4.5 Conclusions 172
4.6 References 173

CHAPTER 5……**176**

5. Design, Synthesis, Catalytic Application, and Strategic Redispersion of Plasmonic Silver Nanoparticles in Ionic Liquid Media

5.1 Abstract 178
5.2 Introduction 179
5.3 Experimental 182
5.4 Results and Discussion 186
5.5 Conclusions 201
5.6 References 203

CHAPTER 6……**206**

6. Optimization of Transition Metal Nanoparticle-Phosphonium Ionic Liquid Composite Catalytic Systems for Deep Hydrogenation and Hydrodeoxygenation Reactions

6.1 Abstract 207
6.2 Introduction 208
6.3 Experimental 211
6.4 Results and Discussion 215
6.5 Conclusions 235
6.6 References 237

CHAPTER 7……**241**

7. Synthesis, Characterization, and Evaluation of Iron Nanoparticles as Hydrogenation Catalysts in Tetraalkylphosphonium Ionic Liquids

7.1 Abstract 240
7.2 Introduction 242
7.3 Experimental 248
7.4 Results and Discussion 251
7.5 Conclusions 264
7.6 References 266

CHAPTER 8……**269**

8.1 Synopsis 270

8.2 Future Work 276
8.2.1 Carbon Dioxide Processing in Tetraalkylphosphonium Ionic Liquids 277
8.2.2 Metallurgy of Gold in Tetraalkylphosphonium Halide Ionic Liquids 280
8.2.3 Enantioselective Catalytic Hydrogenations in Tetraalkylhosphonium Ionic Liquids 283

8.3 Concluding remarks 285

8.4 References 286

List of Figures

Figure 1.1	A guide for solvent selection.	6
Figure 1.2	Some common cations and anions in ILs.	13
Figure 1.3	Novel cations and anions for sustainable and/or biocompatible IL synthesis.	19
Figure 1.4	(a) Some fluorous solvents; (b) A schematic representation of FBC.	25
Figure 1.5	Examples of solvents derived from renewable resources.	28
Figure 1.6	A generic representation of a metal NP, showing metal atoms with varied coordinations.	32
Figure 1.7	Homogeneous, Heterogeneous, and quasi-homogeneous catalysis: a comparison.	33
Figure 1.8	Modes of stabilization of solvent-diffused nanoparticles.	35
Figure 1.9	Ionic copolymers for stabilization of catalytically active Rh NPs in BMIM-BF_4.	37
Figure 1.10	Synthesis of dendrimer-stabilized bimetallic NPs for catalysis.	39
Figure 1.11	Bidentate N-containing ligands can stabilize metal NPs in ILs by coordinating to the NP surface.	41
Figure 1.12	Asymmetric hydrogenation catalyzed by Pt NPs in ILs in the presence of a chiral ligand.	43
Figure 1.13	Interaction of metal NPs with IL supramolecular aggregates: (a) small particles tend to interact preferentially with anionic aggregates of the ILs, whereas (b) large ones probably interact preferentially with the cationic aggregates.	46
Figure 1.14	Cations and anions in functionalized ILs.	49
Figure 1.15	Synthesis of a poly(IL) (EBIB = ethyl 2-bromoisobutyrate, TPMA = tris(2-pyridylmethyl)amine, and $Sn(EH)_2$ = tin(II) 2-ethylhexanoate).	52
Figure 1.16	Au NP catalyzed radical-mediated oxidation of 2-phenylethanol in an IL.	60
Figure 1.17	Tandem phenol HDO on IL-solvated-Ru NPs in the presence a second functionalized Brønsted acidic IL.	62
Figure 2.1	(a) TEM image of Au NPs prepared in P[6,6,6,14]Cl; (b) TEM image of Au NPs prepared in P[4,4,4,1]OTf; (c) UV-Vis spectra of 1.4 mM solutions of $HAuCl_4$, Au NPs in P[6,6,6,14]Cl, and Au NPs in P[6,6,6,14]Br in cyclohexane, (d) Size distribution of Au NPs in P[6,6,6,14]Cl; (e) TEM image of Au NPs prepared in P[6,6,6,14]Br;	90

	(f) a drop of the wine-red Au NP/P[6,6,6,14]Cl on a clean glass slide.	
Figure 2.2	(a) TEM image of Pd NPs prepared in P[6,6,6,14]Cl; (b) (top) a drop of K_2PdCl_4 dissolved in P[6,6,6,14]Cl, (bottom) a drop of 14 mM Pd MNP in P[6,6,6,14]Cl on glass slides; (c) Size distribution of Pd MNPs prepared in P[6,6,6,14]Cl; (d) UV-Vis spectra of 1.4 mM solutions of K_2PdCl_4 and Pd NPs in P[6,6,6,14]Cl in cyclohexane.	91
Figure 2.3	TEM images of (a)Pd NPs and (b) Au NPs in P[6,6,6,14]Cl regenerated after aerial oxidation followed by $LiBH_4$ reduction; and UV-Vis spectra of the re-reduction of (c) Pd NPs and (d) Au NPs in P[6,6,6,14]Cl.	94
Figure 2.4	(a) TON vs. time plot for hydrogenation of 2-methyl-3-buten-2-ol by 14.0 mM Pd MNPs in various phosphonium ILs.; (b) Comparison of the TOF (min^{-1}) of the reaction in different ILs.	99
Figure 2.5	(a) Recyclability of Pd MNPs prepared in P[6,6,6,14]Cl for for hydrogenation of 2-methyl-3-buten-2-ol. Final column shows TOF after complete Pd oxidation at 90^{o}C in air over two days followed by re-reduction of the Pd with $LiBH_4$; (b) From left to right: 14 mM Pd NPs in P[6,6,6,14]Cl after 5 catalytic cycles, after oxidation, and finally, after re-reduction with $LiBH_4$	104
Figure 2.6	(a) TEM image of Pd MNPs in P[6,6,6,14]Cl regenerated after aerial oxidation followed by $LiBH_4$ reduction; (b) TEM image of Pd NPs in P[6,6,6,14]Cl after 5 cycles of catalytic hydrogenations.	105
Figure 3.1	TEM images of PVP-stabilized (A) as-synthesized Au NP seeds and (B) as-synthesized sequentially-reduced 1:3 AuPd NPs and (C) Au NP/Pd(II) 1:3 mixture after 24 h reaction with cinnamyl alcohol and (D) sequentially-grown 1:3 AuPd NPs after 24 h reaction with cinnamyl alcohol.	125
Figure 3.2	UV-Vis spectra of PVP-stabilized Au, Pd, and sequentially-grown 1:3 AuPd NPs in water.	126
Figure 3.3	EXAFS spectra in k-space for monometallic Au, Pd and sequentially-grown 1:3 AuPd NPs and Au NP/Pd(II) 1:3 mixture after 24 h reaction with crotyl alcohol at: (A) Pd K-edge (B)Au-L_{III} edge.	135
Figure 3.4	EXAFS single-shell fits in r-space for sequentially-reduced 1:3 AuPd NPs at the (A) Au-L_{III} and (B) Pd K edges and Au NP/Pd(II) 1:3 mixture after 24h reaction with crotyl alcohol at the (C) Au-L_{III} and	136

(D) Pd K edges
Figure 3.5 UV-Vis spectra of P[6,6,6,14]Cl IL -stabilized Au, Pd, and sequentially-grown 1:3 AuPd NPs. 138
Figure 3.6 TEM images of as-synthesized P[6,6,6,14]Cl IL-stabilized (A) Pd NPs, (B) sequentially-reduced 1:3 AuPd NPs, and (C) Au NPs; and after 24 h reaction with cinnamyl alcohol: (D) Pd NPs, (E) sequentially-reduced 1:3 AuPd NPs, and (F) Au NP/Pd(II) 1:3 mixture. 139
Figure 4.1 TEM images of the as-synthesized metal NPs: (a) Ag(3.5 ± 0.6 nm), (b) Au(3.2 ± 0.8 nm), (c) Co(4.7 ± 1.3 nm), (d) Cu(4.2 ± 1.0 nm), (e) Fe(7.4 ± 2.0 nm), (f) Ni(5.9 ± 1.3 nm), (g) Pd(4.9 ± 2.2 nm), (h) Pt(2.4 ± 0.4 nm), (i) Rh(9.6 ± 3.5 nm) and (j) Ru(4.5 ± 1.2 nm). 159
Figure 4.2 UV-Visible spectra of metal precursor in IL, metal NPs in IL after synthesis, and metal NPs in IL after oxidative degradation for all the metals studied. Spectral features did not deviate significantly from existing literature. 164
Figure 4.3 TEM images of the metal NPs after regeneration: (a) Ag(4.1 ± 0.8 nm), (b) Au(5.5 ± 1.4 nm), (c) Co(12.5 ± 4.1 nm), (d) Cu(9.1 ± 3.7 nm), (e) Fe(8.0 ± 3.1 nm), (f) Ni(6.8 ± 2.1 nm), (g) Pd(3.1 ± 1.1 nm), (h) Pt(2.2 ± 0.7 nm), (i) Rh(11.3 ± 3.9 nm) and (j) Ru(3.5 ± 1.1 nm). 165
Figure 4.4 (a) Time-dependent UV-Vis spectral monitoring of the oxidative degeneration of 2.5 mM Au NPs in P[6,6,6,14]Cl at 60°C in air; plasmon band decay shown on right;
(b) Demonstration of redispersion of larger Au NP aggregates into smaller Au NPs via oxidative etching, with TEM images of the initial large NPs (left) and re-dispersed NPs (right). 168
Figure 4.5 UV-Vis spectrophotometric study of the oxidative degeneration of Ni NPs in P[6,6,6,14]Cl stirred under air at 45°C; inset shows appearance of the sample at t=0 (brown, on the right) and at t=24 hours (turquoise, on the left). 171
Figure 4.6 TEM images of Ni NPs. From left to right: as-synthesized (avg. size: 6.0 ± 1.4 nm), after 3 cycles of hydrogenation (avg. size: 19.2 ± 2.5 nm), and after regeneration (avg. size: 6.8 ± 2.1 nm). Inset shows the beginning of Ni NP coalescence. 171
Figure 5.1 UV-Visible spectra of $AgNO_3$ in P[6,6,6,14]Cl IL, Ag NPs formed by reduction with lithium borohydride, post-etch Ag species in IL, and re-generated Ag NPs. 187

Figure 5.2	TEM images of Ag NPs formed in IL by $LiBH_4$ (A: as-synthesized; B: sintered – 1 hour; C: sintered – 24 hours; D: redispersed; E: after five consecutive cycles of EY degradation).	189
Figure 5.3	Ag NP catalyzed borohydride reduction of Eosin-Y (top), and the color change that accompanies it (bottom).	191
Figure 5.4	(A) Decrease in EY absorption at 536 nm as a function of time both before and after introduction of Ag NPs in the system; (B) First-order regression analysis of EY degradation in the presence as well as the absence of Ag NPs in the reaction system; (C) First-order regression analysis of EY degradation in the presence of freshly synthesized Ag NPs, sintered Ag NPs, and no Ag NPs in the reaction system; (D) First-order regression analysis of EY degradation in the presence of redispersed Ag NPs, sintered Ag NPs, and no Ag NPs in the reaction system.	194
Figure 5.5	(A) Evolution of the UV-Visible spectrum of Ag NPs in P[6,6,6,14]Cl at 65°C in the presence of oxygen: spectrophotometric monitoring of the progress of Ag NP etching; (B) Plot of $-[\ln(A_t - A_\infty)/A0]$ as a function of time for the calculation of pseudo-first-order rate constants for the Ag NP etching process at 65°C in the presence of oxygen.	197
Figure 5.6	Ag L_{III} edge solution phase XANES spectrum of Ag NPs in P[6,6,6,14]Br IL before and after etching in air for 6 hours.	200
Figure 6.1	UV-Visible spectra of Au NPs in various representative ILs recorded immediately after synthesis (light grey solid line), after three days (deep grey dashed line), and after heating under N_2 at 150°C for 1 h (black dotted line).	217
Figure 6.2	TEM images of Au NPs in representative ILs: (a) in P[8,8,8,8]Br after heat treatment- the individual particles (~12 nm average diameter) coalesce to form μm-sized aggregates; (b) in P[4,4,4,14]Cl before heat treatment, with an average particle size of 4.5± 0.6 nm; (c) in P[4,4,4,14]Cl after heat treatment- there is an average particle size growth of ~ 7 nm, with an average final particle size of 11.3 ± 7.1 nm ; (d) in P[6,6,6,14]Cl before heat-treatment, with an average particle size of 4.1 ± 0.6 nm; and (e) in P[6,6,6,14]Cl after heat-treatment- we now see a bimodal distribution of particle sizes, with mean particle diameters of 3.5 ± 0.6 nm (which corresponds to the as-synthesized particle sizes)	218

	and 12.2 ± 3.5 nm (which corresponds to the sintered NP sizes).	
Figure 6.3	TEM images of Pt NPs in P[4,4,4,8]Cl (before heating: (A) after heating: (B) P[6,6,6,14]Cl (before heating: C, after heating: D), and P[6,6,6,14]NTf_2 (before heating: E, after heating: F). Average sizes of NPs are as follows: (A): 4.7 ± 1.2 nm, (B): 12.2 ± 6.1 nm, (C): 2.1 ± 0.4 nm, (D): 3.8 ± 0.9 nm, (E): 5.2 ± 1.2 nm, and (F): 9.2 ± 2.1 nm. Heating was performed under 1 atm hydrogen at 150°C for 12 h.	220
Figure 6.4	(A) TEM images of as-synthesized 10 mM Ru NPs in P[6,6,6,14]Cl. Average particle size is 2.9 ± 1.2 nm. (B,C) TEM images of 10 mM Ru NPs in P[6,6,6,14]Cl after one phenol HDO cycle. Average particle size is 14.6 ± 6.4 nm (ignoring the lighter blobs, which could be droplets of the ionic liquid). The inset in (B) shows two large Ru NPs surrounded by smaller Ru NPs, presumably during the process of particle coalescence.	227
Figure 6.5	(A) ^{1}H NMR spectrum of neat reaction extract (in $CDCl_3$) after phenol HDO. For individual peak assignments, see (B) and (C). (D) ^{13}C NMR spectrum of neat reaction extract (in $CDCl_3$) after phenol HDO.	230
Figure 6.6	^{11}B proton-decoupled NMR spectrum of P[6,6,6,14]Cl/Ru NP system: (A) ~30 minutes synthesis of NPs via borohydride addition; and (B)~24 hours after borohydride addition and quenching. NMR solvent is THF-D8. The peak at δ = -40 could be assigned to a borohydride boron, and the one at δ = 18.5 could be assigned to a borate boron.	234
Figure 7.1	UV-Visible spectra of $Fe(acac)_3$ and Fe NPs in P[6,6,6,14]NTf_2, diluted with THF.	253
Figure 7.2	TEM images of Fe NPs formed in P[6,6,6,14]NTf_2 (A): as-synthesized; (B): as-synthesized in the presence of PVP; (C): after one catalytic cycle in the absence of PVP; (D): PVP-containing sample after one catalytic cycle; (E): after five catalytic cycles in the absence of PVP.	254
Figure 7.3	Fe K edge solution phase XANES spectra: (A) comparing Fe NPs and Fe foil; (B) comparing $Fe(acac)_3$ in THF, $Fe(acac)_3$ in P[6,6,14]NTf_2, as-synthesized Fe NPs in P[6,6,6,14]NTf_2, and the Fe NPs after hydrogenation; (C) Fe NPs in P[6,6,6,14]Cl showing oxidation of Fe(0) in air; and (D) comparing Fe(II) and Fe(III) in P[6,6,6,14]Cl.	263
Figure 8.1	PEG-Pd NPs in P[6,6,6,14]Im with an average particle size of 2.5 ± 0.5 nm	280

Figure 8.2 (a) XANES spectra of Au(III) in P[6,6,6,14]NTf_2 after the initial scan (black) and after two consecutive scans (red), showing changes in speciation; (b) 10 mM Au(III) in P[6,6,6,14]NTf_2 before (bottom) and after (top) exposure to synchrotron X-rays. Au (I) and pre-formed Au NPs in in P[6,6,6,14]NTf_2 have also been shown for comparison purposes. 283

List of Schemes

Scheme 1.1	Selected examples of catalysis in liquid polymer media	10
Scheme 1.2	Synthesis of tetraalkylphosphonium ILs with functional anions	17
Scheme 1.3	Decomposition pathways for tetraalkylphosphonium ILs	17
Scheme 1.4	Selected examples of catalysis in DESs	23
Scheme 2.1	Schematic representation of MNP stabilization by P[6,6,6,14]Cl IL; inset shows Au and Pd MNPs in P[6,6,6,14]Cl stored in capped vials under nitrogen, two months after they were synthesized.	95
Scheme 3.1	Product distributions for oxidation of α,β-unsaturated alcohols.	129
Scheme 6.1	Reaction pathways for phenol HDO by Ru NP in IL.	227
Scheme 6.2	Summary of control experiments performed to evaluate the role of borohydride side products present within the composite catalyst matrix in phenol HDO product distribution. Reaction conditions common to all reactions were as follows: 24 bar Hydrogen pressure; IL P[6,6,6,14]Cl; 120°C, 24 hours. A: in neat P[6,6,6,14]Cl, B: in P[6,6,6,14]Cl containing 10mM Ru NPs synthesized via hydrazine reduction; C: in P[6,6,6,14]Cl containing 10mM Ru NPs synthesized via borohydride reduction; D: in P[6,6,6,14]Cl containing ca. 150 mM soluble borate generated from lithium borohydride.	233
Scheme 8.1	Synthesis of ‘tailored-anion’ tetraalkylphosphonium ILs.	278
Scheme 8.2	CO_2 harvesting by ‘tailored-anion’ tetraalkylphosphonium ILs.	278

List of Tables

Table 1.1	Classes of deep eutectic solvents.	21
Table 2.1	Catalytic hydrogenation of simple organic molecules with single products in the presence of Pd NP/P[6,6,6,14]Cl	100
Table 2.2	Catalytic hydrogenation of organic molecules with multiple hydrogenation products in the presence of Pd NP/P[6,6,6,14]Cl	102
Table 3.1	Summary of Nanoparticle Sizes obtained by TEM	126
Table 3.2	Summary of Catalytic Results for the Oxidation of α,β-Unsaturated alcohols using PVP-stabilized NPs in water.	130
Table 3.3	EXAFS fitting parameters for AuPd NP systems.	134
Table 3.4	Summary of Catalytic Results for the Oxidation of α,β-Unsaturated Alcohols using P[6,6,6,14]Cl-stablized NPs	142
Table 4.1	Redispersion conditions for metal NPs studied in P[6,6,6,14]Cl	154
Table 4.2	Cyclohexene olefination using NiNP/P[6,6,6,14]Cl catalyst	169
Table 5.1	Pseudo-first-order rate constants calculated for the Ag NP etching process in oxygen in ionic liquids with dynamic UV-Vis spectroscopy at 65^0C.	199
Table 6.1	Hydrogenation of 2-methylbut-3-en-2-ol catalyzed by 10 mM NP/IL composites	221
Table 6.2	Hydrogenation of toluene catalyzed by 10 mM NP/IL composites	224
Table 6.3	HDO of phenol catalyzed by 10mM RuNP/IL composites	228
Table 7.1	Performance of Fe NP/IL composites in the catalytic hydrogenation of norbornene	257
Table 8.1	Comparison of the catalytic activities of transition metal NPs in ambient pressure hydrogenations in different solvents. [BMMDPA-PF_6 = 2,3-dimethyl-1-{3-N,N-bis(2-pyridyl)-propylamido} imidazolium hexafluorophosphate].	276

List of Abbreviations

acac	Acetylacetonate
AEMIM	1-(2’-aminoethyl)-3-methylimidazolium
BINAP	2,2'-bis(diphenylphosphino)-1,1'-binaphthyl
BMIM	1-butyl-3-methylimidazolium
C-C	Carbon-Carbon
CLS	Canadian Light Source
CN	Co-ordination Number
cP	Centipoise
CTAB	Cetyltrimethylammonium Bromide
dba	Dibenzylideneacetone
DES	Deep Eutectic Solvent
DLVO Theory	Derjaguin-Lanndau-Verwey-Overbeek Theory
ee	Enantiomeric Excess
EMIM	1-Ethyl-3-Methylimidazolium
EXAFS	Extended X-ray Absorption Fine Structure
EY	Eosin-Y
GC-MS	Gas Chromatography-Mass Spectrometry
GC-FID	Gas Chromatography with Flame Ionization Detector
HDO	Hydrodeoxygenation
HRTEM	High resolution Transmission Electron Microscopy
HXMA	Hard X-ray Microprobe Analysis
Hz	Hertz
IL	Ionic Liquid
Im	Imidazolate
LMCT	Ligand-to-metal charge-transfer
MNP	Metal nanoparticle
MW	Molecular Weight
NHC	N-heterocyclic carbene
NTf_2	Bis(triflimide) [bis(trifluoromethane)sulfonamide]
NMR	Nuclear Magnetic Resonance
NP	Nanoparticle
OTf	Triflate [Trifluoromethanesulfonate]
OTs	Tosylate [p-toluenesulfonate]
PEG	Poly(ethyleneglycol)
ppm	Parts per million
PVP	Poly(vinylpyrrolidone)

$scCO_2$	Supercritical Carbon dioxide
rpm	Revolutions per minute
TEM	Transmission Electron Microscopy
TBAB	Tetrabutylammonium Bromide
TFA	Trifluoroacetate
THF	Tetrahydrofuran
TOAB	Tetraoctylammonium Bromide
TOF	Turnover Frequency
TON	Turnover Number
TTO	Total Turnovers
UV-Vis	Ultraviolet Visible
XAFS	X-ray Absorption Fine Structure
XAS	X-ray Absorption Spectroscopy
XANES	X-ray Absorption Near-edge Structure
XRD	X-ray Diffraction

1.0 Introduction

Catalysis lies at the heart of chemistry in action. From industrial synthetic processes for the manufacture of household chemicals, to exotic methodologies for harvesting renewable energy from sustainable sources and solving the international energy crisis; from the fabrication of complex therapeutic agents for curing devastating diseases, to the routine production of bulk chemicals on a multi-ton scale: catalysis forms an integral part of all these processes.[1-3] Catalysis, in which small amounts of a foreign substrate can have a drastic impact on the efficiency, product composition, and rate of a reaction, is indeed ubiquitous in synthetic chemistry.[4] As we witness a 'quiet revolution' that demands the use of environmentally benign, sustainable, and carbon-neutral processes in the chemical industry, there is no denying that catalysis will be the primary weapon in our arsenal for negotiating cost- and energy-efficient chemical transformations.[5-7]

1.1 Solvents in catalysis

It is widely acknowledged that solvents have drastic effects on reaction pathways, reaction rates, and even product distributions.[8] It is not surprising, therefore, that solvents have several functions in catalytic reactions, including (but not limited to) mass and heat transfer, facilitating separations, and enabling scientists to carry out purification steps.[9] In general, solvents find greater applications in the synthesis of fine

chemicals where the starting materials are often organic solids, which decompose under solvent-free reaction conditions. However, the use of volatile organic solvents in medium- to large-scale industrial synthetic protocols has definite environmental implications that we can no longer afford to ignore. Environmental hazards such as air and water pollution, potential for devastating accidents owing to solvent flammability, and adverse health effects in workers via repeated inhalation and contact, were identified as some of the more pressing concerns, and legislations were passed in several countries to protect the well-being of the environment as well as human resources.[10,11] Furthermore, the question of disposal of contaminated volatile organic solvents after extraction of products can no longer be ignored, given the severely limited recyclability of these solvents.[12] It is imperative for us, therefore, to seek alternatives to solvents that are potentially damaging to the environment, as well as to living beings. Unfortunately, there is another major factor that, until recently, was probably the only consideration in solvent selection for industrial purposes: cost. It was universally acknowledged that organic solvents are cheaper than almost all the so-called 'alternative solvents' which were being discovered and studied, and it was often difficult to convince industrial manufacturers to switch solvents solely on the basis of recommendations of the scientific community.[13]

The scenario in 2015, however, is not as bleak as it appeared to be a couple of decades ago: despite early predictions that alternative solvents would never find application outside research laboratories, Francesca M. Kerton's recent monograph on

the use of alternative solvents in the chemical and manufacturing industries lists several examples of industrial processes that now utilize these solvents on a regular basis, thereby reducing the use of volatile organic solvents, or eliminating them altogether.[14] Since 2000, for instance, Bayer uses water as a solvent in the manufacture of polyurethane coatings; in 1999, Nalco won a Green Chemistry award for synthesizing their acrylamide based polymers in water rather than in volatile organic solvents. The Ruhrchemie hydroformylation process, generating 800,000 tons of products per year, is also carried out in an aqueous medium. Similarly, supercritical CO_2 is used industrially in coffee decaffeination, in dry-cleaning, and in polymer-processing. The BASIL™ (**B**iphasic **A**cid **S**cavenging using **I**onic **L**iquids) process, performed on a multi-tonne scale, proved that handling large quantities of ionic liquids (ILs) is practical. Since 1996, Eastman Chemical Company had been running a process for the isomerisation of 3,4-epoxybut-1-ene to 2,5-dihydrofuran using tri(octyl)octadecylphosphonium iodide as a solvent. The French Petroleum Institute has a patented alkene dimerization process (Difasol™) that utilizes ILs. Currently, the largest industrial facility to use ILs is PetroChina, where a 65,000 ton-per-year sulfuric-acid-based isobutene alkylation plant was retrofitted to use chloroaluminate ILs as the alkylating agent. Numerous other applications of 'alternative solvents' in industry can be unearthed via a cursory search of relevant literature.

The following sections of this chapter are primarily concerned with brief descriptions of the several classes of alternative solvents that have found use in catalysis, along with selected examples of such reactions The concept of catalysis with

stable NPs dispersed in a liquid phase is then introduced, with an emphasis on the use of ILs as a novel media for the synthesis of NP catalysts. Subsequently, selected examples of NP-catalyzed reactions in tetraalkylphosphonium ILs are discussed. Finally, overall research objectives, and the organization and scope of this thesis have been documented. It is to be noted that wherever possible, the catalytic examples have been restricted to processes catalyzed by solvent-dispersed NPs; however, in some cases, examples of homogeneous catalysis have also been described.

1.1.1 Volatile organic solvents

"Weiche, Wotan, weiche", warns Erda, the Earth Goddess, in Richard Wagner's opera 'Das Rheingold': "...all that is will come to an end, as a dark twilight approaches."[15] She might have been talking about the unrestricted use of volatile organic solvents. Health Canada classifies volatile organic solvents as organic compounds with high vapor pressures, low to medium water solubilities, and low molecular weights.[16] They are used extensively in commercial processes where organic substrate and/or organometallic catalysts are involved. As industrial-scale contaminants, these are of particular concern, owing to large environmental releases, human toxicity, and the potential for mixing with groundwater, thereby affecting drinking water supplies. Some typical examples of industrially relevant volatile organic solvents include aliphatic hydrocarbons, acetone, ethyl acetate, ethers, benzene, chlorofluorocarbons, and halogenated hydrocarbons, such as trichloroethylene and dichloromethane. While

it cannot be denied that these solvents have played a vital role in the bulk- and fine-chemicals manufacturing industry, it is daunting to consider some of the detrimental effects that these solvents have on the environment, as well as the human body. The fact that some many of these solvents are human and animal carcinogens and teratogens alone should make us realize how dangerous it is to allow their widespread use and unrestricted disposal.[17] In fact, research has revealed that some of the traditional organic solvents used by the manufacturing industries are so toxic to humans upon continuous exposure that some pharmaceutical companies such as Pfizer have developed a 'blacklist' of solvents that they strongly discourage using in their research and development laboratories and pilot plants.[18,19] Solvents such as hexanes, diethyl ether, DMF, acetonitrile and THF have all been ‘blacklisted’, while attempts are being made to earmark feasible alternatives for these.[20] A model solvent selection guide, classifying solvents on the basis of the desirability of their use in commercial processes, has been shown in Figure 1.1.[21]

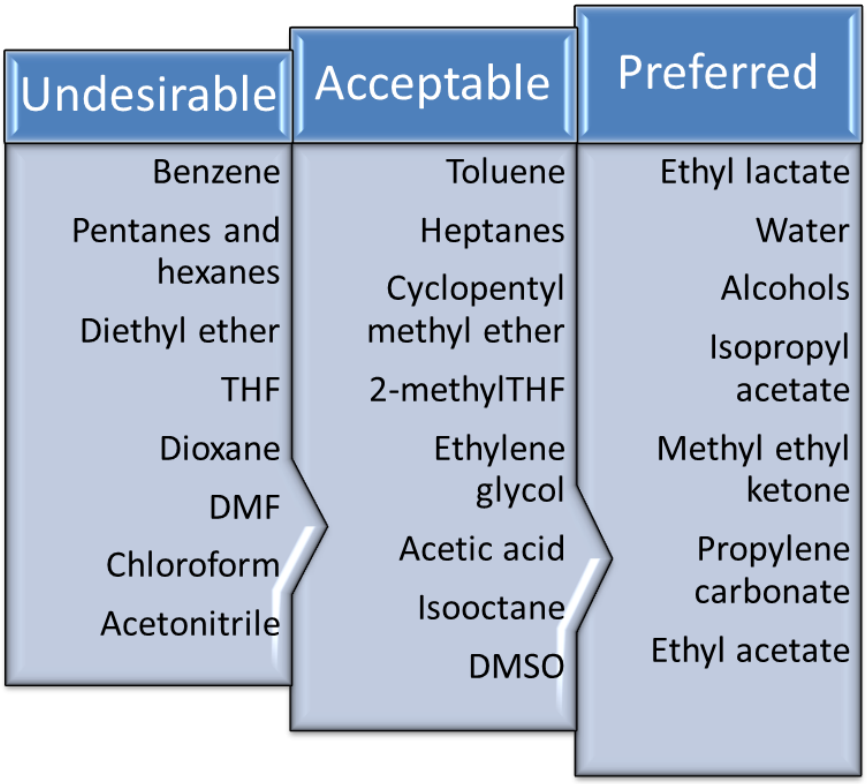

Figure 1.1 A guide for solvent selection (adapted from reference [14]).

1.1.2 Water

Water is nature's reaction medium of choice. Complex enzymatic transformations, responsible for life itself, occur in an aqueous environment.[22] It is not surprising, therefore, that other than volatile organic compounds, water is possibly the only solvent that is used in the chemical industry on a regular basis. Water is one of the most easily available solvents on the planet; it is non-toxic, non-combustible, capable of dissolving a variety of solids, liquids and gases, and highly polar in nature, favoring easy separation of non-polar molecules.[23] It is also, however, highly reactive, especially with organometallic catalysts which are very often moisture-sensitive. Moreover, despite

being called a 'universal solvent', there are many organic compounds that show little to no solubility in water. It has become essential, therefore, to invent new protocols in order to substitute water for volatile organic solvents in catalysis.[24] Addition of surfactants and phase transfer catalysts, for instance, can enhance the solubility of organic molecules in water; addition of hydrophilic groups such as sulfonates, sugars, and carboxylic acids to ligand molecules can produce organometallic catalysts that are soluble and stable in water; and biphasic catalysis often occurs 'on water', where the organic substrates, being hydrophobic in nature, tend to form micelles clusters in an aqueous system, thereby favoring reactions.[25-27] Finally, near-critical water (water heated to temperatures above 100°C but below 374°C in a pressurized vessel; a pressurized vessel is essential since the saturated vapor pressure of water increases with increase in temperature, reaching a value of 1,550 kPa at 200°C) shows unique solvent properties which render it suitable for applications such as devulcanization (partial or total cleavage of cross-links that bridge the polymer chains) of rubber and waste treatment.[28]

A detailed survey of NP catalysts used in aqueous media is beyond the scope of this thesis, but it must be pointed out that many of the earliest examples of catalytic NPs were synthesized in water.[29-31] Presently, there exists a vast body of literature dealing with the synthesis and catalytic applications of metal and semiconductor NPs in aqueous medium, often using plant extracts, unicellular organisms, or bio-molecules for the synthesis.[32-35]

1.1.3 Liquid polymers

Polymers with low glass transition temperatures, commonly called 'liquid polymers', represent an interesting class of alternative solvents for catalytic reactions.[36] Liquid polymer solvents have been shown to enable recyclability of expensive catalysts, eliminate health and environmental risks associated with the use of volatile organic solvents, and facilitate separation of products from reaction media, either by distillation of volatile products, or through extraction with supercritical CO_2.[37] Liquid polymers are also supposed to be tunable over a wide range of polarities by modification of the repeating units. Commonly available liquid polymers such as poly(ethyleneglycol) (PEG), poly(propyleneglycol), and poly(dimethylsiloxane) are nonflammable, biodegradable, and non-cytotoxic to most forms of terrestrial and marine life.[38]

As a number of reviews devoted to this new class of solvents would attest, remarkable progress has been made in this field of research within the last few years. Reports of NO_2-infused poly(ethyleneglycol) for oxidation of hydrazobenzene, partial reductions of alkynes to cis-olefins by Lindlar Catalyst (a heterogeneous catalyst that consists of palladium deposited on calcium carbonate with lead acetate as an additive) in poly(ethyleneglycol), poly-oxometalate catalyzed aerobic oxidations of sulfides and alcohols, generation of uniform silver coatings from silver oxide in poly(ethyleneglycol), oxidation of alcohols to aldehydes and ketones with N-bromosuccinimide in poly(ethyleneglycol), and Baker's Yeast-catalyzed reductions in poly(dimethylsiloxane)

have been published within the last couple of decades (Scheme 1.1).[39] While nanocatalysis in these solvents has not been studied as extensively as some other solvent classes, some examples, such as reports of Fe nanoparticles dispersed in PEG catalyzing Fischer–Tropsch synthesis under mild conditions, and Pd NP-catalyzed C – C cross couplings in PEG do exist in the literature.[40,41] It is definite that they merit a detailed investigation as “green” solvents for nanocatalysis.

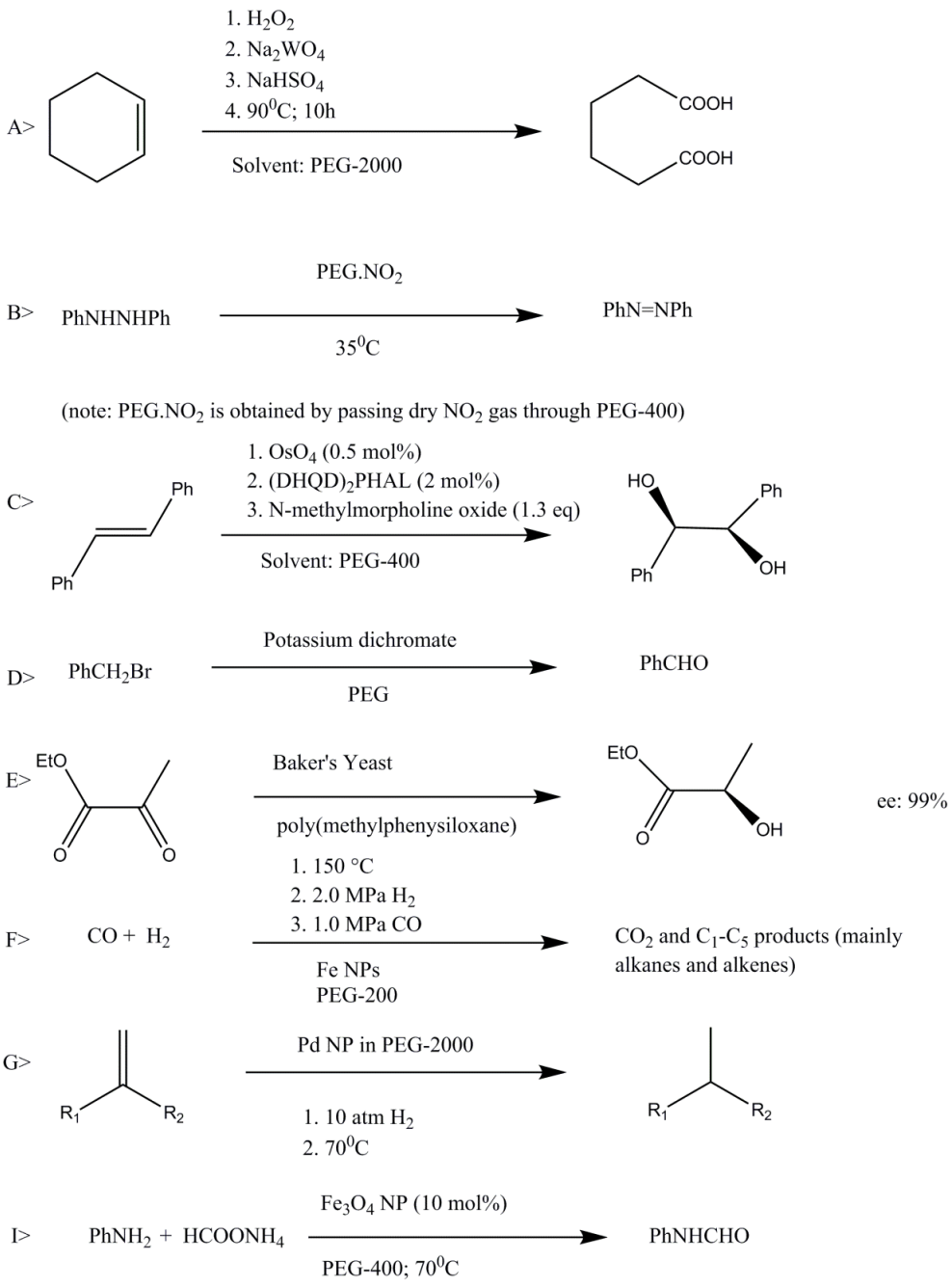

Scheme 1.1 Selected examples of catalysis in liquid polymer media. Adapted from reference [39] and references therein.

1.1.4 Ionic Liquids

ILs are (near)-room-temperature liquids that are dissociated into oppositely charged ion. They have been known to scientists since the early years of the twentieth century, when Paul Walden synthesized ethylammonium nitrate (melting point: 12°C).[42] However, they became popular research topics in their own right only in the 1990s. This is probably because the earliest ILs (such as alkylpyridinium chloroaluminates developed by the United States Air Force Academy) were highly sensitive to air and moisture, a quality that is not particularly desirable in solvents.[43] It is only after air-stable, room-temperature ILs consisting of 1,3-dialkylimidazolium cations and BF_4^- or PF_6^- anions were synthesized independently by several research groups in the 1990s that they were considered to be a more promising class of alternative solvents.[44,45] ILs have a lack of a measurable vapor pressure, non-flammability, high thermal stability, wide range of solubilities and miscibilities, large electrochemical windows, structural tunability, and potential recyclability, which make them attractive alternatives to volatile organic solvents.[46] Recently, an IL has been isolated from the venom of ants, thereby confirming the natural occurrence of ILs and IL-like systems.[47] ILs have been used extensively as non-aqueous polar solvents for transition metal complexes, metal nanocatalysts, and bio-catalysts for the last two decades.[48-50] It has been estimated that approximately 10^{18} different cation-anion combinations in ILs are possible, so it is possible that we have only touched the tip of the iceberg when it comes to design and synthesis of new ILs.[51,52] Figure 1.2 depicts some common cations and anions used in the synthesis of ILs; the

following section discusses two important IL families: the 1,3-dialkylimidazolium ILs, and the tetraalkylphosphonium ILs.

1.1.4.1 Imidazolium ILs

Second generation ILs – a term generally applied to air-stable, non-haloaluminate ILs that can be used outside a glove-box – were synthesized by Wilkes and co-workers in 1992.[43] These contained 1,3-dialkylimidazolium cations with a range of anions, although BF_4^- and PF_6^- were the ones that received the maximum attention. Later, these systems were shown to undergo hydrolysis, thereby generating highly toxic and corrosive HF, fluoride anions; and imidazolium systems with other anions such as acetates, bis-(triflamides), and tosylates were investigated as more practical alternatives.[53] Currently, imidazolium ILs are the best-investigated class of ILs.

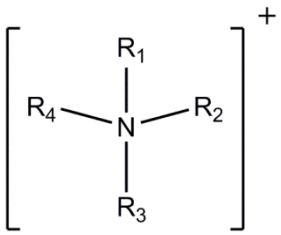

tetraalkylammonium

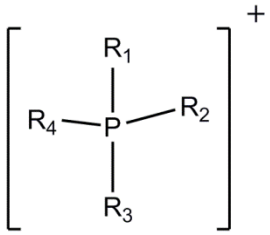

tetraalkylphosphonium

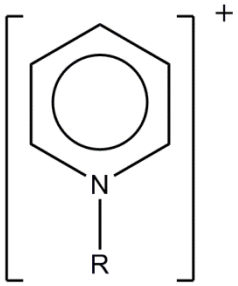

alkylpyridinium

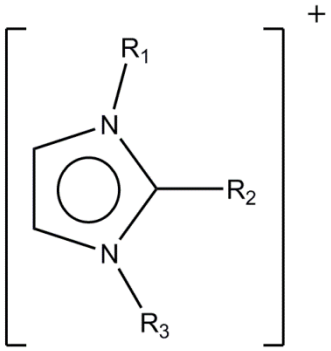

di- or trialkylimidazolium

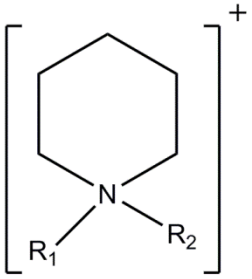

dialkylpiperidinium

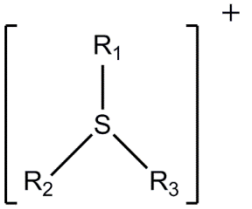

trialkylsulfonium

$^{-}$OAc - acetate
$^{-}BF_4$ - tetrafluoroborate
$^{-}PF_6$ - hexafluorophosphate
$^{-}$OTf - triflate
$^{-}$OTs - tosylate
$^{-}NTf_2$ - N-(bis-triflimide)
$^{-}$X - halides (Cl, Br, I)
$^{-}N(CN)_2$ - dicyanamide

Figure 1.2 Some common cations and anions in ILs.

Several novel applications of imidazolium ILs have been reported within the last few decades. In a seminal study in 2002, Rogers and colleagues showed that cellulose can be dissolved without activation or pretreatment in, and regenerated from, 1-butyl-3-methylimidazolium chloride, and other hydrophilic ILs.[54] Several ILs, based mainly on the 1-alkyl-3-methylimidazolium cation, in combination with anions such as thiocyanate, bromide and chloride, formate, acetate or dialkylphosphates, were found to possess cellulose-dissolution ability, and the mechanism seemed to involve hydrogen-bonding between the carbohydrate hydroxyl protons and the IL chloride ions in a (1:1) stoichiometry.[55] Subsequent studies proved that imidazolium ILs are capable of dissolving other biopolymers such as lignocellulose and chitin.[56,57] Imidazolium ILs also find application in carbon dioxide sequestration, especially in the context of 'designer' ILs, where the covalent tethering of a functional group to the anion or the cation of the IL makes it capable of chemically binding to CO_2.[58] In 2008, for instance, Yokozeki *et al.* found that ILs that show strong chemical absorption with CO_2 contained substituted carboxylate anions.[59] ILs with appended amine groups were also studied extensively for this purpose: Bates and coworkers, for instance, synthesized an amine-functionalized imidazolium hexafluorophosphate IL, and studied its reaction with CO_2. Each CO_2 molecule was seen to react with two IL molecules via the amine termini, forming an ammonium carbamate double salt.[60] Functionalized imidazolium ILs are also used for stabilization of catalytically active metal NPs.[61,62] The structure-property relationships and secondary structures of imidazolium ILs have been subjected to numerous studies,

and their biodegradability and environmental toxicities have also been evaluated.[63,64] It would be impossible to summarize physical and chemical properties of these ILs in this limited space; the interested reader will find numerous reviews, some of them cited in this section, dedicated to this class of ILs. For the purposes of this chapter, it might be concluded that imidazolium ILs are a class of ILs that have been subjected to detailed exploration, often to the detriment of other, less-studied IL families.

1.1.4.2 Tetraalkylphosphonium ILs

While early reports of tetraalkylphosphonium ILs were published by Parshall and Knifton within years of the first reports of imidazolium ILs, these systems, unlike their imidazolium counterparts, never captured the interest of the scientific community.[65,66] Part of this could be attributed to the poor availability of pure trialkylphosphines, which are essential for their synthesis. However, for the last decade or so, a variety of tetraalkylphosphonium ILs have been commercially available, from companies such as Cytec Ltd.[67] These ILs, with four 'customizable' alkyl chains attached to a central phosphorus atom, and an anion that is readily exchanged owing to the base-stability of the phosphonium cations, are finally being given the attention that they deserve from the scientific community.[68] Tetraalkylphosphonium ILs show high degrees of thermal stability, resistance to degradation pathways such as carbene formation via base-induced deprotonation, and are often immiscible in water.[69] Therefore, they can be used for applications such as the biphasic conversion of aromatic chlorides to fluorides

using potassium fluoride at temperatures over 130°C, as halogenating agents for olefins, as solvents for the notoriously reactive Grignard reagents, in separations, extractions, exfoliations, in supercapacitors, and as catalysts.[68]

The tetraalkylphosphonium ILs are usually synthesized via the quaternization of a trialkylphosphine with an alkyl or an aryl halide.[67] There are a number of reasons why the tetraalkylphosphonium cation in unique amongst the several cation families typically found in ILs. The numerous possible permutations that can be generated by selecting the various alkyl and aryl side chains increase the tunability of their resulting physico-chemical properties. The tetraalkylphosphonium ILs lack the weakly acidic ring protons of the more common imidazolium cations – a limitation when strongly basic anions need to be incorporated within the IL system, or during anion exchange protocols. Thermal stabilities of these ILs are also remarkably high, with a typical decomposition temperature of ≤250°C as determined from thermogravimetric studies.[70] The bulk of the alkyl chains on the cation also play a decisive role in determining the properties of these systems: large alkyl chains around the tetraalkylphosphonium cation sterically hinder the electrostatic interactions between the anions and the cation – which is generally localized on the phosphorus – allowing for greater impact of the properties of the anion itself, as compared to salts with more strongly interacting smaller cations. While the high viscosity of these systems can be a nuisance especially when they are used as solvents in a reaction, the viscosity can be reduced by an increase in temperature and/or addition of a diluent.[71]

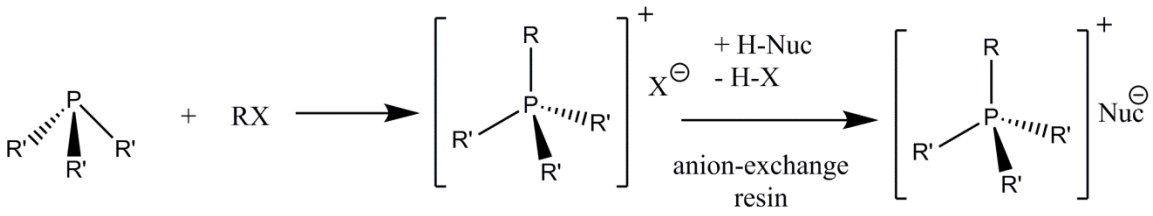

Scheme 1.2 Synthesis of tetraalkylphosphonium ILs with functional anions.

The decomposition pathways of tetraalkylphosphonium ILs have been studied by several groups, and found to proceed through two major pathways, as shown in Scheme 1.4.[72] Generally, elevated temperatures, the presence of oxygen, and high concentrations of small bases (such as the hydroxyl anion) are believed to favor their decomposition, but contradictory studies on the subject are found in the literature.[73,74] Personally, we have observed the formation of trialkylphosphine oxide upon heating the anion-exchanged species tetraalkylphosphonium hydroxide in air at temperatures exceeding 30^0C via ^{31}P NMR studies.

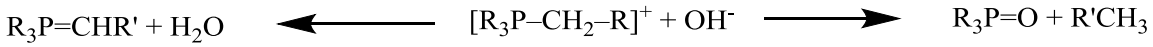

Scheme 1.3 Decomposition pathways for tetraalkylphosphonium ILs.

Experimental details about the preparation and purification of these ILs relevant to this dissertation can be found in Chapter 1; however, for an exhaustive review of this class of ILs, along with detailed preparative strategies, insights into their physico-

chemical properties, and electrochemical applications, see accounts by Clyburne et al., MacFarlane et al., and Zhou et al. [67,68,75]

1.1.4.3 Other ILs

There are numerous other families of ILs that have been studied, but of late, the focus has shifted to IL families based on renewable feedstocks that can be synthesized easily, and without consuming large amount of organic solvents, such as amino-acid based ILs, choline chloride-based ILs, and even ILs based on pharmaceuticals such as ampicillin (Figure 1.3).[76-78] These ILs often have unique advantages associated with them: sugar-derived ILs, for instance, can be chiral in nature, and thus find application as solvents for asymmetric induction in reactions such as the aza-Diels-Alder cycloaddition.[79] Similarly, cholinium alkanoates, which are extraordinarily good solvents for some very recalcitrant plant biocomposites, have been shown to be environmentally benign and biodegradable.[80] It is entirely possible that a new generation of chemists active in this field of research will prioritize the design and synthesis of ILs from cheap, easily available, and environmentally benign starting materials, which would go a long way in putting these solvents at the forefront of the list of alternative solvents for scientific and commercial applications.

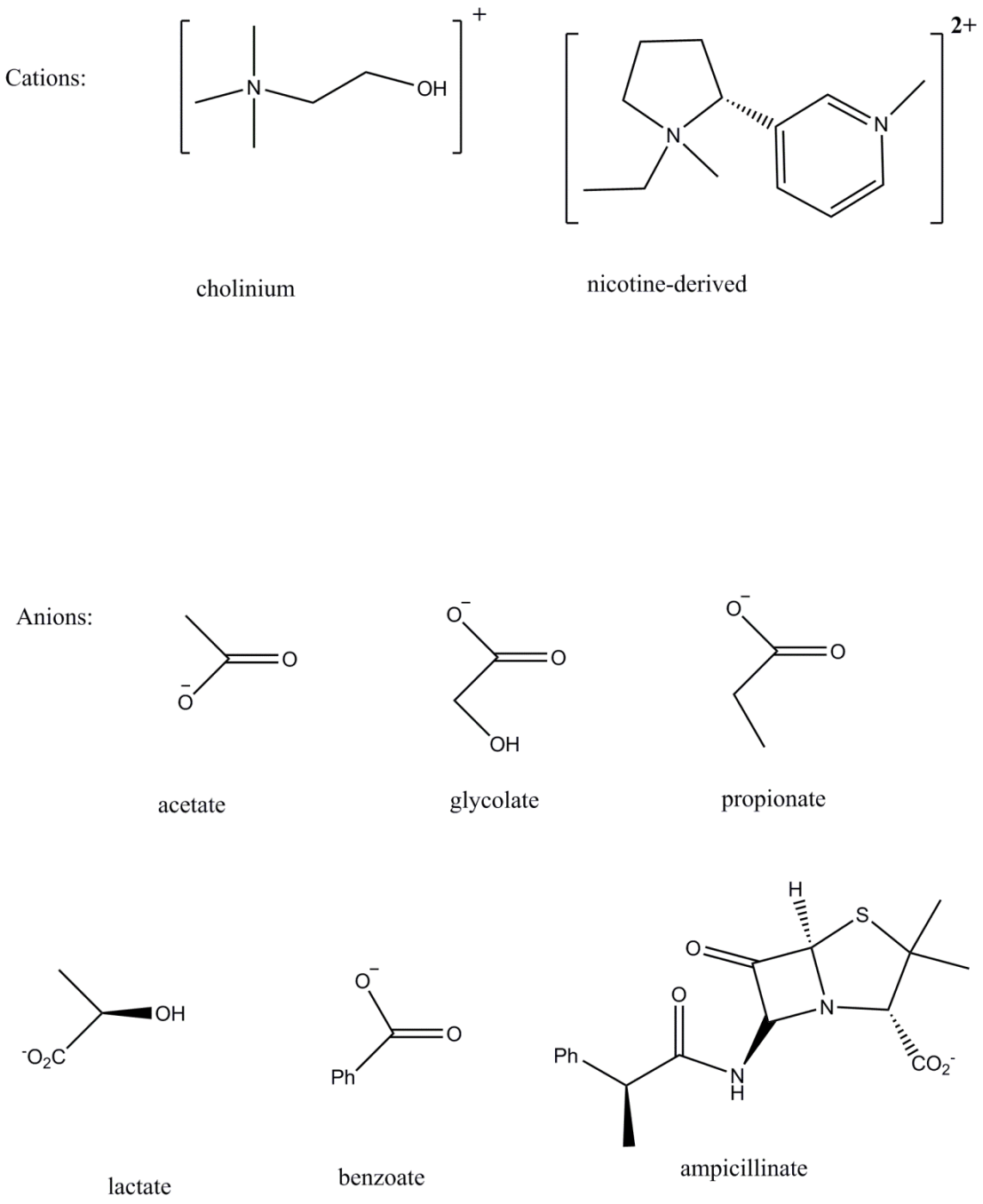

Figure 1.3 Novel cations and anions for sustainable and/or biocompatible IL synthesis.

1.1.5 Deep Eutectic Solvents

Deep eutectic solvents (DESs), previously classified as a subtype of ILs, have attracted considerable interest from the scientific community in the last five years or so, and are now studied as a separate class of green solvents.[81] DESs are eutectic mixtures of Lewis or Brønsted acids and bases. Typically, they contain a variety of anionic and/or cationic species, unlike ILs, which usually consist of a single cation-anion combination.[82] DESs are usually obtained by the complexation of a quaternary ammonium salt with a metal salt or hydrogen bond donor. The resultant charge delocalization occurring through hydrogen bonding reduces the melting point of the mixture relative to the melting points of the individual components. The chemical properties of DESs suggest application areas which are significantly different from those of ILs. Some typical DESs, separated into classes as per an existing nomenclature, have been shown in Table 1.1.[83] Out of these, Class III DESs, comprised of (mostly) non-toxic constituents (often bio-sourced from food grade materials, such as xylitol, proline, fructose, glucose, sucrose, lactic acid, etc.), are truly 'green', in that they are non-cytotoxic.[84] DESs also have low vapor pressures, and can be separated from water, in which they are readily soluble, via evaporation.[85]

Type	General formula	Species
Type I	$[Cat][X].MCl_y$	M=Zn, Sn, Fe, Al, Ga, In
Type II	$[Cat][X].MCl_y.zH_2O$	M=Co, Cr, Cu, Fe, Ni
Type III	[Cat][X].RZ	R=alkyl or aryl groups Z=-$CONH_2$, -COOH, -OH
Type IV	MCl_x.RZ	M=Al, Zn Z=-$CONH_2$, -OH

Table 1.1 Classes of deep eutectic solvents. [Cat] is an organic or inorganic complex cation, such as ammonium, phosphonium, or sulfonium; [X] is a Lewis-basic anion.

Some areas in which DESs find application, albeit not on a commercial scale, include lubrication of steel/steel contacts, electrolysis solvents, in analytical devices for the recognition of analytes such as lithium and sodium ions, synthesis of drug solubilization vehicles, as electrolytes for dye-sensitized solar cells, synthesis of nano- and micro-structures, solvents in biotransformations, and in metal extraction.[81] Examples of catalysis carried out in DESs are comparatively rare, but some notable examples have been depicted in Scheme 1.2. Of these, enzymatic processes are the most common. However, examples of nanocatalytic reactions in DESs do exist: DES-stabilized Au NPs, for instance, can catalyze hydride-induced reduction of *p*-nitrophenol, and Pd-catalyzed C – C cross-couplings involving Pd NPs have been reported in a variety of DESs.[86,87] Wong and co-workers[88] generated 10 nm-thick single-crystalline

mesoporous ZnO nanosheets by initial dissolution of amorphous ZnO in a mixture of choline chloride and urea in a 1:2 molar ratio (known as reline) at 70°C, followed by slow injection into a water bath and calcination of the precipitates, produced mesoporous ZnO. The calcined mesoporous ZnO nanosheets showed high specific surface areas, and proved nearly as effective as commercial P-25 TiO_2 in the photocatalytic degradation of methylene blue.[88] Chirea *et al.*[89] prepared polycrystalline gold nanowire networks via rapid borohydride reduction of $HAuCl_4$ in reline and ethaline (1:2 ratio of choline chloride and ethylene glycol) at 40°C. The nanowire networks produced in reline were shorter and wider, and displayed a higher percentage of [311] facets. This was attributed to a stronger coordination of $[AuCl_4]^-$ in reline. The Au nanowire networks in reline demonstrated improved catalytic activity for *p*-nitrophenol reduction over the ones in ethaline.[89] Finally, Renjith *et al.*[90] reported a single step method for the preparation of Au-core-Pd-shell bimetallic nanoparticles on a graphite rod in a choline chloride-ethylene glycol DES. The core-shell NPs exhibited superior catalytic performance over their corresponding monometallic counterparts, viz., AuNPs and PdNPs, prepared under identical conditions, in the electrochemical oxidation of methanol.[90]

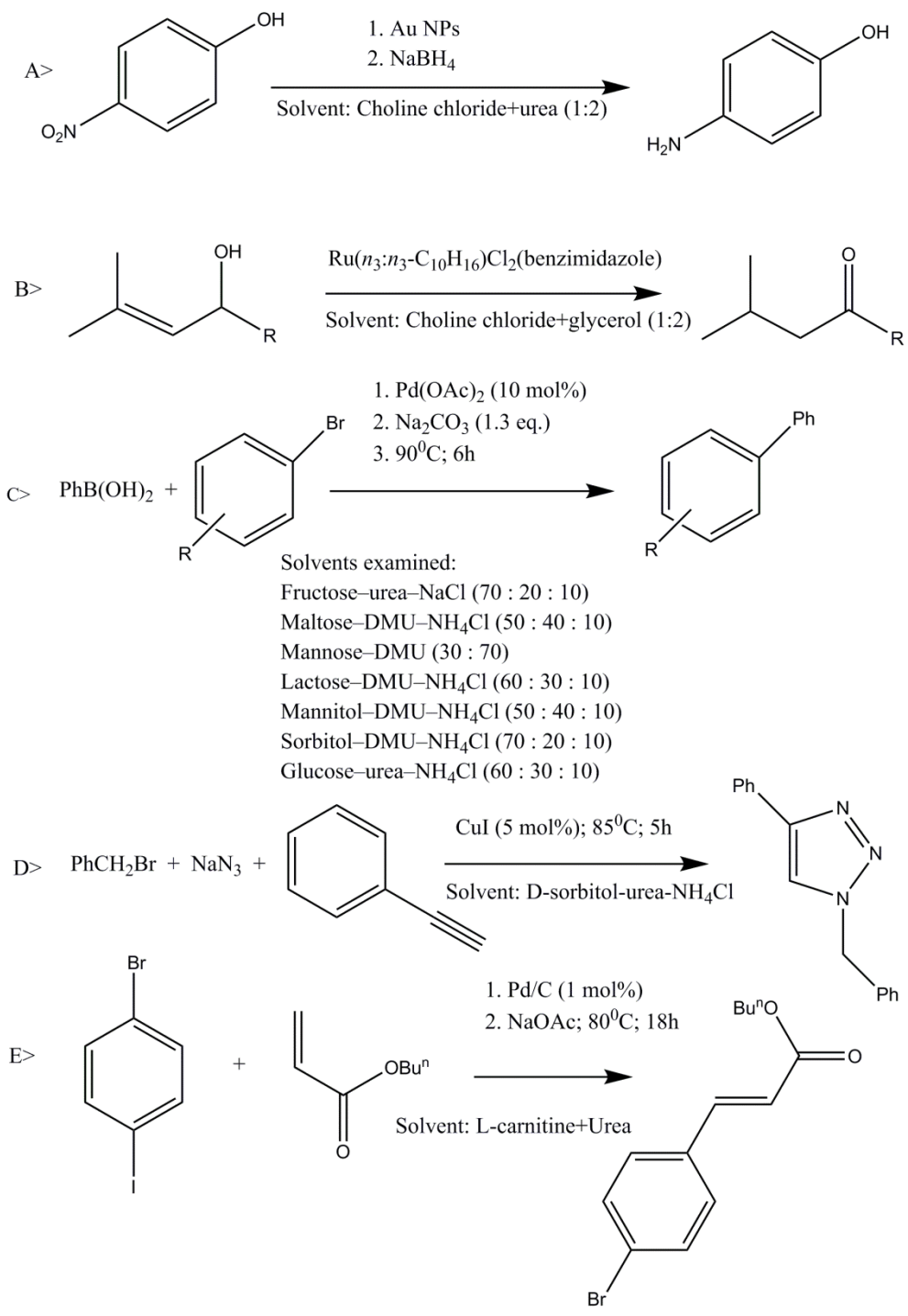

Scheme 1.4 Selected examples of catalysis in DESs.

1.1.6 Fluorous Solvents

Perfluorocarbons [Figure 1.4(a)] emerged as potential solvents for catalysis after a seminal study by Horvath *et al.,* who also coined the phrase "Fluorous Biphasic Catalysis" (FBC).[91,92] These are mostly hydrocarbon-analogues, where the hydrogen atoms have been replaced by fluorine atoms, and they have unique solubility properties that make them good candidates for various applications.[93] They are chemically inert, non-flammable, and can show very low toxicity depending upon their exact chemical structures. They are usually immiscible with volatile organic solvents at room temperatures, and it was this observation that led to the development of the FBC protocol. In FBC, a fluorophilic catalyst in a fluorous solvent and reactant(s) in an organic solvent are heated until they form a single phase. After the completion of the homogeneous catalytic process, cooling leads to a reversal to biphasic conditions, with the product(s) remaining soluble in the organic solvent, while the catalyst is retained in the fluorous phase, and can be separated easily and recycled [Figure 1.4(b)].[92] It is to be noted that a fluorous side-group often needs to be tagged onto the catalyst to render it fluorophilic.[94] Triphasic fluorous process, involving an organic, an aqueous, and a fluorous phase, are also known.[95]

While fluorous-tagged versions of several important organometallic catalysts, such as Wilkinson's catalyst, Grubbs' Ru-carbene metathesis catalyst, the hydroformylation catalyst $HRhCO[P[(CH_2)_2(CF_2)_5CF_3]_3]_3$, and many others, have been studied for FBC, there are fewer examples of catalysis with NPs in fluorous solvents.[96-98]

Mostly, these involve fluorous-tagged NP stabilizers such as dendrimers, used by Crooks and co-workers for the synthesis of Pd NPs for fluorous-phase hydrogenations.[99] Similarly, 1,5-bis(4,4'-bis(perfluorooctyl)phenyl)-1,4-pentadien-3-one-stabilized Pd NPs in perfluorinated solvents proved to be efficient recoverable catalysts for Suzuki cross-couplings and Heck reactions under fluorous biphasic conditions.[100] Fluorinated thiols could also be used for the stabilization of catalytically active Au and Ag NPs.[101] There are examples of catalysis by metal NPs on fluorous supports (rather than solvents), but they are beyond the scope of this brief introduction.

(a)

C_8F_{18}	C_6F_{14}	$CF_3C(=O)CH_2C(=O)C_2F_5$
$C_{10}F_{18}$	$C_{12}F_{27}N$	$C_6F_{11}CF_3$
$CF_3C_6H_5$	$CF_3[(OCF(CF_3)CF_2)_n(OCF_2)_m]OCF_3$	$CF_3[(OCF(CF_3)CF_2)_n(OCF_2)_m]OCF_3$

(b)

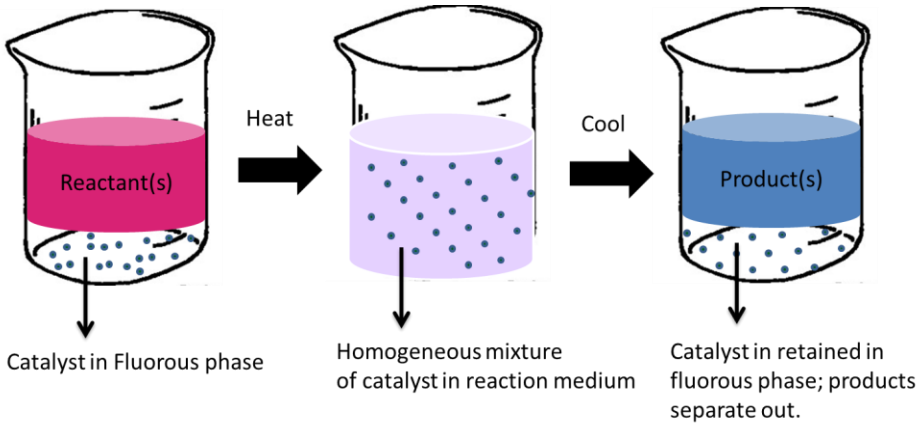

Figure 1.4 (a) Some fluorous solvents; **(b)** a schematic representation of FBC.

1.1.7 Supercritical Fluids

Supercritical fluids (SCFs) were some of the first 'alternative' solvents used in catalytic processes, such as polymerization of ethylene, by Ipatiev and Rutala in 1913.[102] Since the 1990s, there has been extensive research on both homogeneous and heterogeneous catalysis in SCFs, along with the publication of several excellent reviews devoted to the subject.[103-105] SCFs are defined as liquids (either a single liquid or a mixture of liquids) that have been heated to a temperature above their critical temperatures under pressures exceeding their critical pressures. Under these conditions, the substance exists as a single phase. SCFs are known to possess the favorable properties of both liquids and gases. They have numerous other advantages over liquid solvents: higher diffusivity of solutes, enhanced mass transfer owing to reduced viscosity, and the capability to dissolve solutes that are insoluble in their liquid analogues. The two SCFs used most frequently in catalysis ($scCO_2$ and scH_2O) are also non-toxic, non-carcinogenic, non-flammable, and easy to dispose of.[106]

There are numerous examples of catalysis by dispersed NPs in SCFs. In a seminal study by Ohde and co-workers, stable Pd NPs were synthesized by hydrogen reduction of Pd^{2+} ions dissolved in the aqueous core of a water-in-CO_2 microemulsion.[107,108] The Pd NPs were uniformly dispersed in the supercritical fluid phase, and were effective catalysts for hydrogenation of olefins. Leitner *et al.* applied the combination of poly(ethylene glycol) as a catalyst phase and $scCO_2$ as a mobile phase for continuous-flow aerobic oxidation of primary and secondary alcohols by catalytically active Pd NPs;

other studies replaced Pd with Ru or Au, but this did not improve conversions.[109] Bimetallic Au-core-Pd-shell NPs (Au:Pd= 1:3.5) in $scCO_2$ did, however, show improved catalytic activities (compared to monometallic NPs) for base-free benzyl alcohol oxidations.[110] Supported Pt NPs were also seen to hydrogenate substituted nitrobenzenes to anilines in $scCO_2$.[111] Other classes of reactions where stable metal NPs in $scCO_2$ have been used as catalysts include C – C cross-coupling reactions and hydrodechlorinations.[112,113]

1.1.8 Other Solvent Systems

Solventless processes, which represent a rapidly burgeoning field of research in homogeneous catalysis, have little significance in the context of nanocatalysis, since heterogeneous catalysis is already the norm for industrial processes, and is a separate sub-discipline in its own right. Other classes of solvents, such as solvents based on renewable feedstock[114] (Figure 1.5), gas expanded liquids,[115] and solvents with switchable polarities,[116] are all being explored by the scientific community as possible media for catalysis with NPs, but compared to the solvent classes discussed previously, these represent less mature fields of research within the alternative solvents arena.

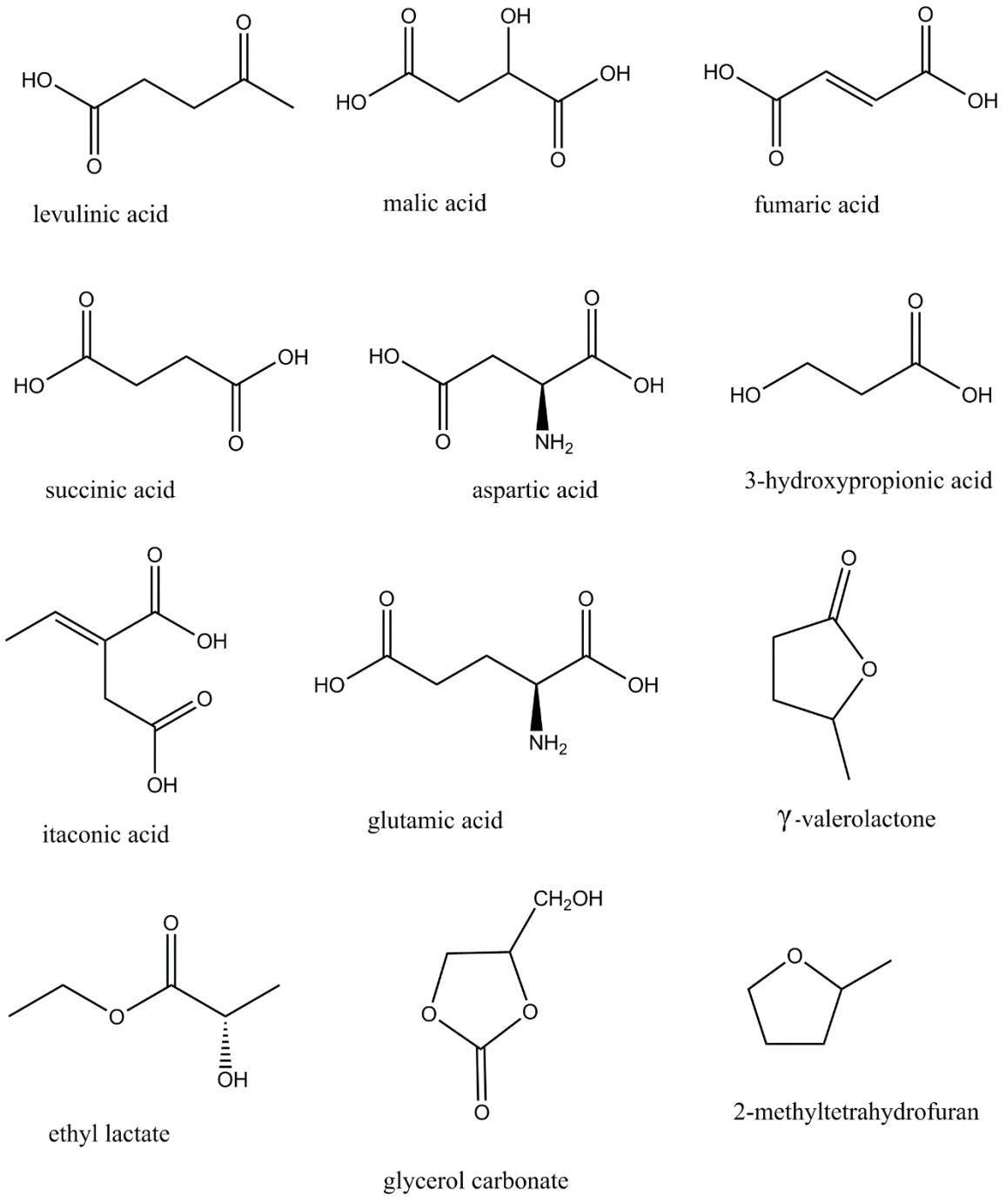

Figure 1.5 Examples of solvents derived from renewable resources.

1.2 Nanoparticle Catalysts

Nanoparticles (NPs) – typically defined as particles between 2 nm to 100 nm (particles of *ca.* 1 nm and less, containing a limited number of atoms, and with sizes comparable to the Fermi wavelengths of metals, are now classified as *clusters*, a kind of a bridge between isolated metal atoms and nanoparticles) in size – are ubiquitous in catalysis, mostly as heterogeneous catalysts on solid supports.[117,118] Their small sizes and large surface-to-volume ratios, exposed active sites, and properties intermediate between those of bulk materials and individual atoms/molecules provide NPs with unique catalytic properties.[119] Materials such as Au and Pt, virtually inert in bulk, can facilitate rapid chemical transformations with high turnover numbers (TONs), when their sizes are brought down to the nanometer regime.[120,121] In fact, the application of NPs in catalysis is by no means a novel strategy: even in the 19th century, Ag NPs were used in photography for negative development, and Pt NPs were used to bring about the decomposition of hydrogen peroxide.[122] Other early examples of nanocatalysis include Nord's report (in 1943!) of nitrobenzene reduction,[123] Parravano's study of hydrogen-atom transfer between benzene and cyclohexane and oxygen-atom transfer between CO and CO_2 using AuNPs,[124] and reports of catalytic isomerization and hydrogenation with oxide-supported metallic gold catalysts. The real breakthrough came with Haruta's seminal studies on oxide-supported AuNP-catalyzed CO oxidation by O_2 at low temperatures.[125] Since then, the study of catalytic activities of NPs has virtually become ubiquitous, finding applications in systems ranging from chemical

reactors to bio-matrices.[126,127] Moreover, unlike some of the earlier studies, which essentially treated the entire concept of nanocatalysis as a black box, the scientific community today places a greater emphasis on 'goal-oriented' design and synthesis of nanocatalysts. With advances in instrumentation and characterization techniques, however, we are in a better position today to identify mechanisms of chemical reactions at the nanoscale. This, in turn, should enable us to design nanocatalysts on the basis of their putative applications, prior to their actual synthesis. Given these developments, it is important that some attempt is made to systematize this enormous superset of materials on the basis of existing classifications in catalysis.

1.2.1 Classification of nanoparticle catalysts

A precise and unambiguous system of classification for metal NPs on the basis of their functional aspects does not exist. Scientists such as Crabtree and Finke have pointed out that premature categorization of catalytic processes as ‘homogeneous’ or ‘heterogeneous’, without a number of control reactions, can be, at best, misleading, and at worst, completely erroneous, hindering the identification of the actual catalytic species.[128-131] A heterogeneous catalyst in a solution-phase reaction may very well serve as a catalytic reservoir or ‘resting state’, from which molecular catalytic species are liberated for catalysis, and re-deposited after the completion of a catalytic cycle.[132] Conversely, many exotic metal-ligand complexes actually function as mere NP precursors under harsh reaction conditions (such as elevated temperatures, extremes of

pH, etc.), with the metallic NPs performing the actual catalysis.[133] Even observations such as kinetic reproducibility, the presence of an induction time in the kinetic profile of the reaction, formation of NPs as evidenced by *ex-situ* electron microscopy, or physical separation of the catalyst are no longer considered to be decisive tests for the homogeneity or heterogeneity of a catalytic process.[132] In fact, a battery of other tests, including selective poisoning, ^{1}H NMR spectroscopy (for hydrogenations), and *in situ* X-ray absorption spectroscopy (XAS), must now be conducted, and the results from these examined for consistency in order to characterize the active species for a catalytic system.[131,134] In order to avoid these pitfalls, and for convenient *ab-initio* characterization, catalytic NPs are often divided into two broad categories: 'polysite' (containing a variety of active catalytic sites, as is the norm in heterogeneous catalysts on oxides and other solid supports) and 'oligosite' (catalysts with a limited number of active sites, with each active site 'motif' repeated over and over; characteristic of stable, monodisperse NP suspensions).[135] A typical metal NP, with some characteristic catalytic sites, has been shown in Figure 1.6.

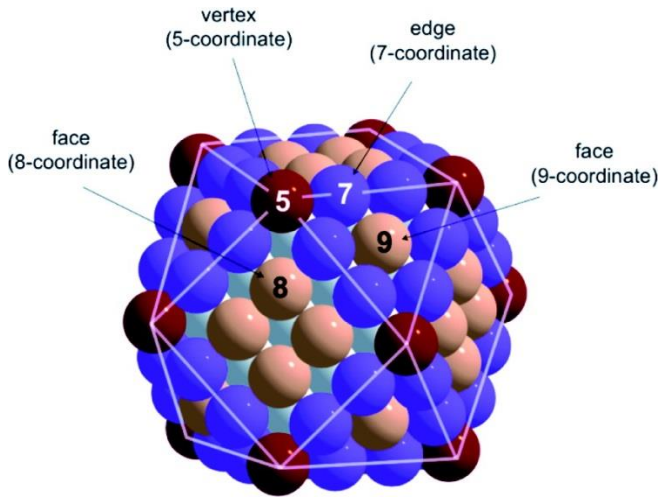

Figure 1.6 A generic representation of a metal NP, showing metal atoms with varied coordinations. Reprinted with permission from reference [135]. Copyright (2011) John Wiley and Sons.

'Quasi-homogeneous catalysis', a classification that has largely been accepted by the catalysis community, is used to describe catalytic processes that reside at the interface between the traditional protocols of homogeneous and heterogeneous catalysis.[122] This category of catalysts consists almost entirely of macroscopically homogeneous but microscopically heterogeneous dispersions of nanoparticles in fluids.[136-138] They combine both the advantages and the challenges of homogeneous and heterogeneous catalysts, as shown in Figure 1.7. The catalytic studies reported in this dissertation can all be classified under the category of 'quasi-homogeneous nanocatalysis' – i.e., they take place on metal NP surfaces in a solvated phase. These systems combine the advantages of solid-supported NP catalysts such as recyclability

with the benefits of a fluid-phase reaction medium, such as uninhibited motion of catalytic particles, and greater number of active sites per NP exposed to the reactants.

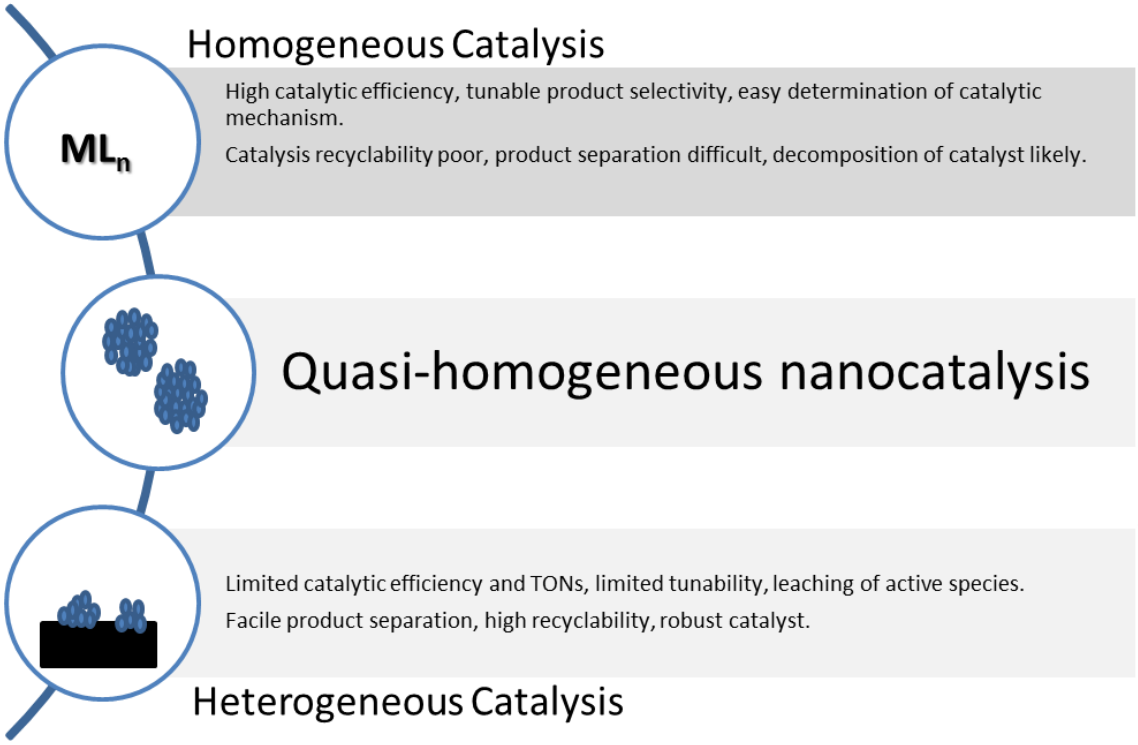

Figure 1.7 Homogeneous, Heterogeneous, and quasi-homogeneous catalysis: a comparison.

1.2.2 Stabilization of NPs in Solution

Nucleation and growth are the two processes that enable the formation of NPs in solution.[139] However, NP growth needs to be stemmed at a certain point in their lifetime. Otherwise, uncontrolled growth would lead to the formation of macroscopic ensembles which, at best, would show reduced catalytic activities owing to loss of surface area, and at worst, would precipitate out of the solution, forming micrometer

sized catalytically inactive agglomerates. The reason behind this behavior is that the NP phase is only kinetically stable; the thermodynamic energy minimum is, of course, the bulk phase.[140] It is essential, therefore, that NPs in solution must be stable to coalescence and aggregation after their formation, as well as under conditions of usage. There are very few strategies available to regenerate small, well-dispersed NPs from their aggregated counterparts, so the easiest way to ensure that the NPs remain active is to prevent their growth. In most of the solvents discussed in the previous section, this is achieved by the addition of an external 'stabilizer': an added protecting agent whose presence ensures that the NPs would remain in solution, with little to no growth or ripening.[141] The stabilizers achieve this by electrostatic ("DLVO-type", named after named after Derjaguin and Landau, Verwey and Overbeek, who provided a quantitative description of the aggregation of aqueous dispersions on the basis of forces between charged surfaces interacting through a liquid medium) stabilization, steric stabilization, or, most often, by a combination of both (Figure 1.8).[142] It is to be noted that the selection of stabilizers is a non-trivial step while designing catalytically active NPs in solution: often, an inverse correlation between high stability and excellent catalytic activity exists, owing to the fact that the stabilizers often ligate to the same coordinatively-unsaturated sites that are essential for catalytic activity.[143,144] We can conclude, therefore, that, *optimal* rather than *maximum* stability of NPs in solution facilitates their use as catalysts.

Unlike water and supercritical fluids, where the addition of an external stabilizer is *de rigueur* for NP stabilization, the situation is more complicated in ILs. There are contradictory reports about the stability of NPs in ILs, both under 'resting' conditions, as well as during reactions.[144-146] The following sections explore the stability of NPs in ILs, both in the presence as well in the absence of a secondary stabilizer. However, studies where ILs were used solely for NP stabilization, and the actual catalytic processes were carried out in a different solvent, or under solventless conditions, have been omitted for the sake of brevity.

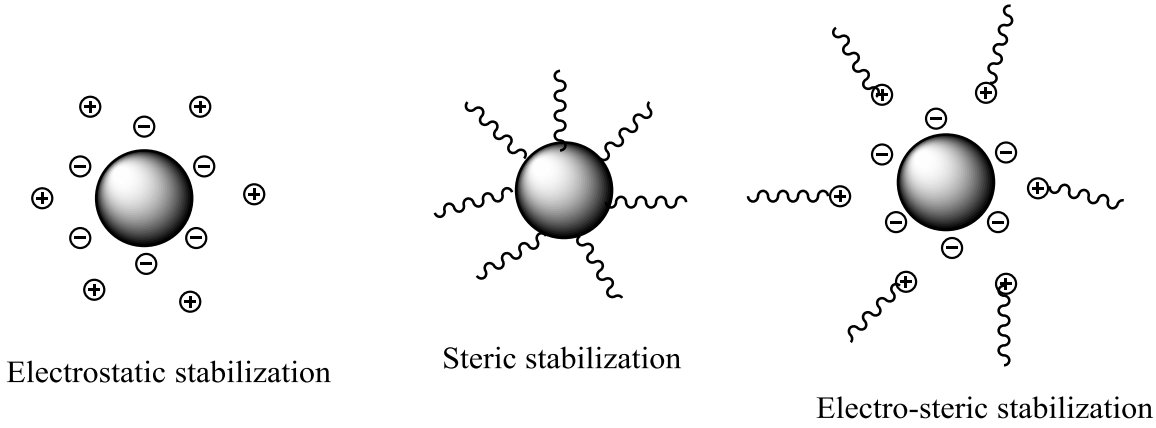

Figure 1.8 Modes of stabilization of solvent-diffused nanoparticles.

1.2.2.1 Extrinsic Stabilization

There are several examples of secondary stabilizers used in IL media for NP stabilization, the most common being polymers, dendrimers, and ligand molecules. Polymers, such poly(vinylpyrrolidone) (PVP), poly(ethylene glycol) (PEG), etc., stabilize

NPs not only because of the steric bulk of their framework, but also via weak ligation to the NP surface by heteroatoms present in their repeating units. It was shown by Wang *et al.* that for PVP-stabilized Ag NPs in water, formed via the reduction of Ag(I) to Ag(0) by glucose, the nitrogen in PVP coordinated with silver for particles of diameter ≤ 50 nm, while for larger particles, both N and O coordinated with the silver.[147] PVP was also seen to stabilize Pt, Pd and Rh NPs in 1-butyl-3-methylimidazolium hexafluorophosphate (BMIM-PF_6), which serve as recyclable catalysts for olefin and benzene hydrogenations at 40^0C.[148] Our group has evaluated PVP-stabilized Pd and AuPd bimetallic NPs in BMIM-PF_6 as recyclable hydrogenation catalysts at ambient hydrogen pressures.[149,150] However, the low solubility of PVP in imidazolium ILs is a challenge, which was overcome by Dyson and co-workers, who synthesized a series of hydroxyl-functionalized ILs, in which PVP proved to be highly soluble.[151] The most 'PVP-philic' IL showed a PVP saturation concentration of >5% by weight, which was a huge improvement over unfunctionalized 1-ethyl-3-methylimidazolium tetrafluoroborate (EMIM-BF_4), which could only dissolve <0.5% PVP. PVP-protected 2.7 nm Rh NPs in these ILs were employed as catalysts for arene hydrogenations. An alternative approach, championed by Kou, Yan, and others, depended on the synthesis of IL-soluble polymers via the incorporation of polymeric chains in IL cations and/or anions.[152,153] These modified polymers were highly soluble in ILs, and could stabilize NPs for catalysis. Kou and co-workers, for instance, fabricated an ionic copolymer containing PVP monomers and vinylimidazolium units (Figure 1.9). This polymer preserved the coordination capacity of

PVP, and proved to be miscible with imidazolium ILs; therefore, it could be used as an IL-selective NP stabilizer. Rh NPs synthesized in BMIM-BF_4 in the presence of this IL-like polymer, poly[(N-vinyl-2-pyrrolidone)-co-(1-vinyl-3-butylimidazolium chloride)], (Figure 1.9) could catalyze arene hydrogenations with a total turnover (TTO) of 20,000 (in five total cycles of 4,000 TTOs each) and a turnover frequency of 250 h^{-1}.[154] Selective hydrogenation of aromatic chloronitro compounds to aromatic chloroamines was also carried out effectively using Pt NPs in BMIM-PF_6 in the presence of these IL-like-polymers.[155] This strategy is now rountinely used for designing IL-soluble polymers such as poly[1-methyl-3-(4-vinylbenzyl)imidazolium chloride and poly[3-(4-vinylbenzyl)-1-methylimidazolium bis(trifluoromethylsulfonyl)imide.

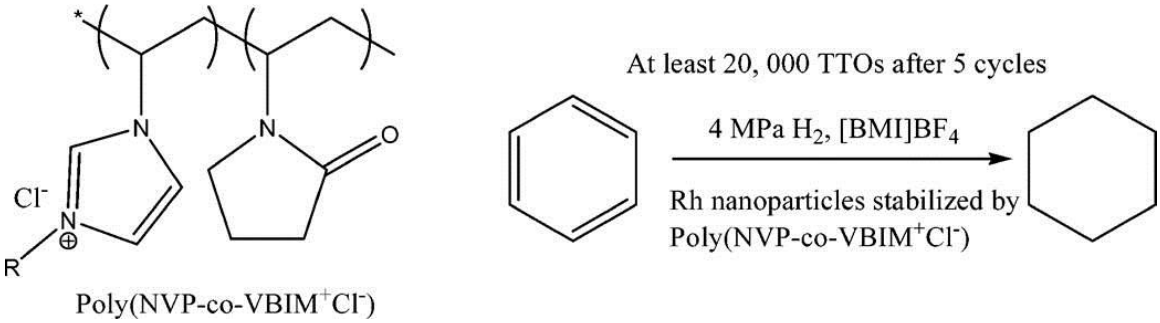

Figure 1.9 Ionic copolymers for stabilization of catalytically active Rh NPs in BMIM-BF_4.

Reprinted with permission from reference [154]. Copyright (2005) American Chemical Society.

A variation of this protocol was used by Dyson and co-workers, who prepared modified PVP having anionic moieties in the polymer backbone.[156] They synthesized 3,3-di(ethoxycarbonyl)-1-vinylpyrrolidin-2-one from N-vinyl-2-pyrrolidone, and then

polymerized this monomer to generate the corresponding polymer poly-3,3-di(ethoxycarbonyl)-1-vinylpyrrolidin-2-one (PDEVP). After hydrolysis of PDEVP in NaOH/ethanol/H_2O and the following cation-exchange step with 1-octyl-3-methylimidazolium chloride, the IL-like polymer 1-methyl-3-octylimidazolium poly(1-vinylpirrolidin-2-one-3-carboxylate) was produced, which could be used to stabilize Rh NPs in BMIM-BF_4 for toluene hydrogenation. However, this synthesis was time-consuming and laborious, and spherical Rh superstructures (40-100 nm) were formed upon repeated recycling. There are numerous other examples of polymer-stabilized NPs, either synthesized directly in ILs or dispersed in ILs after their fabrication, used as recyclable catalysts in IL media, but in all these examples, the solubility of the polymer-coated NPs in ILs remain a concern, unless customized IL-soluble polymers are used as stabilizers. Occasionally, metal NPs are synthesized in an alternative solvent, and then transferred to an IL: Lercher and co-workers, for instance, reduced [Ni(acetylacetonate)$_2$] with Al(^{i}Bu)$_2$H in THF to form air-stable Ni NPs, which were then transferred to tetrahexylammonium tartrate, and the Ni NP/IL dispersion was then used for the catalytic hydrogenation of ketones and ketoesters.[157] Other systems, such as microemulsions of water/IL/polymer, are beyond the scope of this section.

Dendrimers are hyperbranched polymers with well-regulated, cauliflower-like structures containing a central core and branches radiating from it, and have been used extensively for NP stabilization by Crooks and others (Figure 1.10).[158,159] Most of these studies were carried out in aqueous media, although there are some exceptions. Ou *et*

al. reported the first example of highly stable PAMAM dendrimer-encapsulated Pd NPs in BMIM-PF_6 and a functionalized IL [1-(2-hydroxyethyl)-3-methylimidazolium tetrafluoroborate]. These systems catalyzed the hydrogenation of styrene with unmitigated efficiency for at least 12 cycles.[160] Other stabilization strategies, such as anchoring of catalytically active Pd NPs synthesized in BMIM-PF_6 onto the surface of imidazolium-functionalized multi-walled carbon nanotubes in the IL phase, have also been explored with varying degrees of success.[161]

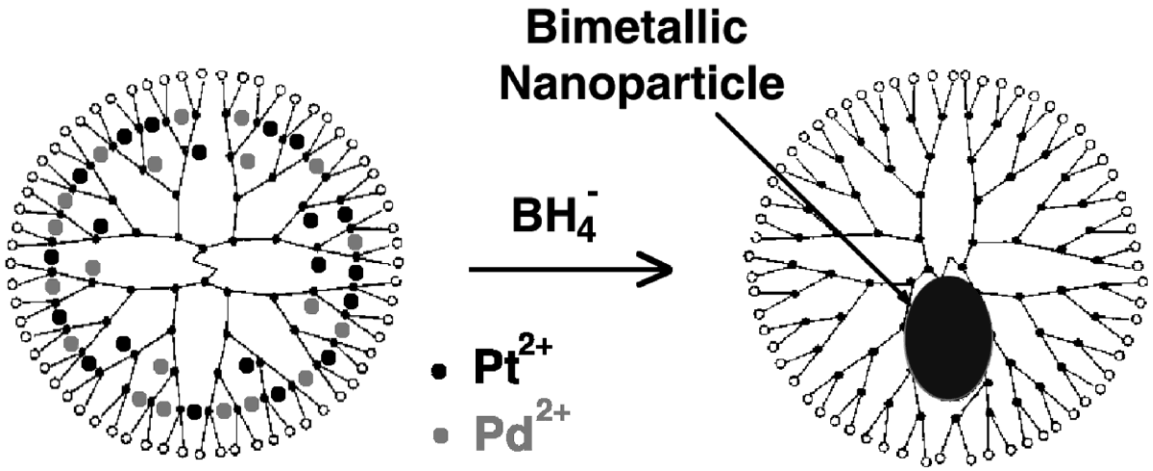

Figure 1.10 Synthesis of dendrimer-stabilized bimetallic NPs for catalysis. Reprinted with permission from reference [159]. Copyright (2003) American Chemical Society.

Ligands – mostly molecules bearing several heteroatoms, possibly capable of chelation – are used extensively as secondary stabilizers for NPs in ILs.[162] Sometimes, these can be impurities present in the IL during its synthesis. For instance, Scott and

Dash showed that traces of 1-methylimidazole, a starting material used in the synthesis of BMIM-PF_6, could stabilize Au and AuPd NPs in these ILs.[146] Phenanthroline has often been used a secondary stabilizer in IL solvents such as BMI-PF_6; protected and well-dispersed Pd NPs (2-5 nm) were obtained from the reduction of $Pd(OAc)_2$ by hydrogen in the IL with the presence of phenanthroline.[163,164] These ligand-protected Pd NPs in ILs were very active catalysts for the hydrogenation of olefins, achieving total conversions in the most cases for over 10 reaction cycles. In the absence of phenanthroline, however, Pd-black precipitation occurred in the IL, and catalytic activities were drastically reduced in the second reaction cycle. Amines and phosphines, especially with bulky alkyl substitutents, are often used as stabilizers: Bras *et al.,* for instance, used a mixture of tributylamine and its quaternary ammonium salt, tetrabutylammonium bromide (TBAB), to protect Pd NPs which catalyzed olefin hydrogenation for five consecutive cycles in BMIM-PF_6.[165] Similarly, Muzart and co-workers used Pd NPs prepared in the presence of TBAB as a capping agent and then dispersed in BMIM-PF_6 for olefin hydrogenations, for which these NPs showed good efficiency and selectivity. In another study, the NP stabilizing powers of a series of structurally similar ligands (2,2'-, 3,3'-, and 4,4'-bipyridine) were compared during the selective hydrogenation of styrene in BMIM-PF_6. It was seen that the yield and the selectivity towards ethylbenzene as a product depended on the coordination modes of the ligands to the Rh NPs, with the bidentate chelating ligand 2,2'-bipyridine favoring greater yields of ethylbenzene (Figure 1.11). Another chelating liagnd, 2,3,5,6-*tetra*-2-pyridinylpyrazine, was able to stabilize

Rh NPs in BMIM-NTf_2, and catalyze various alkylbenzenes to their saturated analogues in >89% yields.[166] Padua *et al.* examined the catalytic hydrogenation of 1,3-cyclohexadiene BMIM-NTf2 as a probe reaction to study the effect of different ligands ($C_8H_{17}NH_2$, H_2O, $PPhH_2$ and PPh_2H) on the catalytic performances of Ru NPs; it was determined that the activity of the Ru NP catalysts was enhanced by σ-donor ligands such as $C_8H_{17}NH_2$ and H_2O, but decreased in the presence of bulkier π-acceptor ligands, $PPhH_2$, PPh_2H and CO.[167]

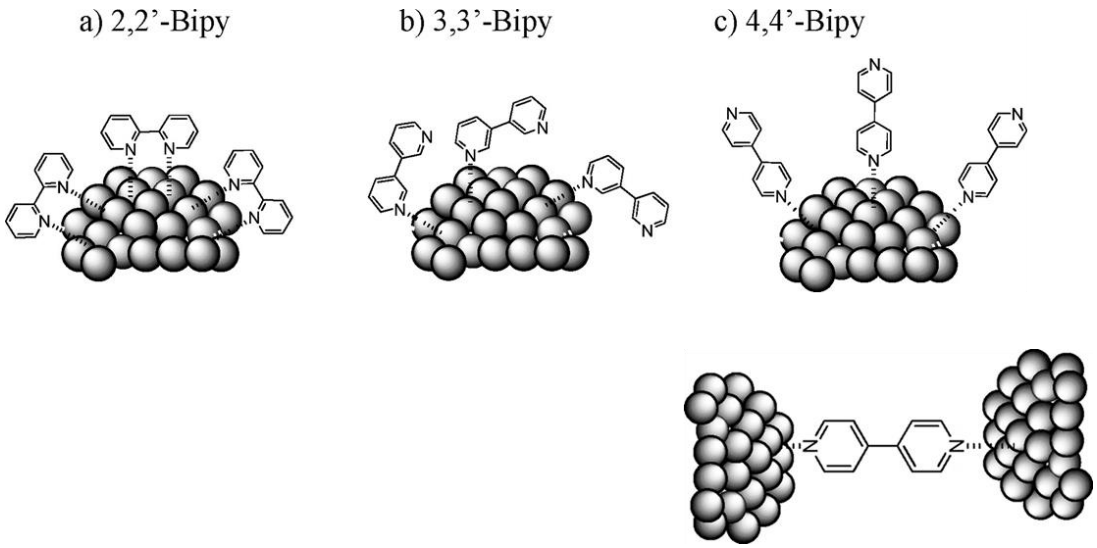

Figure 1.11 Bidentate N-containing ligands can stabilize metal NPs in ILs by coordinating to the NP surface. Reprinted with permission from reference [164]. Copyright (2008) American Chemical Society.

IL/NP/stabilizer systems were also able to catalyze a variety of C–C cross-coupling reactions: Pd NPs in BMIM-PF_6 in the presence of substituted norborn-5-ene-2,3-dicarboxylicanhydrides could catalyze the Suzuki coupling of aryl boronic acids and aryl halides in high yields.[168] There are numerous other reports of C–C cross-coupling

reactions in IL media, but many of them do not explicitly state whether the metal NPs or the metal precursors performed the actual catalysis in the IL phase. The presence of secondary stabilizers bearing chiral centers, such as cinchonidine, which create a chiral environment in the vicinity of the NP surface, have made asymmetric nanocatalysis in IL media possible. Small Pt NPs, for instance, were synthesized in BMIM-PF_6 using $Pt_2(dba)_3$ as a precursor and cinchonidine as a stabilizer, and these NPs could catalyze the enantioselective hydrogenation of methyl benzoylformate with an *ee* of ~78%, and a TOF of 3100 h^{-1} (Figure 1.12).[169]

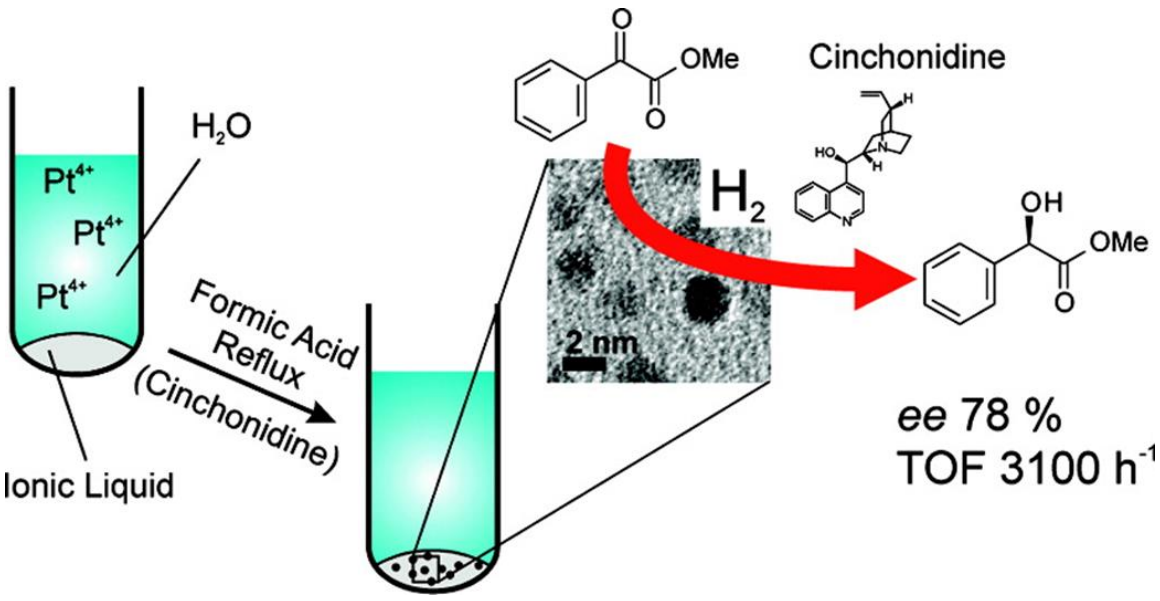

Figure 1.12. Asymmetric hydrogenation catalyzed by Pt NPs in ILs in the presence of a chiral ligand. Reprinted with permission from reference [169]. Copyright (2012) American Chemical Society.

Finally, a word of caution: highly monodisperse, robust NPs are not always the ones that show maximum catalytic activities. In fact, some authors claim that capping ligands with powerful affinities towards NP surfaces that produce near-monodisperse NP systems are actually of little to no use when it comes to nanocatalysis. As an example, one might consider Schmid's "giant Pd clusters" in the aqueous phase hydrogenation of acetophenone, whose catalytic activity reduces to near-zero values in the presence of the capping agent cinchonidine, despite showing a turnover frequency (TOF) of 45.5 h^{-1} in the presence of di-2,9-(2-methyl-butyl)-1,10-phenanthroline.[170] An earlier study by the same group, where ~4 nm nickel NPs were prepared by reduction of $Ni(acac)_2$ with Et_2AlH in diethyl ether, reported that these NPs, while showing a high degree of stability in the absence of oxygen – to the point where they could be stored under nitrogen for months, and re-dispersed in pyridine – showed next to no catalytic activity in the hydrogenation of hex-2-yne.[157] Reviews dealing with modes and types of catalytic deactivation of NPs by capping agents have been published recently.

1.2.2.2 Intrinsic Stabilization

Before we begin to consider specific examples of intrinsic NP stabilization by ILs, let us consider a property that almost all ILs have in common: relatively higher viscosities, especially compared to organic solvents.[46,68] This leads to quenching of the thermal movement of the colloidal NPs, minimizing the probability of close contact between two NPs, and provides a mechanism for NP stabilization based on a physical

property. It has been estimated by Kraynov and Müller that typical collision frequencies and coalescence half-lives for thermal coagulation of 3 nm sized NPs in BMIM-PF_6 (viscosity =376 mPa.s) are 10^3 s^{-1} and 10^{-3} s respectively, which differ by three orders of magnitude from those in an organic solvent, such as tetrahydrofuran (THF).[171] Since the viscosity of a typical IL is a factor of hundred or thousand higher than that of commonly used organic solvents such as THF, the inter-particle collision frequency of NPs in ILs decreases by several orders of magnitude. This results in a longer half-life time of the NPs. Thus, ILs are characterized by very low self-diffusion coefficients. Suppressed diffusion in media with high viscosity cannot be the only mechanism for stabilization of small particles, but it definitely contributes towards the overall stabilization of NPs in IL media.

There are two other proposed mechanisms that attempt to explain the intrinsic stabilization of metal NPs in ILs. The first of these relates specifically to the dialkylimidazolium class of ILs. In a recent review, Dupont and Scholten summarized the concept of ionic aggregates in ILs, and their influence in determining the physico-chemical properties of ILs (Figure 1.13).[172] In a scenario where a generic dialkylimidazolium halide IL, BMIM-X, stabilizes a metal NP, for instance, the following charged species might be considered: $[(BMIM)_x(X)_{x-n}]^{n+}$ and $[(BMIM)_{x-n}(X)_x]^{n-}$, with the anionic species, $[(BMIM)_{x-n}(X)_x]^{n-}$, being found in closer proximity to the surface of a metal NP, and the cationic species, $[(BMIM)_{x(}X)_{x-n}]^{n+}$, balancing the charge in the second coordination sphere.[173,174] XPS analysis of the isolated NPs (Ir, Rh, Pt, Ru and Pd)

prepared in ILs containing the PF_6^- and BF_4^- anions, for instance, have confirmed this hypothesis.[175] It was also suggested that the size of the NPs play a role in determining their surface charge states, and consequently, the identity of the primary stabilizing species in the first coordination sphere.[173] Pensado and Pádua carried out a computational study on the stabilization of Ru NPs by BMIM-NTf_2, in which both the cation and anion were found in close proximity to the metal surface.[176] Many other studies, with similar conclusions, seem to indicate that imidazolium ILs, in particular, form extended hydrogen-bond networks with polar and non-polar nano-domains, and this structural organization of ILs can be used as "entropic drivers" for spontaneous, well-defined, stable and extended ordering of nanoscale structures.[177]

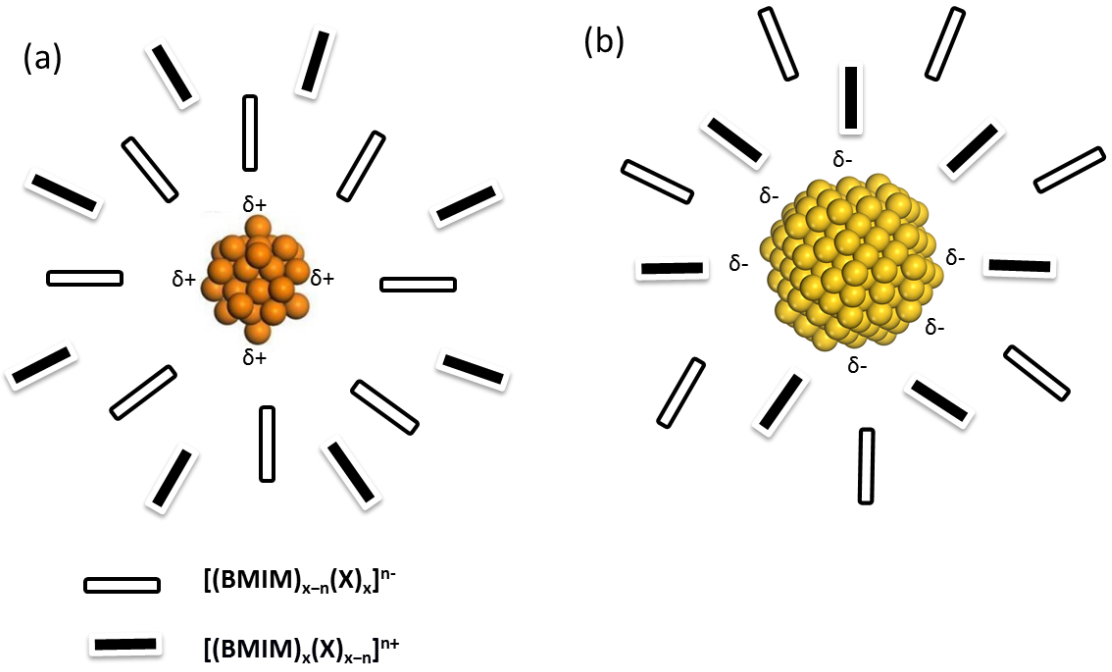

Figure 1.13 Interaction of metal NPs with IL supramolecular aggregates: (a) small particles tend to interact preferentially with anionic aggregates of the ILs, whereas (b) large ones probably interact preferentially with the cationic aggregates.

Finally, the classic theory of electrostatic colloid stabilization ("DLVO theory"), when subjected to modifications such as not treating all counter-ions as point charges, and accounting for "extra-DLVO forces" (hydrogen bonding, hydrophobic interactions, steric effects, etc.), still has its use in providing us with a simplified picture of NP stabilization in ILs that have a structural resemblance to surfactants. It has been emphasized by Finke, for instance, that DLVO theory should be the starting point for all studies on the stability of NP dispersions, since it still yields highly accurate figures in the

presence of highly coordinating anions in a solvent with a high dielectric constant.[141,142,144] This has been explored in the context of our NP/IL systems in the following chapter. Other putative stabilizing agents, such as carbenes, formed by deprotonation of the imidazolium proton, that attach themselves to the electron deficient NP surface, thus passivating them, have also been identified.[145] Elegant labeling experiments, using either D_2 or deuterated imidazolium-based ILs, have shown that the NHCs, as well as hydrides, are present on metal NP surfaces.[178] Similarly, ESI-MS studies also indicate that, when imidazolium-based ILs are employed in solutions, even under relatively "neutral" conditions, stable NHCs are most likely to 'coat' the metal NP surface.[178] The role of these surface-bound NHCs in catalysis remains unclear, with some scientists asserting that they poison active NP surfaces, while others insisting that the N-heterocyclic carbenes (NHCs) are reversibly detached during an induction period, thereby baring catalytically active NP surfaces.[179]

Imidazolium ILs, with the two ring substituents on the ring nitrogen atoms, offer unique opportunities for the introduction of NP-stabilizing functionalities in the imidazolium cation, which have been utilized by several groups. Different functional groups with heteroatoms, such as thiols, amines, cyanides, carboxylic acids and ethers, can be used for providing additional stabilization to the NPs by coordination on the metal surface.[62] For example, stable and well-dispersed Pd NPs with mean diameters of 5–6 nm were prepared in a 2,2'-pyridine-functionalized imidazolium IL, and used as recyclable catalysts for olefin hydrogenation under ambient hydrogen pressures by

Wang *et al*.[180] Similarly, thiol-functionalized ILs were used to stabilize Au NPs via strong Au-S bond formation.[181] Recently, Yan and co-workers fabricated stable AuPd bimetallic NPs via a simple thermal degradation of their respective acetates in 1-(2'-hydroxylethyl)-3-methylimidazolium ILs with a variety of anions, and used these as catalysts for dehalogenation reactions, where they proved to more efficient than commercially available Pd-on-charcoal catalysts by an order of magnitude at similar Pd contents.[182] Figure 1.14 shows some examples of these pendant NP-stabilizing groups. ILs with chiral functionalities appended to the imidazolium ring, such as di(1-phenylethyl)imidazolium nitrate, and 1-methyl-3-[(S)-2'-methyl[butyl]imidazolium tosylate, are often used in processes such as chiral separations, and for creating a chiral environment around the catalytic NPs, thereby favoring reactions such as enantioselective hydrogenations. In particular, Dyson, Yan, Moores, and Roucoux have published several seminal reports related to the design and synthesis of functionalized imidazolium ILs, and a review by Prof. Ralf Giernoth has summarized recent developments in this field of research.[183]

Functionalized cations:

1. Imidazolium-based

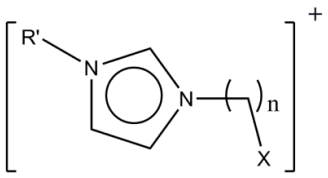

X = -OR
-Si(OR)$_3$
-SO_3^-
-SH
-NHR
-CN
-CO_2H
-CO_2R
-CH=CHR
-PR_2
-P(=O)OR_2
-C*(R^1)(R^2)(R^3)
-C(=O)R

2. Non-imidazolium

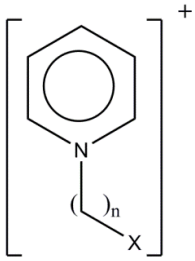

X = -CN
-CF_2SF_5

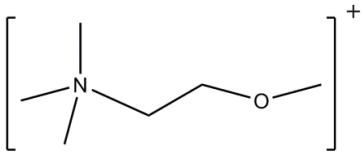

Functional Anions:

$Co(CO)_4^-$
CH_2=CH(SO_3^-)
$CF_3BF_3^-$
polyhalides and interhalides

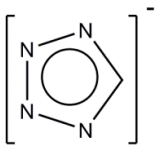

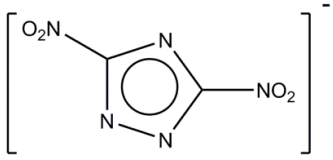

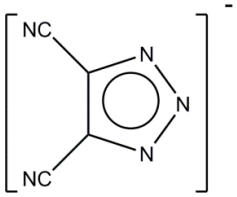

Figure 1.14 Cations and anions in functionalized ILs. Adapted from reference [62].

While cation functionalization is more common in imidazolium ILs, the use of coordinating or chelating ligands as anions – another popular strategy for tuning the structures and properties of ILs – has not been investigated as extensively. A straightforward procedure for obtaining pure functional-anion-containing ILs is the direct neutralization of an organic acid with the appropriate cation hydroxide. However, procurement of the cation hydroxide can be challenging, since exposing a halide salt to a strongly basic ion-exchange resin can lead to deprotonation, especially in nitrogen-containing cation systems. However, in recent years, the increasing demand for alternative solvents derived from renewable resources has led to methods for direct synthesis of ILs containing base-stable cations coupled with bio-sourced ligands such as L-lactate, L-tartrate, malonate, succinate, pyruvate, D-glucuronate, D-galacturonate, citrate, and amino acid anions. Other 'task-specific' anions, such as polyhalides, polycyano-based anions, and polymetallates have been used for applications such as IL-induced halogenation of olefins, as electrolytes in dye-sensitized thin-film solar cells, and, of course, for NP stabilization for catalysis.[62,184] Since anions are the species that preferentially ligate to small metal NPs with charge-depleted surfaces, it is evident that they play an enormous role in NP stabilization, and in determining the exact nature of the catalytic process occurring at the NP surface. Dyson and co-workers studied the effect of the IL anion on Pd NPs synthesized in 1-(2'-hydroxylethyl)-3-methylimidazolium ILs with a variety of anions (Tf_2N^-, PF_6^-, BF_4^- , OTf^-, TFA^-), and concluded that the most nucleophilic anions interact more strongly with the metal

precursor, thereby reducing the nucleation process, and leading to the formation of smaller NPs.[185] Wang *et al.*[186] selected 1-butyl-3-methylimidazolium-lactate IL-stabilized Pd NPs (PdNPs@[Bmim]Lac) as catalysts for the Suzuki-Miyaura reaction at room temperature in air. Lactate, apparently, was selected as the anion of the IL owing to its non-toxicity, facile bioavailability, and the presence of electron-donating hydroxyl and carboxyl groups in the structure of the lactate anion, which were expected to interact with surface metal atoms, thus further stabilizing the Pd NPs. These were seen to be very efficient catalysts, giving high product yields over ten catalytic cycles.[186] Our own studies concerning the effect of the coordination power of the IL anion on the NP catalytic efficiencies for tetraalkylphosphonium ILs can be found in Chapter 2. It is worth noting that the order of stabilization we observed has since been corroborated theoretically by Aleksandrov *et al.,* who performed quantum-chemical simulations of interactions between a Pd_6 cluster and PR_4X (X= PF_6^-, BF_4^-, Tf_2N^-, OTf^-, Br^-, TFA) ILs. They calculated that the binding energy of anions to the Pd_6 cluster, taken as a minimal-size model of the NPs, increases from ~6 to ~27 kcal mol^{-1} in the order $[PF_6]^- \approx [BF_4]^- < [Tf_2N]^- < [OTf]^- < [Br]^- \ll [TFA]$.[187]

It was mentioned in the previous section that polymers can stabilize NPs in a variety of solvents, including ILs; therefore, it is not surprising that attempts have been made to incorporate polymeric moieties within the structures of the ILILs. These polymeric ILs could be divided into two subclasses: ILs with polymeric units built into the structure via co-polymerization functioning as IL-soluble NP stabilizers (mentioned in the

previous section), and poly(ILs), which are fluid phase polyelectrolytes with each monomeric unit containing oppositely charged ions.[188] They are synthesized via radical polymerization of ionic monomers containing suitable substituents such as vinyls (Figure 1.15). It must be mentioned in this context that such polymeric chains could be introduced either in the cations or in the anions, although the former has more examples.[189]

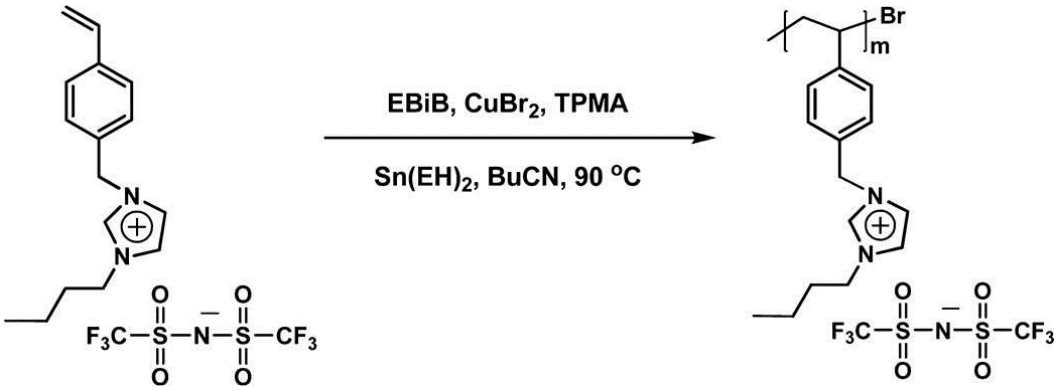

Figure 1.15 Synthesis of a poly(IL) (EBIB = ethyl 2-bromoisobutyrate, TPMA = tris(2-pyridylmethyl)amine, and $Sn(EH)_2$ = tin(II) 2-ethylhexanoate). Reprinted with permission from reference [189]. Copyright (2014) American Chemical Society.

It has been shown in the course of various studies that poly(ILs) can stabilize catalytic NPs, although most of these processes are operationally heterogeneous, and were carried out under solvent free conditions. For instance, sulfonic-acid-terminated poly(ILs) were used by Seidi and co-workers for the stabilization of magnetically recyclable iron oxide NPs. This system catalyzed the synthesis of 1,1'-diacetyls from aldehydes under ambient conditions in good yields.[190] There are, however, almost no

examples where the poly(ILs) are used as both solvents and stabilizers during the course of catalysis with NPs, probably owing to problems in scaling up their syntheses, as well as high viscosities of these polymeric species. Reactions where poly(IL)-coated NPs were isolated and redispersed in water or an organic solvent prior to their application as catalysts have not been been taken into account in this section.

1.3 Reactions catalyzed by metal NPs in an IL phase

Catalytic studies in IL media started with a mere handful of reactions, such as hydrogenations and C–C cross-couplings; today, however, there are hundreds of reactions where metal NPs in ILs find application as catalysts. Reactions such as hydrodehalogenations, hydrosilylations, methoxycarbonylations, Fischer-Tropsch synthesis, borylations, and isotope exchanges (to mention a few) benefit from quasi-homogeneous nanocatalysis, since organic phases can be readily separated from the reaction medium via decantation or vacuum distillation, and the catalyst, retained in the IL, can be recycled.[172] While it would be impossible to cover every reaction where metal NPs in ILs play a role, this section does intend to provide an overview of the three major reactions classes (hydrogenations, oxidations, and hydrodeoxygenations, or HDO) that have been studied during the course of this Ph.D. research project. Reactions such as hydrogenations and oxidations are very important from an industrial perspective, since the synthesis of most commodity chemicals including drugs, dyes, perfumes, flavoring materials, processed food, and cleaning products involve one or more steps where

molecules are either oxidized or reduced, often selectively. HDO is one of the core steps in biofuel processing, where the oxygen-rich pyrolysis oil obtained from biomass must be subjected to hydrodeoxygenation in order to make it usable. It is worthwhile, therefore, to examine these classes of reactions in the light of IL-phase nanocatalysis.

1.3.1 Hydrogenation

Hydrogenation remains the most thoroughly investigated class of reactions when it comes to catalysis with metal NPs in ILs. There are hundreds of reports in the literature of stable metal NPs in ILs serving as active and recyclable catalysts for the hydrogenation of a variety of functional moieties, ranging from simple olefins, to C=X (X= a heteroatom) units, and even arenes.[172] One of the first examples of catalysis by metal NPs generated *in situ* in the IL phase via the reduction of an organometallic precursor was reported by Dupont and co-workers in 1996, who observed that cyclohexene hydrogenation catalyzed by $[Rh(COD)_2]BF_4$ dissolved in BMI-BF_4 proceeded via the involvement of Rh NPs.[191] More definitive examples of metal NP-catalyzed hydrogenations in ILs have been reported by the same group since then.[173] The influence of the olefin structure on the hydrogenation rates have also been reported, with highly substituted alkenes undergoing slower conversions.[192] As suggested by Crabtree, a number of poisoning tests were undertaken as a part of these studies to ensure that the metal NPs formed in the reaction media were, in fact, the actual catalytic species.

There are, however, factors that limit catalytic hydrogenations in ILs from becoming more efficient; the most important limiting factor being the solubility of hydrogen in the IL. Catalytic hydrogenations in ILs proceed under biphasic (or even triphasic) conditions; it is only rarely that a single-phase reaction occurs in these systems. One of the problems of catalytic hydrogenations in ILs is the low miscibility of molecular dihydrogen, and occasionally, also of nonaromatic substrates, such as classical olefins, that may cause mass-flow controlled processes. It is not unusual for the kinetics of multiphase hydrogenation to be determined by the diffusion of the reactants into the IL, where the reaction is supposed to take place.[193] Recently, high-pressure NMR spectroscopy was used for the determination of hydrogen solubility in imidazolium ILs, and the dissolved [H_2] values were seen to vary from 0.7 to 0.9 mM, which is similar to the solubility of H_2 in water (=0.81 mM at P_{H2} =10.1 MPa), and significantly less than that in organic solvents such as toluene (=3.5 mM) and methanol (=3.7 mM). In the tetraalkylphosphonium IL $P(C_6H_{13})_3(C_{14}H_{29})[PF_3(C_2F_5)_3]$, however, [$H_2$] was found to be ~1.9 mM, which is relatively higher, suggesting that tetraalkylphosphonium ILs might be more suitedfor hydrogenation reactions than imidazolium ILs.[194]

There are a few kinetic studies on alkene hydrogenations catalyzed by metal NPs in IL media. In one study by Dupont and co-workers, for instance, it was noticed that Ir NP-catalyzed hydrogenation of 1-decene in BMIM-PF_6 followed the classical Lindemann unimolecular surface reaction mechanism (Rate = $k_c.K[S]/(1 + K[S])$, where [S] is the concentration of 1-decene in the IL phase).[175,192] The reaction was found to be a mass-

flow controlled process under a hydrogen pressure <4 atm. The catalytic kinetic constant (k_c) and the adsorption constant (K) under hydrogen pressures ≥4 atm were independent of the hydrogen concentration, indicating zero-order dependence on hydrogen pressure; the reaction depended only on the alkene concentration in the IL. The solubility effect can, however, be used to great advantage for selective hydrogenation of arenes, where an intermediate product (for e.g., cyclohexene) is sparingly soluble in the reaction medium, and undergoes phase-separation, effectively preventing further hydrogenation.[195] Such selective hydrogenations are very difficult to achieve under heterogeneously catalyzed conditions. There are a number of detailed reviews that deal exclusively with metal NP-catalyzed hydrogenations in IL media.[172,196]

The first reported example of metal NP-catalyzed hydrogenations in tetraalkylphosphonium ILs can be found in Chapter 2 of this thesis; Luska and Moores reported the second example.[197] They compared tetraalkylphosphonium and imidazolium ILs in the synthesis of Ru NPs via hydrogen reduction of an organometallic precursor, and their subsequent use as hydrogenation catalysts in the reduction of cyclohexene. A series of tetraalkylphosphonium ILs was used: $P[4,4,4,1]NTf_2$, $P[4,4,4,8]NTf_2$ and P[4,4,4,14]X (for −X = $-NTf_2$, −OTf, --Cl, $-PF_6$; the numbers in brackets denote the length of the alkyl substituents on the central phosphorus atom), in which the length of the P-alkyl chain and counter anion were varied. Ru NPs in tetraalkylphosphonium ILs were seen to highly efficient hydrogenation catalysts. These systems could also be recycled repeatedly; however, the recyclability was dependent on

the length of the alkyl chains, such that increasing the length of the chain increased the longevity of the catalyst – Ru NPs in P[4,4,4,14]NTf_2, for instance, gave complete conversions over eight runs. In comparison, Ru NPs stabilized in BMIM-NTf_2 showed moderate catalytic activity, which also remained unaffected over eight catalytic cycles.

1.3.2 Oxidations

Unlike hydrogenations, there are not many reports of oxidations catalyzed by metal NPs in IL media, and for good reasons: both metal NPs, as well as the ILs, are susceptible to chemical changes in the presence of oxidants, especially at higher temperatures. For the metal NPs, this might lead to oxidative etching, Ostwald ripening, formation of inert oxide shells, or other changes that diminish their catalytic activities.[198] For the ILs themselves, the presence of oxygen and/or water might lead to anion decomposition (for the halometallate ILs), anion hydrolysis (for ILs containing BF_4^- and PF_6^-), or oxidation of the alkyl side chains. It is imperative, therefore, to consider these factors before designing an oxidative catalytic process in an IL.[199]

The solubility of oxygen in ILs is another factor that has to be considered in the context of MNP-catalyzed oxidations in ILs. It was reported by Maurer and co-workers that the IL BMIM-PF_6 – a commonly used solvent in IL-phase catalysis – is a poor solvent for oxygen; at 9 Mpa of oxygen pressure, only about 0.16 mol of the gas are dissolved in 1 kg of the IL. Furthermore, very little influence of temperature on the solubility of

oxygen in the IL was observed.[200] Brennecke and co-workers have published several studies on the solubility of gases in various ILs; they found that the anion in the IL plays a significant role in determining the gas solubilities.[201] The Tf_2N^- anion, for instance, increased all gas solubilities relative to BF_4 and PF_6 ILs, whereas the BF_4^- anion has little effect on the solubility of these gases relative to PF_6. Changing the cation from imidazolium to quaternary ammonium, phosphonium, or pyrrolidinium, all with the Tf_2N^- anion, made little difference in the CO_2 and O_2 solubility.[202] The solubility of oxygen in the ILs was still found to be exceptionally low.

Despite these limiting factors, however, there have been some studies conducted on possible catalytic routes of oxidations – especially selective oxidations – in IL media. One of the earliest studies by Seddon and Stark, for instance, showed that Pd-catalyzed oxidations of benzyl alcohol to benzaldehyde in various imidazolium ILs were possible, with the product distribution being dependent on the IL anion. The system was recyclable for at least five runs, and could even be used for the oxidation of alkylbenzenes to aromatic carbonyls with decent yields.[203] A similar system was used by Doorslaer and co-workers to demonstrate spontaneous product separation from the catalyst/IL phase after oxidation.[204] Muzart *et al.* heated secondary benzylic alcohols in tetra-^{n}butyl ammonium bromide with catalytic amounts of palladium chloride under Ar to obtain corresponding ketones in good yields, in the absence of cooxidants and additives; the system was recyclable, and the involvement of Pd NPs was suspected,

especially when a control reaction using pre-formed Pd NPs in the same medium led to similar reactions, albeit with reduced efficiency and selectivity.[199] Allylic and saturated alcohols did not show any conversion under identical reaction conditions. In a more recent study by Janiak and co-workers, Au NPs synthesized via thermal reduction of $KAuCl_4$ in the presence of *n*-butylimidazole in BMIM-BF_4 were active catalysts for the oxidation of 1-phenylethanol at 100 and 160^oC under 4 bar pressure of dioxygen in a base-free system in the presence of the radical initiator N-hydroxyphthalimide. The system showed good conversion and selectivity ($TON_{aldehyde}$ = 940 at 160^0C) for the oxidation of 1-phenylethanol to acetophenone through formation of an α-hydroxy carbon free radical (Figure 1.16).[205] In 2014, Mukherjee *et al*. used ~3nm Pt NPs in BMIM-OAc for aerobic oxidation of alcohols under mild conditions; the particles suspended in ILs showed no metal agglomeration or loss of catalytic activity even after repeated use.[206]

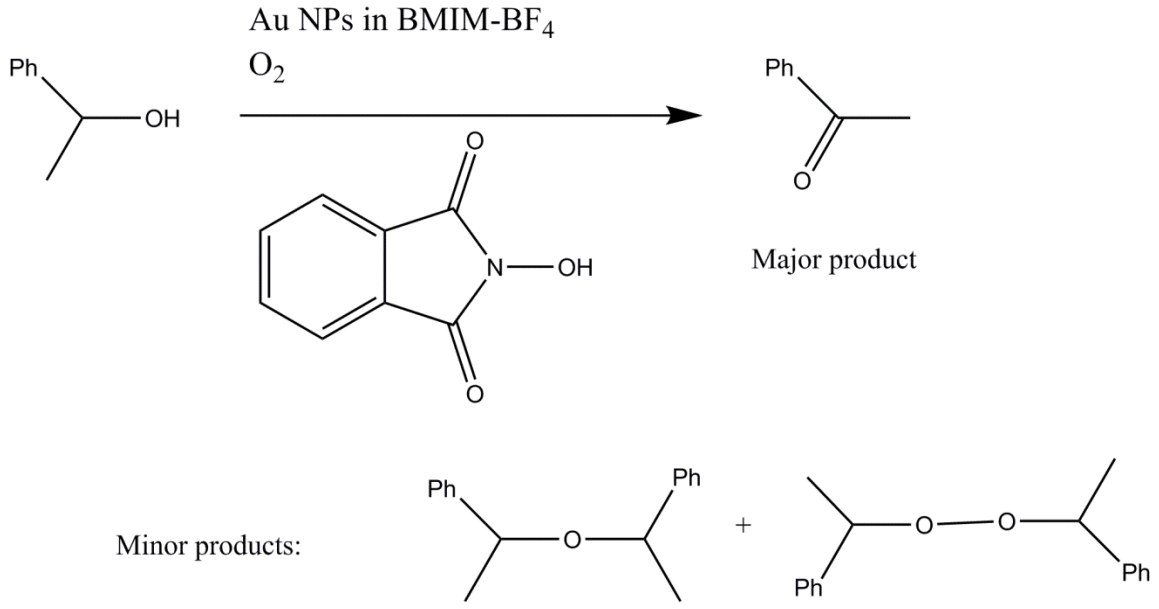

Figure 1.16 Au NP catalyzed radical-mediated oxidation of 2-phenylethanol in an IL.

1.3.3 Hydrodeoxygenation

Chemical processes that attempt to diminish the oxygen content (deoxygenation) as well as augment the hydrogen content (hydrogenation or hydrogenolysis, i.e., hydrogen addition with or without accompanying bond rupture) of the crude bio-oil obtained via the pyrolysis of vegetation bio-mass are promising avenues where metal NP/IL systems might find application, especially since ILs are already used for dissolution of cellulose and lignin.[207-209] While these reactions are often carried out using supported-IL-stabilized metal NPs, there are also examples where HDOs occur under quasi-homogeneous conditions.[210] In a seminal study, Dyson *et al*. achieved the catalytic transformation of lignin-derived phenolic compounds to alkanes

in BMIM-BF_4 and BMIM-NTf_2 ILs.[211] The catalytic system consisted of poly(1-vinyl-3-butylimidazolium chloride-co-N-vinyl-2-pyrrolidone)-stabilized Ru NPs along with a functionalized Brønsted acidic IL suspended in a nonfunctionalized IL, which enabled hydrogenation and dehydration reactions to occur in tandem (Figure 1.17). There are a few other examples of IL-stabilized metal or metal oxide NPs being used as HDO catalysts, but strangely, some of those are carried out in water (despite dehydration being one of the key steps involved in HDO), while others were solventless processes, or used a secondary acidic oxide support to enhance catalytic robustness as well as for the dehydration step.[212,213] It is anticipated that studies in the future will focus on IL-phase HDOs, especially since environmentally benign acids such as boric acids have been shown to be IL-soluble.

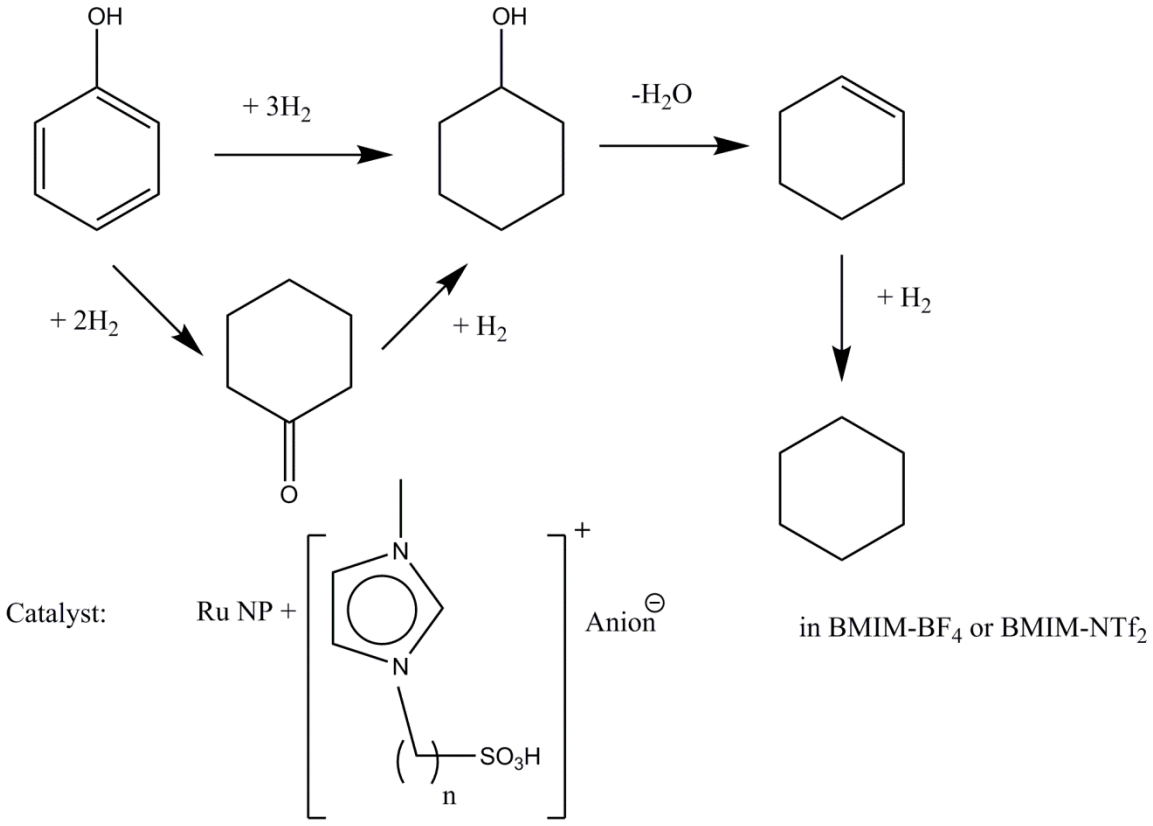

Figure 1.17 Tandem phenol HDO on IL-solvated-Ru NPs in the presence a second functionalized Brønsted acidic IL.

1.3.4 Other reactions

C–C cross-couplings remain the second-most well-investigated class of reactions studied in the context of metal NP catalysis in IL media, with numerous examples of Heck, Sonogashira, Suzuki, Kumada, Negishi, and Stille couplings present in relevant literature.[214] Two of these studies were recently conducted in tetraalkylphosphonium ILs. In 2011, Kerton *et al.* synthesized Pd NPs in a variety of tetraalkylphosphonium ILs without using an external reductant; these were seen to catalyze the Suzuki coupling

reaction of 4-bromotoluene and phenylboronic acid in IL media under microwave conditions. Yields as high as 90% were reached after 15 minutes in the presence of a base such as KOH.[215] Ermolaev *et al.* used 2.5 ± 0.5 nm Pd NPs as catalysts for Suzuki cross-coupling in tri(^{t}-butyl)decylphosphonium tetrafluoroborate under mild conditions in 2012. A variety of chloro- and bromoarenes were evaluated as potential substrates, and yields varied from *ca.* 50% to 90%, depending on individual haloarenes.[216]

Zhu and co-workers used Pd NPs in tri(^{n}-butyl)tetradecylphosphonium dodecylbenzenesulfonate for aminocarbonylation between substituted iodobenzenes and amines at moderate P_{CO}; the catalyst system was recyclable for at least five reaction cycles, yields remained fairly constant, and TEM as well as XPS showed that particle sizes remained unchanged over a number of runs. Leaching of Pd into the product phase was less than 2.0 ppm. These systems could also catalyze diaminocarbonylations in moderate-to-good yields.[217]

Functionalized phosphonium ILs, still a novelty, were synthesized by Moores *et al.* in 2012, and used for catalytic hydroformylation in the presence of [Rh(acac)$(CO)_2$] (acac = acetylacetonate) as a pre-catalyst. The involvement of Rh NPs formed *in situ* in the catalytic process was confirmed, but their exact role (i.e., metal reservoir vs. active catalyst) remained open to speculation. A control experiment, however, proved that pre-formed Rh NPs in these ILs could also catalyze the same reaction, albeit with reduced yields and selectivities.[218]

Another example of metal NPs in tetraalkylphosphonium ILs serving as catalyst reservoirs was published in 2011, where Ni NPs, formed via the in-situ reduction of $NiBr_2$ in tetra(octyl)phosphonium bromide, tri(hexyl)tetradecylphosphonium chloride or tri(butyl)tetradecylphosphonium chloride, catalyzed the coupling of 4-chlorobenzonitrile with morpholine. The authors addressed the issue concerning the role of Ni NPs in the reaction: i.e., whether the Ni NPs themselves catalyzed the reaction, or served as a nickel source from which homogeneous nickel complexes entered the reaction cycle. It was decided that the latter hypothesis was more plausible, although Ni NPs were observed via TEM imaging, and catalytic efficiencies reduced drastically upon changing the reaction medium to less-coordinating imidazolium ILs. It was hypothesized that upon reduction of the active nickel complex, the zerovalent nickel species formed needed to be stabilized. Tetraalkylphosphonium ILs inhibited aggregation of the nickel metal and prevented deposition, which would result in loss of activity. The final conclusion was that this reaction thus proceeded "on the border between homogeneous and heterogeneous catalysis."[219]

1.4 Organization and Scope

This Ph.D. dissertation is an account of catalysis by metallic NPs conducted in the tetraalkylphosphonium family of ILs. It consists of eight chapters. Chapter 2-6 are near-verbatim copies of articles published in different scientific journals, with minor formatting changes. Chapter 7 is a manuscript to be submitted for publication in the near future. At the beginning of each chapter, a synopsis has been provided, including comments on the relation between that particular chapter with the overall goal of the research program, and the name of the scientific journal where the manuscript was published.

Chapter 1 is concerned with the importance of catalytic processes in alternative solvents. From this general introduction, it segues into a description of nanocatalyzed processes in ILs, which are perhaps one of the most intensely studied alternative solvents. It documents the use of the tetraalkylphosphonium family of ILs, which are less well-known to the catalysis community than their imidazolium counterparts, as media for the synthesis of metal NPs. A detailed literature survey is carried out to identify catalytic reactions involving NPs in this under-studied class of IL. In Chapter 2, the synthesis of tetraalkylphosphonium ILs and their use as solvents, as well as stabilizers, for Au and Pd NPs are described. Additionally, the catalytic applications of Pd NPs in these ILs and their recyclabilities are addressed. Chapter 3 presents a comparative study of Au, Pd and bimetallic AuPd NPs as catalysts for the oxidation of α,β-unsaturated

alcohols in water and in tetraalkylphosphonium ILs. In Chapter 4, a previously undocumented mode of catalyst regeneration, viz., the conversion of larger metal aggregates into smaller, catalytically active NPs via a two-step strategy in tetraalkylphosphonium halide ILs is introduced. Chapter 5 continues this narrative, showing that Ag NPs in tetraalkylphosphonium halides regain not only their sizes but also their catalytic activities upon being subjected to the regeneration protocol; it also attempts to corroborate our hypothesis about facile oxidation of metal NPs in tetraalkylphosphonium halides via X-ray absorption studies. Chapter 6 documents our attempts to select a stable NP/IL composite catalytic system for deep hydrogenations, and describes how the presence of synthetic by-products in these composite catalysts can lead to phenol hydrodeoxygenation (HDO). In Chapter 7, earth-abundant Fe NPs are evaluated as hydrogenation catalysts in tetraalkylphosphonium ILs. Finally, in Chapter 8, a summary, an outlook, and possible future work in this field of research, including three research topics briefly examined during the course of this Ph.D., are presented.

1.5 References

[1] Lyons, J.; Parshall, G. *Catal. Today* **1994**, *22*, 313-333.

[2] George, S. M. *Chem. Rev.* **1995**, *95*, 475-476.

[3] Somorjai, G. A.; Li, Y. *Introduction to Surface Chemistry and Catalysis*; Wiley & Sons: New York, 2010.

[4] Kolb, D. *J. Chem. Educ.* **1979**, *56*, 743.

[5] Dimitratos, N.; Lopez-Sanchez, J. A.; Hutchings, G. J. *Top. Catal.* **2009**, *52*, 258-268.

[6] Fukuoka, A.; Dhepe, P. L. *Chem. Rec.* **2009**, *9*, 224-235.

[7] Sheldon, R. A.; Arends, I.; Hanefeld, U. *Green Chemistry and Catalysis*; Wiley & Sons: New York, 2007.

[8] Reichardt, C.; Welton, T. *Solvents and Solvent Effects in Organic Chemistry*; Wiley & Sons: New York, 2011.

[9] Hynes, J. T. *Ann. Rev. Phys. Chem.* **1985**, *36*, 573-597.

[10] Harrison, R. M. *Pollution: causes, effects and control*; RSC Publishing: Cambridge, 2001.

[11] Rana, S. *Environmental Pollution: health and toxicology*; Alpha Science International Ltd.: Oxford, 2006.

[12] Lichtfouse, E.; Schwarzbauer, J.; Robert, D. *Pollutant Diseases, Remediation and Recycling*; Springer-Verlag: New York, 2013.

[13] Blaser, H.-U.; Studer, M. *Green Chem.* **2003**, *5*, 112-117.

[14] Kerton, F. M.; Marriott, R. *Alternative Solvents for Green Chemistry*; RSC Publishing: Cambridge, 2013.

[15] Sabor, R. *Richard Wagner, Der Ring des Nibelungen: a companion volume*; Phaidon Press: New York, 1997; Vol. 1.

[16] *Impurities: Guideline for Residual Solvents*; Health Canada Publications: Ottawa, ON, 1999.

[17] Ikeda, M. *Toxicol. Lett.* **1999**, *64*, 191-201.

[18] Alfonsi, K.; Colberg, J.; Dunn, P. J.; Fevig, T.; Jennings, S.; Johnson, T. A.; Kleine, H. P.; Knight, C.; Nagy, M. A.; Perry, D. A.; Stefaniak, M. *Green Chem.* **2008**, *10*, 31-36.

[19] Adams, J. P.; Alder, C. M.; Andrews, I.; Bullion, A. M.; Campbell-Crawford, M.; Darcy, M. G.; Hayler, J. D.; Henderson, R. K.; Oare, C. A.; Pendrak, I.; Redman, A. M.; Shuster, L. E.; Sneddon, H. F.; Walker, M. D. *Green Chem.* **2013**, *15*, 1542-1549.

[20] Capello, C.; Fischer, U.; Hungerbuhler, K. *Green Chem.* **2007**, *9*, 927-934.

[21] Prat, D.; Hayler, J.; Wells, A. *Green Chem.* **2014**, *16*, 4546-4551.

[22] Breslow, R. A Fifty-year Perspective of Chemistry in Water. In *Organic Reactions in Water*; U. M. Lindstörm, Ed.; Blackwell Publishing: Cambridge, MA, 2007; pp 1-23.

[23] Engberts, J.B.F.N. Structure and Properties of Water. In *Organic Reactions in Water*; U. M. Lindstörm, Ed.; Blackwell Publishing: Cambridge, MA, 2007; pp 29-54.

[24] Gawande, M. B.; Bonifácio, V. D.; Luque, R.; Branco, P. S.; Varma, R. S. *Chem. Soc. Rev.* **2013**, *42*, 5522-5551.

[25] Herriott, A.W.; Picker, D. *J. Am. Chem. Soc.* **1975**, *97*, 2345-2349.

[26] Jung, Y.; Marcus, R. *J. Am. Chem. Soc.* **2007**, *129*, 5492-5502.

[27] Pirkanniemi, K.; Sillanpää, M. *Chemosphere* **2002**, *48*, 1047-1060.

[28] Patrick, H. R.; Griffith, K.; Liotta, C. L.; Eckert, C. A.; Gläser, R. *Ind. Eng. Chem. Res.* **2001**, *40*, 6063-6067.

[29] Cushing, B. L.; Kolesnichenko, V. L.; O'Connor, C. J. *Chem. Rev.* **2004**, *104*, 3893-3946.

[30] Roucoux, A.; Schulz, J.; Patin, H. *Chem. Rev.* **2002**, *102*, 3757-3778.

[31] Lu, Z.; Yin, Y. *Chem. Soc. Rev.* **2012**, *41*, 6874-6887.

[32] Duan, H.; Wang, D.; Li, Y. *Chem. Soc. Rev.* **2015**.

[33] Hulkoti, N. I.; Taranath, T. C. *Colloids Surf., B* **2014**, *121*, 474-483.

[34] Makarov, V. V.; Love, A. J.; Sinitsyna, O. V.; Makarova, S. S.; Yaminsky, I. V.; Taliansky, M. E.; Kalinina, N. O. *Acta Nat.* **2014**, *6*, 35-44.

[35] Iravani, S. *Green Chem.* **2011**, *13*, 2638-2650.

[36] Heldebrant, D. J.; Witt, H. N.; Walsh, S. M.; Ellis, T.; Rauscher, J.; Jessop, P. G. *Green Chem.* **2006**, *8*, 807-815.

[37] Rodríguez, H.; Rogers, R. D. *Fluid Phase Equilib.* **2010**, *294*, 7-14.

[38] Chen, J.; Spear, S. K.; Huddleston, J. G.; Rogers, R. D. *Green Chem.* **2005**, *7*, 64-82.

[39] Colacino, E.; Martinez, J.; Lamaty, F.; Patrikeeva, L. S.; Khemchyan, L. L.; Ananikov, V. P.; Beletskaya, I. P. *Coord. Chem. Rev.* **2012**, *256*, 2893-2920.

[40] Fan, X.-B.; Tao, Z.-Y.; Xiao, C.-X.; Liu, F.; Kou, Y. *Green Chem.* **2010**, *12*, 795-797.

[41] Han, W.; Liu, C.; Jin, Z.-L. *Org. Lett.* **2007**, *9*, 4005-4007.

[42] Walden, P. *Bull. Acad. Imper. Sci. St. Petersbourg* **1914**, *8*, 405-422.

[43] Wilkes, J. S.; Levisky, J. A.; Wilson, R. A.; Hussey, C. L. *Inorganic Chem.* **1982**, *21*, 1263-1264.

[44] Wilkes, J. S.; Zaworotko, M. J. *J. Chem. Soc., Chem. Commun.* **1992**, 965-967.

[45] Green, M. D.; Long, T. E. *Polymer Rev.* **2009**, *49*, 291-314.

[46] Freemantle, M. *An Introduction to Ionic Liquids*; RSC Publishing: Cambridge, 2010.

[47] Chen, L.; Mullen, G. E.; Le Roch, M.; Cassity, C. G.; Gouault, N.; Fadamiro, H. Y.; Barletta, R. E.; O'Brien, R. A.; Sykora, R. E.; Stenson, A. C.; West, K. N.; Horne, H. E.; Hendrich, J. M.; Xiang, K. R.; Davis, J. H. *Angew. Chem. Int. Ed.* **2014**, *53*, 11762-11765.

[48] Migowski, P.; Dupont, J. *Chem. Eur. J.* **2007**, *13*, 32-39.

[49] Welton, T. *Chem. Rev.* **1999**, *99*, 2071-2084.

[50] Lozano, P. *Green Chem.* **2010**, *12*, 555-569.

[51] Branco, L. C.; Afonso, C. A.; Carrera, G. V.; Martin, I. L.; Aires, J.; Frade, R. *Physico-Chemical Properties of Task-specific Ionic Liquids*; INTECH Open Access Publisher, 2011.

[52] Mohammad, A. *Green solvents II: properties and applications ionic liquids*; Springer Science & Business Media, 2012; Vol. 2.

[53] Freire, M. G.; Neves, C. M. S. S.; Marrucho, I. M.; Coutinho, J. A. P.; Fernandes, A. M. *J. Phys. Chem. A* **2010**, *114*, 3744-3749.

[54] Swatloski, R. P.; Spear, S. K.; Holbrey, J. D.; Rogers, R. D. *J. Am. Chem. Soc.* **2002**, *124*, 4974-4975.

[55] Remsing, R. C.; Swatloski, R. P.; Rogers, R. D.; Moyna, G. *Chem. Commun.* **2006**, 1271-1273.

[56] Xie, H.; Zhang, S.; Li, S. *Green Chem.* **2006**, *8*, 630-633.

[57] Sun, N.; Rahman, M.; Qin, Y.; Maxim, M. L.; Rodriguez, H.; Rogers, R. D. *Green Chem.* **2009**, *11*, 646-655.

[58] Torralba-Calleja, E.; Skinner, J.; Gutierrez-Tauste, D. *J. Chem.* **2013**, *2013*, 16.

[59] Yokozeki, A.; Shiflett, M. B.; Junk, C. P.; Grieco, L. M.; Foo, T. *J. Phys. Chem. B* **2008**, *112*, 16654-16663.

[60] Bates, E. D.; Mayton, R. D.; Ntai, I.; Davis, J. H. *J. Am. Chem. Soc.* **2002**, *124*, 926-927.

[61] Yue, C.; Fang, D.; Liu, L.; Yi, T.-F. *J. Mol. Liq.* **2011**, *163*, 99-121.

[62] Zhen, L.; Zhao, Y.W.; Feng, H.; Lei, Y.; HeYuan, S.; Chen, J.; ChunGu, X. *Sci. Sin. Chim.* **2012**, *42*, 502-524.

[63] Zaitsau, D. H.; Yermalayeu, A. V.; Verevkin, S. P.; Bara, J. E.; Stanton, A. D. *Ind. Eng. Chem. Res.* **2013**, *52*, 16615-16621.

[64] Romero, A.; Santos, A.; Tojo, J.; Rodríguez, A. *J. Hazard. Mater.* **2008**, *151*, 268-273.

[65] Knifton, J. F. *J. Am. Chem. Soc.* **1981**, *103*, 3959-3961.

[66] Muetterties, E. L.; Gerlach, D. H.; Kane, A. R.; Parshall, G. W.; Jesson, J. P. *J. Am. Chem. Soc.* **1971**, *93*, 3543-3544.

[67] Bradaric, C. J.; Downard, A.; Kennedy, C.; Robertson, A. J.; Zhou, Y. *Green Chem.* **2003**, *5*, 143-152.

[68] Fraser, K. J.; MacFarlane, D. R. *Aust. J. Chem.* **2009**, *62*, 309-321.

[69] Del Sesto, R. E.; Corley, C.; Robertson, A.; Wilkes, J. S. *J. Organomet. Chem.* **2005**, *690*, 2536-2542.

[70] Ferreira, A. F.; Simões, P. N.; Ferreira, A. G. M. *J. Chem. Thermodyn.* **2012**, *45*, 16-27.

[71] Tsunashima, K.; Sugiya, M. *Electrochem. Commun.* **2007**, *9*, 2353-2358.

[72] Marsi, K. L.; Oberlander, J. E. *J. Am. Chem. Soc.* **1973**, *95*, 200-204.

[73] Tseng, M.-C.; Kan, H.-C.; Chu, Y.-H. *Tetrahedron Lett.* **2007**, *48*, 9085-9089.

[74] Ramnial, T.; Ino, D. D.; Clyburne, J. A. C. *Chem. Commun.* **2005**, 325-327.

[75] McNulty, J.; Capretta, A.; Cheekoori, S.; Clyburne, J. A. C.; Robertson, A. J. *Chim. Oggi.* **2004**, *22*, 13-16.

[76] Fukaya, Y.; Iizuka, Y.; Sekikawa, K.; Ohno, H. *Green Chem.* **2007**, *9*, 1155-1157.

[77] Ohno, H.; Fukumoto, K. *Acc. Chem. Res.* **2007**, *40*, 1122-1129.

[78] Ferraz, R.; Branco, L. C.; Marrucho, I. M.; Araujo, J. M. M.; Rebelo, L. P. N.; da Ponte, M. N.; Prudencio, C.; Noronha, J. P.; Petrovski, Z. *Med. Chem. Commun.* **2012**, *3*, 494-497.

[79] Poletti, L.; Chiappe, C.; Lay, L.; Pieraccini, D.; Polito, L.; Russo, G. *Green Chem.* **2007**, *9*, 337-341.

[80] Petkovic, M.; Ferguson, J. L.; Gunaratne, H. Q. N.; Ferreira, R.; Leitao, M. C.; Seddon, K. R.; Rebelo, L. P. N.; Pereira, C. S. *Green Chem.* **2010**, *12*, 643-649.

[81] Smith, E. L.; Abbott, A. P.; Ryder, K. S. *Chem. Rev.* **2014**, *114*, 11060-11082.

[82] Abbott, A. P.; Barron, J. C.; Ryder, K. S.; Wilson, D. *Chem. Eur. J.* **2007**, *13*, 6495-6501.

[83] Abbott, A. P.; Al-Barzinjy, A. A.; Abbott, P. D.; Frisch, G.; Harris, R. C.; Hartley, J.; Ryder, K. S. *Phys. Chem. Chem. Phys.* **2014**, *16*, 9047-9055.

[84] Dai, Y.; van Spronsen, J.; Witkamp, G.-J.; Verpoorte, R.; Choi, Y. H. *Anal. Chim. Acta* **2013**, *766*, 61-68.

[85] Abbott, A. P.; Ahmed, E. I.; Harris, R. C.; Ryder, K. S. *Green Chem.* **2014**, *16*, 4156-4161.

[86] O'Neill, M.; Raghuwanshi, V. S.; Wendt, R.; Wollgarten, M.; Hoell, A.; Rademann, K. *Z. Phys. Chem.* **2015**, *229*, 221-234.

[87] Russ, C.; Konig, B. *Green Chem.* **2012**, *14*, 2969-2982.

[88] Dong, J.-Y.; Lin, C.-H.; Hsu, Y.-J.; Lu, S.-Y.; Wong, D. S.-H. *CrystEngComm* **2012**, *14*, 4732-4737.

[89] Chirea, M.; Freitas, A.; Vasile, B. S.; Ghitulica, C.; Pereira, C. M.; Silva, F. *Langmuir* **2011**, *27*, 3906-3913.

[90] Renjith, A.; Lakshminarayanan, V. *J. Mater. Chem., A* **2015**, *3*, 3019-3028.

[91] Rábai, J.; Szlávik, Z.; Horváth, I. T. In *Handbook Green Chemistry and Technology*; Blackwell Science Ltd.: 2007, p 502-523.

[92] Horváth, I. T. *Acc. Chem. Res.* **1998**, *31*, 641-650.

[93] Mathison, C.; Cole-Hamilton, D. In *Catalyst Separation, Recovery and Recycling*; Cole-Hamilton, D., Tooze, R., Eds.; Springer Netherlands: 2006; Vol. 30, p 145-181.

[94] Chen, L. D.; Mandal, D.; Gladysz, J. A.; Buhlmann, P. *New J. Chem.* **2010**, *34*, 1867-1874.

[95] Nakamura, H.; Linclau, B.; Curran, D. P. *J. Am. Chem. Soc.* **2001**, *123*, 10119-10120.

[96] Horváth, I. T.; Rábai, J. *Science* **1994**, *266*, 72-75.

[97] Horváth, I. T.; Kiss, G.; Cook, R. A.; Bond, J. E.; Stevens, P. A.; Rábai, J.; Mozeleski, E. J. *J. Am. Chem. Soc.* **1998**, *120*, 3133-3143.

[98] Richter, B.; Spek, A. L.; van Koten, G.; Deelman, B.-J. *J. Am. Chem. Soc.* **2000**, *122*, 3945-3951.

[99] Chechik, V.; Crooks, R. M. *J. Am. Chem. Soc.* **2000**, *122*, 1243-1244.

[100] Moreno-Mañas, M.; Pleixats, R.; Villarroya, S. *Organometallics* **2001**, *20*, 4524-4528.

[101] Yonezawa, T.; Onoue, S.-y.; Kimizuka, N. *Langmuir* **2001**, *17*, 2291-2293.

[102] Ipatiev, V.; Rutala, O. *Ber. Dtsch. Chem. Ges.* **1913**, *46*, 1748-1750.

[103] Eckert, C. A. *Nature* **1996**, *383*, 313-318.

[104] Jessop, P. G.; Leitner, W. *Chemical Synthesis using Supercritical Fluids*; Wiley & Sons: New York, 2008.

[105] Subramaniam, B.; McHugh, M. A. *Ind. Eng. Chem. Process Des.Dev.* **1986**, *25*, 1-12.

[106] Clifford, A.; Clifford, T. *Fundamentals of Supercritical Fluids*; Oxford University Press: New York, 1999.

[107] Ohde, H.; Wai, C. M.; Kim, H.; Kim, J.; Ohde, M. *J. Am. Chem. Soc.* **2002**, *124*, 4540-4541.

[108] Ohde, M.; Ohde, H.; Wai, C. M. *Chem. Commun.* **2002**, 2388-2389.

[109] Hou, Z.; Theyssen, N.; Brinkmann, A.; Leitner, W. *Angew. Chem. Int. Ed.* **2005**, *117*, 1370-1373.

[110] Kameo, A.; Yoshimura, T.; Esumi, K. *Colloids Surf., A* **2003**, *215*, 181-189.

[111] Zhao, F.; Ikushima, Y.; Arai, M. *J. Catal.* **2004**, *224*, 479-483.

[112] Gordon, R. S.; Holmes, A. B. *Chem. Commun.* **2002**, 640-641.

[113] Liao, W.; Chen, Y.-C.; Wang, J. S.; Yak, H. K.; Wai, C. M. *Ind. Eng. Chem. Res.* **2007**, *46*, 5089-5093.

[114] Spear, S. K.; Griffin, S. T.; Granger, K. S.; Huddleston, J. G.; Rogers, R. D. *Green Chem.* **2007**, *9*, 1008-1015.

[115] Subramaniam, B.; Akien, G. R. *Curr. Opin. Chem. Eng.* **2012**, *1*, 336-341.

[116] Jessop, P. G.; Phan, L.; Carrier, A.; Robinson, S.; Durr, C. J.; Harjani, J. R. *Green Chem.* **2010**, *12*, 809-814.

[117] Johnson, B. F. *Top. Catal.* **2003**, *24*, 147-159.

[118] Xia, Y.; Yang, H.; Campbell, C. T. *Acc. Chem. Res.* **2013**, *46*, 1671-1672.

[119] Johnson, B. F. *Coord. Chem. Rev.* **1999**, *190*, 1269-1285.

[120] Thompson, D. T. *Nano Today* **2007**, *2*, 40-43.

[121] Toshima, N. In *Nanoscale Materials*; Springer-Verlag: New York, 2003, pp 79-96.

[122] Astruc, D.; Lu, F.; Aranzaes, J. R. *Angew. Chem. Int. Ed.* **2005**, *44*, 7852-7872.

[123] Kavanagh, K. E.; Nord, F. F. *J. Am. Chem. Soc.* **1943**, *65*, 2121-2125.

[124] Cha, D. Y.; Parravano, G. *J. Catal.* **1970**, *18*, 200-211.

[125] Haruta, M.; Kobayashi, T.; Sano, H.; Yamada, N. *Chem. Lett.* **1987**, *16*, 405-408.

[126] Parker, H. L.; Rylott, E. L.; Hunt, A. J.; Dodson, J. R.; Taylor, A. F.; Bruce, N. C.; Clark, J. H. *PloS one* **2014**, *9*, e87192.

[127] Cho, K.; Wang, X.; Nie, S.; Shin, D. M. *Clin. Cancer Res.* **2008**, *14*, 1310-1316.

[128] Bayram, E.; Linehan, J. C.; Fulton, J. L.; Roberts, J. A. S.; Szymczak, N. K.; Smurthwaite, T. D.; Özkar, S.; Balasubramanian, M.; Finke, R. G. *J. Am. Chem. Soc.* **2011**, *133*, 18889-18902.

[129] Artero, V.; Fontecave, M. *Chem. Soc. Rev.* **2013**, *42*, 2338-2356.

[130] Yan, N.; Yuan, Y.; Dyson, P. J. *Dalton Trans.* **2013**, *42*, 13294-13304.

[131] Crabtree, R. H. *Chem. Rev.* **2012**, *112*, 1536-1554.

[132] Sonnenberg, J. F.; Morris, R. H. *Catal. Sci. Technol.* **2014**, *4*, 3426-3438.

[133] Widegren, J. A.; Finke, R. G. *J. Mol. Catal. A: Chem.* **2003**, *198*, 317-341.

[134] Glöggler, S.; Grunfeld, A. M.; Ertas, Y. N.; McCormick, J.; Wagner, S.; Schleker, P. P. M.; Bouchard, L.-S. *Angew. Chem. Int. Ed.* **2015**, *54*, 2452-2456.

[135] Umpierre, A. P.; de Jesus, E.; Dupont, J. *ChemCatChem* **2011**, *3*, 1413-1418.

[136] Xu, R.; Xie, T.; Zhao, Y.; Li, Y. *Nanotechnology* **2007**, *18*, 055602.

[137] Herrmann, W. A.; Kohlpaintner, C. W. *Angew. Chem. Int. Ed.* **1993**, *32*, 1524-1544.

[138] Coperet, C.; Chabanas, M.; Petroff Saint-Arroman, R.; Basset, J. M. *Angew. Chem. Int. Ed.* **2003**, *42*, 156-181.

[139] Finney, E. E.; Finke, R. G. *J. Colloid Interface Sci.* **2008**, *317*, 351-374.

[140] Finney, E. E.; Finke, R. G. *Chem. Mater.* **2008**, *20*, 1956-1970.

[141] Ott, L. S.; Finke, R. G. *Coord. Chem. Rev.* **2007**, *251*, 1075-1100.

[142] Ott, L. S.; Cline, M. L.; Finke, R. G. *J. Nanosci. Nanotechnol.* **2007**, *7*, 2400-2410.

[143] Ott, L. S.; Hornstein, B. J.; Finke, R. G. *Langmuir* **2006**, *22*, 9357-9367.

[144] Ott, L. S.; Finke, R. G. *Inorg. Chem.* **2006**, *45*, 8382-8393.

[145] Ott, L. S.; Campbell, S.; Seddon, K. R.; Finke, R. G. *Inorg. Chem.* **2007**, *46*, 10335-10344.

[146] Dash, P.; Scott, R. W. J. *Chem. Commun.* **2009**, 812-814.

[147] Wang, H.; Qiao, X.; Chen, J.; Wang, X.; Ding, S. *Mater. Chem. Phys.* **2005**, *94*, 449-453.

[148] Mu, X.-d.; Evans, D.; Kou, Y. *Catal. Lett.* **2004**, *97*, 151-154.

[149] Dash, P.; Miller, S. M.; Scott, R. W. J. *J. Mol. Catal. A: Chem.* **2010**, *329*, 86-95.

[150] Dash, P.; Dehm, N. A.; Scott, R. W. J. *J. Mol. Catal. A: Chem.* **2008**, *286*, 114-119.

[151] Yang, X.; Yan, N.; Fei, Z.; Crespo-Quesada, R. M.; Laurenczy, G.; Kiwi-Minsker, L.; Kou, Y.; Li, Y.; Dyson, P. J. *Inorg. Chem.* **2008**, *47*, 7444-7446.

[152] Zou, M.; Mu, X.; Yan, N.; Kou, Y. *Chin. J. Catal.* **2007**, *28*, 389-391.

[153] Zhao, C.; Wang, H.-z.; Yan, N.; Xiao, C.-x.; Mu, X.-d.; Dyson, P. J.; Kou, Y. *J. Catal.* **2007**, *250*, 33-40.

[154] Mu, X.-d.; Meng, J.-q.; Li, Z.-C.; Kou, Y. *J. Am. Chem. Soc.* **2005**, *127*, 9694-9695.

[155] Yuan, X.; Yan, N.; Xiao, C.; Li, C.; Fei, Z.; Cai, Z.; Kou, Y.; Dyson, P. J. *Green Chem.* **2010**, *12*, 228-233.

[156] Yan, N.; Yuan, Y.; Dyson, P. J. *Chem. Commun.* **2011**, *47*, 2529-2531.

[157] Duteil, A.; Schmid, G.; Meyer-Zaika, W. *J. Chem. Society, Chem. Commun.* **1995**, 31-32.

[158] Crooks, R. M.; Zhao, M.; Sun, L.; Chechik, V.; Yeung, L. K. *Acc. Chem. Res.* **2001**, *34*, 181-190.

[159] Scott, R. W. J.; Datye, A. K.; Crooks, R. M. *J. Am. Chem. Soc.* **2003**, *125*, 3708-3709.

[160] Ou, G.; Xu, L.; He, B.; Yuan, Y. *Chem. Commun.* **2008**, 4210-4212.

[161] Rodríguez-Pérez, L.; Pradel, C.; Serp, P.; Gómez, M.; Teuma, E. *ChemCatChem* **2011**, *3*, 749-754.

[162] Dykeman, R. R.; Yuan, Y.; Yan, N.; Asakura, H.; Teramura, K.; Tanaka, T.; Dyson, P. J. *ChemCatChem* **2012**, *4*, 1907-1910.

[163] Denicourt-Nowicki, A.; Leger, B.; Roucoux, A. *Phys. Chem. Chem. Phys.* **2011**, *13*, 13510-13517.

[164] Léger, B.; Denicourt-Nowicki, A.; Olivier-Bourbigou, H.; Roucoux, A. *Inorg. Chem.* **2008**, *47*, 9090-9096.

[165] Le Bras, J.; Mukherjee, D. K.; Gonzalez, S.; Tristany, M.; Ganchegui, B.; Moreno-Manas, M.; Pleixats, R.; Henin, F.; Muzart, J. *New J. Chem.* **2004**, *28*, 1550-1553.

[166] Léger, B.; Denicourt-Nowicki, A.; Olivier-Bourbigou, H.; Roucoux, A. *ChemSusChem* **2008**, *1*, 984-987.

[167] Salas, G.; Campbell, P. S.; Santini, C. C.; Philippot, K.; Costa Gomes, M. F.; Padua, A. A. H. *Dalton Trans.* **2012**, *41*, 13919-13926.

[168] Fernandez, F.; Cordero, B.; Durand, J.; Muller, G.; Malbosc, F.; Kihn, Y.; Teuma, E.; Gomez, M. *Dalton Trans.* **2007**, 5572-5581.

[169] Beier, M. J.; Andanson, J.-M.; Mallat, T.; Krumeich, F.; Baiker, A. *ACS Catal.* **2012**, *2*, 337-340.

[170] Schmid, G.; Emde, S.; Maihack, V.; Meyer-Zaika, W.; Peschel, S. *J. Mol. Catal. A: Chem.* **1996**, *107*, 95-104.

[171] Kraynov, A.; Mueller, T. E. In *Applications of Ionic Liquids in Science and Technology*; Handy, S., Ed.; INTECH Open Access Publisher, 2011.

[172] Scholten, J. D.; Leal, B. C.; Dupont, J. *ACS Catal.* **2012**, *2*, 184-200.

[173] Dupont, J. *Acc. Chem. Res.* **2011**, *44*, 1223-1231.

[174] Consorti, C. S.; Suarez, P. A. Z.; de Souza, R. F.; Burrow, R. A.; Farrar, D. H.; Lough, A. J.; Loh, W.; da Silva, L. H. M.; Dupont, J. *J. Phys. Chem. B* **2005**, *109*, 4341-4349.

[175] Fonseca, G. S.; Machado, G.; Teixeira, S. R.; Fecher, G. H.; Morais, J.; Alves, M. C. M.; Dupont, J. *J. Colloid Interface Sci.* **2006**, *301*, 193-204.

[176] Pensado, A. S.; Pádua, A. A. H. *Angew. Chem. Int. Ed.* **2011**, *50*, 8683-8687.

[177] Dupont, J.; Meneghetti, M. R. *Curr. Opin. Colloid Interface Sci.* **2013**, *18*, 54-60.

[178] Scholten, J. D.; Ebeling, G.; Dupont, J. *Dalton Trans.* **2007**, 5554-5560.

[179] Prechtl, M. H. G.; Campbell, P. S.; Scholten, J. D.; Fraser, G. B.; Machado, G.; Santini, C. C.; Dupont, J.; Chauvin, Y. *Nanoscale* **2010**, *2*, 2601-2606.

[180] Wang, R.; Xiao, J.-C.; Twamley, B.; Shreeve, J. n. M. *Org. Biomol. Chem.* **2007**, *5*, 671-678.

[181] Pucheault, M.; Vaultier, M. In *Ionic Liquids*; Kirchner, B., Ed.; Springer Berlin: Heidelberg, 2010; Vol. 290, pp 83-126.

[182] Yuan, X.; Sun, G.; Asakura, H.; Tanaka, T.; Chen, X.; Yuan, Y.; Laurenczy, G.; Kou, Y.; Dyson, P. J.; Yan, N. *Chem. Eur. J.* **2013**, *19*, 1227-1234.

[183] Giernoth, R. *Angew. Chem. Int. Ed.* **2010**, *49*, 2834-2839.

[184] Li, X.; Zhao, D.; Fei, Z.; Wang, L. *Sci. China, Ser. B: Chem.* **2006**, *49*, 385-401.

[185] Chiappe, C.; Pieraccini, D.; Zhao, D.; Fei, Z.; Dyson, P. J. *Adv. Synth. Catal.* **2006**, *348*, 68-74.

[186] Wang, F.; Tang, S.; Ma, H.; Wang, L.; Li, X.; Yin, B. *Chin. J. Chem.* **2014**, *32*, 1225-1232.

[187] Zvereva, E. E.; Grimme, S.; Katsyuba, S. A.; Ermolaev, V. V.; Arkhipova, D. A.; Yan, N.; Miluykov, V. A.; Sinyashin, O. G.; Aleksandrov, A. *Phys. Chem. Chem. Phys.* **2014**, *16*, 20672-20680.

[188] Yuan, J.; Mecerreyes, D.; Antonietti, M. *Prog. Polym. Sci.* **2013**, *38*, 1009-1036.

[189] He, H.; Luebke, D.; Nulwala, H.; Matyjaszewski, K. *Macromolecules* **2014**, *47*, 6601-6609.

[190] Pourjavadi, A.; Hosseini, S. H.; Doulabi, M.; Fakoorpoor, S. M.; Seidi, F. *ACS Catal.* **2012**, *2*, 1259-1266.

[191] Suarez, P. A. Z.; Dullius, J. E. L.; Einloft, S.; De Souza, R. F.; Dupont, J. *Polyhedron* **1996**, *15*, 1217-1219.

[192] Fonseca, G. S.; Domingos, J. B.; Nome, F.; Dupont, J. *J. Mol. Catal. A: Chem.* **2006**, *248*, 10-16.

[193] Dupont, J.; Scholten, J. D. *Chem. Soc. Rev.* **2010**, *39*, 1780-1804.

[194] Dyson, P. J.; Laurenczy, G.; Andre Ohlin, C.; Vallance, J.; Welton, T. *Chem. Commun.* **2003**, 2418-2419.

[195] Schwab, F.; Lucas, M.; Claus, P. *Angew. Chem. Int. Ed.* **2011**, *50*, 10453-10456.

[196] Narayanan, R. In *Nanocatalysis: Synthesis and Applications*; Polshettiwar, V., Asefa, T., Eds.; Wiley: New York, 2013, pp 405-442.

[197] Luska, K. L.; Moores, A. *Green Chem.* **2012**, *14*, 1736-1742.

[198] Chernavskii, P. A.; Peskov, N. V.; Mugtasimov, A. V.; Lunin, V. V. *Russ. J. Phys. Chem. B* **2007**, *1*, 394-411.

[199] Muzart, J. *Adv. Synth. Catal.* **2006**, *348*, 275-295.

[200] Kumełan, J.; Kamps, Á. P.-S.; Urukova, I.; Tuma, D.; Maurer, G. *J. Chem. Thermodyn.* **2005**, *37*, 595-602.

[201] Anthony, J. L.; Anderson, J. L.; Maginn, E. J.; Brennecke, J. F. *J. Phys. Chem. B* **2005**, *109*, 6366-6374.

[202] Lei, Z.; Dai, C.; Chen, B. *Chem. Rev.* **2014**, *114*, 1289-1326.

[203] Seddon, K. R.; Stark, A. *Green Chem.* **2002**, *4*, 119-123.

[204] Van Doorslaer, C.; Schellekens, Y.; Mertens, P.; Binnemans, K.; De Vos, D. *Phys. Chem. Chem. Phys.* **2010**, *12*, 1741-1749.

[205] Hosseini-Monfared, H.; Meyer, H.; Janiak, C. *J. Mol. Catal. A: Chem.* **2013**, *372*, 72-78.

[206] Mondal, A.; Das, A.; Adhikary, B.; Mukherjee, D. *J .Nanopart. Res.* **2014**, *16*, 1-10.

[207] Nagy, M.; David, K.; Britovsek, J. P.G.; Ragauskas, J.A. *Holzforschung* **2009,** *63*, 513-520.

[208] Mora-Pale, M.; Meli, L.; Doherty, T. V.; Linhardt, R. J.; Dordick, J. S. *Biotechnol. Bioeng.* **2011**, *108*, 1229-1245.

[209] Tadesse, H.; Luque, R. *Energy Environ. Sci.* **2011**, *4*, 3913-3929.

[210] Chen, J.; Huang, J.; Chen, L.; Ma, L.; Wang, T.; Zakai, U. I. *ChemCatChem* **2013**, *5*, 1598-1605.

[211] Yan, N.; Yuan, Y.; Dykeman, R.; Kou, Y.; Dyson, P. J. *Angew. Chem. Int. Ed.* **2010**, *49*, 5549-5553.

[212] Konnerth, H.; Zhang, J.; Ma, D.; Prechtl, M. H. G.; Yan, N. *Chem. Eng. Sci.* **2015**, *123*, 155-163.

[213] Chen, M.-Y.; Huang, Y.-B.; Pang, H.; Liu, X.-X.; Fu, Y. *Green Chem.* **2015**, *17*, 1710-1717.

[214] Banerjee, A.; Scott, R. W. J. In *Nanocatalysis: Synthesis and Applications*; Polshettiwar, V., Asefa, T., Eds.; Wiley: New York, 2013, pp 133-188.

[215] Kalviri, H. A.; Kerton, F. M. *Green Chem.* **2011**, *13*, 681-686.

[216] Ermolaev, V. V.; Arkhipova, D. M.; Nigmatullina, L. S.; Rizvanov, I. K.; Milyukov, V. A.; Sinyashin, O. G. *Russ Chem Bull* **2013**, *62*, 657-660.

[217] Zhu, Y.; Chuanzhao, L.; Biying, A. O.; Sudarmadji, M.; Chen, A.; Tuan, D. T.; Seayad, A. M. *Dalton Trans.* **2011**, *40*, 9320-9325.

[218] Luska, K. L.; Demmans, K. Z.; Stratton, S. A.; Moores, A. *Dalton Trans.* **2012**, *41*, 13533-13540.

[219] Geukens, I.; Fransaer, J.; De Vos, D. E. *ChemCatChem* **2011**, *3*, 1431-1434.

2 Highly Stable Noble Metal Nanoparticles in Tetraalkylphosphonium Ionic Liquids for *in situ* Catalysis

Herein, we evaluate the tetraalkylphosphonium family of ionic liquids as potential solvent-cum-stabilizers for transition metal NPs, and use stable Pd NPs synthesized in these ILs as quasi-homogeneous catalysts for hydrogenation reactions at ambient pressures. The influence of the IL anion on the stability of the synthesized NPs, and consequently on their catalytic efficiency is also probed.

This has been reprinted with minor changes from a previous publication ("Highly stable noble-metal nanoparticles in tetraalkylphosphonium ionic liquids for in situ catalysis", Abhinandan Banerjee, Robin Theron, Robert W J Scott, *ChemSusChem*, **2011**, *5*, 109-116, © 2011) with permission from John Wiley and Sons.

The author would like to acknowledge Robin Theron for her involvement in this study. The author's contributions to this report include: synthesis of all ionic liquids, synthesis of the NPs in the IL media, design and execution of the catalytic reactions, and design of the experiment related to the influence of the IL anions on the catalytic activities of the IL/NP systems. The experiments on the influence of the IL anions on the catalytic activities of the IL/NP systems were performed by Robin Theron. The author also analyzed the experimental results and prepared a manuscript from the same, which was revised by Dr. Scott prior to publication.

Highly Stable Noble Metal Nanoparticles in Tetraalkylphosphonium Ionic Liquids for *in-situ* Catalysis

Abhinandan Banerjee, Robin Theron, and Robert W.J. Scott
Department of Chemistry, University of Saskatchewan
110 Science Place, Saskatoon, Saskatchewan, Canada.

2.1 ABSTRACT

Au and Pd nanoparticles were prepared by lithium borohydride reduction of the metal salt precursors in tetraalkylphosphonium halide ionic liquids in the absence of any organic solvents or external nanoparticle stabilizers. These colloidal suspensions remained stable and showed no nanoparticle agglomeration over many months. A combination of electrostatic interactions between the coordinatively unsaturated metal nanoparticle surface and the ionic liquid anions, bolstered by steric protection offered by the bulky alkylated phosphonium cations, is likely to be the reason behind such stabilization. The halide anion strongly absorbs to the nanoparticle surface leading to exceptional nanoparticle stability in halide ionic liquids; other tetralkylphosphonium ionic liquids with non-coordinating anions such as tosylate and hexafluorophosphate show much lower affinities towards the stabilization of nanoparticles. Pd nanoparticles stabilized in the tetraalkylphosphonium halide ionic liquid were found to be stable, efficient and recyclable catalysts for a variety of hydrogenation reactions at ambient pressures with sustained activity. Aerial oxidation of the metal nanoparticles was seen to occur over time, and was readily reversed by re-reduction of oxidized metal salts.

2.2 Introduction

Nanosized materials have attracted extensive interest in recent years due to their unique structural and chemical properties which can often be modulated by changing parameters such as size, shape, and the surrounding environment of the nanomaterials.[1-5] Noble metal nanoparticles (NPs), in particular, have shown impressive catalytic abilities for reactions of both scientific and industrial importance.[6-9] While supported NPs have traditionally been used as heterogeneous catalysts for enhanced reusability and facile product recovery, recent research has been focused on their use as "quasi-homogeneous" catalysts.[10-12] "Quasi-homogeneous" nanocatalysis involves the synthesis and use of stable and catalytically active nanoparticles in solution, combining the benefits of catalyst modulation and recyclability without having to heterogenize a homogeneous catalyst.[13-15] While there is no dearth of either materials or methodologies for the synthesis of NPs in solution, their lack of thermodynamic stability and consequent tendency to agglomerate and precipitate often prevent their effective application as efficient catalytic systems.[16,17] To date, the electrostatic and/or steric protection that stabilizes such nanoparticles is introduced via addition of an external stabilizer; synthetic strategies where such stabilization is inherent in the reaction system are few and far between. While stabilizers such as poly(vinylpyrrolidone), poly-N-donor ligands, and molecular stabilizers such as alkanethiolates can stabilize MNPs, they can suffer from numerous disadvantages: very efficient capping ligands often passivate the catalytic activity of NPs, and the protective ligand may not be soluble in the medium of

dispersion of NPs.[18-22] Moreover, the concept of involving a secondary stabilizer in a catalyst system just for the sake of protection may have undesirable effects on the selectivity and the reactivity of the reaction being catalyzed. Herein we show a process involving the use of tetraalkylphosphonium halide ionic liquid solvents that allows for a robust and reusable catalytic NP system in the absence of organic solvents, secondary stabilizers, and excessive functionalization of the medium of dispersion.

In the last decade, many groups have shown that ionic liquids (ILs) can be used as an intriguing media for the stabilization of NPs.[23-26] Immobilization of nanoparticles by supporting them in an IL rather than on a surface provides catalytic centers in the liquid phase; indeed there have been many reports in the literature exploring the catalytic properties of NPs in imidazolium-based ILs since the pioneering work of Dupont and coworkers.[27-29] Well-defined Pd NPs have earlier been prepared in-situ and used for C-C coupling reactions such as Heck and Suzuki processes,[30-32] while we have shown that bimetallic NPs can be transferred from water to imidazolium ILs for efficient nanocatalysis.[33,34] The reasons behind such efforts can be understood if we consider the numerous attractive chemical properties of ILs such as limited volatility and flammability, recyclability, wide ranges of solubility and miscibility, structural tunability (through both the cation and anion), although their green credentials are a matter of debate.[35-38] In spite of these developments, the optimal strategies for NP stability in ILs are still being determined; there is some evidence that NP dispersions are inherently more stable in ILs due to the IL microstructure and/or weak interactions of the anions

and/or cations of ILs with the nanoparticle surface, though we have previously shown that inherent impurities in imidazolium ILs (such as unreacted 1-methylimidazole) and/or secondary stabilizers can dramatically affect stability.[39] In addition, "task-specific" functionalized imidazolium and pyridinium ILs with thiol, alcohol, and nitrile moieties have been used for the synthesis of NPs by many groups.[40-43]

The majority of research to date concerned with NP catalysts in ILs has involved imidazolium-based ILs, likely due to the moderate viscosities of room-temperature imidazolium ILs.[44] The room-temperature imidazolium ILs have feebly coordinating anions such as tetrafluoroborate and hexafluorophosphate with limited NP stabilization capabilities. Moreover, the imidazolium cation can undergo deprotonation in the presence of strong bases to form carbenes,[45] and hexafluorophosphate groups can undergo anion hydrolysis to produce strongly toxic HF at moderate temperatures.[46] Another class of ILs is the tetraalkylphosphonium family of ILs, which are much more stable in strongly basic media,[47] lower-cost, and are fairly chemical inert (though Wittig substitution reactions on the phosphonium center have been reported).[48] Several other groups have previously shown that tetraalkylphosphonium ILs can be used successfully for NP stabilization and catalysis. In particular, Kalviri et al. reported a Suzuki coupling reaction catalyzed by Pd NPs formed in phosphonium ILs in the absence of an external reductant; and it was postulated that the IL itself was acting as a reducing agent.[49] Yinghuai *et al.* used the same IL to prepare Ru NPs from an organometallic precursor with ethylene glycol as a reductant.[50] However, to the best of our knowledge, all the

tetraalkylphosphonium IL systems that have been studied to date have anions that either do not coordinate or coordinate weakly to metal surfaces. We were particularly intrigued by the P[6,6,6,14]X (X=Cl, Br) family of room-temperature ILs (where P[6,6,6,14] refers to the trihexyl(tetradecyl)phosphonium cation), given their striking structural resemblance to the quaternary ammonium surfactants that have already been used successfully for electrostatic NP stabilization.[51] We postulated that such P[6,6,6,14]X (X=Cl, Br) ILs would be particularly interesting to examine as efficient dual "solvent/stabilizers" for NP synthesis.

In this report, we outline the synthesis of a catalytic system of NPs dispersed in several tetraalkylphosphonium ILs in the absence of organic solvents and external stabilizers conventionally used for protection against NP agglomeration. Au and Pd NPs synthesized directly in P[6,6,6,14]X (X=Cl, Br) ILs showed prolonged stability over several months, while NPs formed in systems with weakly-coordinating tosylate and hexafluorophosphate anions showed poor stability towards aggregation. Pd NPs dispersed in the P[6,6,6,14]X (X=Cl, Br) ILs were found to be recyclable catalysts for the hydrogenation of olefinic alcohols, aromatic nitro compounds, 1,2-unsaturated carbonyls, and alkynes. The dependence of the catalytic activities on the nature of the IL used for dispersion of the NPs further confirms the important role played by the ILs in NP stabilization, and sheds light on the exact mechanism of protection against aggregation. In addition, we show that while both the Au and Pd NPs dispersed in P[6,6,6,14]X (X=Cl, Br) ILs are prone to oxidation in the presence of air, the NPs can be

easily regenerated via re-reduction of the metal salts to reform MNPs, thus enhancing the recyclability of such NP/IL composites.

2.3 Experimental

2.3.1 Materials

All chemicals except for the ones listed below were purchased from Sigma Aldrich and used as received. Tetrachloroauric acid, $HAuCl_4.4H_2O$ and potassium tetrachloropalladate, K_2PdCl_4, (both 99.9%, metals basis) were obtained from Alfa Aesar, and were stored under vacuum and flushed with nitrogen after every use. Trihexylphosphine (98%) as well as commercial samples of the ILs were generously donated by Cytec Industries Ltd. Commercial samples of ILs were dried under vacuum at 70°C for 10-12 h with stirring before use. Deuterated solvents were purchased from Cambridge Isotope Laboratories. 18 MΩcm Milli-Q water (Millipore, Bedford, MA) was used.

2.3.2 Synthesis of the tetraalkylphosphonium ILs

Synthesis of P[6,6,6,14]Cl and the generation of nanosized Au and Pd clusters in the IL were carried out using standard Schlenk-line techniques. For a typical synthesis of P[6,6,6,14]Cl, trihexylphosphine was added to a slight excess of 1-chlorotetradecane under nitrogen at 145^{0}C, stirred overnight, and vacuum-stripped to remove volatile impurities.[52] A transparent, pale-yellow viscous IL was generated in 90% yield. Chloride contents of the ILs prepared by metathesis were checked via $AgNO_3$ test. ^{1}H NMR and

^{31}P NMR spectra of the as-prepared samples matched with those obtained from literature. The commercial sample of P[6,6,6,14]Cl supplied by Cytec was of comparable purity. P[6,6,6,14]Br was synthesized by an identical procedure, and turned out to be a deep yellow viscous liquid obtained in 93% yield, and was also indistinguishable from the dried Cytec samples in terms of purity. The P[6,6,6,14]PF_6 was synthesized from P[6,6,6,14]Cl by an additional ion exchange step, where HPF6 was added drop-wise to ice-cold P[6,6,6,14]Cl under nitrogen and stirred overnight under ambient temperatures. The waxy white solid generated was washed repeatedly with de-ionized water until the washings failed to generate a precipitate upon reaction with a large excess of 0.05M $AgNO_3$ solution. It was then dried under vacuum, giving a yield of 95%. The P[4,4,4,1]OTs, P[4,4,4,1]OSO_3Me and P[6,6,6,14]$N(CN)_2$ ILs were donated by Cytec, and were moderately heated under vacuum to remove volatile impurities prior to use.

2.3.3 Synthesis of Pd and Au NPs in ILs

For the synthesis of Pd MNPs, 45 mg of K_2PdCl_4 (0.14 mmol on the basis of Pd content) was added under nitrogen to a 10mL sample of the IL at 80^oC (all the ILs studied are liquids at this temperature), and vigorously stirred to give a 14 mM solution. The solution was cooled to 60^oC, and a stoichiometric excess of $LiBH_4$ reagent (1.5 mL, 2.0 M in THF) was injected drop-wise into it over a period of five minutes. A brisk effervescence followed, and the entire solution turned brown, indicating nanoparticle formation. After the addition of $LiBH_4$, volatile impurities were removed by vacuum-stripping the system at 80^oC. The Pd NP solution thus obtained was stored under

nitrogen in capped vials until use. For the synthesis of Au MNPs, an identical solvent-free procedure was followed, except the reactions were done in air. Tetrachloroauric acid (20 mg, equivalent to 0.05 mmol of Au) was dissolved in 10 mL P[6,6,6,14]X (X=Cl, Br) at 80°C to give a golden yellow solution which turned violet and then wine-red upon drop-wise addition of 1.5 mL of a 2.0 M $LiBH_4$ reagent after cooling the solution down to 60°C.

2.3.4 General Procedure for Hydrogenation Reactions

Hydrogenation reactions were carried out in a Schlenk flask, with the stem connected to a H_2 gas source, and the sealed neck linked to a differential pressure gauge (Model 407910, Extech Instruments Corp. with a resolution of 0.001 atm and accuracy of 5% at 23±5°C). The hydrogen supply was stopped and the stopcock closed before the reactant was injected into the reaction vessel. The progress of the reaction was monitored by time-dependent measurement of the hydrogen pressure inside the sealed flask. The temperatures to which the reaction mixtures were heated, and the reaction times of the systems studied may be found in Table 1. The accuracy of the pressure data was verified by vacuum-stripping the product and leftover substrate from the reaction mixture and using ^1H NMR spectroscopy to determine the ratio between the product(s) and the unreacted substrate (if any) from their peak areas. In all cases, no significant difference was found between the two sets of data. The catalytic systems were used repeatedly for recyclability studies. Parameters such as turnover number (TON) and effective turnover frequency [TOF, (mol $_{hydrogen}$/ mol $_{metal}$). time^{-1}] could be determined

from the hydrogen pressure data. TOFs from NMR were also determined from the slope of linear plots of TON as a function of time, and were consistently found to be within 5% of values obtained by differential pressure measurements. Yields and product distributions were determined using relative quantification of distinct ^{1}H NMR peaks. To ensure reproducibility, each reaction was performed at least twice; the yields, etc., were found to vary by no more than ±1-2%.

2.3.5 Characterization

UV-Vis spectra were obtained using a Varian Cary 50 Bio UV-Visible spectrophotometer with a scan range of 300-800 nm and an optical path length of 1.0 cm. ^{1}H and ^{31}P NMR spectra were obtained using a Bruker 500 MHz Avance NMR spectrometer; chemical shifts were referenced to the residual protons of the deuterated solvent. TEM analyses of the Au and Pd NPs in different ILs, both before and after catalytic cycles, were conducted using a Philips 410 microscope operating at 100 keV. The samples were prepared by ultrasonication of a 1% solution of the MNP/IL solution in chloroform followed by drop-wise addition onto a carbon-coated copper TEM grid (Electron Microscopy Sciences, Hatfield, PA). To determine particle diameters, a minimum of 100 particles from each sample were manually measured from several TEM images using the ImageJ program.[53]

2.4 Results and Discussion

2.4.1 Synthesis of NPs in tetraalkylphosphonium ILs

Inherently stabilized Au and Pd NPs were synthesized in tetraalkylphosphonium ILs via *in-situ* $LiBH_4$ reduction, without the involvement of any organic solvents or secondary stabilizers. Since these ILs are considerably viscous, cooling of the product led to highly viscous systems; however, the viscosity was seen to reduce drastically upon heating.

TEM images of Au NPs synthesized P[6,6,6,14]Cl and P[6,6,6,14]Br are shown in Figure 2.1(a) and 2.1(e), respectively. The average size of the free Au NPs synthesized in P[6,6,6,14]Cl and P[6,6,6,14]Br determined from the TEM images was found to be 4.1 ± 0.7 nm and 5.4 ± 0.9 nm, respectively. This is in agreement with the UV-Vis spectra of the NPs [Figure 2.1(c)]. From the spectra, it can be seen that the Au NPs in P[6,6,6,14]Cl show a broad plasmon band at 520 nm after reduction. For Au NPs in P[6,6,6,14]Br, the plasmon band is signficantly shifted to higher wavelengths due to the larger average particle size. Au NPs synthesized in P[4,4,4,1]OTs aggregated quickly (TEM micrograph shown in [Figure 2.1(b)]) and precipitated within a day. Pd NPs synthesized in P[6,6,6,14]Cl had a deep brown color, as seen in Fig 2(b). A TEM of Pd NPs synthesized in P[6,6,6,14]Cl is shown in Figure 2.2(b); the average sizes of these particles was 2.3±0.6 nm. The UV-Vis spectrum, shown in Figure 2.2(d), shows an exponential rise in absorbance with decreasing wavelength which is typical of Pd NPs in solution.

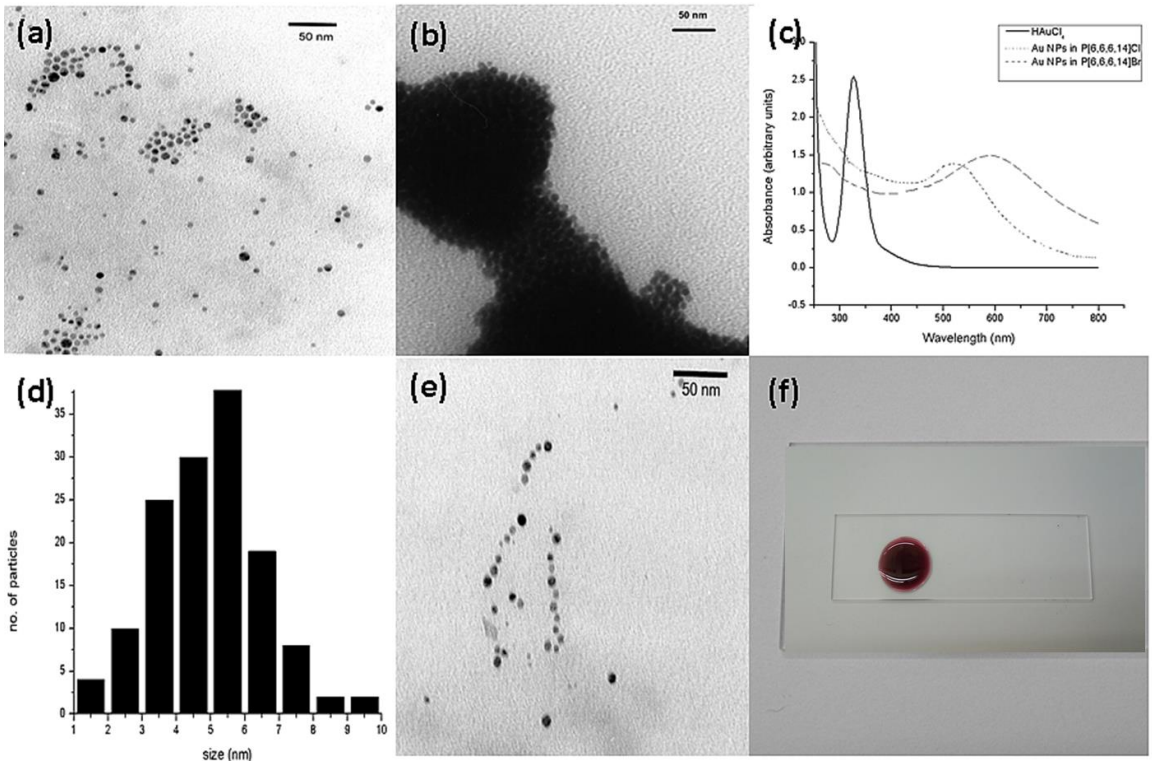

Figure 2.1 (a) TEM image of Au NPs prepared in P[6,6,6,14]Cl; **(b)** TEM image of Au NPs prepared in P[4,4,4,1]OTf; **(c)** UV-Vis spectra of 1.4 mM solutions of HAuCl4, Au NPs in P[6,6,6,14]Cl, and Au NPs in P[6,6,6,14]Br in cyclohexane, **(d)** Size distribution of Au NPs in P[6,6,6,14]Cl; **(e)** TEM image of Au NPs prepared in P[6,6,6,14]Br; **(f)** a drop of the wine-red Au NP/P[6,6,6,14]Cl on a clean glass slide.

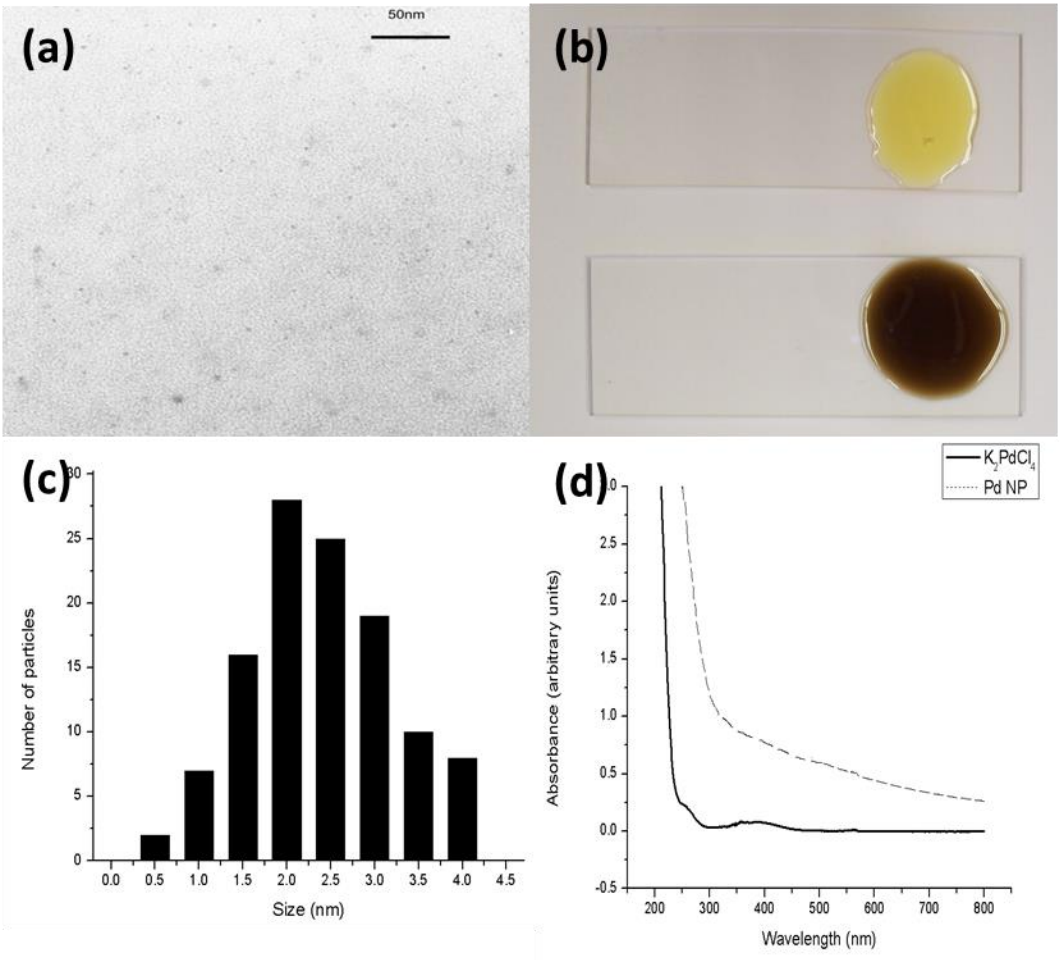

Figure 2.2 **(a)** TEM image of Pd NPs prepared in P[6,6,6,14]Cl; **(b)** (top) a drop of K_2PdCl_4 dissolved in P[6,6,6,14]Cl, (bottom) a drop of 14mM Pd NP in P[6,6,6,14]Cl on glass slides; **(c)** Size distribution of Pd NPs prepared in P[6,6,6,14]Cl; **(d)** UV-Vis spectra of 1.4 mM solutions of K_2PdCl_4 and Pd NPs in P[6,6,6,14]Cl in cyclohexane.

2.4.2 Nanoparticle stability and regeneration

The P[6,6,6,14]Cl-stabilized NPs remained unagglomerated for months under nitrogen. This stability is exceptional compared to that of NPs stabilized with poorly coordinating anions such as dicyanamide, tosylate, and methylsulfate in which

precipitation of the particles is seen within 12 to 24 h, or NPs stabilized directly in imidazolium ILs which tend to precipitate over several days or almost immediately under hydrogenation conditions.[33] Under air at elevated temperatures, NPs in the P[6,6,6,14]Cl IL show a very slow aerial oxidation, as the red Au(0) system turns colorless, and then pale yellow, likely due to oxidative etching of gold assisted by halide absorption on the surface, leading to the formation of Au(I), Au(III), or a mixture of both.[54] The Pd NPs in the P[6,6,6,14]Cl IL also oxidize upon heating in air. Oxidative etching of Pd in presence of O_2 and Cl^- is well-known; Kalviri *et al.* attribute their failure to grow Pd NPs in P[6,6,6,14]Cl in the absence of reductants to this effect.[49] In both cases the oxidized metal species could be readily re-reduced by drop-wise addition of excess $LiBH_4$. At ambient temperatures, this aerial oxidation was, however, extremely slow (proceeded over a period of months). For Pd NPs, heating of the system at 90°C in an atmosphere of oxygen for 48 h produced what closely resembled the orange-yellow precursor solution; re-reduction of this solution with $LiBH_4$ generated deep brown NPs. UV-Vis spectra before and after re-generation and TEM images of the particles after re-reduction are shown in Figure 2.3. For Au – which is known to offer greater resistance to oxidative etching than Pd – this method led to a partial decolorization of the NP dispersion. However, addition of ~2mL of ethanolic HNO_3 followed by heating at 90°C for 24 h and vacuum stripping of volatiles produced a golden-yellow solution, which turned wine-red upon $LiBH_4$ re-reduction. After oxidation and re-formation of the Pd and Au NPs in P[6,6,6,14]Cl, TEM analysis revealed the average particle sizes to be 3.9 ± 1.1 nm

and 3.5 ± 1.1 nm, respectively. The reasons for the moderate increase in Pd NP particle size are still unknown.

Borohydride reduction is a well-documented method for synthesis of NPs in conventional solvents, and its mechanism has been thoroughly studied.[55] Reduction of dissolved metal salts gives metal atoms in the embryonic stage of nucleation, followed by irreversible ion/atom or atom/atom collision producing metal cluster "seeds". It has been pointed out by Dupont *et al.* that there are electrostatic forces at play between the charged NP surfaces and the three-dimensional network of cations and anions that constitute the ILs.

Dupont proposed a two-phase system to explain imidazolium ionic liquid stabilization of NPs: a crystalline NP, and a semi-ordered IL phase.[56,57] A simpler model may be applied to the tetraalkylammonium phosphonium IL systems, (Scheme 1), in which the halide anions bind strongly to the metal surface and the associated bulky tetraalkylphosphonium cations offer steric protection. Indeed, significant work in with tetralkylammonium halide systems such as CTAB and TOAB have shown that halide absorption onto metal surfaces can lead to significant stability of the resulting particles.[58,59] Another significant validation for this model is the direct dependence of NP stability on the anion composition of the IL; the stronger the coordinating ability of the anion (e.g. chloride > tosylate), the greater the protection of the NP surface, which leads to increased stability of the NP in the IL.

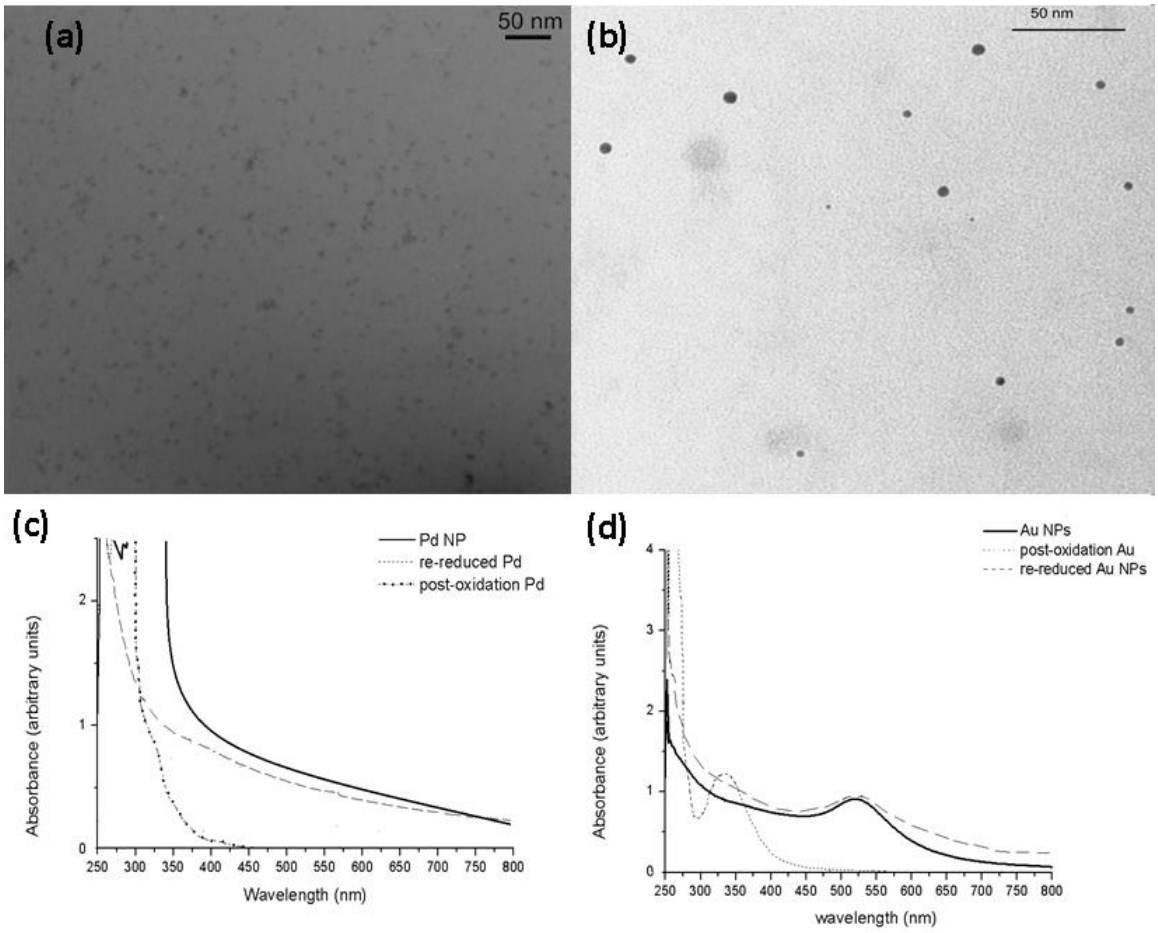

Figure 2.3 TEM images of **(a)** Pd NPs and **(b)** Au NPs in P[6,6,6,14]Cl regenerated after aerial oxidation followed by $LiBH_4$ reduction; and UV-Vis spectra of the re-reduction of **(c)** Pd NPs and **(d)** Au NPs in P[6,6,6,14]Cl.

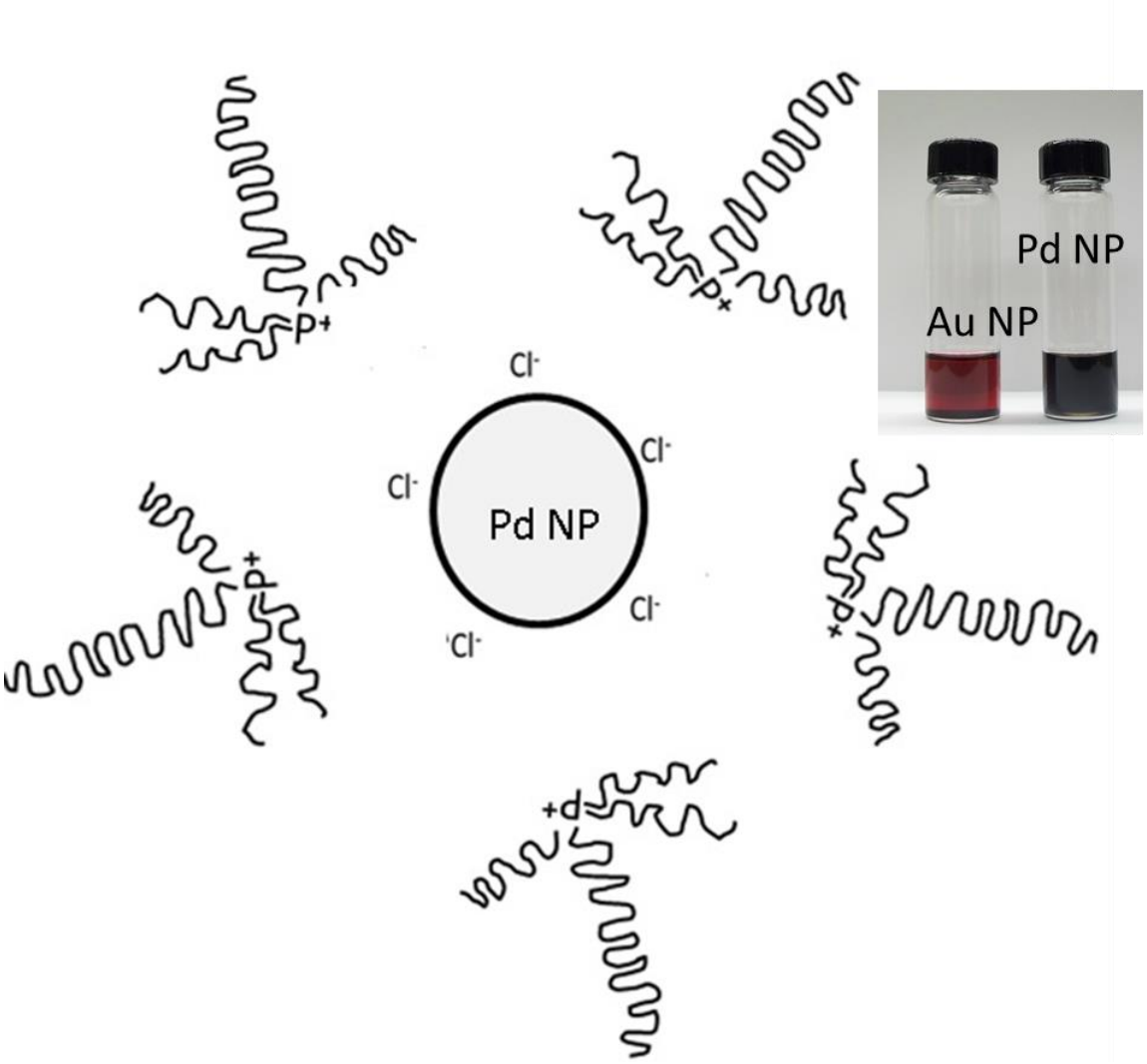

Scheme 2.1 Schematic representation of NP stabilisation by P[6,6,6,14]Cl IL; **inset** shows Au and Pd NPs in P[6,6,6,14]Cl stored in capped vials under nitrogen, two months after they were synthesized.

2.4.3 Application of Pd NPs in P[6,6,6,14]Cl IL for Catalytic Hydrogenations

The catalytic behavior of Pd NPs in P[6,6,6,14]Cl IL was evaluated via the hydrogenation of several organic compounds with unsaturated moieties present in their structures. Slightly elevated temperatures were necessary to reduce the viscosities of

the ionic liquids for attenuation of mass-transfer effects. While the solubility of hydrogen in ILs is moderate, it has also been observed that at higher temperatures, this solubility actually increases, in contrast to other gases such as CO_2.[60] Seminal work by Brennecke and colleagues showed the dependence of gas solubility in an ionic liquid on the nature of the anion present in it.[61] Earlier, Dyson *et al.* determined the Henry's Constant for hydrogen in P[6,6,6,14][$PF_3(C_2F_5)_3$] to be 700 bar at 293 K, which indicates that hydrogen is more soluble in many phosphonium ionic liquids than imidazolium or pyridinium ones by an order of magnitude.[62]

For the Pd NP/P[6,6,6,14]Cl system, most of the hydrogenations reached completion within a few hours. The progress of the reaction was followed by differential hydrogen pressure measurement, the details of which may be found in the experimental section. The monometallic Pd NPs in the P[6,6,6,14]Cl IL showed high catalytic activity and considerable stability. It was noted earlier that the mechanism of stabilization of NPs involves protective anchoring of the IL anions onto NP surfaces; the better the coordinating ability of the anion, the greater the stabilization provided by it to the MNP. Similarly, one should expect a similar trend in catalytic activities. This is borne out by Figure 2.4 which shows the hydrogenation of 2-methyl-3-butene-2-ol at 75°C by 14.0 mM Pd NPs in different ILs. The relative TOFs of this reaction over the first half-hour can be seen in Figure 2.3(b); with the largest TOF of 10.2 min^{-1} seen for P[6,6,6,14]Cl compared to just 1.8 min^{-1} for P[6,6,6,14]$N(CN)_2$. Traces of precipitate were observed in the reaction flask after completion of the reaction in case of Pd NPs in

P[6,6,6,14]N(CN)$_2$, P[4,4,4,1]OTs and P[4,4,4,1]OSO$_3$Me. It can be seen from Figure 2.4(b) that the TOFs increase in the following order: P[6,6,6,14]N(CN)$_2$ < P[4,4,4,1]OTs < P[4,4,4,1]OSO$_3$Me < P[6,6,6,14]PF$_6$ < P[6,6,6,14]Br << P[6,6,6,14]Cl. The activities here are substantial; we previously observed significantly lower TOFs (about 4.5 min^{-1}) for hydrogenations with PVP-stabilized Pd NPs in imidazolium ILs.[33]

From this order, a couple of trends emerge: namely, shorter alkyl chain-bearing tetraalkylphosphonium ILs are less efficient at protecting against agglomeration than those having longer chains, and the halides in general provide maximum stability to NPs leading to high catalytic activities. The first observation could easily be justified if we consider Scheme 2.1, where a surrounding layer of tetraalkylphosphonium ions is shown to offer steric protection to the MNPs; obviously, shorter alkyl chains would be less efficient in offering resistance to aggregation than longer ones. A number of other factors make P[6,6,6,14]Cl the best IL for Pd NP stabilization and catalysis. Ferguson and coworkers found that the diffusivity of many gases at 30°C was maximum in P[6,6,6,14]Cl,[63] and observed that gas diffusivity in phosphonium-based ILs is significantly higher than diffusivity in imidazolium-based ILs of equal viscosity. Indeed, P[6,6,6,14][NTf$_2$] with a viscosity of 200 cP has the same gas diffusivity as an imidazolium-based ionic liquid with a viscosity of 20 cP. The high gas diffusivity noted for P[6,6,6,14]Cl was attributed to the small size of Cl$^-$, which prevents it from competing with the diffusing gas molecules to fill the same microvoids within the IL. However, of greater importance here is the idea of NP stabilization by the anionic species of the IL. It

is seen that amongst all the ILs studied, the anion having the largest surface charge density is Cl^-. In other words, the catalytic activities of NPs dispersed in ILs depend overwhelmingly on the stability of the NPs in those ILs. Since Cl^- is capable of offering excellent electrostatic protection to the NP surface, it enhances the catalytic abilities of the NPs dispersed in Cl^- bearing ILs. A similar effect is observed for Br^-, but to a smaller extent, which may be explained by the larger size and smaller surface charge density of Br^-. All other anions show comparatively smaller catalytic efficiencies, and in the case of OTs^- and OSO_3Me^- ILs, precipitation of Pd NPs was seen within several days. The only IL that shows a slight deviation from this trend is P[6,6,6,14]PF_6, whose large, poorly coordinating anion should lead to poor NP stabilization: however, the comparatively higher stability of Pd NPs in this IL can be explained by the moderate Cl^- content of the IL of 200 ppm even after repeated washings (P[6,6,6,14]PF_6 was synthesized via ion exchange from P[6,6,6,14]Cl).

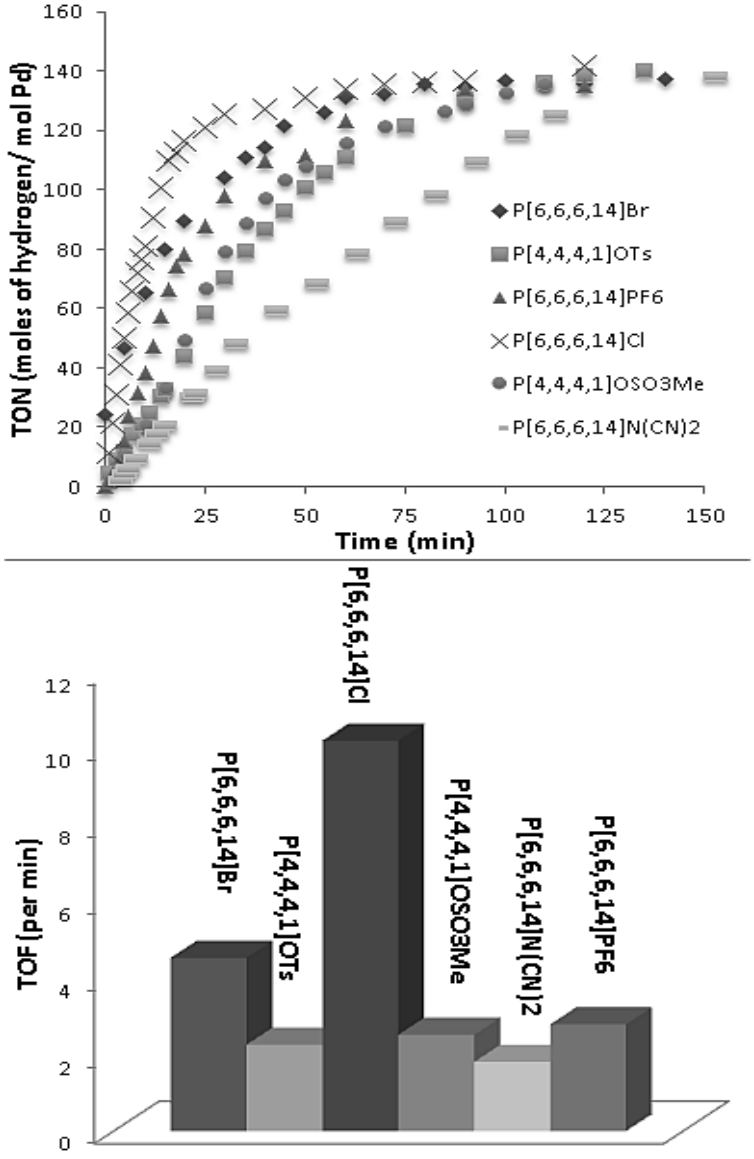

Figure 2.4 (a) TON vs. time plot for hydrogenation of 2-methyl-3-buten-2-ol by 14.0 mM Pd NPs in various phosphonium ILs.; **(b)** Comparison of the TOF (min^{-1}) of the reaction in different ILs.

The selectivity of a catalyzed reaction is also profoundly influenced by the surrounding environment of the catalyst. The Pd NPs in P[6,6,6,14]Cl were seen to catalyze the hydrogenation of various organic molecules with unsaturated moieties

(such as olefinic and acetylenic multiple bonds) in their structures. It can be seen from Table 2.1 that yields were almost quantitative, except for styrene, where polystyrene was also obtained. The aromatic moiety remained unaffected in all relevant reactions. The Pd NPs in P[6,6,6,14]Cl showed very high thermal stability to relatively elevated temperatures (up to about 140°C), thus a relatively higher reaction temperature was chosen for several of the hydrogenations. Arene hydrogenation, partial or complete, was not noted for any of the molecules containing aromatic rings.

Reactant	**Product**	**Conversion[(a)]**	**Temp.**	**Time (h)**
CH_2=$CHCMe_2OH$	$CH_3CH_2CMe_2OH$	>99%	75°C	2
Cyclohexene	Cyclohexane	90%	70°C	2.5
Styrene	Ethylbenzene	52%[(b)]	100°C	2
Nitrobenzene	Aniline	95%	115°C	6

Conditions: 1 mL of the substrate added to 10 mL, 14 mM Pd NP/P[6,6,6,14]Cl catalyst system, and heated at the given temperature for the given length of time under a hydrogen balloon. (a) Conversions calculated via relative quantization from the peak areas of individual, well-separated reactant and product peaks from ^{1}H NMR spectra; (b) poly(styrene) formation and precipitation of minute granules were observed.

Table 2.1 Catalytic hydrogenation of simple organic molecules with single products in the presence of Pd NP/P[6,6,6,14]Cl

Among the various organic molecules hydrogenated, the catalytic activity was seen to be the lowest for the hydrogenation of *trans*-cinnamaldehyde; this could be

because of the presence of highly conjugated unsaturation, along with steric effects of the bulky benzene ring attached to the double bond. The selectivity towards partial hydrogenation of 1,3-cyclooctadiene to generate cyclooctene (rather than the completely saturated cyclooctane) was investigated; this was seen to be a function of time and temperature of reaction. A 4.5 h reaction at 80°C not only reduced the extent of conversion to about 90%, but also gave more cyclooctene (78%, as opposed to 61% for a 8 h reaction at 110°C). Similar observations were recorded for trans-cinnamaldehyde and 3-hexyn-1-ol. For the former, a 5 h reaction at 90°C produced 79% 3-phenylpropanal and 21% of the phenyl alcohol; the extent of conversion was also seen to drop to about 85%. Note that another possible hydrogenation product, cinnamyl alcohol, was not seen at all. This is in accordance with previous results in other systems.[33] In the hydrogenation of 3-hexyn-1-ol, hexenols and hexanol were formed as the only products; for a 6 h reaction at 60°C, the respective yields were 18% and 82%. When the reaction time was reduced to 2.5 h, and the temperature to 55°C, the hexenol yield increased to 41%, while 59% hexanol was produced. Combined evidence, therefore, indicates that the hydrogenations proceed via the accepted Horiuti-Polanyi mechanism, with one unsaturated moiety reduced at a time. Obviously, exposure to hydrogen for smaller amounts of time and/or at a lower temperature favors the partially hydrogenated product. These observations have been summarized in Table 2.2.

Reactant	Product (Selectivity%)	Conversion[(a)]	Temp.	Time(h)
1,3-cyclooctadiene	Cyclooctene (61%) Cyclooctane (38%)	>99%	110°C	8
	Cyclooctene (78%) Cyclooctane (22%)	90%	80°C	4.5
3-hexyn-1-ol	3-hexen-1-ol (17%) 1-hexanol (82%)	>99%	100°C	6
	3-hexen-1-ol (41%) 1-hexanol(59%)	92%	115°C	2.5
Cinnamaldehyde	3-phenylpropionaldehyde (8%) 3-Phenyl-1-propanol (92%)	>99%	120°C	8
	3-phenylpropionaldehyde (21%) 3-Phenyl-1-propanol (79%)	85%	90°C	5

Conditions: 1 mL of the substrate added to 10 mL, 14 mM Pd NP/P[6,6,6,14]Cl catalyst system, and heated at the given temperature for the given length of time under a hydrogen balloon. (a) Conversions calculated via relative quantization from the peak areas of individual, well-separated reactant and product peaks from ^{1}H NMR spectra; later confirmed via GC-FID analysis.

Table 2.2 Catalytic hydrogenation of organic molecules with multiple hydrogenation products in the presence of Pd NP/P[6,6,6,14]Cl

The catalytic efficiency of the regenerated NPs in IL is shown in Figure 2.5, which shows the recyclability of this system for the hydrogenation of 2-methyl-3-

butene-2-ol. For the recyclability evaluation, the same system (Pd NPs in P[6,6,6,14]Cl) was used repeatedly for the reduction of 2-methyl-3-butene-2-ol at 75°C. For each cycle, the catalytic activity was obtained by differential pressure measurement of hydrogen inside the sealed reaction flask, the products and unreacted substrate removed by vacuum-stripping, and the catalyst system used for the next cycle. After removal of volatiles from the catalytic mixture, there was very little loss in activity for the hydrogenation of the substituted allyl alcohol (<5% after 5 cycles), confirming their re-usability/recyclability as catalysts. The physical appearance of the system could be seen from Figure 2.5(b); there were no significant differences either after 5 catalytic cycles, or after the oxidation/reduction procedure.

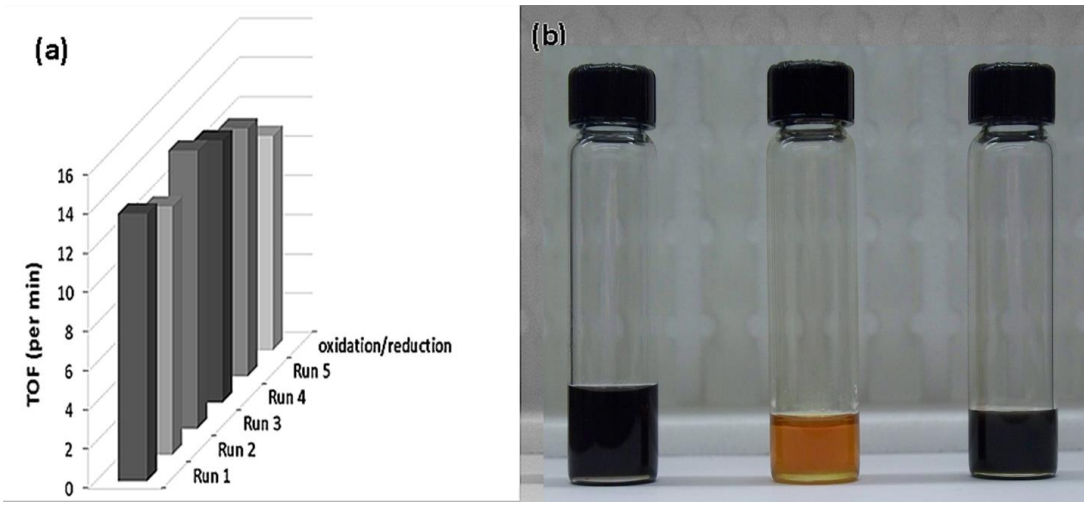

Figure 2.5 (a) Recyclability of Pd NPs prepared in P[6,6,6,14]Cl for for hydrogenation of 2-methyl-3-buten-2-ol. Final column shows TOF after complete Pd oxidation at 90°C in air over two days followed by re-reduction of the Pd with $LiBH_4$; (b) From left to right: 14mM Pd NPs in P[6,6,6,14]Cl after 5 catalytic cycles, after oxidation, and finally, after re-reduction with $LiBH_4$

However, it must be noted that moderate particle size growth was seen upon use of the Pd NPs as hydrogenation catalysts as shown in Figure 2.6(b); after 5 cycles the average size of the particles grew to 5.5 ± 1.9 nm. We are uncertain as to why this particle size growth is seen, but note that still no NP precipitation is seen in the system after multiple cycles. This growth could be reversed via Pd oxidation in air at elevated temperature followed by re-reduction of the Pd salts [(Figure 2.5(b)].

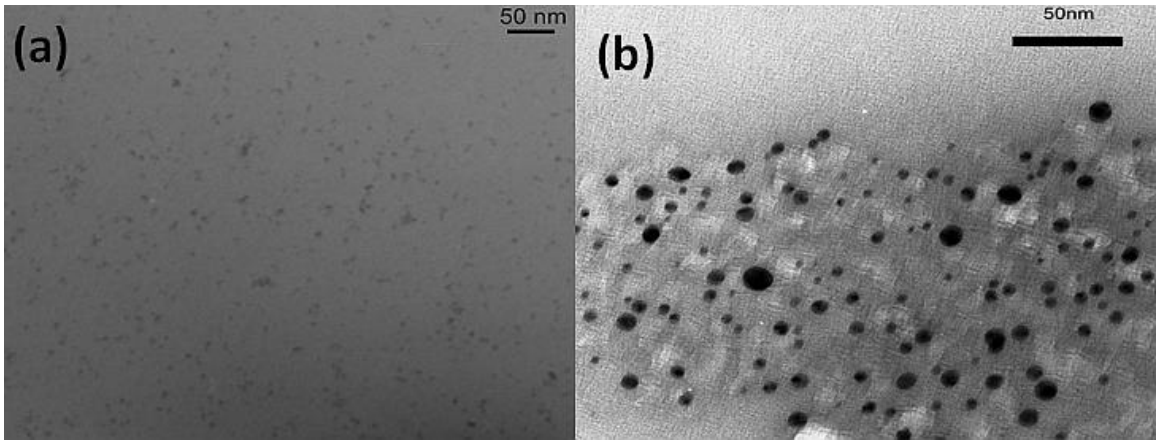

Figure 2.6 (a) TEM image of Pd NPs in P[6,6,6,14]Cl regenerated after aerial oxidation followed by $LiBH_4$ reduction**; (b)** TEM image of Pd NPs in P[6,6,6,14]Cl after 5 cycles of catalytic hydrogenations.

2.5 Conclusion

In summary, we have synthesized Au and Pd NPs in a variety of tetraalkylphosphonium ILs by in-situ reduction, without the use of any organic solvents. These NPs were seen to have stabilities ranging from days to months depending upon the composition of the IL. The Pd NPs showed excellent activities for the hydrogenation of a range of substrates (cyclohexene, 2-methyl-3-butene-2-ol, nitrobenzene, 1,3-cyclooctadiene, trans-cinnamaldehyde, and 3-hexyn-1-ol), with dihydrogen at ambient pressures. Unreacted substrates (if any) and products were easily removed from the catalytic mixture by vacuum treatment. The catalytic dispersions of Pd NPs in P[6,6,6,14]Cl were seen to be stable for months, highly recyclable, and could be readily regenerated after aerial oxidation.

Acknowledgements

The authors would like to thank NSERC and the University of Saskatchewan for funding, Dr. Pia Wennek for her help and support, and Tesfalidet Balcha for help with the TEM imaging and pictures of the samples. AB would like to acknowledge scholarships from the University of Saskatchewan and VWR. The authors would also like to express their gratitude towards Al Robertson of Cytec for donation of the phosphonium ILs as well at the phosphine precursors.

2.6 References

[1] Bonnemann, H.; Brijoux, W.; Brinkmann, R.; Dinjus, E.; Joussen, T.; Korall, B. *Angew. Chem. Int. Ed.* **1991**, *30*, 1312-1314.

[2] *Nanoparticles and Catalysis*; Astruc, D., Ed.; Wiley-VCH, Weinheim, 2008.

[3] Schmid, G. *Chem. Rev.* **1992**, *92*, 1709-1727.

[4] Roduner, E. *Chem. Soc. Rev.* **2006**, *35*, 583-592.

[5] Zeng, T.; Chen, W.-W.; Cirtiu, C.M.; Moores, A.; Song, G.; Li, C.-J. *Green Chem.*, **2010**, *12*, 570-573.

[6] Bonnemann, H.; Braun, G.; Brijoux, W.; Brinkmann, R.; Tilling, A.S.; Seevogel, K.; Siepen, K. *J Organomet. Chem.* **1996**, *520*, 143-162.

[7] Rao, C.N.R.; Kulkarni, G.U.; Thomas, P.J.; Edwards, P.P. *Chem. Soc. Rev.* **2000**, *29*, 27-35.

[8] Toshima, N.; Yonezawa, T. *New J. Chem.* **1998**, *22*, 1179-1201.

[9] Cirtiu, C.M.; Dunlop-Brière, A.F.; Moores, A. *Green Chem.*, **2011**, *13*, 288-291.

[10] Biffis, A.; Cunial, S.; Spontoni, P.; Prati, L. *J. Catal.* **2007**, *251*, 1-6.

[11] Rangheard, C.; Fernandez, C.-d.J.; Phua, P.-H.; Hoorn, J.; Lefort, L.; De Vries, J.G. *Dalton Trans.* **2010**, *39*, 8464-8471.

[12] Zhang, S. M.; Zhang, C. L.; Zhang, J. W.; Zhang, Z. J.; Dang, H. X.; Wu, Z. S.; Liu, W. M. *Acta. Phys. Chim. Sin.* **2004**, *20*, 554-556.

[13] Safavi, A.; Zeinali, S. *Colloids Surf. A: Physicochem. Eng. Aspects* **2010**, *362*, 121-126.

[14] Fonseca, G.S.; Domingos, J.B.; Nome, F.; Dupont, J. *J. Mol. Catal. A: Chem.* **2006**, *248*, 10-16.

[15] Salprima, Y.S.; Dhital, R.N.; Sakurai, H. *Tetrahedron Lett.* **2011**, *52*, 2633-2637.

[16] Schwarzer, H.-C.; Peukert, W. *AIChE J.* **2004**, *50*, 3234-3247.

[17] Manteghian, M; Ghader, S. *Chem. Eng. Technol.* **2009**, *32*, 835-839.

[18] Nagabhushana, K.S.; Bonnemann, H. In *Nanotechnology in Catalysis*; Zhou, B.; Hermans, S.; Somorjai, G.A., Eds.; Vol. 1; Kluwer Academic Plenum Publishers; New York, 2004; pp 51-82.

[19] Yan, N.; Yuan, Y.; Dyson, P.J. *Chem. Commun.* **2011**, *47*, 2529-2531.

[20] Calo, V; Nacci, A.; Monopoli, A.; Detomaso, A,; Iliade, P. *Organometallics* **2003**, *22*, 4193-4197.

[21] Mu, X.; Meng, J.; Li, Z.; Kou, Y. *J. Am. Chem. Soc.* **2005**, *127*, 9694-9695.

[22] Leger, B.; Denicourt-Nowicki, A.; Olivier- Bourbigou, H.; Roucoux, A. *ChemSusChem* **2008**, *1*, 984-987.

[23] Astruc, D.; Lu, F.; Aranzaes, J.R. *Angew. Chem. Int. Ed.* **2005**, *117*, 8062-8072.

[24] Dupont, J.; de Oliviera Silva, D. In *Nanoparticles and Catalysis*; D. Astruc, Ed.; Wiley VCH, 2008; p 195.

[25] Migowski, P.; Dupont, J. *Chem. Eur. J.*, **2007**, *13*, 32-39.

[26] Huang, J.; Jiang, T.; Gao, H.X.; Han, B.X.; Liu, Z.M.; Wu, W.Z.; Chang, Y.H.; Zhao, G.Y. *Angew. Chem. Int. Ed.* **2004**, *43*, 1397-1399.

[27] Suarez, P.A.Z.; Dullius, J.E.L.; Einloft, S.; DeSouza, R.F.; Dupont, J. *Polyhedron* **1996**, *15,* 1217-1219.

[28] Dupont, J.; Fonseca, G.S.; Umpierre, A.P; Fichtner, P.F.P; Teixeira, S.R. *J. Am. Chem. Soc.* **2002**, *124*, 4228-4229.

[29] Fonseca, G.S.; Umpierre, A.P; Fichtner, P.F.P.; Teixeira, S.R.; Dupont, J. *Chem. Eur. J.* **2003**, *9*, 3263-3269.

[30] Calo, V.; Nacci, A.; Monopoli, A,; Fornaro, A.; Sabbatini, L.; Cioffi, N.; Ditaranto, N. *Organometallics* **2004**, *23*, 5154-5158.

[31] Moreno-Manas, M.; Pleixats, R. *Acc. Chem. Res.* **2003,** *36*, 638-643.

[32] de Vries, J.G. *Dalton Trans.* **2006**, 421-429.

[33] Dash, P.; Dehm, N.A.; Scott, R.W.J. *J. Mol. Catal. A. Chem.* **2008**, *286*, 114-119.

[34] Dash, P.; Miller, S.; Scott, R.W.J. *J. Mol. Catal. A: Chem*., **2010**, *329*, 86-95.

[35] Freemantle, M. *An Introduction to Ionic Liquids;* RSC Publishing: Cambridge, 2010; Chapter 1.

[36] Kerton, F. M. *Alternative Solvents for Green Chemistry*, RSC Publishing: Cambridge, 2009; Chapter 6.

[37] Welton, T. *Green Chem.* **2011**, *13*, 225-226.

[38] Hallett, J.P.; Welton, T. *Chem. Rev.* **2011**, *111*, 3508-3576.

[39] Dash, P.; Scott, R.W.J. *Chem. Commun.* **2009**, 812-814.

[40] Luo, L.; Yu, N.; Tan, R.; Jin, Y.; Yin, D.; Yin, D. *Catal. Lett.* **2009**, *130*, 489-495.

[42] Stojanovic, A.; Kogelnig, D.; Fischer, L.; Hann, S.; Galanski, M.; Groessl, M.; Krachler, R.; Keppler, B.K. *Aust. J. Chem.*, **2010**, *63*, 511-524.

[43] Kim, K.S.; Demberelnyamba, D.; Lee, H. *Langmuir* **2004**, *20*, 556-560.

[44] Vilain, C.; Goettmann, F.; Moores, A; Le Floch, P.; Sanchez, C. J *Mater. Chem.* **2007**, *17*, 3509-3514.

[45] Sanchez, L.G.; Espel, J.R.; Onink, F.; Meindersma, G.W.; de Haan, A.B. *J. Chem. Eng. Data* **2009**, *54,* 2803-2812.

[46] Ott, L.S.; Cline, M.L.; M. Deetlefs,M.; K. R. Seddon, K.R.; R. G. Finke, R.G. *J. Am. Chem. Soc.* **2005**, *127*, 5758-5759.

[47] Freire, M.G.; Neves, C.M.S.S.; Marrucho, I.M.; Coutinho, J.A.P.; Fernandes, A.M. *J. Phys. Chem. A* **2010**, *114*, 3744-3749.

[48] Tseng, M.-C.; Kan, H.-C.; Chu, Y.-H. *Tetrahedron Lett.* **2007**, *48*, 9085-9089.

[49] Kalviri, H.A.; Kerton, F.M. *Green Chem.* **2011**, *13*, 681-686.

[50] Yinghuai, Z,; Widjaja, E.; Sia, S.L.P.; Zhan, W.; Carpenter, K.; Maguire, J.A.; Hosmane, N.S.; Hawthorne, M.F. *J. Am. Chem. Soc.* **2007**, *129*, 6507-6512.

[51] Bile, E.G.; Sassine, R.; Denicourt-Nowicki, A.; Launay, F.; Roucoux, A. *Dalton Trans.* **2011**, *40*, 6524-6531.

[52] Bradaric, C.J.; Downard, A.; Kennedy, C.; Robertson, A.J.; Zhou, Y.H. *Green Chem.* **2003**, *5*, 143-152.

[53] Woehrle, G. H.; Hutchison, J. E.; Ozkar, S.; Finke, R. G. *Turk. J. Chem.* **2006**, *30*, 1-13.

[54] Dasog, M.; Scott, R.W.J. *Langmuir,* **2007**, *23*, 3381-3387.

[55] Bonnemann, H.; Nagabhushana, K.S. In *Surface and Nanomolecular Catalysis*; Richards, R. Ed.; Taylor and Francis, 2006, Chap. 3, pp. 63-73.

[56] Hardacre, C.; Holbrey, J. D.; McMath, S. E. J.; Bowron, D. T.; Soper, A. K. *J. Chem. Phys.* **2003**, *118*, 273-278.

[57] Dyson, P. J.; McIndoe, J. S.; Zhao, D. B. *Chem. Commun.* **2003**, 508-509.

[58] Miranda, O. R.; Dollahon, N. R.; Ahmadi, T. S. *Cryst. Growth Des.* **2006**, *6*, 2747-2753.

[59] Chen, F. X.; Xu, G. Q.; Hor, T. S. A. *Mater. Lett.* **2003**, *57*, 3282-3286.

[60] Kumelan, J.; Kamps, A. P.-S.; Tuma, D.; Maurer, G. *J. Chem. Eng. Data* **2006**, *51*, 1364-1367.

[61] Anthony, J. L.; Anderson, J. L.; Maginn, E.J.; Brennecke, J.F. *J. Phys. Chem. B,* **2005**, *109*, 6366–6374.

[62] Dyson, P.J.; Laurenczy, G.; Ohlin, C.A.; Vallance, J.; Welton, T. *Chem. Commun.* **2003**, 2418-2419.

[63] Ferguson, L.; Scovazzo, P. *Ind. Eng. Chem. Res.* **2007**, 46, 1369-1374.

3 Oxidation of α,β-unsaturated Alcohols Using Sequentially-Grown AuPd Nanoparticles in Water and Tetraalkylphosphonium Ionic Liquids

Following our successful foray into the synthesis and catalysis of Pd NPs in tetraalkylphosphonium ILs, we attempted to gather more information about these unique NP-stabilizing solvent systems. It was essential for us to compare these systems to another, better-studied catalytic system, and Aimee Maclennan, who was investigating the chemistry of bimetallic NPs in water in the presence of PVP, became a collaborator in this comparative study. It was found that sequentially reduced AuPd NPs in IL were at least as good for the catalysis of α,β-unsaturated alcohol oxidation as their PVP-protected aqueous counterparts, and Pd NPs in IL decisively so, but they fared badly when it came to recyclability: AuPd NPs were stripped of their Pd shells, and bare Pd NPs showed non-negligible size and morphological changes, after one catalytic cycle. It was hypothesized that oxidative etching in tetraalkylphosphonium halides was responsible for this behavior. These results were highlighted in the 2013 Annual Research Report of the Canadian Light Source.

This has been reprinted with minor changes from a previous publication ("Oxidation of α,β-unsaturated Alcohols Using Sequentially-Grown AuPd Nanoparticles in Water and Tetraalkylphosphonium Ionic Liquids", Aimee Maclennan, Abhinandan Banerjee, Robert W J Scott, *Catal. Today*, **2013**, *207*, 170-179, © 2013), with permission from Elsevier. The first-author credit for this publication was shared by Abhinandan

Banerjee and Aimee Maclennan. Aimee Mclennan performed the catalytic experiments in water, as well as the EXAFS studies and associated data interpretation. IL-phase catalytic studies recorded in this paper were performed by Abhinandan Banerjee, who was also responsible for the preparation and editing of the manuscript. It is to be noted that this publication was previously included in the M.Sc. thesis of Aimee Maclennan.

Oxidation of α,β-unsaturated Alcohols Using Sequentially-Grown AuPd Nanoparticles in Water and Tetraalkylphosphonium Ionic Liquids

Aimee Maclennan, Abhinandan Banerjee, and Robert W.J. Scott
Department of Chemistry, University of Saskatchewan
110 Science Place, Saskatoon, Saskatchewan, Canada.

3.1 ABSTRACT

Metallic and bimetallic nanoparticles (Au, Pd, and AuPd NPs) were synthesized in water with PVP as a polymer stabilizer, as well as in tetraalkylphosphonium halide ionic liquids. A borohydride reduction technique was used for the preparation of the monometallic NPs, while a sequential reduction strategy was seen to generate the putative core-shell varieties. Pd and sequentially grown AuPd NPs were seen to serve as efficient catalysts for the oxidation of α,β-unsaturated alcohols, while the Au NPs themselves showed minimal activity. However, a system with both Au NPs and a Pd(II) salt (K_2PdCl_4) also efficiently catalyzed the oxidation reaction in water. A number of aliphatic and aromatic unsaturated alcohols were oxidized using oxygen as an oxidant with these as-prepared catalysts at 60^{o}C in the absence of base. TEM and EXAFS studies of the nanoparticle catalysts before and after the oxidation reaction revealed that the Pd(II) salt was reduced *in situ* during catalytic conditions, and that there was large changes in particle size and morphology after catalysis, which suggests Ostwald ripening, and the presence

of a redox mechanism. In the IL system, the ease of Pd reduction led to high activities for many α,β-unsaturated alcohols in the absence of the Au promoter.

3.2 Introduction

The oxidation of alcohols to their respective carbonyl compounds, although known to the scientific community since the 19th century,[1] continues to represent a major challenge as far as the industrial implementation of such processes is concerned. Traditionally, in the laboratory, such conversions have been performed using highly toxic transition metal compounds (such as chromium salts) in volatile and flammable organic solvents.[2] Such systems are rife with disadvantages: the reaction mixtures are inherently toxic, often corrosive, and the process can pose a serious threat to the environment if performed regularly on a large scale.[3] Another point worth noting is the probability of "over-oxidation" of primary alcohols in such systems, where the reaction proceeds to give the carboxylic acid rather than halt at the aldehyde stage. Moreover, from the standpoint of green chemistry, catalytic processes are preferred over stoichiometric ones. While the application of novel sources of oxygen such as ozone, PhOI, N-morpholine-N-oxide, or urea-hydrogen peroxide have notable utility, for industrial processes either air or oxygen are the oxidants of choice if they can be used safely, simply for the sake of accessibility and cost-effectiveness.[4]

Our group and many others are examining the "greening" of important chemical reactions by developing methods by which reactions of industrial importance (such as oxidations, hydrogenations, and so on) can be carried out in solvents ear-marked as

"green", and with catalysts that are readily recyclable, with high yields and minimal waste products (e.g. high selectivities). Stable metal nanoparticles (NPs) in solvents such as water, supercritical carbon dioxide, ionic liquids, or eutectic mixtures provide an alternative route to traditional homogeneous or heterogeneous catalysis.[5] In fact, such "quasi-homogeneous" nanocatalysis involving suspended nanoparticle catalysts in liquid media straddles the boundaries between homogeneous and heterogeneous catalysis, combining some of the advantages of both approaches. While the catalytic versatility of metal NPs is well-known, their tendency to agglomerate and precipitate in the absence of stabilizers can restrict their catalytic uses: however, several strategies have been successfully applied to minimize such catalyst deactivation, and many different reactions have been screened for potential application of quasi-homogeneous nanocatalysis.

After the pioneering work by Haruta, it is now well-known that Au NPs below a certain critical size are capable of efficient catalysis of oxidation reactions at low temperatures.[6] In 2005, Tsunoyama *et al.* showed that PVP-stabilised Au NPs in water selectively catalyze the oxidation of benzyl alcohol to benzaldehyde in the presence of base,[7-9] and many other groups have also reported alcohol oxidations with Au NPs,[3, 10-15] as well as enhanced activities for AuPd NPs for mild alcohol oxidations.[16-26] We previously studied alcohol oxidations in aqueous solutions using Au, Pd, and bimetallic AuPd NP catalysts in aqueous solutions, and determined that AuPd systems were much more reactive than their monometallic Au and Pd counterparts.[18] Recently, both

ourselves,[25] and others,[21, 24] have shown that core-shell AuPd NPs (either as-synthesized or synthesized *in situ* during reaction conditions) are particularly active for alcohol oxidations, with substantial activities and selectivities for α,β-unsaturated alcohols such as crotyl alcohol at room temperature in the absence of bases. However, it was not apparent how generic such results were to other alcohol systems, and what the dominant mechanism was in the reaction. In addition, not many of these studies comment on the recyclability of such nanoparticle systems. Catalytic oxidations in ionic liquids are rather less well-known than those in other media: even in cases where such studies have been carried out, the actual catalytic species are often transition metal complexes (such as methyltrioxorhenium,[27] OsO_4,[28] $RuCl_3$,[29] and so on), and/or the oxygen is harvested from novel oxidants rather than using molecular oxygen or air. Recently, heteropolyacids have been immobilised on imidazolium IL modified SBA-15 for alcohol oxidations,[30] and ILs such as choline hydroxide have also been used to stabilize Ru NPs on MgO supports for oxidations.[31] However, AuPd systems have not been well explored in IL systems to date.

In this study, the oxidation of a variety of α,β-unsaturated alcohols (aliphatic as well as aromatic) in the presence of molecular oxygen has been investigated. The catalytic systems of choice are Au, Pd, Au/Pd(II), and sequentially grown AuPd NPs, while the reaction media include water in the presence of PVP stabilizer as well as a tetraalkylphosphonium chloride IL capable of inherent NP stabilization. Careful growth of Pd shells on Au seeds using mild reductants such as ascorbic acid have been used to

generate sequentially grown AuPd NPs while minimizing secondary nucleation of Pd NPs. *In situ* formation of Pd shells on Au cores may also be achieved by the oxidation of the substrate itself, and concurrent reduction of Pd(II) in the presence of Au NPs, while individually each of these show very little catalytic activity. Similar catalytic NP systems are generated in trihexyl(tetradecyl)phosphonium halide ILs in the absence of any external stabilizers, and the resulting Pd NPs show high activities even in the absence of the Au promoter. Tentative mechanisms for α,β-unsaturated alcohol oxidation in water and in trihexyl(tetradecyl)phosphonium halide ionic liquids have been suggested, and the influence of the anion of the ionic liquid on the catalytic activity of the NPs is noted. Finally, TEM and EXAFS studies of core-shell catalyst before and after reaction, as well as of Au NP/Pd(II) salt after reaction has been conducted to study the structure of these NP catalysts, and results suggest that the initial step of the oxidation reaction with Au NPs in the presence of Pd (II) salts leads to *in situ* formation of AuPd catalysts. Since allylic aldehydes are valuable fine chemicals finding extensive use in the pharmaceutical, agrochemical and cosmetic industries, we believe it is worthwhile to seek clean technologies for their synthesis via atom-efficient oxidations that also address issues of catalyst reusability, environmental impact, waste disposal, and renewable feedstock.

3.3 Experimental

3.3.1 Materials

All chemicals except for the ones listed below were purchased from Sigma Aldrich and used as received. Poly(vinylpyrrolidone) (PVP) (M.W. 58,000 g/mol), tetrachloroauric acid, $HAuCl_4.4H_2O$ and potassium tetrachloropalladate, K_2PdCl_4, (both 99.9%, metals basis) were all obtained from Alfa Aesar, and the metal salts were stored under vacuum and flushed with nitrogen after every use. Commercial samples of the trihexyl(tetradecyl)phosphonium chloride (P[6,6,6,14]Cl) room-temperature ionic liquid (IL) were generously donated by Cytec Industries Ltd. Commercial samples of ILs were dried under vacuum at 70^oC for 10-12 hours with stirring before use. Deuterated solvents were purchased from Cambridge Isotope Laboratories. 18 MΩcm Milli-Q water (Millipore, Bedford, MA) was used throughout.

3.3.2 Synthesis of PVP stabilized Pd, Au and AuPd NPs in water

PVP-stabilized metallic and sequentially grown bimetallic NPs were synthesized by previously reported procedures;[18,25] metallic NPs were reduced using sodium borohydride while sequentially grown AuPd NPs were synthesized using ascorbic acid as the selective reducing agent for the Pd shell. To prepare the Au NPs (also used as "seed" particles), 50 mL of 0.35 mM PVP (1.75×10^{-5} mol) was added to 5 mL of 10 mM $HAuCl_4 \cdot 3H_2O$ (5×10^{-5} mol) and stirred at 800 rpm for 30 minutes. The solution was then placed on ice, stirring set to 1200 rpm, and 5 mL of 100 mM $NaBH_4$ (5×10^{-4} mol) was added quickly to the solution. The reaction was left to stir for 30 min on ice, and then

stirred for another 30 minutes at room temperature. To quench the reaction, 5 mL of 100 mM HCl (5×10^{-4} mol) was added to the solution and stirred for 30 min. To further stabilize the NPs, 35 mL of 1.0 mM PVP (3.5×10^{-4} mol) was added to the final solution and stirred for 30 min. The particles were dialyzed overnight using cellulose dialysis membrane with a molecular cut off of 12,400 g/mol under N_2. Pd NPs were synthesized using the same procedure, but K_2PdCl_4 was used instead of $HAuCl_4 \cdot 3H_2O$. The sequentially-grown 1:3 AuPd NPs were synthesized by mixing 100 mL of previously made Au "seed" particles (5×10^{-5} mol) with 15 mL of 100 mM ascorbic acid (1.5×10^{-3} mol) on ice, stirring at 800 rpm. To this solution, 15 mL of 10 mM K_2PdCl_4 (1.5×10^{-4} mol) was added then left to stir at 800 rpm on ice for 1 hour. Upon completion, the particles were dialyzed overnight in the same manner as the Au seed particles. For the generation of the Au NP/ Pd(II) system, an identical procedure was followed, except for the addition of ascorbic acid and the second dialysis step.

3.3.3 Synthesis of Pd, Au and AuPd NPs in IL

For the synthesis of Pd NPs in IL, 1.6 mg of K_2PdCl_4 (5.0×10^{-6} mol) was added to a 10 mL sample of the trihexyl(tetradecyl)phosphonium chloride IL mixed with 2 mL 1,4-dioxane at room temperature, and vigorously stirred. To this solution, a stoichiometric excess of $LiBH_4$ reagent (1.0 mL, 2.0 M in THF) was injected drop-wise over a period of five minutes.[32] A brisk effervescence followed, and the entire solution turned brown, indicating nanoparticle formation. After the addition of $LiBH_4$, volatile impurities including the dioxane were removed by vacuum-stripping the system at 70°C. The Pd NP

solution thus obtained was stored under nitrogen in capped vials until use. For the synthesis of Au NPs, a similar procedure was followed. Tetrachloroauric acid (2.0 mg, 5.0 x 10^{-6} mol) was dissolved in 10 mL P[6,6,6,14]Cl diluted with 2 mL 1,4-dioxane at room temperature to give a golden yellow solution which turned colorless, violet and then wine-red upon drop-wise addition of 1.0 mL of a 2.0 M $LiBH_4$ reagent. Excess $LiBH_4$ was quenched with methanol and volatiles were subsequently removed by vacuum-stripping. For the synthesis of sequentially grown AuPd NPs, a sequential reduction procedure was followed using the Au NP seeds as synthesized above, followed by the addition of 200 mg ascorbic acid added to the reaction medium. While stirring this mixture under ice, a 5 mL solution of K_2PdCl_4 (15.0 x 10^{-6} mol) dissolved in methanol was added to it all at once. The mixture was then stirred under ice for ~1 h, and volatiles were removed from it by vacuum-stripping. For the generation of the Au NP/Pd(II) system, an identical procedure was followed, except for the addition of ascorbic acid.

3.3.4 General Procedure for Oxidation Reactions

Oxidation reactions were carried out in a round-bottomed flask, sealed with a septum. In a general procedure, 10 mL of the NP solution (in water or IL) was stirred and heated to 60^{o}C under a flow of oxygen for about 10 min for aqueous systems, and for about 1 h in IL systems to compensate for the higher viscosity of the IL. After this, 500 or 5000 equivalents (based on 1 equivalent of metal catalyst) of the alcohol substrate was injected into the flask. For aqueous work, at incremental times 1.0 mL of the reaction mixture was sampled and the products were then extracted by two, 0.5 mL aliquots of

ethyl acetate, shaking in 1 minute intervals for 5 minutes per extraction. For IL samples, after ~12 h, the reaction vessel was removed from the constant temperature bath, and subjected to vacuum-stripping while being heated for extraction of the products and/or unreacted substrate. Conversion and selectivity were obtained from GC using a FID detector (Agilent Technologies 7890A) and a HP-Innowax capillary column. Two reactions were typically run for each sample. The neat organic liquids extracted were subsequently characterised by ^{1}H NMR, ^{13}C NMR, and GC-FID techniques. For GC-FID analysis, 25µL of a neat extract was mixed with 1 mL ethyl acetate in a GC-vial, and subjected to analysis. To ensure reproducibility, each reaction was performed at least twice; the yields, etc., were found to vary by no more than ±2-3% between different replicates of the experiment.

3.3.5 Characterization

UV-Vis spectra were obtained using a Varian Cary 50 Bio UV-Visible spectrophotometer with a scan range of 200-800 nm and an optical path length of 1.0 cm. ^{1}H and ^{13}C NMR spectra were obtained using a Bruker 500 MHz Avance NMR spectrometer; chemical shifts were referenced to the residual protons of the deuterated solvent. TEM analyses of the NPs in IL and water, both before and after catalytic cycles, were conducted using a Philips 410 microscope operating at 100 kV. The samples in IL were prepared by ultrasonication of a 1% solution of the NP/IL solution in DCM followed by drop-wise addition onto a carbon-coated copper TEM grid (Electron Microscopy Sciences, Hatfield, PA). To determine average particle diameters, a minimum of 100

particles from each sample were manually measured from several TEM images using the ImageJ program. The Hard X-ray Micro Analysis beamline (HXMA) 061D-1 (energy range, 5-30 keV; resolution, 1 x 10^4 ΔE/E) at the Canadian Light Source was used for recording X-ray absorption spectra at the Pd K-edge and the Au L_{III}-edge. The beamline optics include water-cooled collimating KB mirrors (Rh for the Au L_{III}-edge and Pt for Pd K-edge), and a liquid nitrogen cooled double crystal monochromator housing two crystal pairs Si (111) and Si (220). The X-ray measurements were conducted in an ion chamber filled with a helium and nitrogen mixture for the Au L_{III}-edge and pure helium for the Pd K-edge. The energy scan range for the measurement was between -200 eV to +1000 eV at each edge. Pd and Au foils were used for the respective edges as references. All EXAFS measurements were conducted in transmission mode at room temperature using samples trapped in alumina at 2.5% by weight metal and pressed into pellets.33 The software package IFEFFIT was used for data processing which included fitting the pre-edge region to a straight line, and the background above the edge was fit to a cubic spline function.[34, 35] The EXAFS function, χ, was obtained by subtracting the post-edge background from the overall absorption and then normalizing with respect to the edge jump step. The EXAFS fitting was performed in R-space between 1.4 to 3.4 Å for the Au edge and 1.4 to 3.0 Å for the Pd-edge using theoretical phase-shifts and amplitudes generated by FEFF. Bulk lattice parameters for an *fcc* system (i.e., first shell coordination numbers of 12) were used to determine the amplitude reduction factor, S_o^2, for Au and Pd by analyzing Au and Pd reference foils.[36]

3.4 Results and Discussion

3.4.1 Oxidation Reactions in Water

PVP-stabilized Au, Pd, sequentially grown 1:3 AuPd NPs and Au NP/Pd(II) 1:3 mixtures were synthesized. Figure 3.1(A, B) shows representative TEM images of samples of PVP-stabilized Au NPs and sequentially grown 1:3 AuPd NPs. Average particle sizes were found to be 2.9 ± 1.4 nm and 3.9 ± 1.7 nm for these systems, respectively, which is in general agreement with previous work, although the Au NP sample showed some larger particles present and thus were not as monodisperse as could be desired. Pd NPs were 2.7 ± 1.0 nm, which within error is similar to that of the Au NPs; particle sizes of all samples by TEM are listed in Table 3.1. The *ca.* 1 nm increase of size for the sequentially-grown particles is consistent with, but does not in itself prove, core-shell type growth of the particles. The UV-Vis spectra of Au, Pd, and sequentially grown 1:3 AuPd NPs are shown in Figure 3.2. There is a slight plasmon shoulder at ~530 nm in the Au NP sample, which is no longer apparent in the sequentially grown AuPd NP sample, which is similar to results seen before in this system,[25, 33, 37] and is in agreement with TEM results which suggest Pd growth on the Au NP seeds. However, no information about whether the final particles have specific structures (core-shell, cluster on cluster, etc.) can be obtained from this TEM and UV-Vis information alone.

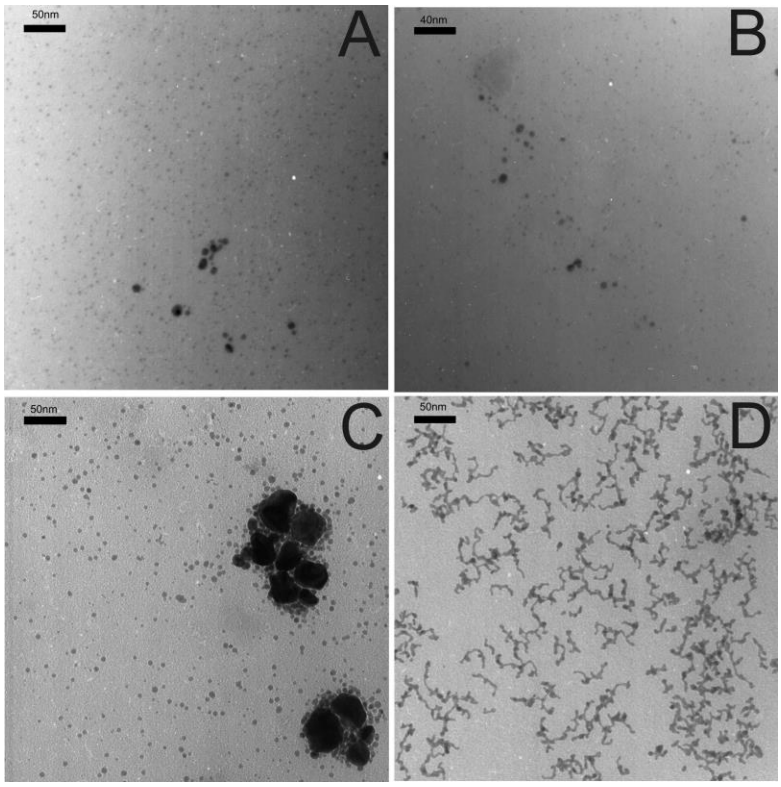

Figure 3.1 TEM images of PVP-stabilized (A) as-synthesized Au NP seeds and (B) as-synthesized sequentially-reduced 1:3 AuPd NPs and (C) Au NP/Pd(II) 1:3 mixture after 24 h reaction with cinnamyl alcohol and (D) sequentially-grown 1:3 AuPd NPs after 24 h reaction with cinnamyl alcohol.

Nanoparticle	Size in water (nm)	Size in ionic liquid (nm)
Au NPs	2.9 (1.4)	2.2 (0.8)
Pd NPs	2.7 (1.0)	4.3 (1.3)
1:3 AuPd Seq. Grown NPs	3.9 (1.7)	3.7 (1.0)
1:3 AuPd Seq. Grown NPs after reaction	--- [a]	8.0 (5.0)[b]
1:3 Au NPs/Pd(II) after reaction	6.4 (7.8)[b]	8.7 (3.9)
Pd NPs after reaction	---	9.0 (2.9)

[a] Particles formed worm-like structures; [b]Bimodal distribution of particles

Table 3.1 Summary of Nanoparticle Sizes obtained by TEM

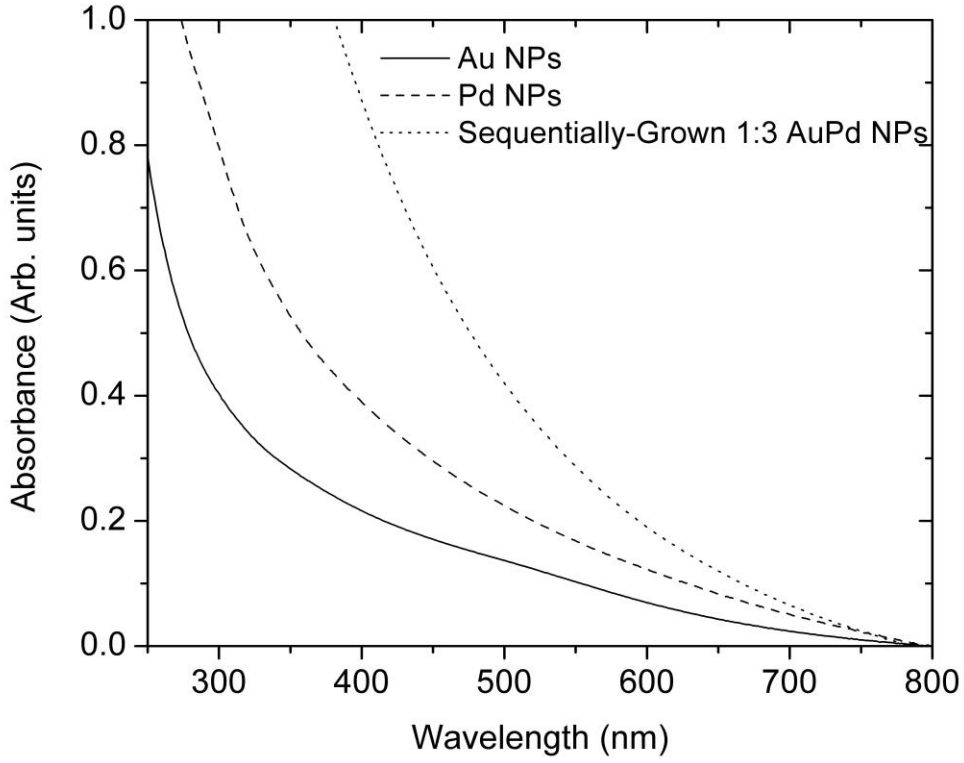

Figure 3.2 UV-Vis spectra of PVP-stabilized Au, Pd, and sequentially-grown 1:3 AuPd NPs in water.

We have previously shown that sequentially-grown PVP-stabilized 1:3 AuPd NPs were optimal catalysts for the room-temperature oxidation of crotyl alcohol in water in the absence of base;[25] however, it was noted in the previous study that crotyl alcohol was an unusual substrate in this regard (e.g. room temperature/base free activation) and other allyl and benzyl alcohols showed much lower activity at these conditions. We also noted in the previous study that Au NPs in the presence of Pd(II) salts (specifically K_2PdCl_4) also showed tremendous activity for crotyl alcohol oxidation activation at room temperature while the individual Au NPs and Pd(II) salts showed next to no activity, and hypothesized that in situ reduction of Pd onto the Au NPs was responsible for this activity.[25] Thus, in this study, we wished to test the generality of both the high activity of sequentially-grown 1:3 AuPd NPs for other allylic and benzylic alcohols (e.g. α,β-unsaturated alcohols) and whether the Au NP/Pd(II) salt mixtures showed strong activities for other substrates as well. In order to activate other allylic and benzylic alcohols with moderate conversions, it was necessary to increase reaction temperatures to 60^{o}C using 1 atm oxygen as the oxidant (but no external base has been added to the system). Catalysis results for the five chosen α,β-unsaturated alcohols are shown in Table 3.2, and the major and minor products are shown in Scheme 1. For all the systems studied, Au NPs showed no or next to no activity under these conditions. Results for the K_2PdCl_4 salt by itself were non-uniform; both cinnamyl alcohol and crotyl alcohol showed significant conversions over 24 hours in the presence of the Pd(II) salt alone, while the other substrates did not react to any significant extent. Similarly, Pd NPs by

themselves did not show significant activities for many substrates, although nearly 12% conversion was seen for allyl alcohol. Interestingly, both the sequentially-grown 1:3 AuPd NPs and the 1:3 Au NP/Pd(II) mixtures showed moderate activity for most substrates, typically with similar conversions and selectivities towards the aldehyde (or ketone in the case of 1-hexen-3-ol) product. For 1-hexen-3-ol, the 1:3 Au NP/Pd(II) mixture showed significantly higher reactivity, for reasons that are not known at this time. High selectivities towards the aldehyde product were seen for benzyl and cinnamyl alcohols, while moderate selectivities were seen in the crotyl alcohol reaction, in which significant hydrogenation and isomerization products were also seen at short time periods. For 1-hexen-3-ol, the major product of the reaction was actually the saturated ketone, 3-hexanone, which is an isomerization/tautomerization product (or a hydrogenation+oxidation product);[38,39] while the expected oxidation product, 1-hexen-3-one was formed in much lower amounts. Similarly, the major product for the allyl alcohol oxidation reaction was the isomerization/tautomerization product, 1-propanal. Similar reactivity of allyl alcohol to give large amounts of 1-propanal has been previously documented by our group using Pd catalysts under hydrogenation conditions.[39] The formation of minor hydrogenation products in many reactions can be attributed to a partial hydrogen coating on the NP surface, since it has been shown by Schwabe that even during oxidation of alcohols, the potential of Pt-group metals lie in the “hydrogen region”.[40]

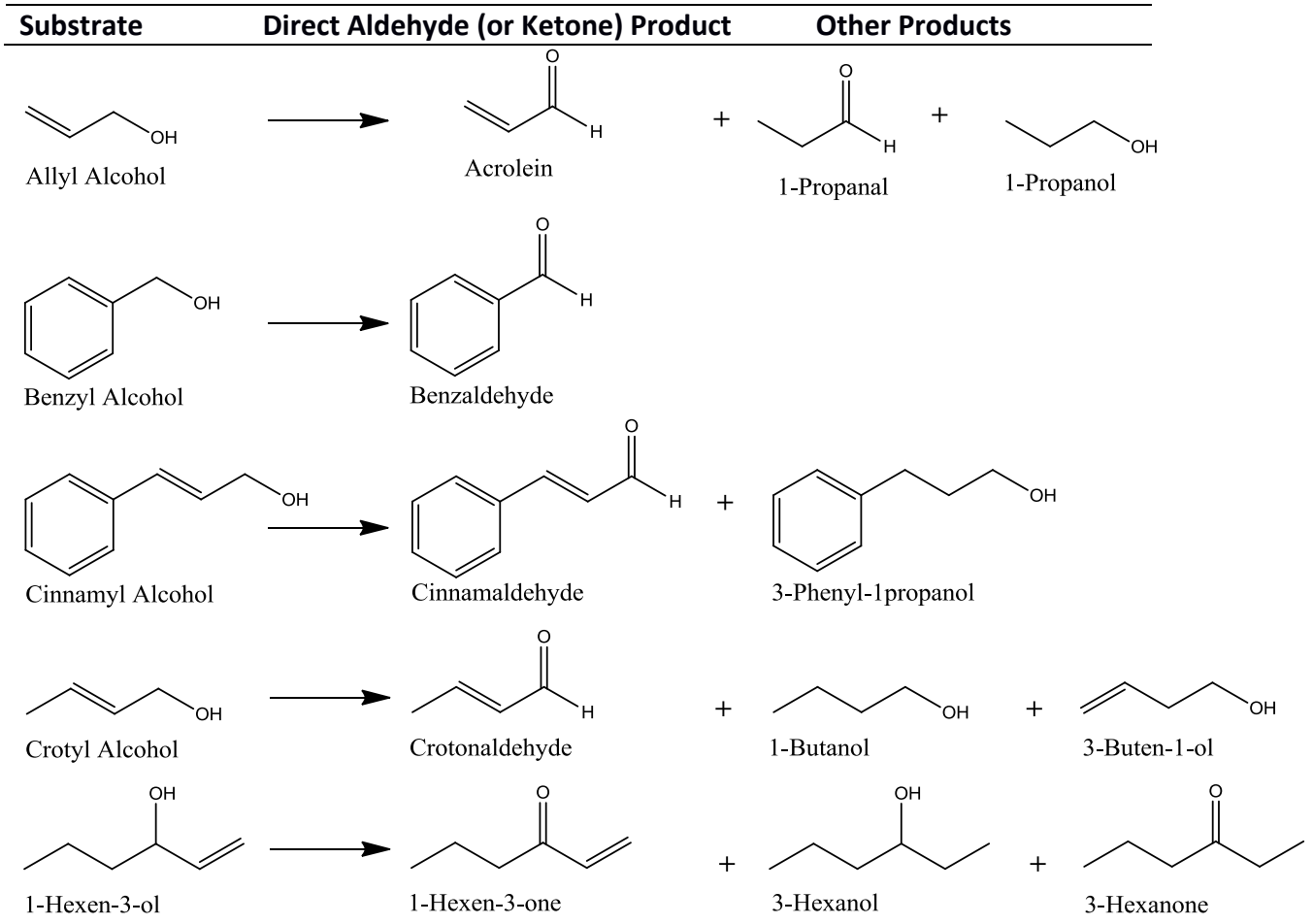

Scheme 3.1 Product distributions for oxidation of α,β-unsaturated alcohols

Substrate	NP Catalyst	Conversion[1]	Selectivity (%)	
			Aldehyde or Ketone	Other
Allyl Alcohol	Au NPs	0	0	0
	K_2PdCl_4	2	66	34
	Pd NPs	11.6	29	71[3]
	1:3 AuPd Seq. NPs	19.9	14	86[3]
	1:3 Au/Pd(II)	17.1	9	91[3]
Benzyl Alcohol	Au NPs	0	0	0
	K_2PdCl_4	2.3	100	0
	Pd NPs	2.7	100	0
	1:3 AuPd Seq. NPs	4.3	100	0
	1:3 Au/Pd(II)	3.1	100	0
Cinnamyl Alcohol	Au NPs	0	0	0
	K_2PdCl_4	34.3	96	4
	Pd NPs	6.8	100	0
	1:3 AuPd Seq. NPs	34.2	89	11
	1:3 Au/Pd(II)	29.3	90	10
Crotyl Alcohol	Au NPs	-	-	-
	K_2PdCl_4	14.0	34	66
	Pd NPs	-	-	-
	1:3 AuPd Seq. NPs	36.9	73	27
	1:3 Au/Pd(II)	37.9	65	35
1-Hexen-3-ol	Au NPs	0	0	0
	K_2PdCl_4	trace amounts	~97	~3
	Pd NPs	trace amounts	~37	~63
	1:3 AuPd Seq. NPs	17.3[2]	29	71[4]
	1:3 Au/Pd(II)	35.1[2]	27	73[4]

Reaction conditions: All reactions are carried out at 60°C with a substrate:catalyst ratio of 500:1. [1]Conversions and selectivities listed over 24h. [2]Conversions and selectivities listed after 4h. [3]Major product for allyl alcohol reaction 1-propanal (isomerization product), α,β-unsaturated ketone (prop-2-en-1-al) was minor product. [4]Major product for 1-hexen-3-ol reaction is 3-hexanone (isomerization product), α,β-unsaturated ketone (1-hexen-3-one) was minor product.

Table 3.2 Summary of Catalytic Results for the Oxidation of α,β-Unsaturated alcohols using PVP-stabilized NPs in water.

Interestingly, for crotyl alcohol, which we have previously shown can be activated at room temperature in the absence of base with excellent conversions and a high selectivity to crotonaldehyde,[25] the harsher reaction conditions (60^{o}C) here generally lead to lower overall conversions for both the AuPd NPs and Au NP/Pd(II) systems with moderate selectivities to crotonaldehyde; also, moderate decompositions to CO and propene were seen after 8 hours.[21,41] The reaction has a TOF of 120 moles product/moles catalyst h^{-1} over the first hour, which is comparable to earlier room-temperature work,[18, 25] followed by a drastic reduction in the reaction rate after 1 hour. We believe that the reduced TOF after one hour, and thus the lower overall conversions after 24 h, seen at these higher temperature conditions, are due to significant Ostwald ripening of the particles during the catalyst experiment. To further explore this, the nanoparticle catalysts were examined after the catalytic reaction. Figure 1(C, D) show the final TEM images of the Au NP/Pd(II) and sequentially-grown AuPd NP systems, respectively, after 24 h reaction. Significant growth in the NPs are seen in both systems; the Au NP/Pd(II) system showed a bimodal distribution with the presence of extremely large particles and an average particle size of 6.4 ± 7.8 nm, while the sequentially-grown AuPd NP system showed wormlike particles after the 24 h reaction (no particle size is reported due to the change in morphology). In the absence of a catalytic reaction (e.g. just heating to 60^{o}C) there is typically no change in average particle sizes in these systems. Both of these results suggest significant ripening of particles during the catalytic reaction, likely due to an Ostwald ripening mechanism. Previously we indicated

that the mechanism for this reaction may be a redox mechanism in which the Pd is oxidized to Pd(II) and reformed upon reaction with the alcohol substrate;[25] and others have also supported a Pd(II) oxidation mechanism.[24] Such a mechanism is likely to lead to homogeneous Pd(II) species in solution during the catalytic reaction which would greatly enhance Ostwald ripening. Indeed, others have shown that Pd(II) species can react stoichiometrically with many α,β-unsaturated alcohols.[42, 43] Thus the lower activities seen for crotyl alcohol at 60°C seems mostly due to the large changes seen in particle size during the reaction; at lower temperatures the Ostwald ripening is much slower, thus allowing for higher-surface area NPs to remain active for longer periods of time. We believe the role of the Au in this reaction is to destabilize the Pd to oxidation by oxygen, thus allowing the reaction to turnover.

Finally, in order to further examine both the structure of the sequentially grown AuPd NPs and the reaction product in the Au NP/Pd(II) system, EXAFS analysis of these systems was performed. Figure 3 shows the Au L_{III}-edge and Pd K-edge EXAFS spectra in k-space for the pure Au and Pd NPs, sequentially grown AuPd NPs, and the reaction product in the Au NP/Pd(II) system (after 24 h reaction with crotyl alcohol); high quality data was collected over a k-range from 0 to 14 for the Au edge and 0 to 10 for the Pd edge. Both the Pd and Au edge k-space data show that the reaction product in the Au NP/Pd(II) system has similar chemical environments around the Au and Pd absorber atoms as the as-synthesized sequentially grown AuPd NPs. The shift in periodicity on the Au k-space data suggests some alloying of Au and Pd in both the bimetallic samples.[33, 44,

[45] Figure 4 shows the experimentally obtained EXAFS data in R-space with the single-shell theoretical fits for sequentially grown AuPd NPs and the reaction product in the Au NP/Pd(II) system. For the bimetallic NPs, the Au and Pd EXAFS data of the same sample were simultaneously fit using the IFEFFIT software package.[35] High-quality fits have been obtained for both the bimetallic AuPd samples. We note that the Pd data shows significant Pd-Pd and Pd-Au coordination environments but minimal Pd-O and/or Pd-Cl contributions (a very small shoulder can be seen on the low r-side of the Pd data); thus during the reaction, the Pd(II) is definitively reduced to form bimetallic NPs in the Au NP/Pd(II) system. The structural fit parameters for the sequentially grown AuPd NPs and the reaction product in the Au NP/Pd(II) system generated from the EXAFS fitting parameters are presented in Table 3.3. In both cases, reasonable fits were obtained; however, higher errors in coordination number for the Pd nearest neighbour were seen, which is likely both due to the lower quality of Pd edge data and inhomogeneities in the actual samples (which are particularly evident in the TEM of the reaction product in the Au NP/Pd(II) system). Higher Pd loadings in sample may allow for quality data acquisition to higher k-space values in the future, though heterogeneity problems will likely compromise data quality regardless. We note that because of these errors one cannot make any definitive conclusions regarding the final structures of the AuPd particles; however, the EXAFS data unambiguously indicates that nearly all the Pd is in the zerovalent state in both systems, and that core-shell morphologies are unlikely as the total first shell Au coordination number (e.g. N[Au-Au] + N[Au-Pd]) is significantly

below the bulk fcc value of 12 for both systems. The moderate N[Au-Pd] and N[Pd-Au] values (albeit with high errors on the latter) also indicate that significant Au/Pd mixing is seen in both these systems.

Nanoparticle Sample	Shell	N	R (A^o)	ΔE^o(eV)	σ ^{2}(A^o ^{2})	R-factor
1:3 AuPd Sequentially Grown NPs	Au-Au	5.9 (0.8)	2.812 (0.008)	4.4 (0.5)	0.010 (0.001)	0.020
	Au-Pd	2.4 (0.4)	2.768 (0.009)		0.008 (0.001)	
	Pd-Pd	6.0 (2.6)	2.73 (0.02)	-4.1 (2.6)	0.008 (0.004)	
	Pd-Au	3.8 (2.5)	2.768 (0.009)		0.008 (0.001)	
1:3 Au NPs/ Pd(II) After Reaction	Au-Au	6.4 (0.7)	2.814 (0.007)	4.9 (0.4)	0.009 (0.001)	0.014
	Au-Pd	3.4 (0.4)	2.777 (0.007)		0.007 (0.001)	
	Pd-Pd	7.0 (3.1)	2.76 (0.02)	3.0 (1.2)	0.008 (0.004)	
	Pd-Au	2.9 (2.7)	2.777 (0.007)		0.007 (0.001)	

Table 3.3 EXAFS fitting parameters for AuPd NP systems.

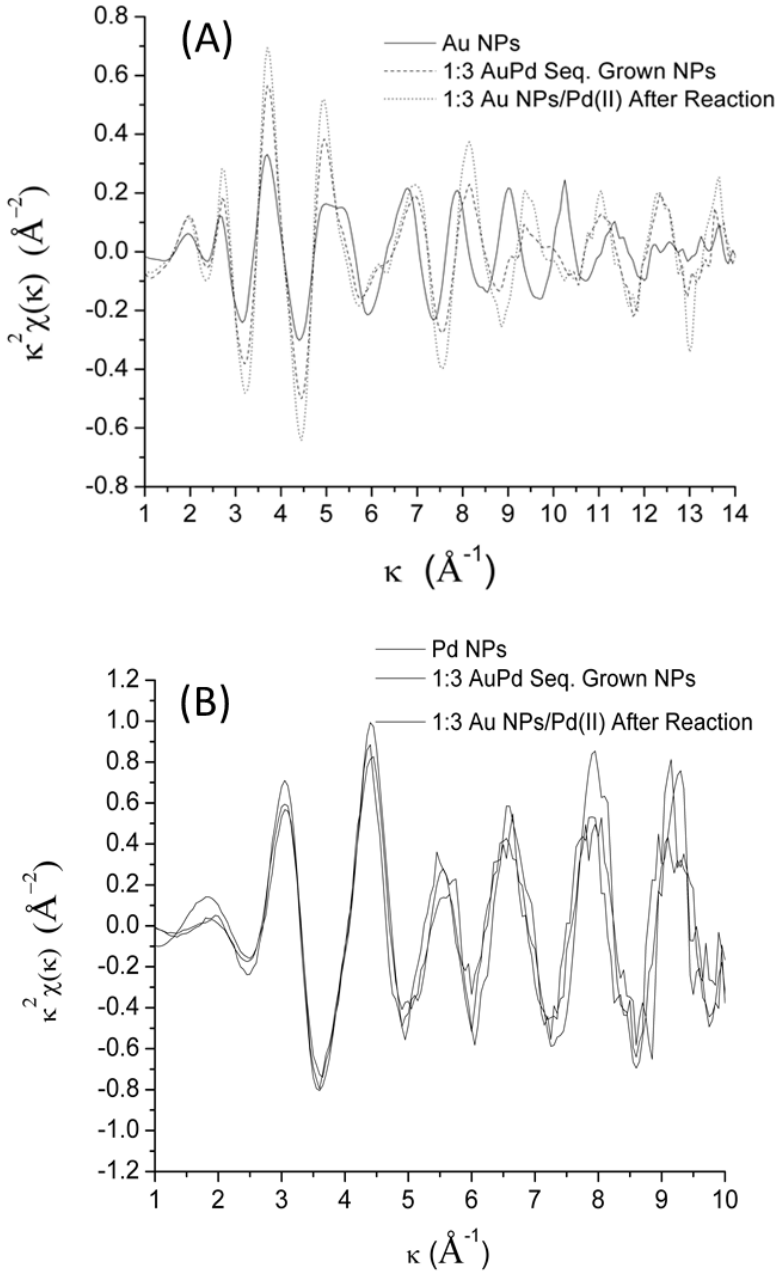

Figure 3.3 EXAFS spectra in k-space for monometallic Au, Pd and sequentially-grown 1:3 AuPd NPs and Au NP/Pd(II) 1:3 mixture after 24 h reaction with crotyl alcohol at: (A) Pd K-edge (B)Au-L_{III} edge.

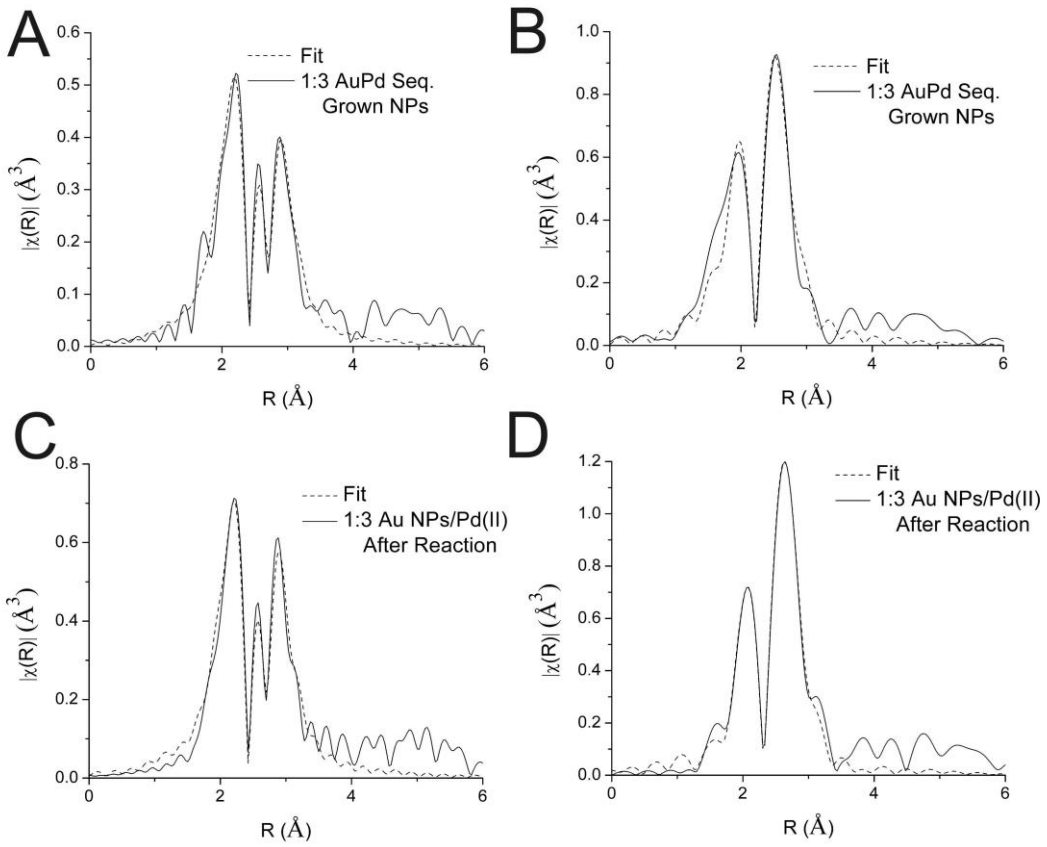

Figure 3.4 EXAFS single-shell fits in r-space for sequentially-reduced 1:3 AuPd NPs at the (A) Au-L_{III} and (B) Pd K edges and Au NP/Pd(II) 1:3 mixture after 24h reaction with crotyl alcohol at the (C) Au-L_{III} and (D) Pd K edges

3.4.2 Oxidation Reactions in ILs

We have recently shown that trihexyl(tetradecyl)phosphonium chloride IL is an excellent stabilizer for both Au and Pd NPs for hydrogenation reactions.[32] In this IL, the source of NP stabilization is thought to be two-fold: the halide ions that interact with the NP surface, and the long-chain hydrocarbons that provide steric protection in the form of a secondary coordination shell. Weaker coordinating anions such as BF_4^- were

found to have much lower stabilizing effects in previous work. As AuPd NP recyclability is a major challenge in the water system above (since the products need to be extracted using ethyl acetate or a similar solvent), we were curious as to whether the reaction could proceed in a more recyclable solvent system such as an IL. This system is attractive as it would allow for the products and un-reacted substrates to be removed from the reaction mixture by vacuum extraction, allowing for a potential re-use of the IL/NP catalyst system.

TEM images in Figure 3.6 show the Au, Pd NPs and sequentially grown 1:3 AuPd NPs before and after reaction. Before reaction, the Au, AuPd and Pd NPs are 2.2 ± 0.8 nm, 3.7 ± 1.0 nm, and 4.3 ± 1.3 nm respectively (see Table 3.1). The Pd NPs are larger than those formed in the aqueous system above, but in general agreement with our previous work.[32] The larger size of the NPs is confirmed by UV-Vis spectroscopy as shown in Figure 3.5; a significant plasmon band at 530 nm is seen for the Au NPs, which dampens significantly upon sequential Pd deposition. However, there is a significant growth of particles during a 12 h catalytic cycle, as seen in Figure 3.6(D, E, F); the Pd and Au NP/Pd(II) system grow to 9.0 ± 2.9 nm and 8.7 ± 3.9 nm, respectively, while the sequentially grown AuPd system shows a bimodal distribution with a significant number of particles above 10 nm. Since halide ions are also known to promote oxidative etching of Pd, NPs in halide ILs in the presence of oxygen form an unique system in which both Pd and Au oxidation can occur.[46] Evidently an Ostwald ripening mechanism in which Pd (and potentially Au as well) are oxidized and re-reduced upon stoichiometric reactions

with the alcohol substrates is occurring to an even greater extent in the IL system as compared to the aqueous system above, due to the extremely high chloride environment in these ILs.

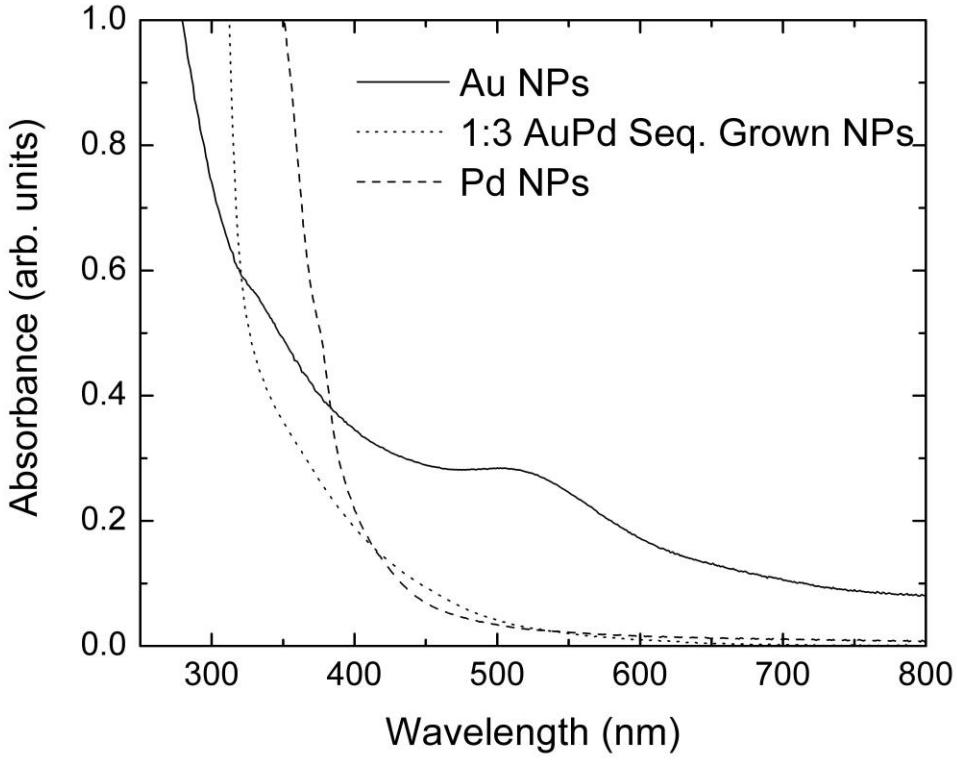

Figure 3.5 UV-Vis spectra of P[6,6,6,14]Cl IL -stabilized Au, Pd, and sequentially-grown 1:3 AuPd NPs.

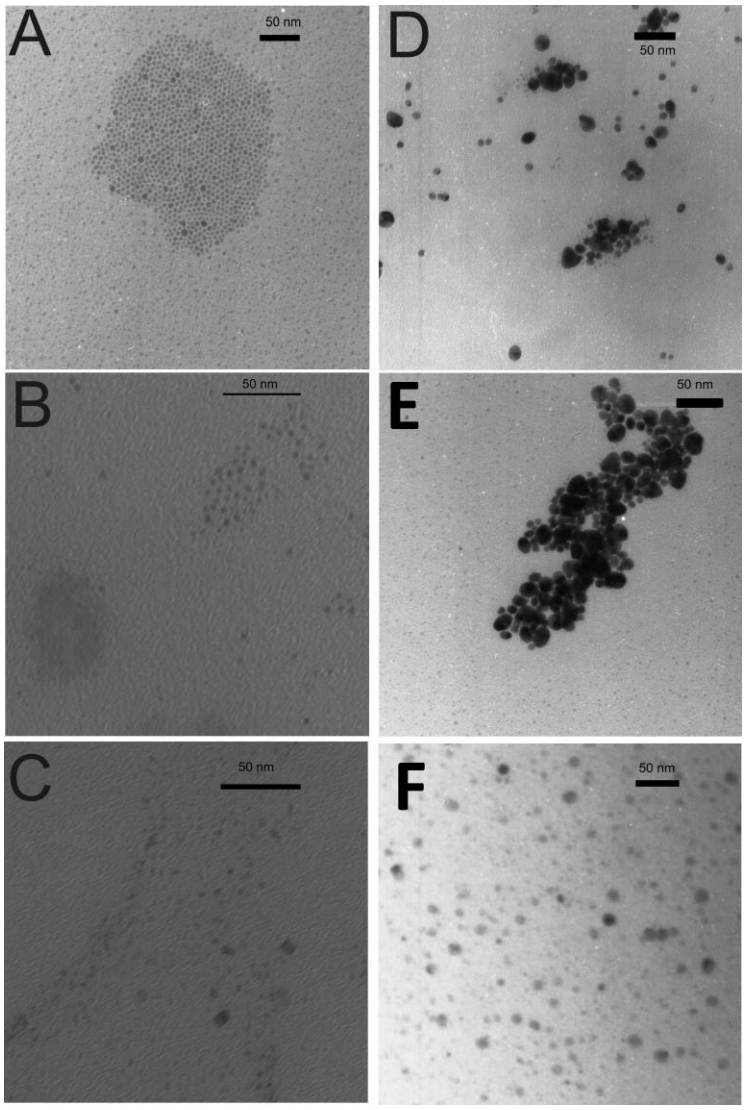

Figure 3.6 TEM images of as-synthesized P[6,6,6,14]Cl IL-stabilized (A) Pd NPs, (B) sequentially-reduced 1:3 AuPd NPs, and (C) Au NPs; and after 24 h reaction with cinnamyl alcohol: (D) Pd NPs, (E) sequentially-reduced 1:3 AuPd NPs, and (F) Au NP/Pd(II) 1:3 mixture.

Table 3.4 shows the product distributions for the catalytic oxidations of four of the various α,β-unsaturated alcohols in trihexyl(tetradecyl)phosphonium chloride. We

note that 5000:1 ratios of substrate to catalyst were used for the IL work, rather than the 500:1 ratios in the aqueous work, as vacuum stripping of the products and leftover substrates was more reliable at higher substrate levels and IL-stabilized NPs were still quite stable in the presence of larger amounts of substrate. While the Au NPs showed almost no catalytic activity in the absence of Pd(II) salts, but were active with Pd(II) salts present, Pd NPs and 1:3 AuPd NPs showed variable degrees of conversion for most of the substrates under the reaction conditions. Several things can be noted from the catalytic data; first, the overall conversions over 12 hours for reactions in the IL are in most cases much higher than their respective aqueous systems. In particular, aromatic systems such as benzyl alcohol and cinnamyl alcohol show extremely high conversions with high and moderate selectivities towards the aldehyde, respectively. Again, the major product for the allyl alcohol oxidation reaction is actually the isomerization/tautomerization product, 1-propanal (which could also be formed as a hydrogenation + oxidation product). The activities towards crotyl alcohol oxidation are somewhat similar to that of the aqueous system, albeit with significantly lower selectivities. In order to ensure that the change in substrate:catalyst ratio did not adversely affect the comparison of aqueous/IL systems, crotyl alcohol oxidation was examined in the IL system with a 500:1 substrate:product ratio, and similar yields and selectivities to crotonaldehyde were seen for both Pd NPs (62% conversion, 43% selectivity) and sequentially grown 1:3 AuPd NPs (66% conversion, 56% selectivity) systems. The major finding is that AuPd NPs show no exceptional abilities in terms of

catalytic performance and/or product selectivity compared to Pd NPs in this particular system, likely due to the ease at which Pd can be oxidized in this IL as compared to water. Indeed, we have previously noted facile oxidation of Pd NPs upon heating in the P[6,6,6,14]Cl ILs.[32] This easier oxidation of Pd in the IL system allows for higher turnovers of the redox catalytic cycle even in the absence of the Au promoter. Thus the Pd NP/IL system has some promise for the possibility of high activities for mild alcohol oxidations; however, in order to optimize the system, it would be desirable to attempt to minimize the particle growth occurring in the system.

Substrate	NP Catalyst	Conversion[1]	Selectivity (%)	
			Aldehyde	Other
Allyl Alcohol	Pd NPs	66	17	83[2]
	1:3 AuPd Seq. NPs	47	21	79[2]
	1:3 Au/Pd(II)	45	27	73[2]
Benzyl Alcohol	Pd NPs	97	99	1
	1:3 AuPd Seq. NPs	84	97	3
	1:3 Au/Pd(II)	90	98	2
Cinnamyl Alcohol	Pd NPs	99	70	30
	1:3 AuPd Seq. NPs	81	91	9
	1:3 Au/Pd(II)	98	74	26
Crotyl Alcohol	Pd NPs	53	47	53
	1:3 AuPd Seq. NPs	50	46	54
	1:3 Au/Pd(II)	50	58	42

Reaction conditions: All reactions are carried out at 60°C with a substrate:catalyst ratio of 5000:1. [1]Conversions and selectivities listed over 12 h. [2]Major product for allyl alcohol reaction is 1-propanal (isomerization product), α,β-unsaturated ketone (prop-2-en-1-al) was minor product.

Table 3.4 Summary of Catalytic Results for the Oxidation of α,β-Unsaturated Alcohols using P[6,6,6,14]Cl -stablized NPs

3.5 Conclusion

In summary, the present study considers the NP-catalyzed oxidation of α,β-unsaturated alcohols in water and in a tetraalkylphosphonium IL at 60°C. In water sequentially grown AuPd NPs, either formed intentionally or *in situ*, were found to be active for most α,β-unsaturated alcohols; although particle size growth due to Ostwald ripening was problematic. TEM and EXAFS studies of sequentially grown AuPd NPs and Au NP/Pd(II) mixtures indicated that both systems led to the formation of AuPd NPs with some mixing of Pd and Au in their structures. Conversely, we found that Pd NPs

alone have significant catalytic activity in tetraalkylphosphonium chloride ILs, likely due to the ease of oxidation of Pd in the high chloride environment. As such, Au promoters have little to no effect on Pd catalytic activity in the IL system. The concept of using a recyclable solvent in catalytic alcohol oxidations still remains a problem worthy of intensive research.

Acknowledgements

The authors would like to thank Dr. Weifeng Chen and Ning Chen at the Canadian Light Source (CLS) for the assistance with EXAFS measurements, Al Robertson at Cytec for donation of tetraalkylphosphonium chloride ionic liquids and NSERC and the University of Saskatchewan for funding. Some of the research described in this paper was performed at the Canadian Light Source, which is supported by the Natural Sciences and Engineering Research Council of Canada, the National Research Council Canada, the Canadian Institutes of Health Research, the Province of Saskatchewan, Western Economic Diversification Canada, and the University of Saskatchewan.

3.5 References

[1] March, J. *Advanced Organic Chemistry: Reactions, Mechanisms, And Structure*

Wiley: New York, 1992.

[2] Lee, D. G.; Spitzer, U. A. *J. Org. Chem.* **1970**, *35*, 3589-3590.

[3] Abad, A.; Almela, C.; Corma, A.; Garcia, H. *Chem. Commun.* **2006**, 3178-3180.

[4] Dyson, P. J.; Geldbach, T. J. Metal Catalyzed Reactions in Ionic Liquids. In *Catalysis By Metal Complexes*; James, B.; van Leeuwen, P.W.M.N., Eds.; Springer: The Netherlands, 2005; Vol 29, Chapter 2, pp 90-113.

[5] Astruc, D.; Lu, F.; Aranzaes, J. R. *Angew. Chem. Int. Ed.* **2005**, *44*, 7852-7872.

[6] Haruta, M. *Catal. Today* **1997**, *36*, 153-166.

[7] Tsunoyama, H.; Sakurai, H.; Negishi, Y.; Tsukuda, T. *J. Am. Chem. Soc.* **2005**, *127*, 9374-9375.

[8] Tsunoyama, H.; Tsukuda, T.; Sakurai, H. *Chem. Lett.* **2007**, *36*, 212-213.

[9] Tsunoyama, H.; Ichikuni, N.; Sakurai, H.; Tsukuda, T. *J. Am. Chem. Soc.* **2009**, *131*, 7086-7093.

[10] Prati, L.; Rossi, M. *J. Catal.* **1998**, *176*, 552-560.

[11] Enache, D. I.; Knight, D. W.; Hutchings, G. J. *Catal. Lett.* **2005**, *103*, 43-52.

[12] Li, H. R.; Guan, B. T.; Wang, W. J.; Xing, D.; Fang, Z.; Wan, X. B.; Yang, L. P.; Shi, Z. J. *Tetrahedron* **2007**, *63*, 8430-8434.

[13] Hu, J.; Chen, L.; Zhu, K.; Suchopar, A.; Richards, R. *Catal. Today* **2007**, *122*, 277-283.

[14] Casanova, O.; Iborra, S.; Corma, A. *J. Catal.* **2009**, *265*, 109-116.

[15] Liu, H.; Liu, Y.; Li, Y.; Tang, Z.; Jiang, H. *J. Phys. Chem. C* **2010**, *114*, 13362-13369.

[16] Enache, D. I.; Edwards, J. K.; Landon, P.; Solsona-Espriu, B.; Carley, A. F.; Herzing, A. A.; Watanabe, M.; Kiely, C. J.; Knight, D. W.; Hutchings, G. J. *Science* **2006**, *311*, 362-365.

[17] Dimitratos, N.; Lopez-Sanchez, J. A.; Lennon, D.; Porta, F.; Prati, L.; Villa, A. *Catal. Lett.* **2006**, *108*, 147-153.

[18] Hou, W. B.; Dehm, N. A.; Scott, R. W. J. *J. Catal.* **2008**, *253*, 22-27.

[19] Villa, A.; Janjic, N.; Spontoni, P.; Wang, D.; Su, D. S.; Prati, L. *Appl. Catal., A* **2009**, *364*, 221-228.

[20] Marx, S.; Baiker, A. *J. Phys. Chem. C.* **2009**, *113*, 6191-6201.

[21] Lee, A. F.; Hackett, S. F. J.; Hutchings, G. J.; Lizzit, S.; Naughton, J.; Wilson, K. *Catal. Today* **2009**, *145*, 251-257.

[22] Frank, A. J.; Rawski, J.; Maly, K. E.; Kitaev, V. *Green Chem.* **2010**, *12*, 1615-1622.

[23] Chen, Y. T.; Lim, H. M.; Tang, Q. H.; Gao, Y. T.; Sun, T.; Yan, Q. Y.; Yang, Y. H. *Appl. Catal., A* **2010**, *380*, 55-65.

[24] Wang, D.; Villa, A.; Spontoni, P.; Su, D. S.; Prati, L. *Chem. Eur. J.* **2010**, *16*, 10007-10013.

[25] Balcha, T.; Strobl, J. R.; Fowler, C.; Dash, P.; Scott, R. W. J. *ACS Catal.* **2011**, *1*, 425-436.

[26] Vinod, C. P.; Wilson, K.; Lee, A. F. *J. Chem. Tech. Biotech.* **2011**, *86*, 161-171.

[27] Owens, G. S.; Abu-Omar, M. M. *Chem. Commun.* **2000**, 1165-1166.

[28] Laszlo, J. A.; Compton, D. L. *J. Mol. Catal. B* **2002**, *18*, 109-120.

[29] Wolfson, A.; Wuyts, S.; De Vos, D. E.; Vankelecom, I. F. J.; Jacobs, P. A. *Tet. Lett.* **2002**, *43*, 8107-8110.

[30] Bordoloi, A.; Sahoo, S.; Lefebvre, F.; Halligudi, S. B. *J. Catal.* **2008**, *259*, 232-239.

[31] Kantam, M. L.; Pal, U.; Sreedhar, B.; Bhargava, S.; Iwasawa, Y.; Tada, M.; Choudary, B. M. *Adv. Synth. Catal.* **2008**, *350*, 1225-1229.

[32] Banerjee, A.; Theron, R.; Scott, R. W. J. *ChemSusChem* **2012**, *5*, 109-116.

[33] Dash, P.; Bond, T.; Fowler, C.; Hou, W.; Coombs, N.; Scott, R. W. J. *J. Phys. Chem.C.* **2009**, *113*, 12719-12730.

[34] Newville, M.; Ravel, B.; Haskel, D.; Rehr, J. J.; Stern, E. A.; Yacoby, Y. *Physica B.* **1995**, *208*, 154-156.

[35] Newville, M. *J. Synchrotron Radiat.* **2001**, *8*, 322-324.

[36] Maeland, A.; Flanagan, T. B. *Can. J. Phys.* **1964**, *42*, 2364-&.

[37] Scott, R. W. J.; Wilson, O. M.; Oh, S. K.; Kenik, E. A.; Crooks, R. M. *J. Am. Chem. Soc.* **2004**, *126*, 15583-15591.

[38] Bergens, S. H.; Bosnich, B. *J. Am. Chem. Soc.* **1991**, *131*, 5734-5735.

[39] Calver, C. F.; Dash, P.; Scott, R. W. J. *ChemCatChem* **2001**, *3*, 695-697.

[40] Müller, E.; Schwabe, K. *Z. Elektrochem. Angew. Phys. Chem.* **1928**, *34*, 170-172.

[41] Lee, A. F.; Chang, Z.; Ellis, P.; Hackett, S. F. J.; Wilson, K. *J. Phys. Chem. C.* **2007**, *111*, 18844-18847.

[42] Zaw, K.; Lautens, M.; Henry, P. M.; *Organometallics* **1983**, *2*, 197-199.

[43] Muzart, J. *Tetrahedron* **2003**, *59*, 5789-5816.

[44] Liu, F.; Wechsler, D.; Zhang, P. *Chem. Phys. Lett.* **2008**, *461*, 254-259.

[45] Knecht, M. R.; Weir, M. G.; Frenkel, A. I.; Crooks, R. M. *Chem. Mater.* **2008**, *20*, 1019-1028.

[46] Kalviri, H. A.; Kerton, F. M. *Green Chem.* **2011**, *13*, 681-686.

4 Redispersion of Transition Metal Nanoparticle Catalysts in Tetraalkylphosphonium Ionic Liquids

During the course of the two studies described in Chapters 1 and 2, we noticed that: (a) NP-sintering is a problem with metal NP/tetraalkylphosphonium ILs, especially during catalysis under high temperatures; and (b) the presence of an oxidant leads to rapid etching of Au and Pd NPs in tetraalkylphosphonium halides. In the field of heterogeneous catalysis, there are a few existing studies that seem to suggest that large gold agglomerates on solid supports could be reduced in size via oxidative etching using organic halides. Since halides ions were already present in our ILs, such an oxidative degradation of large metal micro- and nanostructures was expected to proceed smoothly in these ILs. Testing the generality of the protocol, especially in the context of hydrogenation reactions, where metal NP/IL catalysts have been used extensively, seemed to be a goal worth pursuing.

This has been reprinted after minor changes from a previous publication ("Redispersion of transition metal nanoparticle catalysts in tetraalkylphosphonium ionic liquids", Abhinandan Banerjee, Robin Theron, Robert W J Scott. *Chem. Commun*. **2013**, *49*, 3227-3229, © 2013), with permission from the Royal Society of Chemistry.

The author would like to acknowledge Robin Theron for her involvement in this study. The author's contributions to this report include: design of a strategy for the dissolution of sintered NPs in tetraalkylphosphonium halide ILs, evaluation of the

generality of the redispersion strategy, kinetic profiling of Au and Ni NP etching, and application of different oxidants for accelerated NP digestion in ILs. Time-resolved spectrophotometric monitoring of Au, Ag and Cu NP etching via oxidation was carried out by the author and Robin Theron. The author also analyzed the experimental results and prepared a manuscript from the same, which was revised by Dr. Scott prior to publication.

Redispersion of Transition Metal Nanoparticle Catalysts in Tetraalkylphosphonium ILs

Abhinandan Banerjee, Robin Theron, and Robert W. J. Scott
Department of Chemistry, University of Saskatchewan
110 Science Place, Saskatoon, Saskatchewan, Canada.

4.1 ABSTRACT

Despite the fact that particle sintering is one of the most common events leading to the deactivation of metal nanoparticle (NP) catalysts, there is a paucity of studies investigating potential routes for the regeneration of smaller, catalytically active nanoparticles from larger particles formed after repeated catalytic cycles. Here, we reveal a simple yet elegant technique for the 'redispersion' of sintered NPs in tetraalkylphosphonium halide ILs. The procedure described can use environmentally benign oxidants, be carried out at mild temperatures, and is shown to be applicable to a large number of catalytically important transition metals. TEM and UV-Vis spectroscopy reveal that this methodology can indeed regenerate smaller NPs from sintered systems. A sample catalytic reaction reveals that the redispersed NPs are as catalytically active as they were prior to sintering.

4.2 Introduction

Metal NPs have found extensive use as catalytically active species in reactions of scientific as well as commercial importance.[1] Traditionally, homogeneous and heterogeneous catalysis have been examined as the two major catalytic protocols.[2] However, of late, research has focused on quasi-homogeneous nanocatalysis, in which NPs dispersed in liquids are used for catalytic reactions, thereby combining the benefits of homogeneous and heterogeneous catalysis.[3-5] Within the last decade, the quasi-homogeneous nanocatalysis approach has been applied successfully in reactions as varied as hydrogenations, oxidations, and C-C cross-couplings.[6-9] These catalytic systems are typically recyclable, and therefore, can be used repeatedly after product recovery.[10] However, catalytically active NPs, even in the presence of capping agents that protect them from agglomeration and sintering, begin to grow after a finite number of catalytic cycles, leading to subsequent loss of surface area and catalytic activity.[11,12] Many groups have conducted studies to minimize or reverse catalyst deactivation owing to sintering, although most of the research in this field has been confined to supported metal catalysts.[13-18] While prevention of agglomeration/sintering would be even more desirable, very strong capping agents can also block reactive sites on the NP, reducing catalytic activities.[19] This is a serious concern for a number of reasons: catalytically active metals such as Pt, Pd, Ru, and Rh are expensive, the media in which quasi-homogeneous nanocatalysis is carried out can often be exotic substances such as functionalized ILs that need special preparation, and the disposal of potentially toxic

heavy metal waste is, in itself, a serious problem.[20,21] Quasi-homogenous nanocatalysis might be applied to industrial processes if it is made cost-effective and environmentally benign via a recycling procedure that can be applied to the agglomerated/sintered NPs to convert them back into their smaller, catalytically-active counterparts.

In traditional heterogeneous catalysis using metal NPs on solid supports, catalyst-specific methods do exist for such regeneration processes.[19,20] For example, Sá et al. have shown that Au NPs can be redipsersed on oxides using CH_3I treatment at moderate to high temperatures.[20] Laser-induced fragmentation or high velocity impaction of agglomerates for the regeneration of smaller NPs in a homogeneous system have also been reported.[22-24] In this paper, we present a method for a facile, one-pot redispersion of sintered NPs in tetraalkylphosphonium halide ILs via halide-promoted oxidation. The redispersed NPs are seen to be approximately of the same size as the freshly prepared ones, and are catalytically just as efficient. This protocol has been shown to be workable for a wide variety of transition metal nanoparticles that find application as catalysts in scientific/ industrial research (Au, Pd, Pt, Ru, Rh, Ni, Co, Fe, Ag, and Cu).

4.3 Experimental

4.3.1 Materials

Unless otherwise mentioned, all chemicals were used as received. Commercially available reagents (such as metal precursors from Sigma Aldrich) were used without purification unless noted otherwise. High purity solvents were purchased from Fischer Scientific and 100% ethanol was purchased from Commercial Alcohols. 18MΩ cm Milli-Q (Millipore, Bedford, MA) was used throughout. 6.0 M ^{t}Butyl hydroperoxide (in decane) and 2.0 M $LiBH_4$ (in THF) were purchased from Sigma Aldrich. The tri(hexyl)tetradecylphosphonium ILs were provided by Cytec Industries Ltd., and were dried under vacuum at 60^{o}C for 8 h.

4.3.2 Synthesis of NPs in IL

Methods described by us and others for the synthesis of metal NPs in tetraalkylphosphonium ILs were followed.[3,25] In a representative synthesis, Pd NPs were generated in trihexyl(tetradecyl)phosphonium chloride as follows: K_2PdCl_4 (16 mg; 0.05 mmol on the basis of Pd content) was added under N_2 to a sample of the IL (10 mL) at 70°C, and vigorously stirred to give a reddish-brown solution. The solution was cooled to 60°C, and a stoichiometric excess of $LiBH_4$ reagent (1.5 mL, 2.0 M in THF) was injected drop-wise over a period of 5 minutes. Rapid effervescence followed, and the entire solution turned mink-brown, indicating NP formation. After the addition of $LiBH_4$, volatile impurities were removed by vacuum stripping the system at 80°C. The Pd NP solution thus obtained was stored under N_2 in capped vials until use. UV-Visible spectra

of the precursor in the IL, as well as the NPs, were recorded after dilution to ~0.5 mM with methanol, with neat methanol as the blank, and compared with the literature. Similar spectra were recorded after the oxidative degeneration of the NPs to show that the systems reverted to their precursors under these conditions. It is to be noted that the excess reductant present in the system offers protection against accidental exposure of NPs to air, especially for the 3d transition metal NPs, which are readily oxidized upon aerial exposure. For Ag NPs, synthesis in the absence of light produced reproducible results. For all the systems, information about precursors, NP sizes, etc. can be found in Table 4.1.

4.3.3 Procedure for oxidative degradation and regeneration of metal NPs in ILs

For oxidative etching of the NPs, the systems were typically heated to 60-65°C under air or oxygen for variable amounts of time, and the progress of the oxidative degeneration was monitored by UV-Vis spectroscopy (Figure 4.2). In all cases, metal oxidation was noticed; the rate of etching of NPs was seen to depend on the chemical identity of the IL in which they were synthesized, the nature of the metal, and the temperature.[26,27] While Co, Ni and Fe NPs showed complete oxidative etching over a period of 2-2.5 h when exposed to air at 40°C (in fact, these NPs could only be generated under an atmosphere of nitrogen), Au, Pd, and Pt NPs took 3-4 h (Au) to 9-12 h (Pd and Pt) at 60°C, respectively, to complete oxidize in 1 atm oxygen, while Ru and Rh NPs oxidized very slowly even under oxygen. For the NPs recalcitrant to oxidation, drop-wise addition of a 20-fold molar excess of 6.0 M ^{t}butyl hydroperoxide (in decane) to the

NP dispersion after quenching of excess reductant, followed by slow heating to 80°C, sped up the oxidative etching considerably. We hypothesize that the tetraalkylphosphonium halide ILs provide a unique environment which promotes facile oxidation of metal aggregates in the presence of an oxidant such as oxygen.[25,28,29] In no cases were oxide nanoparticles observed; Cu, Ag, Ni and Fe all oxidized back to their respective metal halide solutions. NPs were regenerated upon treatment with the reductant of choice; details are in the table below.

Metal	**Precursor**	**Reductant**	**NP size (nm)**	**NP size after regeneration (nm)**	**Oxidant**
Ag	$AgNO_3$	$LiBH_4$	3.5 ± 0.6	4.1 ± 0.8	Oxygen
Au	$HAuCl_4.4H_2O$	$LiBH_4$	3.2 ± 0.8	5.5 ± 1.4	Oxygen
Cu	$Cu(NO_3)_{2.}2.5\,H_2O$	$LiAiH_4$	4.2 ± 1.0	9.1 ± 3.7	Air
Co	$CoCl_2$	$LiAlH_4$	4.7 ± 1.3	12.5 ± 4.1	Air
Fe	$FeCl_3.6H_2O$	$LiAlH_4$	7.4 ± 2.0	8.0 ± 3.1	Air
Ni	$NiCl_2.6H_2O$	$LiAlH_4$ or $LiBH_4$	5.9 ± 1.3	6.8 ± 2.1	Air
Pd	K_2PdCl_4	$LiBH_4$	4.9 ± 2.2	3.1 ± 1.1	$^{t}BuOOH$

Pt	$Pt(acac)_2$	$LiBH_4$	2.4 ± 0.4	2.2 ± 0.7	^{t}BuOOH
Rh	Na_3RhCl_6	$LiBH_4$	9.6 ± 3.5	11.3 ± 3.9	^{t}BuOOH
Ru	$RuCl_3.3H_2O$	$LiBH_4$	4.5 ± 1.2	3.5 ± 1.1	^{t}BuOOH

Table 4.1 Redispersion conditions for metal NPs studied in P[6,6,6,14]Cl

4.3.4 Hydrogenation catalysis with Ni NPs in P[6,6,6,14]Cl

Hydrogenation reactions were performed in a Schlenk flask, with the stem initially connected to an H_2 gas source. In a representative reaction, 10mL of 10mM Ni NPs in P[6,6,6,14]Cl synthesized under N_2 in a Schlenk flask was flushed with H_2 for 15 minutes at 65^{o}C, and the reactant (cyclohexene, 2mL) was injected into the reaction vessel. The Schlenk flask was then closed, connected to a reflux condenser, and the reaction was allowed to progress at this temperature for 8 hours under constant hydrogen supply via a hydrogen-filled balloon connected securely to the top of the reflux condenser using a Schlenk adapter. Vacuum stripping at elevated temperatures was used to recover the product and leftover substrate from the reaction mixture, and ^{1}H NMR spectroscopy was used to determine the ratio between the product(s) and the unreacted substrate (if any) from the areas of the signals. It was observed that after each cycle, the yield of cyclohexane went down, and the initially transparent brown Ni NP solution became cloudy (likely due to suspended agglomerates). For the

regeneration procedure, the Ni NPs in P[6,6,6,14]Cl were exposed to air, and heated at 65^{o}C with stirring, which led to the development of a greenish-blue solution. This, upon reduction by $LiBH_4$ under nitrogen after de-aeration, regenerated the brown Ni NPs. TEMs were taken after the regeneration to ensure that NPs were indeed being formed. These 're-formed' NPs were used for another cycle of catalytic hydrogenation, and it was seen that they produced yields similar to the first cycle. To ensure reproducibility, each reaction was performed at least twice; the yields, etc., were found to vary by no more than ±1-2% between replicate experiments.

4.3.5 Characterization Techniques.

Unless otherwise stated, all reactions were performed using standard Schlenk techniques, with nitrogen to provide an inert atmosphere, in oven-dried Schlenk glassware. ^{1}H and ^{13}C-NMR spectra were recorded at 500 MHz on a Brüker Avance spectrometer. NMR spectra were recorded in deuterated chloroform ($CDCl_3$) solutions, with residual chloroform (δ = 7.27 ppm for ^{1}H NMR and δ = 77.23 ppm for ^{13}C-NMR) taken as the internal standard, and were reported in parts per million (ppm). For ambient temperature UV/Vis spectra, a Varian Cary 50 Bio UV/Visible spectrophotometer with a scan range of λ=200–800 nm and quartz cuvettes with optical path lengths of 0.4 cm were used. A Cary 6000i spectrophotometer, equipped with a sample changer and a constant temperature bath capable of holding cuvettes and stirring their contents with the aid of a magnetic stirrer while recording their spectra, was used for the etching studies. To avoid effects of oxygen depletion on etching of NPs,

the contents of the cuvettes were flushed with oxygen between readings. TEM analyses of the NPs in different ILs were conducted by using a Philips 410 TEM operating at 100 kV. The TEM samples were prepared by ultrasonication of ~5% solution of the NP/IL solution in $CHCl_3$ followed by drop-wise addition onto a carbon-coated copper TEM grid (Electron Microscopy Sciences, Hatfield, PA). For Cu, Fe and Co NPs, TEM sample preparation was performed using de-aerated 1,4-dioxane under nitrogen. For Ni NPs, which oxidized quickly in air while in the IL, the NPs were extracted from the IL matrix into a toluene layer containing phenylethanethiol, and this Ni-enriched layer was used for drop-coating the TEM grid under nitrogen. To determine particle diameters, a minimum of 100 particles from each sample from several TEM images were manually measured by using the ImageJ program.

4.4 Results and Discussion

4.4.1 Metal NPs in ILs: UV-Vis and TEM studies

We,[3,8] and others,[5,25] have previously shown that ultra-stable NPs can be synthesized in tetraalkylphosphonium ILs. Briefly, requisite amounts of the chosen precursor (usually a metal chloride salt, although acetylacetonates were also used in some cases) were dissolved in the tetraalkylphosphonium halide ILs (typically trihexyl(tetradecyl)phosphonium chloride, P[6,6,6,14]Cl, where the integer values refer to the alkyl chain lengths on the phosphonium centre) at 60^{o}C under nitrogen, and reduced with an excess of the reducing agent used (see Table 4.1 for more details). This

generated NPs in concentrations ranging from 5 mM to 0.5 mM. For most of the NPs considered in this study the reductant of choice was $LiBH_4$, however, for the more oxophilic 3d transition metals such as Co, Ni, and Cu, a stronger hydride reducing agent such as $LiAlH_4$ was necessary for facile reduction of the metal ions to their zerovalent state. The final NP/IL composite was vacuum-stripped for removal of volatiles, and stored in capped vials under nitrogen until use. In the following pages, Figure 4.1 shows the TEM images of the as-synthesized metal NPs in P[6,6,6,14]Cl; Figure 4.2 shows the UV Visible spectra of the metal ions as well as the metal NPs in the P[6,6,6,14]Cl, both before and after oxidative degeneration; and Figure 4.3 shows the TEM images of the metal NPs in P[6,6,6,14]Cl after their redispersion. Note that for Fe NPs, large aggregates were not taken into account while measuring particle sizes.

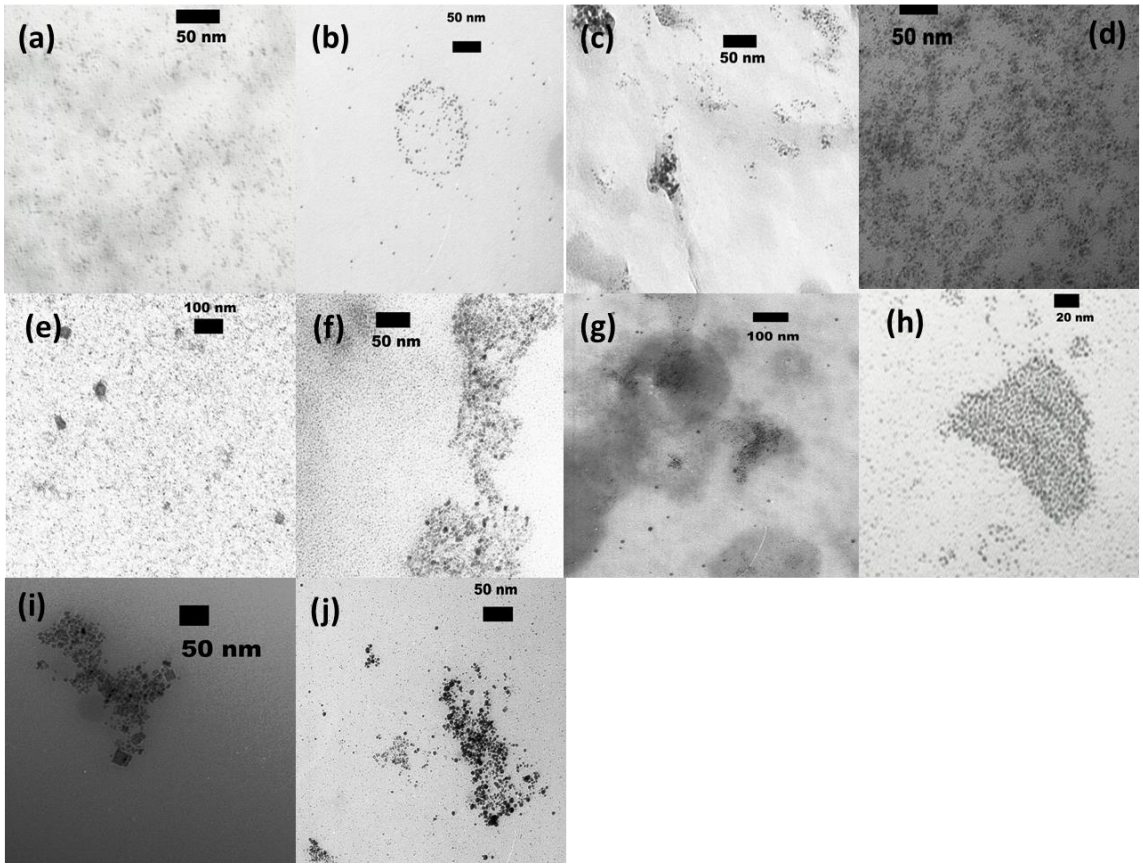

Figure 4.1 TEM images of the as-synthesized metal NPs: (a) Ag(3.5 ± 0.6 nm), (b) Au(3.2 ± 0.8 nm), (c) Co(4.7 ± 1.3 nm), (d) Cu(4.2 ± 1.0 nm), (e) Fe(7.4 ± 2.0 nm), (f) Ni(5.9 ± 1.3 nm), (g) Pd(4.9 ± 2.2 nm), (h) Pt(2.4 ± 0.4 nm), (i) Rh(9.6 ± 3.5 nm) and (j) Ru(4.5 ± 1.2 nm).

Figure 4.2 UV-Visible spectra of metal precursor in IL, metal NPs in IL after synthesis, and metal NPs in IL after oxidative degradation for all the metals studied.

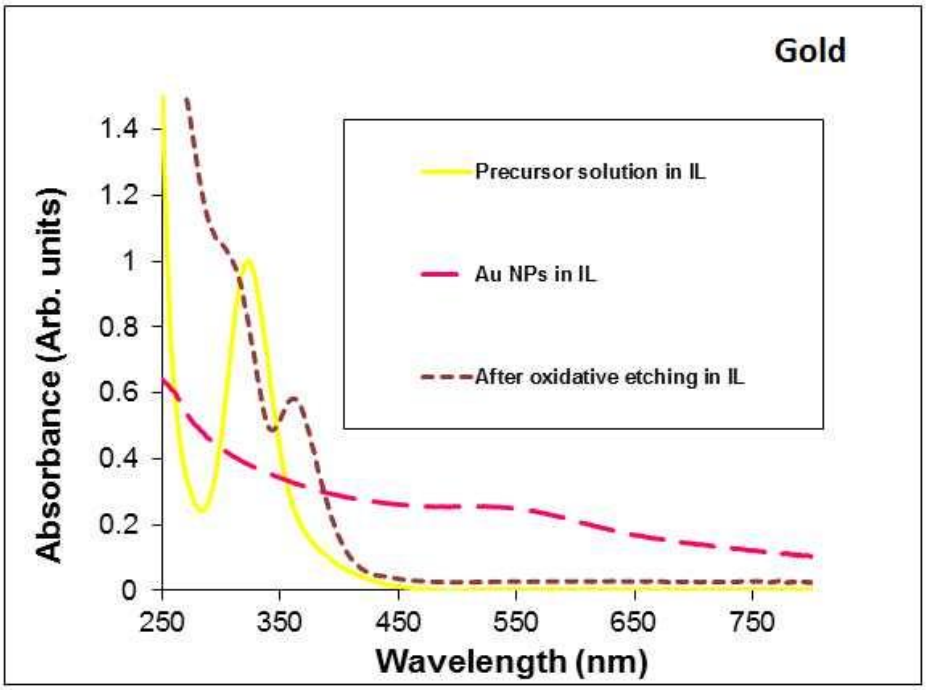

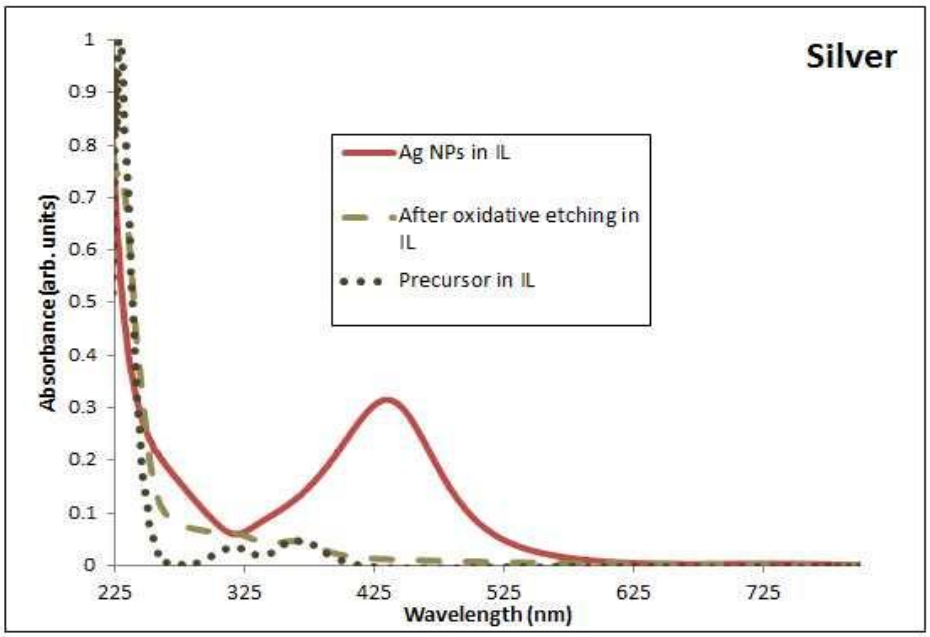

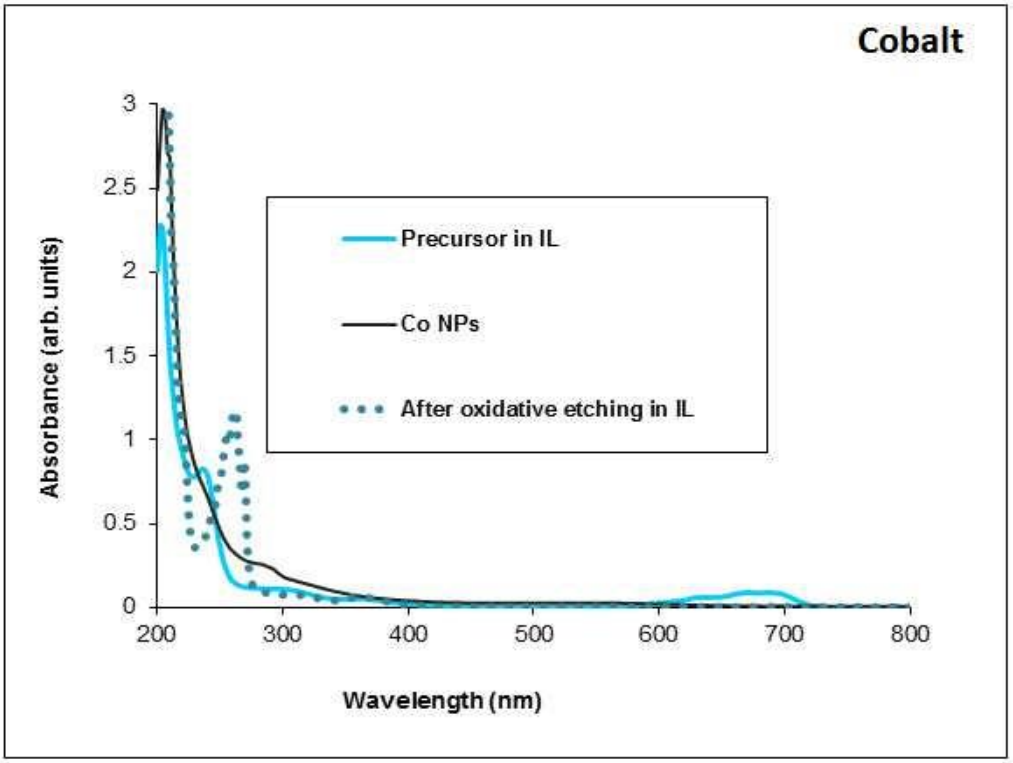
Cobalt
Absorbance (arb. units)
Wavelength (nm)
Precursor in IL
Co NPs
After oxidative etching in IL
0
0.5
1
1.5
2
2.5
3
200
300
400
500
600
700
800

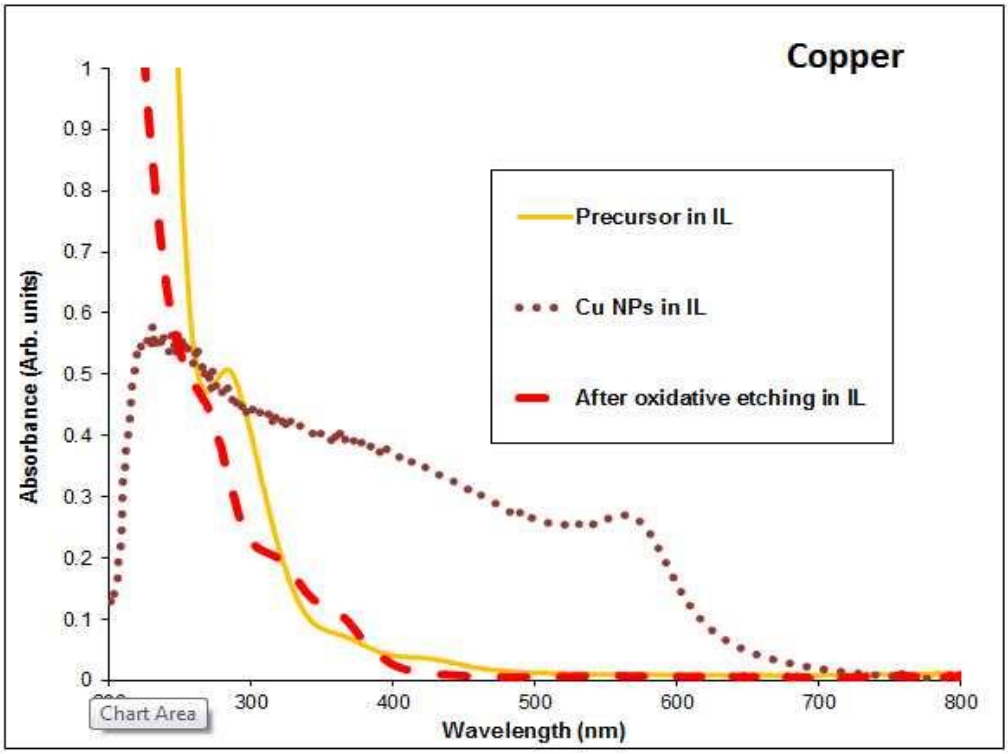
Copper
Absorbance (Arb. units)
Wavelength (nm)
Precursor in IL
Cu NPs in IL
After oxidative etching in IL
Chart Area
0
0.1
0.2
0.3
0.4
0.5
0.6
0.7
0.8
0.9
1
300
400
500
600
700
800

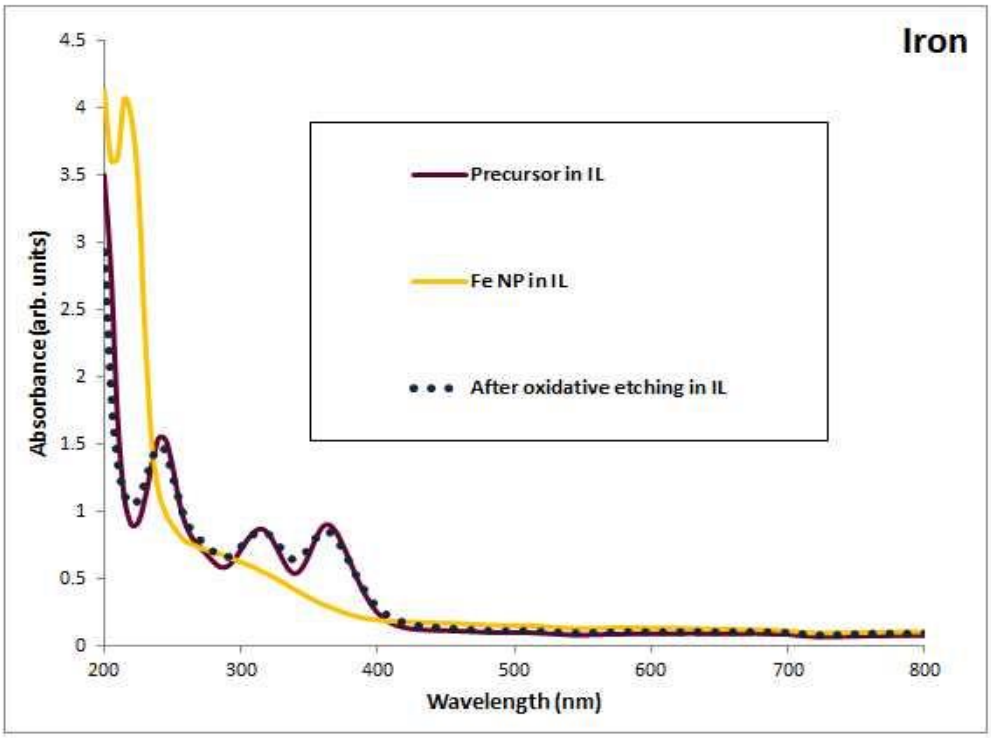
Iron
Absorbance (arb. units)
Wavelength (nm)
Precursor in IL
Fe NP in IL
After oxidative etching in IL

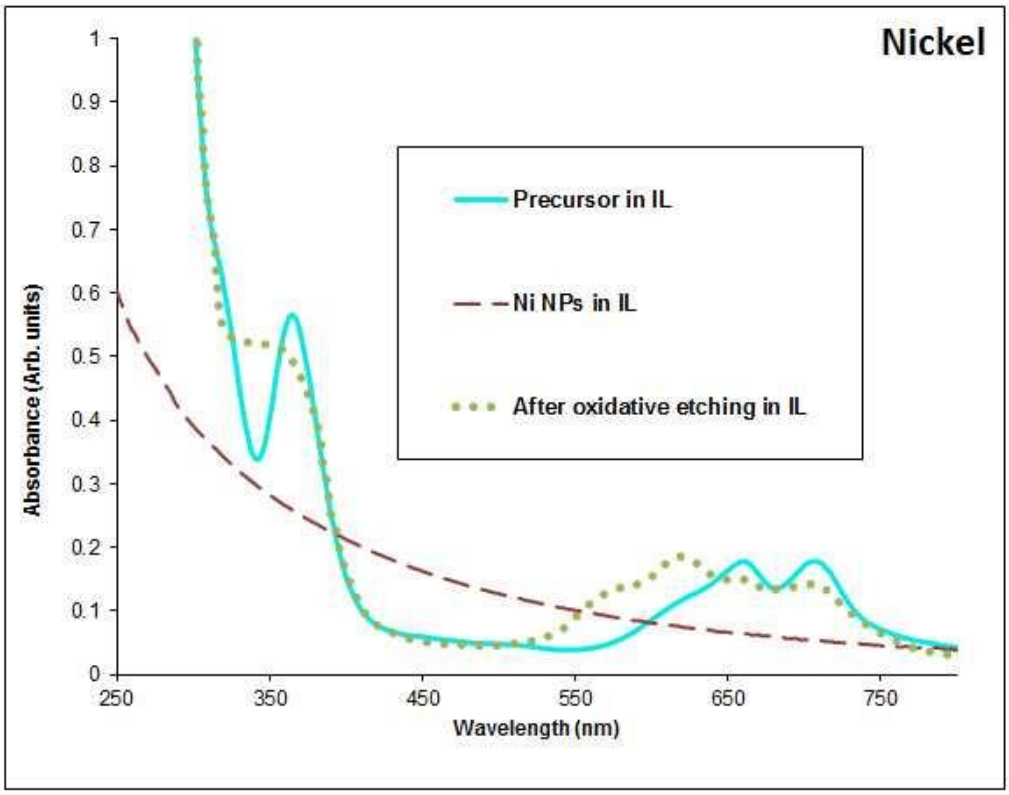
Nickel
Absorbance (Arb. units)
Wavelength (nm)
Precursor in IL
Ni NPs in IL
After oxidative etching in IL

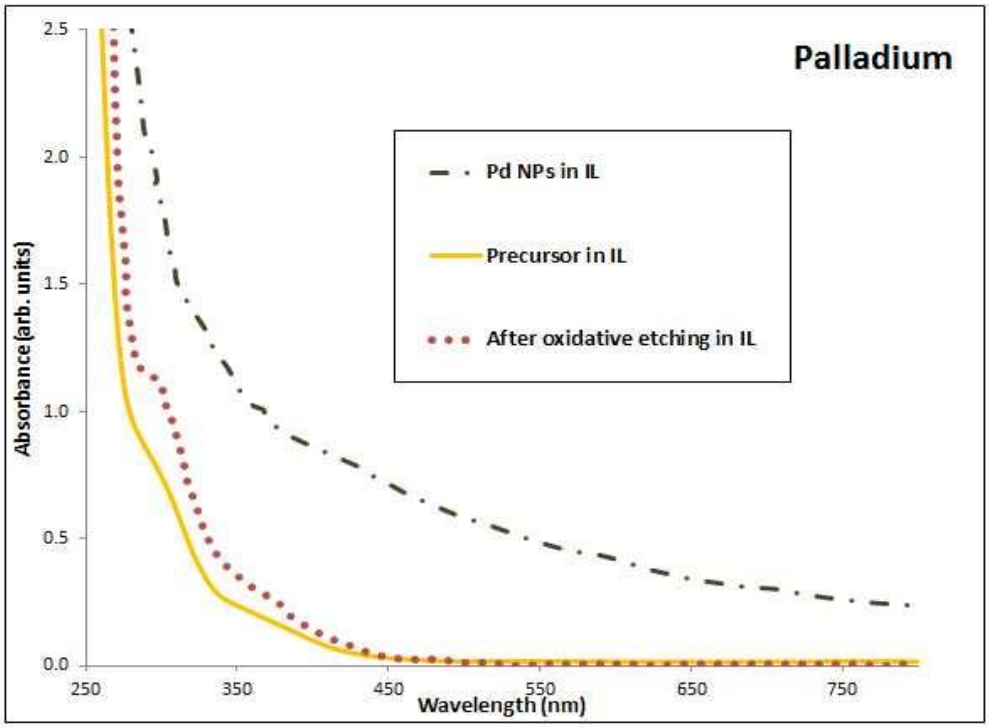
Palladium
Pd NPs in IL
Precursor in IL
After oxidative etching in IL
Absorbance (arb. units)
Wavelength (nm)
2.5
2.0
1.5
1.0
0.5
0.0
250
350
450
550
650
750

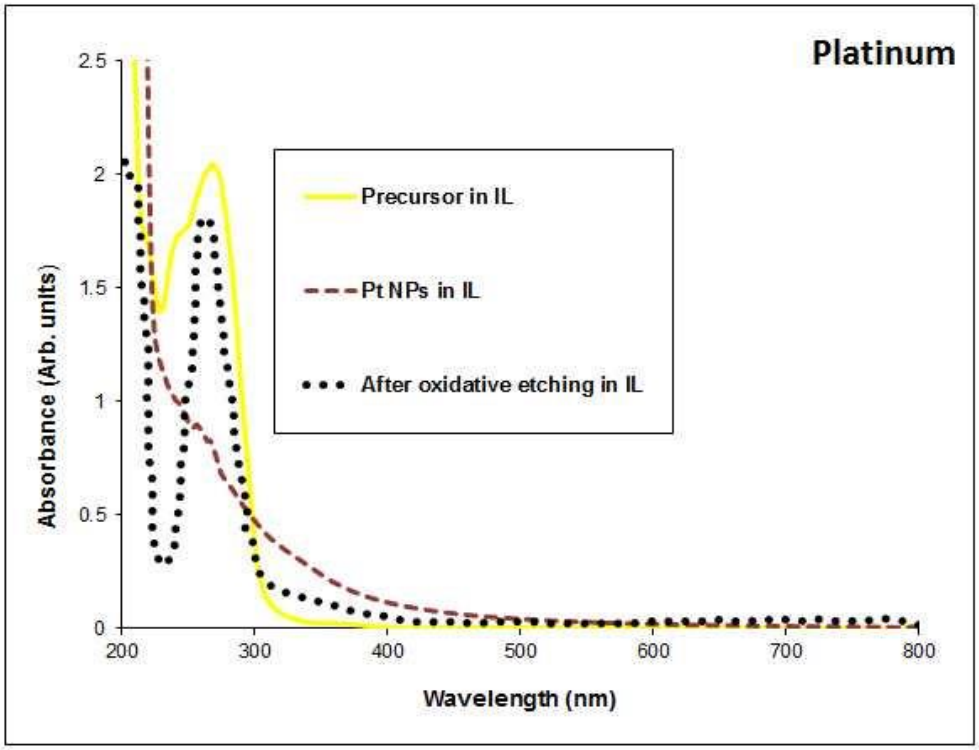
Platinum
Precursor in IL
Pt NPs in IL
After oxidative etching in IL
Absorbance (Arb. units)
Wavelength (nm)
2.5
2
1.5
1
0.5
0
200
300
400
500
600
700
800

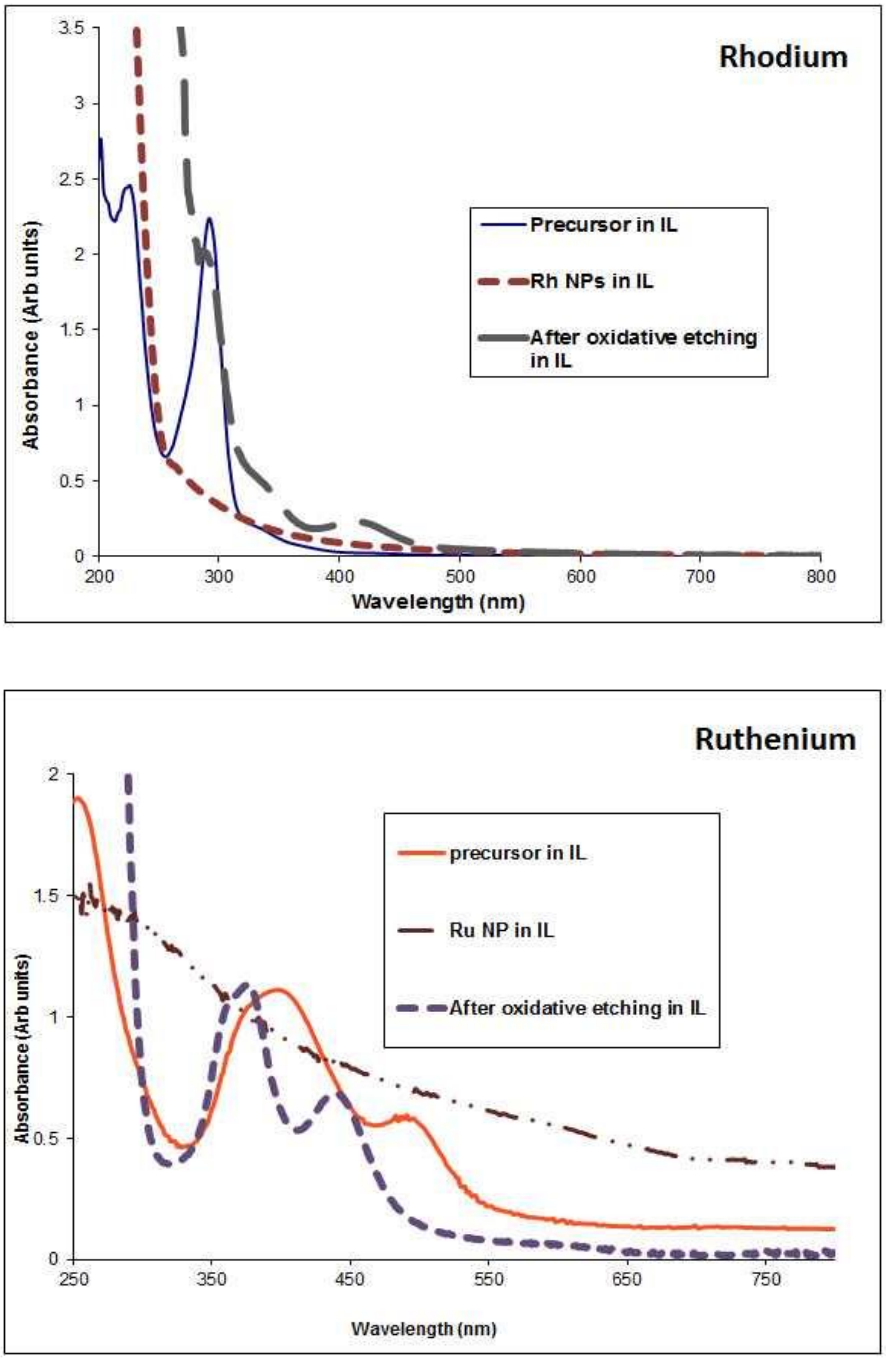

Figure 4.2 UV-Visible spectra of metal precursor in IL, metal NPs in IL after synthesis, and metal NPs in IL after oxidative degradation for all the metals studied. Spectral features did not deviate significantly from existing literature.[30]

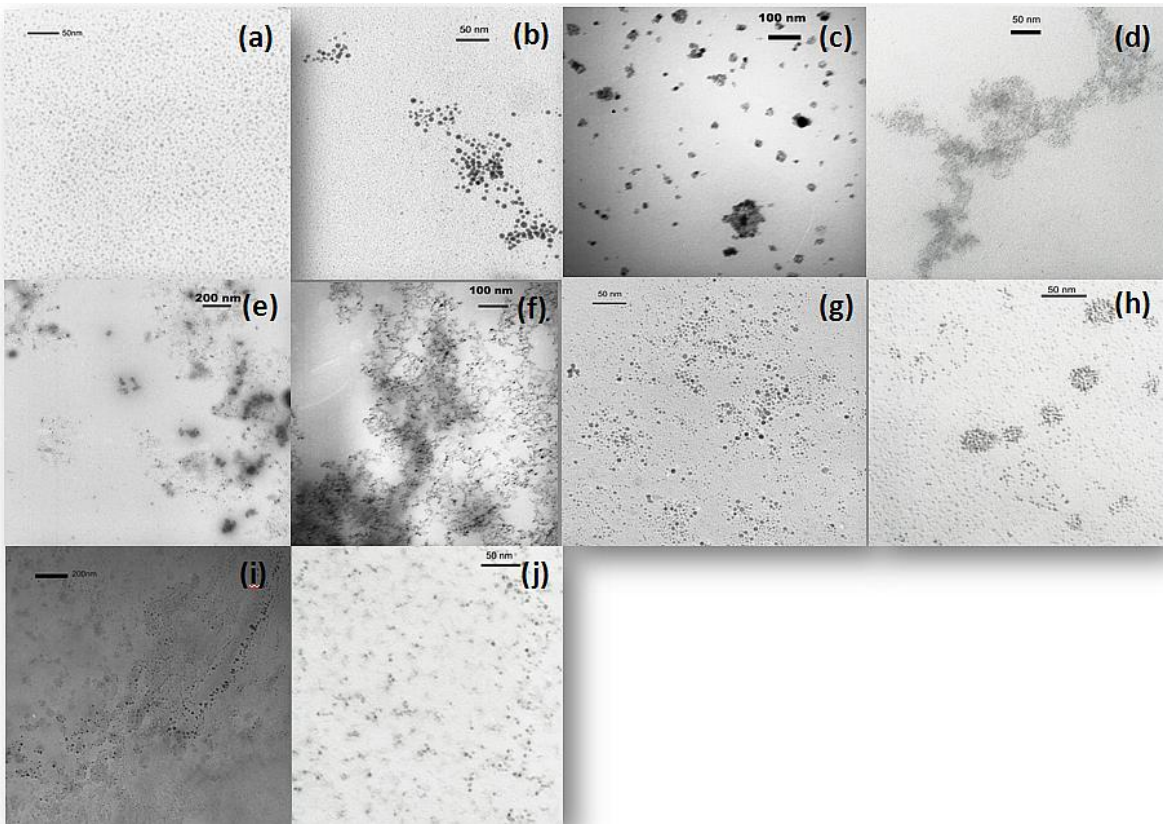

Figure 4.3 TEM images of the metal NPs after regeneration: (a) Ag(4.1 ± 0.8 nm), (b) Au(5.5 ± 1.4 nm), (c) Co(12.5 ± 4.1 nm), (d) Cu(9.1 ± 3.7 nm), (e) Fe(8.0 ± 3.1 nm), (f) Ni(6.8 ± 2.1 nm), (g) Pd(3.1 ± 1.1 nm), (h) Pt(2.2 ± 0.7 nm), (i) Rh(11.3 ± 3.9 nm) and (j) Ru(3.5 ± 1.1 nm).

4.4.2 Dissolution and regeneration of Au NPs in tetraalkylphosphonium halide.

We followed the progress of the oxidative etching of 5.0 mM Au NPs using UV-Vis spectroscopy with a constant temperature bath. Oxygen was bubbled through the samples between successive spectra to avoid oxygen depletion in the system. Figure 4.4(a) shows the surface plasmon resonance peak at ~525 nm due to the Au NPs vanishing with time, while new peaks characteristic of the Au salts dissolved in the IL appear, clearly indicating the oxidation of the NPs. The appearance of Au(III)-Cl LMCT bands in the UV-Vis spectra of this system clearly confirms the formation of Au-Cl entities.[31] $AuCl_4^-$ species are the most likely gold-halide complexes formed, however the possibility of formation of $AuCl_5^{2-}$, $AuCl_6^{3-}$, and dimeric species such as $Au_2Cl_{10}^{4-}$ cannot be ignored, especially in the presence of a vast excess of Cl^- in the IL. The emergent peaks observed in this spectral system, such as the Au-Cl charge transfer band at 365 nm showing a blue shift and reduced intensity, can all be explained on the basis of previous studies.[32]

In order to test the redispersion process, large sintered Au NPs in the P[6,6,6,14]Cl IL (generated by heating at 150°C under nitrogen for 24 hours) were oxidized, followed by re-reduction with $LiBH_4$ to produce small Au NPs, comparable in size to the ones initially formed [Figure 4.4(b)]. TEM images show that the initial sintered Au NPs were 8.9 ± 2.7 nm in size, while after redispersion the particle size decreased to 5.5 ± 1.4 nm. Sá et al. proposed two possible mechanistic scenarios for the etching of Au NPs supported on carbon by CH_3I: namely, repeated particle rupture

owing to Au-halide interactions until atomic dispersions are generated and progressive shrinkage of particle diameter due to leaching of individual Au-halide species from the particle surface.[20] It is quite likely that in this system, both these mechanisms operate. It is seen that the presence of halide ions is necessary for the oxidative etching process: Au NPs in trihexyl(tetradecyl) dicyanamide and tributyl(methyl) mesylate ILs showed a very slow decay of the plasmon band upon being heated, possibly indicating particle fragmentation via thermolysis to generate small, non-plasmonic Au NPs, and/or formation of Au(I) species. No UV-Vis LMCT bands could be detected in either of these systems even after prolonged heating under oxygen.

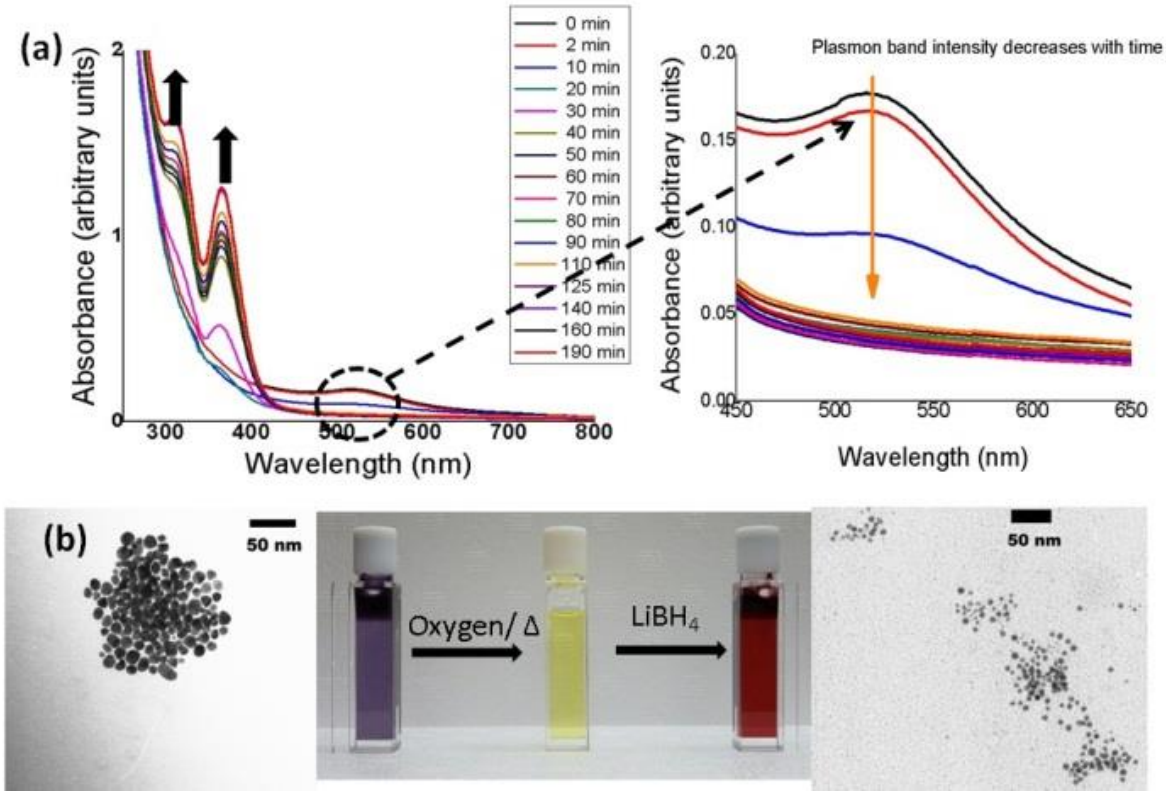

Figure 4.4 (a) Time-dependent UV-Vis spectral monitoring of the oxidative degeneration of 2.5mM Au NPs in P[6,6,6,14]Cl at 60°C in air; plasmon band decay shown on right; (b) Demonstration of redispersion of larger Au NP aggregates into smaller Au NPs via oxidative etching, with TEM images of the initial large NPs (left) and re-dispersed NPs (right).

4.4.3 Olefin hydrogenation with Ni NPs in P[6,6,6,14]Cl

A catalytic test cycle was devised to examine the viability of this regeneration protocol using Ni, a 3d transition metal which is cheaper than the traditional precious metals used for catalysis. Finely divided Ni and IL-supported Ni NPs have already been used as quasi-homogeneous catalysts in the past; although mostly without recycling.[33,34,35] From Table 4.2, we can see that their repeated use as hydrogenation catalysts leads to reduced conversions, likely due to size increases from 6.0 ±1.4 nm to

19.5 ±2.5 nm (Figure 4.6). In P[6,6,6,14]Cl, the Ni NPs show enhanced catalytic activity for cyclohexene hydrogenation under ambient hydrogen pressures after being subjected to the regeneration protocol. TEM measurements revealed that the regenerated NPs (6.8 ± 2.1 nm) were similar in size to the freshly prepared ones.

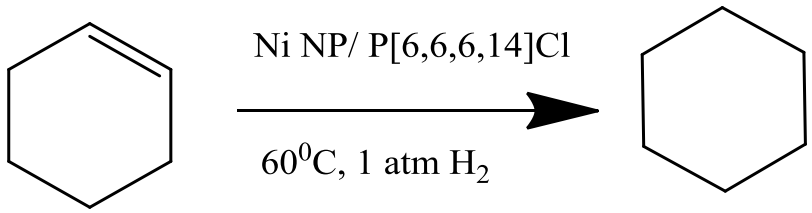

Entry[a]	Cycle Number	%Yield (NMR)
1	1	46
2	2	37
3	3	25
4	After oxidation and redispersion	44

[a]2.0 mL of neat cyclohexene injected in a 10mL, 10mM Ni NP/ P[6,6,6,14]Cl system at 60-65◦C ([cyclohexene]/[Ni]=198), refluxed under hydrogen for 8 h with stirring. Products extracted from the reaction mixture under reduced pressure. [b]from ^{1}H NMR data.

Table 4.2 Cyclohexene olefination using NiNP/P[6,6,6,14]Cl catalyst

4.4.4 TEM and UV-Vis spectroscopic study of Ni NP redispersion

While Ni NPs in P[6,6,6,14]Cl can serve as hydrogenation catalysts in the presence of gaseous hydrogen at temperatures well below 100°C, repeated use of the same catalyst affects the yields adversely, likely due to increase in size from 6.0 ±1.4 nm to 19.5 ±2.5 nm.[33] To counter this, Ni NPs in the IL were heated to 65°C in air to oxidize Ni^0 to $NiCl_4^{2-}$, followed by re-reduction of the Ni salts. This transformation could be followed spectroscopically for a diluted Ni NP system (2.5mM Ni^0 in P[6,6,6,14]Cl), as shown in Figure 4.5. Several prominent peaks appeared gradually as the dispersion changed colour upon being heated and stirred. The intense bands at ~365nm were clearly LMCT bands, while weaker bands at higher wavelengths (659nm, 710nm) could be attributed to LaPorté forbidden *d-d* transitions in the metal cation and their splitting owing to lowering of symmetry of the Ni-complexes due to the non-uniform fields of the tetraalkylphosphonium cations.[36,37] As Ni is more susceptible to oxidation than Au, the oxidation process was significantly faster, and bubbling of oxygen through the dispersion was not necessary. The turquoise Ni(II)/IL system could then be re-reduced with a stoichiometric excess of $LiAlH_4$ or $LiBH_4$ to regenerate small NPs. In P[6,6,6,14]Cl, the regenerated Ni NPs show enhanced catalytic activity for cyclohexene hydrogenation under ambient hydrogen pressures.

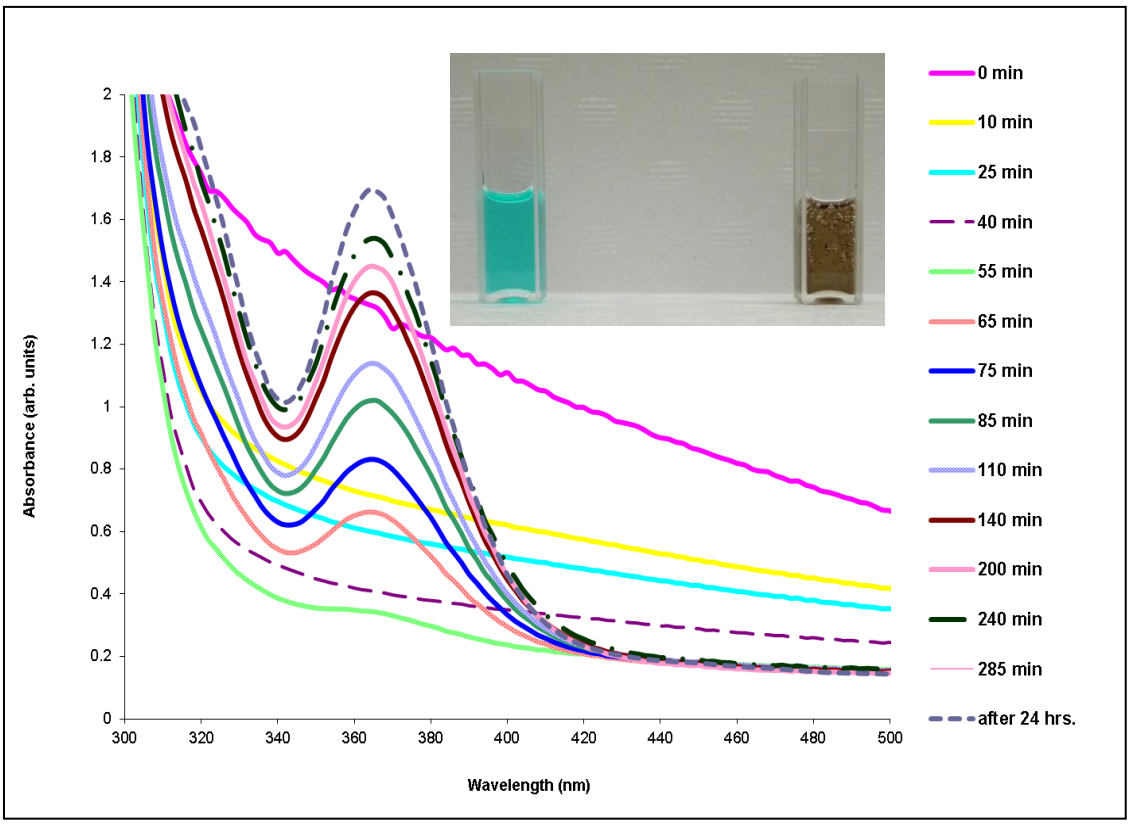

Figure 4.5 UV-Vis spectrophotometric study of the oxidative degeneration of Ni NPs in P[6,6,6,14]Cl stirred under air at 45^0C; inset shows appearance of the sample at t=0 (brown, on the right) and at t=24 hours (turquoise, on the left).

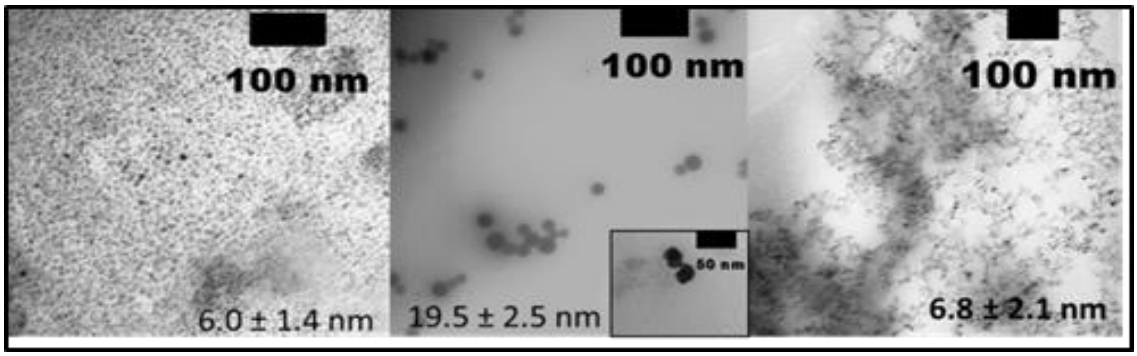

Figure 4.6 TEM images of Ni NPs. From left to right: as-synthesized, after 3 cycles of hydrogenation, and after regeneration. Inset shows the beginning of Ni NP coalescence.

4.5 Conclusion

To conclude, we have formulated an efficient and versatile protocol for redispersion of sintered catalytic NPs in tetraalkylphosphonium halide ILs. The presence of a huge excess of halide ions offers a unique environment which makes facile oxidative etching of large NP agglomerates possible, and the post-oxidation system is susceptible to re-reduction, thereby regenerating small, catalytically active NPs. While the presence of halide ions seems imperative, we are in the process of studying the effect of other variables on the greenness and efficiency of this protocol.

Acknowledgements

We acknowledge financial assistance from the National Sciences and Engineering Research Council of Canada (NSERC) and Al Robertson and Jeff Dyck at Cytec Canada for generously providing ILs for this work. AB would also like to thank the Saskatchewan Innovation Scholarship Trust.

4.6 References

[1] Astruc, D. *Nanoparticles and catalysis,* 1st ed.; Wiley VCH: Weinheim, 2008.

[2] Bengalia, M. *Recoverable and Recyclable Catalysts,* 1st ed.; John Wiley and Sons, Inc.: Wiltshire, U.K., 2009.

[3] Banerjee, A.; Theron, R.; Scott, R. W. J. *ChemSusChem* **2012**, *5*, 109-116.

[4] Dash, P.; Dehm, N. A.; Scott, R. W. J. *J. Mol. Catal. A: Chem.* **2008**, *286*, 114-119.

[5] Luska, K. L.; Moores, A. *ChemCatChem* **2012**, *4*, 1534-1546.

[6] Migowski, P.; Dupont, J. *Chem. Eur. J.* **2007**, *13*, 32-39.

[7] Dupont, J.; Fonseca, G. S.; Umpierre, A. P.; Fichtner, P. F. P.; Teixeira, S. R. *J. Am. Chem. Soc.* **2002**, *124*, 4228-4229.

[8] Maclennan, A.; Banerjee, A.; Scott, R. W. J. *Catal. Today* **2013**, *207*, 170-179.

[9] Cassol, C. C.; Umpierre, A. P.; Machado, G.; Wolke, S. I.; Dupont, J. *J. Am. Chem. Soc.* **2005**, *127*, 3298-3299.

[10] Yu, Y.; Hu, T.; Chen, X.; Xu, K.; Zhang, J.; Huang, J. *Chem. Commun.* **2011**, *47*, 3592-3594.

[11] Bernardi, F.; Scholten, J. D.; Fecher, G. H.; Dupont, J.; Morais, J. *Chem. Phys. Lett.* **2009**, *479*, 113-116.

[12] Prechtl, M. H. G.; Campbell, P. S.; Scholten, J. D.; Fraser, G. B.; Machado, G.; Santini, C. C.; Dupont, J.; Chauvin, Y. *Nanoscale* **2010**, *2*, 2601-2606.

[13] Goodman, D. *Catal. Lett.* **2005**, *99*, 1-4.

[14] Aydin, C.; Lu, J.; Browning, N. D.; Gates, B. C. *Angew. Chem. Int. Ed.* **2012**, *51*, 5929-5934.

[15] Farmer, J. A.; Campbell, C. T. *Science* **2010**, *329*, 933-936.

[16] Somorjai, G.; Park, J. *Top. Catal.* **2008**, *49*, 126-135.

[17] Kartusch, C.; Krumeich, F.; Safonova, O.; Hartfelder, U.; Makosch, M.; Sa, J.; van Bokhoven, J. A. *ACS Catal.* **2012**, *2*, 1394-1403.

[18] Sa, J.; Taylor, S. F. R.; Daly, H.; Goguet, A.; Tiruvalam, R.; He, Q.; Kiely, C. J.; Hutchings, G. J.; Hardacre, C. *ACS Catal.* **2012**, *2*, 552-560.

[19] Dupont, J.; Scholten, J. D. *Chem. Soc. Rev.* **2010**, *39*, 1780-1804.

[20] Dupont, J.; de Oliveira Silva, D. In *Nanoparticles and Catalysis*; Astruc, D., Ed.; Wiley VCH: Weinheim, 2007.

[21] Freemantle, M. *An Introduction to Ionic Liquids*; RSC: Cambridge, U.K., 2009.

[22] Gelesky, M. A.; Umpierre, A. P.; Machado, G.; Correia, R. R. B.; Magno, W. C.; Morais, J.; Ebeling, G.; Dupont, J. *J. Am. Chem. Soc.* **2005**, *127*, 4588-4589.

[23] Seipenbusch, M.; Toneva, P.; Peukert, W.; Weber, A. P. *Part. Part. Syst. Char.* **2007**, *24*, 193-200.

[24] Zeng, H.; Du, X.-W.; Singh, S. C.; Kulinich, S. A.; Yang, S.; He, J.; Cai, W. *Adv. Funct. Mater.* **2012**, *22*, 1333-1353.

[25] Kalviri, H. A.; Kerton, F. M. *Green Chem.* **2011**, *13*, 681-686.

[26] Luska, K. L.; Moores, A. *Green Chem.* **2012**, *14*, 1736-1742.

[27] Zhao, Y.; Cui, G.; Wang, J.; Fan, M. *Inorg. Chem.* **2009**, *48*, 10435-10441.

[28] Mulvihill, M. J.; Ling, X. Y.; Henzie, J.; Yang, P. *J. Am. Chem. Soc.* **2009**, *132*, 268-274.

[29] Whitehead, J. A.; Lawrance, G. A.; McCluskey, A. *Green Chem.* **2004**, *6*, 313-315.

[30] Creighton, J.A.; Eadon, D.G. *J. Chem. Soc., Faraday Trans*., **1991**, 87, 3881-3891.

[31] Mason, W. R.; Gray, H. B. *Inorg. Chem.* **1968**, *7*, 55-58.

[32] Gangopadhayay, A. K.; Chakravorty, A. *J. Chem. Phys.* **1961**, *35*, 2206-2209.

[33] Migowski, P.; Machado, G.; Texeira, S. R.; Alves, M. C. M.; Morais, J.; Traverse, A.; Dupont, J. *Phys. Chem. Chem. Phys.* **2007**, *9*, 4814-4821.

[34] Geukens, I.; Fransaer, J.; De Vos, D. E. *ChemCatChem* **2011**, *3*, 1431-1434.

[35] Duteil, A.; Schmid, G.; Meyer-Zaika, W. *J. Chem. Soc., Chem. Commun*. **1995**, 31-40.

[36] Khokhryakov, A.; Mikhaleva, M.; Paivin, A. *Russ. J. Inorg. Chem*., **2006**, *51*, 1311-1314.

[37] Boston, C.R.; Brynestad, J.; Smith, G.P. *J. Chem. Phys*., **1967**, *47*, 3193-3197.

5 Design, synthesis, catalytic application, and strategic redispersion of plasmonic silver nanoparticles in ionic liquid media

This was a natural successor to our study on the redispersal of large metallic aggregates formed via NP agglomeration in tetraalkylphosphonium halide media during catalysis. As mentioned before, we were inspired by an account published by Hutchings and colleagues, in which they employed methyl halide as an etchant to fragment large gold agglomerates on oxide supports, with the fragmented gold NPs presumably regaining their initial catalytic activities. No such studies, however, have been done in IL media, so we attempted to fill that void by using Ag-NP-induced borohydride reduction of Eosin Y in IL media as a probe reaction to prove that upon redispersal, the smaller NPs regain not only their sizes but also their catalytic activities. Finally, XANES at the Ag L_{III} edge indicated that aerial oxidation of Ag NPs in tetraalkylphosphonium halides does, indeed, facilitate a $[Ag(0)]_n \rightarrow \mathbf{n}\ Ag(I)X_y^{(y-1)-}$ reaction step (X = a halide).

The contents of this chapter has been reprinted after minor changes from a previous publication ("Design, synthesis, catalytic application, and strategic redispersion of plasmonic silver nanoparticles in ionic liquid media", Abhinandan Banerjee, Robin Theron, Robert W.J. Scott, *J. Mol. Catal. A: Chem*. **2014**, *393*, 105-111, © 2014) with permission from Elsevier. The author would like to acknowledge Robin Theron for her involvement in this study. Robin Theron performed the initial synthesis of Ag NPs in tetraalkylphosphonium halide ILs, and recorded the X-ray absorption spectra included in

the paper. Other experimental work recorded in this paper was performed by the first author, who was also responsible for the preparation and editing of the manuscript, including the XANES spectra. The author subsequently prepared a manuscript from the same, which was revised by Dr. Scott prior to publication.

Design, synthesis, catalytic application, and strategic redispersion of plasmonic silver nanoparticles in ionic liquid media

Abhinandan Banerjee, Robin Theron, and Robert W. J. Scott
Department of Chemistry, University of Saskatchewan
110 Science Place, Saskatoon, Saskatchewan, Canada.

5.1 ABSTRACT

Silver nanoparticles, synthesized in tetraalkylphosphonium ionic liquids via a one-pot chemical reduction strategy, are found to be excellent catalysts for borohydride-induced reductive degeneration of Eosin-Y, a commercially available dye that has been classified as a Class 3 carcinogen by the International Agency for Research on Cancer. Transmission electron microscopic images indicated that the size of the Ag nanoparticles was significantly influenced by heat-induced sintering. A strategy was devised to redisperse smaller Ag nanoparticles from their aggregated counterparts via a facile two-step protocol. This protocol involves oxidative etching of Ag nanoparticles in the presence of the halide counter-ions of the ionic liquid media, followed by a reduction step. This reduced the Ag NP size from 15.7 ± 6.1 nm to 3.7 ± 0.8 nm. The as-synthesized and the redispersed Ag nanoparticles were found to catalyze the bleaching of Eosin-Y with comparable efficiencies. A preliminary examination of the kinetics of Ag nanoparticle etching was performed via temperature-controlled UV-Visible spectroscopy. Changes in the oxidation state of Ag during this sequence of events were

also followed by in situ X-ray Absorption Near Edge Structure of Ag nanoparticles in the ionic liquid.

5.2 Introduction

Nanoparticles dispersed in ionic liquids represent an interesting class of composite materials that are being studied extensively by the scientific community owing to their unique physical and chemical properties, which make them promising candidates in catalysis.[1-5] One of the several intriguing properties of ionic liquids is their well-documented capability to act both as solvents and as stabilizers when it comes to stable NP dispersions.[6-8] In imidazolium ILs, this is often due to functionalities deliberately appended to the substituents on the imidazolium cations, but there have been other examples where stabilization stems directly from the nature of the anions.[9-12] Tetraalkylphosphonium halides (P[6,6,6,14]X; X=Cl, Br) represent a class of ionic liquids with intrinsic NP stabilizing abilities.[6, 13-15] While these ILs remain less studied for their applications in quasi-homogeneous nanocatalysis than their imidazolium counterparts, recent research indicates that NPs stabilized by these ILs are similar to traditional metal-surfactant combinations that have been used for nanoparticle stabilization for many years, such as CTAB-stabilized metal nanoparticles, which rely on strong halide absorption to the NP surface, along with steric stabilization by the charge balancing cation.[16-19] The exact nature of the forces that stabilize small NPs in tetraalkylphosphonium halide ILs have remained unidentified so far, although it has been suggested by us that a surfactant-like double layer, aided by the high viscosity

coefficients of these systems, might contribute towards preventing NP coalescence in P[6,6,6,14]Cl ILs.[6, 20, 21] Others have suggested that this interaction originates in the well-ordered three-dimensional network structure of ionic liquids, which leads to the formation of well-defined hydrophobic and hydrophilic zones, with pockets where the NPs might find accommodation.[14] Presumably, the catalytic behavior of the NPs formed within these ILs would be influenced by the nature of both the metal used and the ILs.[22] It is essential, therefore, to examine NP/P[6,6,6,14]Cl IL systems in greater detail, which would give us valuable information not only about the individual systems under scrutiny, but also on the chemical and catalytic behaviors of this class of composite materials as a whole.

While Au, Pt, Pd, Ru and Rh NPs in tetraalkylphosphonium ILs have been studied by several groups in the recent past from the point of view of their catalytic behavior, Ag NPs in P[6,6,6,14]Cl ILs are yet to be explored as catalytic systems.[13, 14, 23, 24] This is surprising, since Ag is one of the cheaper 'noble metals'; also, it also has various applications in areas as diverse as photography, anti-bacterial coatings and surface-enhanced Raman spectroscopy.[25-27] The presence of a well-characterized, intense surface plasmon resonance (SPR) band for silver nanoparticles in the visible region also makes them attractive candidates for morphological studies, since it is known that the size, shape and intensity of these bands depend upon the size and shape of the NPs being studied.[28-30] It has been recently been shown by us that Ag NPs can be synthesized in trihexyl(tetradecyl)phosphonium halides via a conventional borohydride reduction

protocol. It has also been demonstrated that these NPs etch upon exposure to oxygen at high temperatures, presumably aided by the presence of a large excess of halide ions in the system.[31]

For testing the catalytic behaviour of these systems, we selected a well-studied reaction whose progress could be followed spectrophotometrically. The reaction chosen was the borohydride-induced discoloration of Eosin-Y (EY), an organic dye used extensively in staining of histological tissue samples, in photoelectrochemical cells, and as a fluorescent pigment.[32-34] The addition of Ag NPs to this system leads to complete discoloration of Eosin-Y. This is in accordance with previous reports, which indicate that coinage metal NPs serve as electron-transfer relays in borohydride-induced reductive discoloration of dyes, with the nucleophilic borohydride ions transferring electron density onto the NP surface, which in turn injects those electrons into the dye molecule.[35-39] Most studies carried out in this context focus on the discoloration of EY in water phase. Since ILs as solvents show behaviors drastically different from those of water as well as conventional organic solvents, it is worthwhile to examine such electron-transfer processes in these novel media.[40]

In this paper, we show the synthesis of Ag NPs in tetraalkylphosphonium halide ILs via reduction of Ag(I) salts with lithium borohydride. The Ag NPs formed in tetraalkylphosphonium halide ILs remained stable for months. These Ag NPs were also able to catalyze the borohydride-induced degeneration of EY in non-aqueous media. It was found that over a large number of catalytic cycles and/or higher temperatures, Ag

NPs aggregated in the IL media. We show that the resulting particles could then be etched via exposure to air or oxygen, which, followed by chemical reduction, can redisperse smaller Ag NPs. The kinetics of the oxidative etching of Ag NPs in P[6,6,6,14]Cl and P[6,6,6,14]Br were examined in this study by in situ UV-Vis spectroscopy and X-ray absorption near edge spectroscopy. The catalytic activity of the redispersed Ag NPs was determined to be similar to freshly synthesized NPs.

5.3 Experimental

5.3.1 Materials

Unless otherwise mentioned, all chemicals were used as received. Silver nitrate (>99.7%) was purchased from Fisher Scientific. Eosin-Y and 2.0 M $LiBH_4$ (in THF) were purchased from Sigma Aldrich. THF was purchased from EMD and used as received. The tri(hexyl)tetradecylphosphonium halide (P[6,6,6,14]X; X= Cl or Br) ILs were provided by Cytec Industries Ltd., and were dried under vacuum at 70^oC for 10-12 hours with stirring before use. 18 MΩcm Milli-Q water (Millipore, Bedford, MA) was used throughout.

5.3.2 Synthesis of Ag NPs in IL using lithium borohydride

In a representative synthesis of 5.0 mM Ag NPs in P[6,6,6,14]Cl, 8.5 mg of $AgNO_3$ (0.050 mmol) was added under nitrogen to a 10 mL sample of the IL at 80^oC (all the ILs studied are liquids at this temperature) in a Schlenk flask, and vigorously stirred. The solution was cooled to 50^oC, and a stoichiometric excess of $LiBH_4$ reagent (1.5 mL, 2.0 M in THF) was injected drop-wise into it over a period of 2-3 minutes. A brisk effervescence

followed, and the entire solution turned deep yellowish-brown, indicating nanoparticle formation. After the addition of $LiBH_4$, volatile impurities were removed by vacuum-stripping the system at 80^oC. The Ag NP-IL composites thus obtained was stored under nitrogen in capped vials wrapped with foil until use.

5.3.3 Procedure for EY discoloration

In a typical experiment, 0.2 mL of a 0.2 mM EY solution in THF was added to a 7 mL (5:2) mixture of IL/THF in a foil-wrapped vial under nitrogen. A stoichiometric excess of $LiBH_4$ (0.1 mL, 2.0 M in THF) was then added to the system, and stirring was commenced. After the desired time-interval, 200 μL of 5.0 mM Ag NPs in P[6,6,6,14]Cl was added to the system. UV-Vis spectra of the 'blank' sample (i.e., without added Ag NPs) was also recorded. A quartz cuvette was then filled with the aliquot, and recording of spectra was initiated. Between successive readings, the cuvette was taken out of the spectrophotometer, wrapped in tinfoil to minimize exposure to ambient light, and manually shaken to ensure homogeneity of analyte. It has been noted by others that effervescence owing to the presence of borohydride in the reaction mixture also promotes thorough mixing, even in absence of a magnetic stir-bar.[41] The recording of spectra was continued at suitable intervals of time, until the pink color of the solution faded to straw-yellow.

5.3.4 Procedure for Ag NP sintering

To bring about heat-induced growth in particle size, nitrogen was bubbled through Ag NPs in P[6,6,6,14]Cl at 135^{o}C for an hour, followed by overnight heating under a nitrogen atmosphere at the same temperature. To check for increase in Ag NP size after repeated catalytic cycles, five portions of 0.2 mL, 0.2 mM EY solution in THF were added to a single 7 mL (5:2) mixture of IL:THF, containing 500µL of 5.0 mM Ag NP, in a foil-wrapped vial under nitrogen, with a gap of one hour between each successive addition. 0.1 mL portions of $LiBH_4$ (2.0 M in THF) were also added to the system after each dye addition, and stirring was commenced. After five such cycles of EY discoloration, a TEM sample was prepared from the reaction mixture, and Ag NP sizes were studied. We note that our reaction of choice is conducted at room temperature, rather than at elevated temperatures, where greater particle sintering might be expected after repeated reaction cycles as compared to a reaction that occurs under mild, ambient conditions.

5.3.5 Procedure for Ag NP oxidative etching and redispersion.

The following procedure was adopted to redisperse the agglomerated Ag NPs back to *ca.* their initial sizes: oxygen was flushed through the Ag NP/P[6,6,6,14]Cl system at 65^{o}C until the characteristic yellow color of the NPs disappeared, followed by re-reduction of the redispersed precursor by drop-wise addition of 1.5mL $LiBH_4$ solution in THF, followed by quenching of excess reductant and low-pressure removal of volatiles from the medium. The progress of the oxidative etching of Ag NPs in various

tetraalkylphosphonium halide ILs was monitored spectrophotometrically by UV-Vis spectroscopy. The kinetic studies were conducted in a Cary 6000i spectrophotometer. Ag NP/P[6,6,6,14]Cl samples were taken in quartz cuvettes and small Teflon®-coated magnetic stir-bars were immersed in them; they were then placed in a constant-temperature bath with a magnetic stirring base inside the spectrophotometer. Oxygen from a compressed gas cylinder was passed directly into the contents of the cuvettes at regular intervals using a gas regulator connected to a system of hoses, syringes and needles.

5.3.6 Characterization Techniques.

Unless otherwise stated, all reactions were performed using standard Schlenk techniques, with nitrogen to provide an inert atmosphere, in oven-dried Schlenk glassware. A Varian Cary 50 Bio UV-Visible spectrophotometer with a scan range of λ=200–800 nm and quartz cuvettes with optical path lengths of 0.4 cm or 1 cm were used for ambient temperature UV-Vis spectra and spectrophotometric studies of EY discoloration. A Cary 6000i spectrophotometer, equipped with an auto-sampler, a constant temperature bath, and magnetic stirring capabilities was used for the etching studies. To avoid effects of oxygen depletion on etching of NPs, the contents of the cuvettes were flushed with oxygen between readings. TEM analyses of the NPs in ILs were conducted by using a Philips 410 microscope operating at 100 kV. The TEM samples were prepared by ultrasonication of ~5% solution of the NP/IL solution in $CHCl_3$ followed by drop-wise addition onto a carbon-coated copper TEM grid (Electron

Microscopy Sciences, Hatfield, PA). To determine particle diameters, a minimum of 100 particles from each sample from several TEM images were manually measured by using the ImageJ program.

Ag XANES spectroscopy was carried out on the SXRMB Beamline (06B1-1) at the Canadian Light Source (CLS). The beamline was equipped with InSb(111) and Si(111) crystals, and has an energy range of 1700 - 10000 eV with a resolution of 1×10^{-4} ΔE/E. XANES spectra were obtained in fluorescence mode. The setup for liquid XANES work was similar to previous investigations; solution samples were placed in SPEX CertiPrep Disposable XRF X-Cell sample cups fitted with polypropylene inserts and sealed with an X-ray transparent film (Ultralene film, 4 μm thick, purchased from Fisher Scientific, Ottawa, ON).[42, 43] The sample solution cell was placed on the sample holder that faces the incident beam at 45° angle. The software package IFEFFIT was used for data processing.

5.4 Results and Discussion

5.4.1 Characterization of Ag NPs.

It has been previously shown by us and others that tetraalkylphosphonium ILs are excellent solvents and stabilizers for NPs. NPs synthesized in these ILs via borohydride reduction tend to remain stable for months or even years depending upon storage conditions.[6] The Ag NPs synthesized in the P[6,6,6,14]Cl were characterized via UV-Vis spectroscopy and TEM. Figure 5.1 shows the UV-Vis spectra of the $AgNO_3$

precursor (which, upon dissolution in a chloride-rich solvent, presumably forms $AgCl_2^-$), the as-synthesized Ag NPs, the Ag NPs after being subjected to an etching regimen, as well as after regeneration in P[6,6,6,14]Cl.[44] The surface plasmon resonance band of Ag at ~400 nm could be observed in the NP samples.

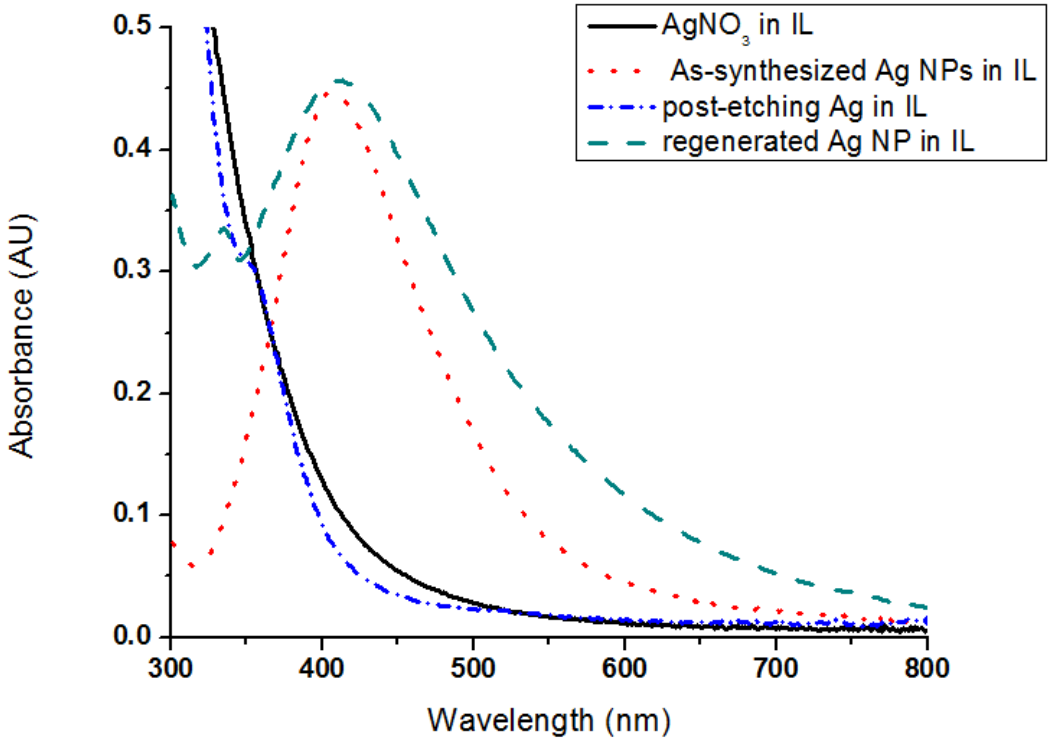

Figure 5.1 UV-Visible spectra of $AgNO_3$ in P[6,6,6,14]Cl IL, Ag NPs formed by reduction with lithium borohydride, post-etch Ag species in IL, and re-generated Ag NPs.

Figure 5.2 shows TEM images of the Ag NP samples as-synthesized and after one cycle of oxidation and re-reduction. The average particle sizes of the as-synthesized Ag NPs formed in IL was 4.8 ± 0.9 nm. Higher temperatures favor NP aggregation and

sintering; NP growth was seen after heating the Ag NPs at 135^{o}C under a nitrogen atmosphere [Figure 5.2(B),(C)] TEMs after 1 hour and 24 hours of heating under a nitrogen atmosphere show gradual increase in particle size over time (average particle sizes: 8.9 ± 2.8 nm after one hour, 15.7 ± 6.1 nm after 24 hours). The polydispersity of the Ag NP samples also increased significantly after the thermal treatment. Ag NPs could be redispersed after oxidative etching, using $LiBH_4$; the sizes of the redispersed NPs do not differ significantly from the initial values (3.7 ± 0.8 nm). Figure 5.2(E), which shows the Ag NPs after five consecutive cycles of EY discoloration at room temperature, has an approximately bimodal particle distribution, with maxima at 4.7 ± 0.8 nm and 6.1 ± 1.3 nm, presumably corresponding to the sizes of the as-synthesized and grown NPs.

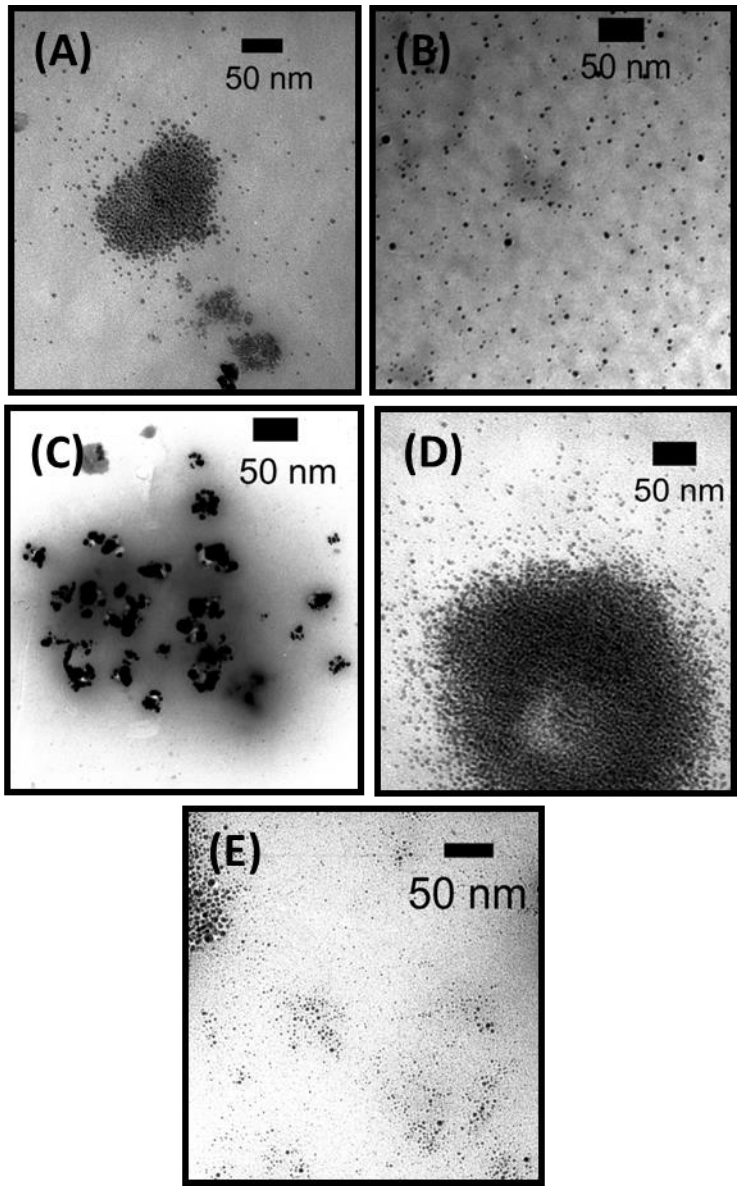

Figure 5.2 TEM images of Ag NPs formed in IL by $LiBH_4$ (A: as-synthesized; B: sintered – 1 hour; C: sintered – 24 hours; D: redispersed; E: after five consecutive cycles of EY discoloration).

5.4.2 EY discoloration by Ag NPs.

While the borohydride-induced discoloration of EY has been used for years as a probe for testing the surface activity of NPs, it is only recently that the mechanism of this process is being studied in detail.[41, 45] It is to be noted that EY shows multiple reductive pathways in the presence and absence of light.[45] We have observed that EY undergoes a slow reduction via an uncatalyzed pathway upon exposure to excess $LiBH_4$ in a THF/IL medium. This bleaches the dye solution from a bright pink to a pale yellow, possibly owing to a reduction of a double bond in the heterocyclic ring structure, thereby decreasing the length of the electron delocalization trajectory (Figure 5.3).[46] The reaction follows a pseudo-first-order kinetics, with the reaction rate being dependent on the concentration of the dye, while the borohydride concentration remains virtually unchanged. Weng *et al.* established that in aqueous solutions, EY hydrolyzes to produce EY^{2-}, which then undergoes a slow two-electron reduction in the presence of borohydride to generate colorless EY^{4-}.[41] In the presence of metal NPs, however, a one-electron reduction pathway generates EY^{3-} which can then undergo a photochemical fragmentation to generate a 'green dye', or be subjected to another single-electron reduction pathway in the dark to generate colorless EY^{4-}.[45] It has already been established in several studies that reduction of EY in the presence of borohydride proceeds at a moderate rate in the absence of catalysts such as Au, Ag, or Cu NPs; the reaction rate, however, is accelerated when coinage metal nanostructures are added to the reaction medium.[47] The spectral signature for this mechanistic shift – the

appearance of a characteristic peak of the single-electron reduction product (EY^{3-}) at ~405 nm (in water) – is not easily visible in the presence of Ag NPs, which have a large surface plasmon resonance around the same region.[45]

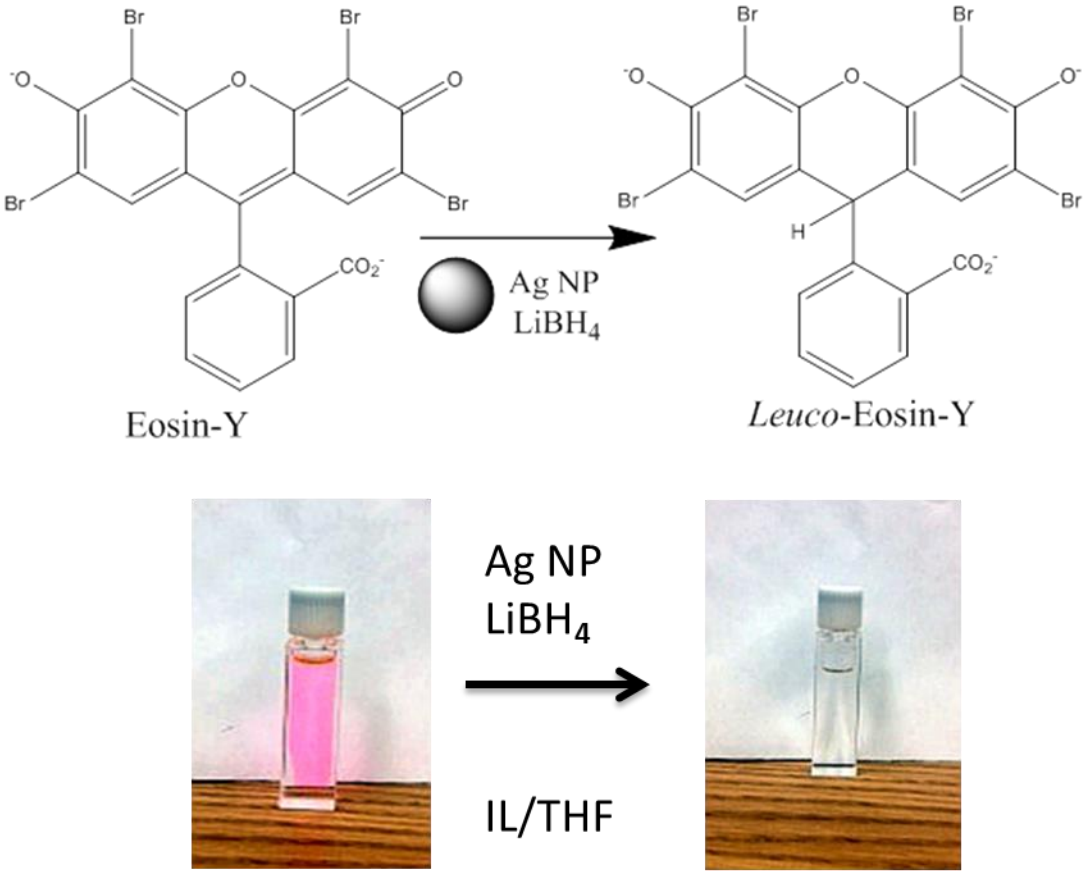

Figure 5.3 Ag NP catalyzed borohydride reduction of Eosin-Y (top), and the color change that accompanies it (bottom).

In the presence of Ag NPs and $LiBH_4$, the progress of the catalytic dye discoloration in THF/P[6,6,6,14]Cl mixtures could be followed by monitoring the absorbance of the solution at the wavelength of maximum absorption of EY. The role of the THF is to reduce the viscosity of the reaction mixture so that the reactants can be evenly distributed; this might also be achieved by heating the neat IL, but at higher temperatures it was very difficult for us to follow the progress of the reaction within the experimental time-scale. It can be seen from the UV-Vis spectra (Figure 5.4) that EY in the THF/IL mixture has two absorption maxima (500 nm and 536 nm): the latter, more intense absorption wavelength was selected for this study. The intensity of the band at 536 nm decreased with an increase in time, although the shape and the position of the peak remained unaltered once the Ag NPs and $LiBH_4$ have been added to the reaction mixture. A control reaction [Figure 5.4(A,B)] demonstrated that in the absence of Ag NPs, the degeneration of EY proceeded at a much slower rate ($\boldsymbol{k}_{\mathbf{cat}}/\boldsymbol{k}_{\mathbf{uncat}} \sim 10$).

The kinetics of reductive degeneration of EY in the THF/IL mixture can be described by the Langmuir-Hinshelwood equation (1):

$$\text{Rate} = \frac{dE}{dt} = \frac{kKE}{1+KE} \quad \text{..... (1)}$$

As the product of K and E is very small compared to unity, we replaced the (1+KE) term in the denominator by unity, and integrated with respect to time, which produced the pseudo-first-order kinetic equation (2):

$$\ln \frac{E}{E_0} = kKt = k_{app}t \quad \text{.....(2)}$$

where E_0 is the initial EY concentration, E is the EY concentration at time t, k is the reaction rate constant, k_{app} is the pseudo-first-order rate constant, and K is the absorption coefficient of EY onto Ag NPs in the reaction medium.[47] Some representative plots for changes in the absorbance of EY in a IL/THF mixture as a function of time under the reaction conditions can be seen in Figure 5.4. It is evident from an examination of the plots that the kinetics of the reaction undergoes a drastic change upon addition of the Ag NPs, presumably owing to a shift to a different mechanistic regimen [Figure 5.4(A)]. Assuming a first-order kinetic scenario in the presence of excess borohydride, a linear kinetic plot was obtained for the Ag NP catalyzed EY discoloration [Figure 5.4(B)], which is in accordance with several studies conducted in the past in aqueous media.[32, 36, 38, 39, 41, 45, 47]

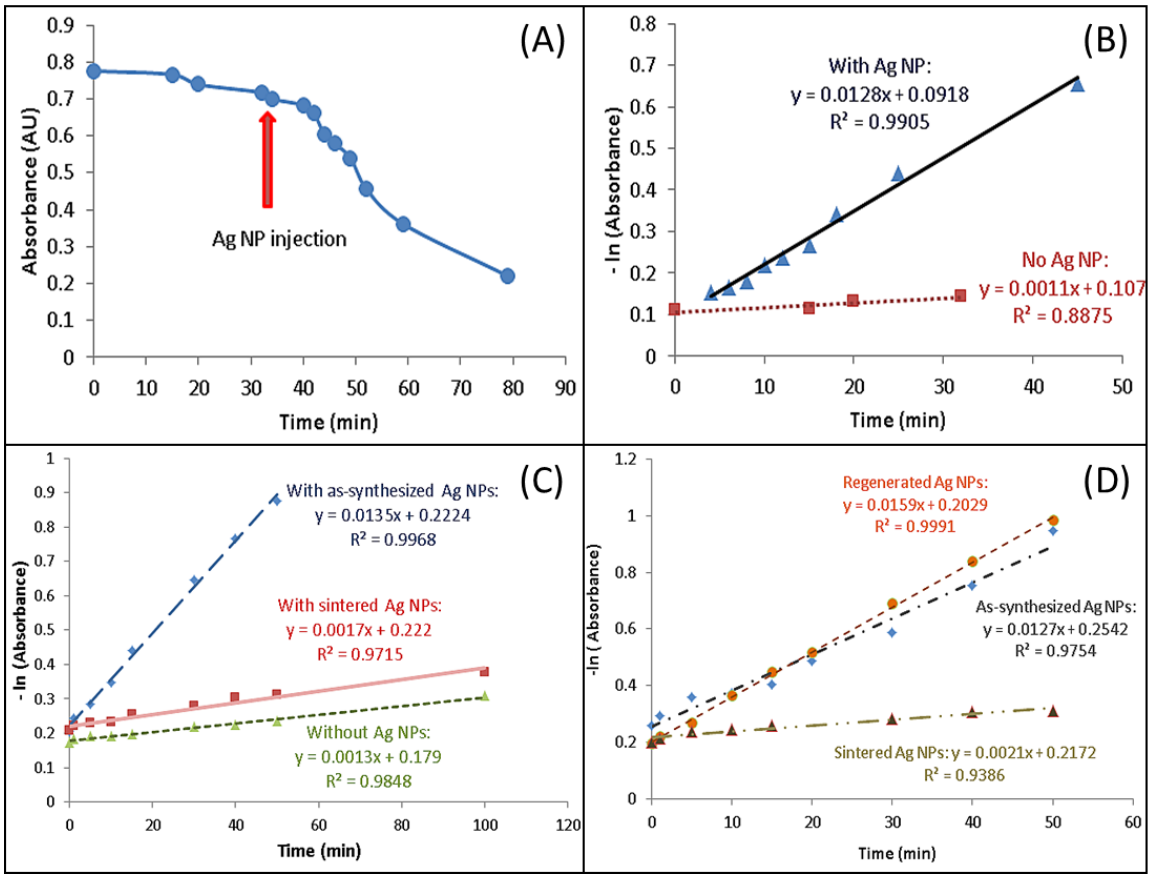

Figure 5.4 (A) Decrease in EY absorption at 536 nm as a function of time both before and after introduction of Ag NPs in the system; (B) First-order regression analysis of EY discoloration in the presence as well as the absence of Ag NPs in the reaction system; (C) First-order regression analysis of EY discoloration in the presence of freshly synthesized Ag NPs, sintered Ag NPs, and no Ag NPs in the reaction system; (D) First-order regression analysis of EY discoloration in the presence of redispersed Ag NPs, sintered Ag NPs, and no Ag NPs in the reaction system.

It is well-known that larger NPs are less efficient than smaller ones at catalyzing reactions, presumably owing to a reduced surface area. Therefore, the sintered Ag NP samples are expected to show a reduced rate for EY discoloration. However, the time-

scale for this process turned out to be of the same order as that of the uncatalyzed reaction; therefore, it was impossible to separate the two reaction pathways on the basis of a simple kinetic study [Figure 5.4(C)]. We measured the ratio between the pseudo-first-order rate constants for the sintered and the as-synthesized Ag NPs, which turned out to be approximately equal to the ratio between the pseudo-first-order rate constants for the sintered and the redispersed Ag NPs [Figure 5.4(D)] [$k_{fresh}/k_{sinter} = k_{redispersed}/k_{sinter} \sim 8$]. This confirms our original hypothesis: namely, the process of regeneration of small Ag NPs from larger aggregates restores their original catalytic activities. The results are also in accordance with previous experimental findings by Pal and co-workers, who demonstrated that the rate of Eosin-Y discoloration in the presence of metal NPs depends considerably on the size of the NPs, with enhanced catalytic activities exhibited by smaller NPs.[48]

5.4.3 Dissolution of Ag NPs in tetraalkylphosphonium halide ILs and their regeneration.

Coinage metal NPs are susceptible to oxidative etching in the presence of a halide and an oxidant.[49, 50] Tetraalkylphosphonium ILs containing halide counter-ions provide a unique oxidizing atmosphere within which agglomerated NPs can be oxidized to their halometallate ions (such as $AgCl_2^-$). For Ag NPs, the progress of oxidative etching can be followed spectrophotometrically via the evolution of the Ag NP SPR band at ~400 nm [Figure 5.4(A)]. A continuous decay in the intensity of this band was observed when the Ag NPs were exposed to oxygen at 65°C.[51, 52] Figure 5.5(A) shows the changes in the

spectral landscape of 400 μM Ag NPs in P[6,6,6,14]Cl as a function of time. It is likely that the formation of $AgCl_2^-$ from Ag(0) is the major pathway through which this discoloration proceeds: however, other possibilities, such as formation of non-plasmonic Ag clusters from plasmonic Ag NPs prior to their reversion to Ag(I) species, cannot be ruled out. A similar case of Ag NP dissolution can be observed in P[6,6,6,14]Br, where the Br^- ion, in the presence of oxygen, oxidizes Ag to $AgBr_2^-$. For 400 μM Ag NPs in P[6,6,6,14]Cl, the absorption at λ_{max} (=415 nm) decreases consistently upon exposure to oxygen at 65^{o}C with continual stirring. The excess borohydride present in our dispersions was quenched prior to etching experiments. It is to be noted that even at slightly elevated temperatures, solubility of oxygen in the ILs was a rate-limiting factor: to avoid this, oxygen was bubbled through the samples between successive readings. When these solutions were left overnight for automated spectral data collection, manual oxygen replenishment was not possible, and the kinetics quickly deteriorated into a mass-transfer-limited regime. A specific example of the first-order regression plot of the data is shown in Figure 5.5(B).

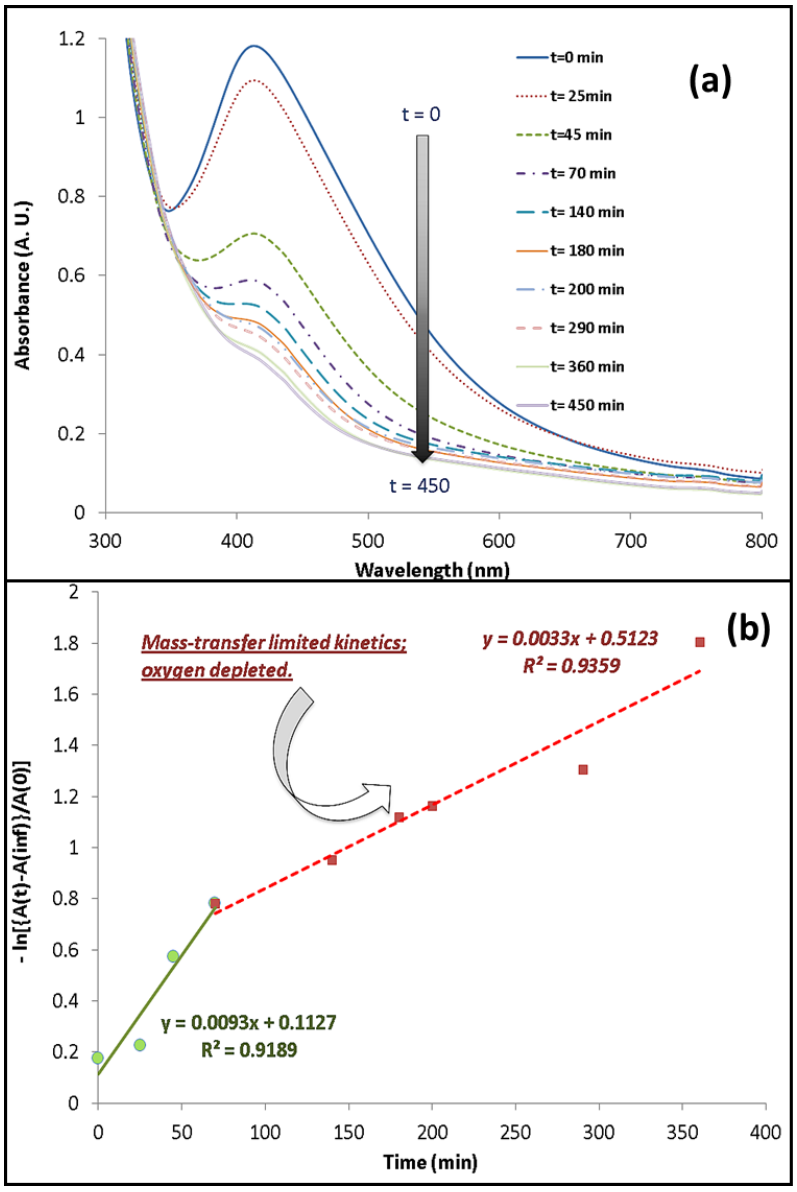

Figure 5.5 (A) Evolution of the UV-Visible spectrum of Ag NPs in P[6,6,6,14]Cl at 65°C in the presence of oxygen: spectrophotometric monitoring of the progress of Ag NP etching; (B) Plot of $-[\ln(A_t - A\infty)/A_0]$ as a function of time for the calculation of pseudo-first-order rate constants for the Ag NP etching process at 65°C in the presence of oxygen.

The Ag NP etching data were fit to a general first-order equation, $A_t = A_\infty + A_0.\exp(-k.t)$, following a kinetic treatment used for NP etching by Murray *et al.,* where

A_∞ is the absorbance (i.e., loss of transmittance) due to light scattering which was invariant with time.[53, 54] The pseudo-first-order rate constants obtained from these experiments have been collected in Table 5.1. For all samples other than #2, repeated flushing of cuvette contents with oxygen was performed initially, but stopped after a certain interval and data points collected after that time were not taken into account for kinetic calculations, owing to a documented shift to mass-transfer-limited regimes. The values of the rate constants are of the same order of magnitude for both the chloride and the bromide ILs, indicating that the etching mechanism is likely identical in both cases. It has already been shown that the nature of the soluble Ag species that forms in halide-rich solutions varies as a function of total Ag and halide (X) concentration; these may be formulated as Ag^+, AgX(solvated), AgX_2^-, AgX_3^{2-}, and AgX_4^{3-}, as predicted by thermodynamics.[55] Generally, in environments as halide-rich as the ILs studied, with the molar ratio (X/Ag) ~ 170 for a 10mM, 10mL Ag NP/IL sample, a range of $AgX_y^{(y-1)-}$ soluble species might be formed, making their exact characterization somewhat difficult.

Serial No.	[Ag NP] (mM)	Ionic Liquid	Temperature (°C)	Rate constant (k, min^{-1})	R^2
1	0.4	P[6,6,6,14]Cl	65 ± 1	9.3×10^{-3}	0.9189
2[a]	0.7	P[6,6,6,14]Cl	65 ± 1	2.3×10^{-3}	0.9017
3	0.5	P[6,6,6,14]Br	65 ± 1	8.1×10^{-3}	0.9849

[a]This experiment was conducted entirely in air, and all data points recorded were used for calculations.

Table 5.1 Pseudo-first-order rate constants calculated for the Ag NP etching process in oxygen in ionic liquids with dynamic UV-Vis spectroscopy at 65^0C.

5.4.4 Speciation of Ag in P[6,6,614]Cl using XANES.

Further proof of Ag NP oxidation over time was followed by XANES spectroscopy at the Ag L_{III} edge; Ag NPs stabilized in the P[6,6,6,14]Br IL were placed in XRF liquid cell holders as detailed in the experimental section. P[6,6,6,14]Br ILs were used instead of P[6,6,6,14]Cl ILs as the Cl K edge is slightly lower in energy than the Ag L_{III} edge and thus makes collection of good signal/noise data in fluorescence mode nearly impossible.

Figure 5.6 shows XANES spectra of the Ag NPs in the IL before and after etching for 6 hours in air. The major change in the spectra is an enhanced white line at the edge which is due to Ag(I) species forming; this peak is attributed to a 2p → 4d transition of Ag(I) (i.e. $AgBr_2^-$), the intensity of which is greatly enhanced by s–d hybridization which leaves vacancies in the 4d band.[43] No efforts were made to quantify the level of Ag(I) species in these solutions, nor have we been able to qualitatively identify $AgBr_2^-$ vs. other possible Ag(I) bromide species in these solutions.

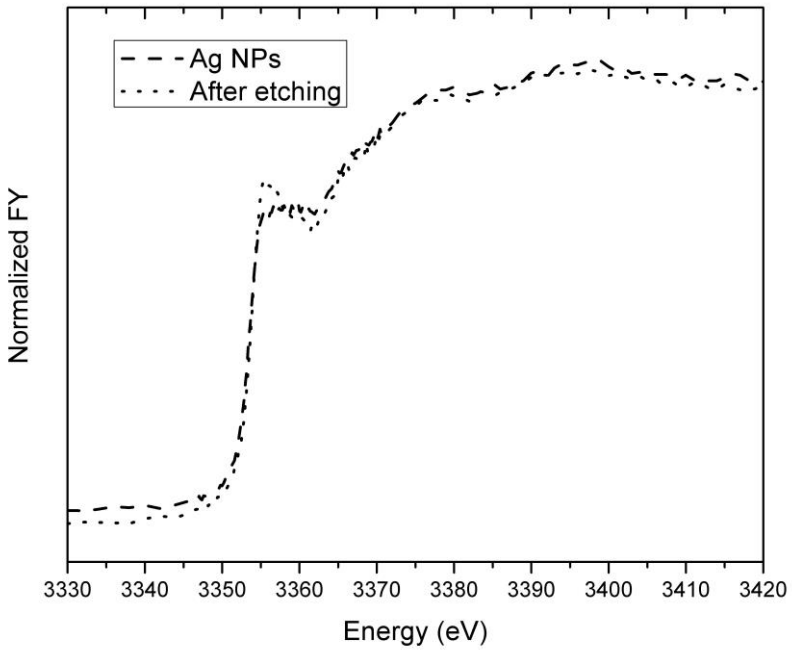

Figure 5.6 Ag L_{III} edge solution phase XANES spectrum of Ag NPs in P[6,6,6,14]Br IL before and after etching in air for 6 hours.

5.5 Conclusions

The present results are from a detailed study of the catalytic behavior of Ag NPs towards EY reduction in tetraalkylphosphonium ILs. Key findings regarding the nature of these systems can be summarized as follows:

(i) Ag NPs generated in P[6,6,6,14]Cl ILs via a bottom-up strategy using lithium borohydride as a reductant were stable to aggregation over a period of months under nitrogen, owing to a combination of factors, such as the presence of strongly coordinating halide ions within the IL medium, steric protection offered by the bulky tetraalkylphosphonium cations, and the high viscosity of the ILs.

(ii) Ag NPs catalyzed the discoloration of EY in the presence of $LiBH_4$ in P[6,6,6,14]Cl/THF medium, with almost a tenfold increase in rate compared to the uncatalyzed counterpart of the reaction.

(iii) Sintered Ag NPs generated by heating the smaller NPs under an inert atmosphere showed reduced catalytic activity. However, the facile dissolution of Ag NPs in in P[6,6,6,14]Cl in the presence of oxygen, and their regeneration via repeated reduction provided us with a pathway for redispersing large, catalytically inactive Ag NPs to smaller, more active ones. From preliminary survey of data, this etching process seems to follow pseudo-first order kinetics. The redispersed Ag NPs showed EY reduction rates comparable to that of the as-synthesized Ag NPs.

(v) XANES spectroscopy of the Ag NPs in P[6,6,6,14]Br shows evidence of etching of the particles over time in air via the appearance of Ag(I) features at the edge.

It is expected that as we explore the chemistry and catalytic behavior of metal nanoparticles (such as Ag NPs) in alternative solvents, we would gain valuable insights into these promising catalytic systems.

Acknowledgements

The authors acknowledge financial assistance from the National Sciences and Engineering Research Council of Canada (NSERC). XANES experiments described in this paper were performed at the Canadian Light Source, which is supported by the Natural Sciences and Engineering Research Council of Canada, the National Research Council Canada, the Canadian Institutes of Health Research, the Province of Saskatchewan, Western Economic Diversification Canada, and the University of Saskatchewan. AB would like to thank the Saskatchewan Innovation and Opportunity Scholarship Foundation for a scholarship.

5.6 References

[1] Astruc, D. *Nanoparticles and catalysis*; Wiley VCH: Weinheim, 2008.

[2] Banerjee, A.; Scott, R. W. J. In *Nanocatalysis: Synthesis and Applications*; 1st ed.; Polshettiwar, V., Asefa, T., Eds.; John Wiley & Sons: Hoboken, New Jersey, 2013.

[3] Gellman, A.J.; Shukla, N. *Nat. Mater*. **2009**, *8*, 87-88.

[4] Yan, N.; Zhang, J.; Yuan, Y.; Chen, G.-T.; Dyson, P. J.; Li, Z.-C.; Kou, Y. *Chem. Commun.* **2010**, *46*, 1631-1633.

[5] Zhang, J.; Yuan, Y.; Kilpin, K. J.; Kou, Y.; Dyson, P. J.; Yan, N. *J. Mol. Catal. A: Chem.* **2013**, *371*, 29-35.

[6] Banerjee, A.; Theron, R.; Scott, R. W. J. *ChemSusChem* **2012**, *5*, 109-116.

[7] Dash, P.; Dehm, N. A.; Scott, R. W. J. *J. Mol. Catal. A: Chem* **2008**, *286*, 114-119.

[8] Fonseca, G. S.; Umpierre, A. P.; Fichtner, P. F.; Teixeira, S. R.; Dupont, J. *Chem. Eur. J.* **2003**, *9*, 3263-3269.

[9] Chen, S.; Liu, Y.; Wu, G. *Nanotechnology* **2005**, *16*, 2360.

[10] Schrekker, H. S.; Gelesky, M. A.; Stracke, M. P.; Schrekker, C. M.; Machado, G.; Teixeira, S. R.; Rubim, J. C.; Dupont, J. *J. Colloid Interface Sci.* **2007**, *316*, 189-195.

[11] Wang, Z.; Zhang, Q.; Kuehner, D.; Ivaska, A.; Niu, L. *Green Chem.* **2008**, *10*, 907-909.

[12] Dash, P.; Scott, R. W. J. *Chem. Commun.* **2009**, 812-814.

[13] Kalviri, H. A.; Kerton, F. M. *Green Chem.* **2011**, *13*, 681-686.

[14] Luska, K. L.; Moores, A. *Green Chem.* **2012**, *14*, 1736-1742.

[15] Ermolaev, V.; Arkhipova, D.; Nigmatullina, L. S.; Rizvanov, I. K.; Milyukov, V.; Sinyashin, O. *Russ. Chem. Bull.* **2013**, *62*, 657-660.

[16] Pal, T.; Sau, T. K.; Jana, N. R. *Langmuir* **1997**, *13*, 1481-1485.

[17] Yu, Y.-Y.; Chang, S.-S.; Lee, C.-L.; Wang, C. C. *J. Phys. Chem. B* **1997**, *101*, 6661-6664.

[18] Astruc, D. *Inorg. Chem.* **2007**, *46*, 1884-1894.

[19] Kvitek, L.; Panáček, A.; Soukupova, J.; Kolar, M.; Vecerova, R.; Prucek, R.; Holecová, M.; Zboril, R. *J. Phys. Chem. C* **2008**, *112*, 5825-5834.

[20] Reinaudi, L.; Giménez, M. C. *J. Comput. Theo. Nanos.* **2013**, *10*, 2507-2519.

[21] Fritz, G.; Schädler, V.; Willenbacher, N.; Wagner, N. J. *Langmuir* **2002**, *18*, 6381-6390.

[22] Zhao, Y.; Cui, G.; Wang, J.; Fan, M. *Inorg. Chem.* **2009**, *48*, 10435-10441.

[23] Prechtl, M. H.; Campbell, P. S. *Nanotech. Rev.* **2013**, *2*, 577-595.

[24] Maclennan, A.; Banerjee, A.; Scott, R. W. J. *Catal. Today* **2013**, *207*, 170-179.

[25] Ahamed, M.; AlSalhi, M. S.; Siddiqui, M. *Clin. Chim. Acta* **2010**, *411*, 1841-1848.

[26] Murphy, C. J.; Sau, T. K.; Gole, A. M.; Orendorff, C. J.; Gao, J.; Gou, L.; Hunyadi, S. E.; Li, T. *J. Phys. Chem. B* **2005**, *109*, 13857-13870.

[27] Wang, H. H.; Liu, C. Y.; Wu, S. B.; Liu, N. W.; Peng, C. Y.; Chan, T. H.; Hsu, C. F.; Wang, J. K.; Wang, Y. L. *Adv. Mater.* **2006**, *18*, 491-495.

[28] Moores, A.; Goettmann, F. *New J. Chem.* **2006**, *30*, 1121-1132.

[29] Lee, K.-S.; El-Sayed, M. A. *J. Phys. Chem. B* **2006**, *110*, 19220-19225.

[30] Amendola, V.; Bakr, O. M.; Stellacci, F. *Plasmonics* **2010**, *5*, 85-97.

[31] Banerjee, A.; Theron, R.; Scott, R. W. J. *Chem. Commun.* **2013**, *49*, 3227-3229.

[32] Kim, S.-S.; Yum, J.-H.; Sung, Y.-E. *Sol. Energy Mater. Sol. Cells* **2003**, *79*, 495-505.

[33] Skou, J.; Esmann, M. *Biochim. Biophys. Acta* **1981**, *647*, 232-240.

[34] Wittekind, D.; Gehring, T. *Histochem. J.* **1985**, *17*, 263-289.

[35] Jiang, Z.-J.; Liu, C.-Y.; Sun, L.-W. *J. Phys. Chem. B* **2005**, *109*, 1730-1735.

[36] Vidhu, V.; Philip, D. *Micron* **2014**, *56*, 54-62.

[37] Jana, N. R.; Sau, T. K.; Pal, T. *J. Phys. Chem. B* **1999**, *103*, 115-121.

[38] Komalam, A.; Muraleegharan, L. G.; Subburaj, S.; Suseela, S.; Babu, A.; George, S. *Int. Nano Lett.* **2012**, *2*, 1-9.

[39] Santhanalakshmi, J.; Venkatesan, P. *J. Nanopart. Res.* **2011**, *13*, 479-490.

[40] Freemantle, M. *An Introduction to ionic liquids*; RSC: Cambridge, U.K., 2009.

[41] Weng, G.; Mahmoud, M. A.; El-Sayed, M. A. *J. Phys. Chem. C* **2012**, *116*, 24171-24176.

[42] Maclennan, A.; Banerjee, A.; Hu, Y.; Miller, J. T.; Scott, R. W. J. *ACS Catalysis* **2013**, *3*, 1411-1419.

[43] Liu, L.; Burnyeat, C. A.; Lepsenyi, R. S.; Nwabuko, I. O.; Kelly, T. L. *Chem. Mater.* **2013**, *25*, 4206-4214.

[44] Estager, J.; Holbrey, J. D.; Swadzba-Kwasny, M. *Chem. Soc. Rev.* **2014**, *43*, 847-886.

[45] Mahmoud, M. A.; Weng, G. *Catal. Commun.* **2013**, *38*, 63-66.

[46] Zhang, J.; Sun, L.; Yoshida, T. *J. Electroanal. Chem.*

6 Optimization of transition metal nanoparticle-phosphonium IL composite catalytic systems for deep hydrogenation and hydrodeoxygenation reactions

This study resulted from an attempt to select a NP/IL system capable of catalyzing the hydrogenation of aromatic species under high hydrogen pressures, and at elevated temperatures. Au NPs were used as an initial probe for the selection of an optimal NP-stabilizing IL; these ILs were then used to stabilize transition metal NPs for the hydrogenation of toluene and phenol. It was surprising to us, however, when the phenol hydrogenation with Ru NPs in P[6,6,6,14]Cl generated not only the hydrogenation but also the hydrodeoxygenation products. After a series of control experiments, we concluded that the borates formed in the IL during the synthesis of metal NPs via borohydride reduction were responsible for the dehydration step, thus effectively generating a tandem catalytic system.

This chapter has been reprinted after minor changes from a recent publication ("Optimization of transition metal nanoparticle- phosphonium ionic liquid composite catalytic systems for deep hydrogenation and hydrodeoxygenation reactions", Abhinandan Banerjee, Robert W J Scott *Green Chem*. **2015**, *17*, 1597-1604, © 2015) with permission from the Royal Society of Chemistry.

Optimization of transition metal nanoparticle-phosphonium IL composite catalytic systems for deep hydrogenation and hydrodeoxygenation reactions

Abhinandan Banerjee and Robert W. J. Scott
Department of Chemistry, University of Saskatchewan
110 Science Place, Saskatoon, Saskatchewan, Canada.

6.1 ABSTRACT

A variety of metal nanoparticle (NP)/tetraalkylphosphonium ionic liquid (IL) composite systems were evaluated as potential catalysts for the deep hydrogenation of aromatic molecules. Particles were synthesized by reducing appropriate metal salts by $LiBH_4$ in a variety of ILs. Gold NPs were used as probes to investigate the effect of both chain lengths of the alkyl substituents on the phosphonium cation and the nature of anions, on the stability of NPs dispersed in the ILs. The presence of three medium-to-long alkyl chains (such as hexyl) along with one long alkyl chain (such as tetradecyl) in the IL, coupled with highly coordinating anions (such as halides, or to a smaller extent, bis-triflimides) produced the most stable dispersions. These ILs also showed maximum resistance to heat-induced sintering; for example, TEM studies of Pt NPs heated under hydrogen to 120^{o}C showed only moderate sintering in trihexyl(tetradecyl)phosphonium chloride and bis(triflimide) ILs. Finally, olefinic hydrogenations, aromatic hydrogenations, and hydrodeoxygenation of phenol were carried out with Ru, Pt, Rh and PtRh NPs using hydrogen at elevated pressures. From preliminary studies, Ru NPs dispersed in trihexyl(tetradecyl)phosphonium chloride emerged as the catalyst system

of choice. The presence of borate Lewis-Acid by-products in the reaction medium (from the borohydride reduction step) allowed for partial phenol hydrodeoxygenation.

6.2 Introduction

In recent years, ionic liquids (ILs) have been used extensively for the stabilization of metal nanoparticles (NPs) and/or as reaction media for metal NP-catalysed reactions.[1-5] Imidazolium ILs, in particular, have been studied extensively for their remarkable ability to serve as reaction media and/or stabilizers for such NP-catalysed transformations.[6-10] However, the imidazolium ILs offer challenges such as base-induced deprotonation and consequent carbene formation,[11] hydrolysis of anions such as PF_6^- and BF_4^- to generate corrosive acids,[12] variations in the efficiency of NP stabilization induced by the presence of trace amounts of impurities such as unreacted IL precursors,[8,13] and comparatively higher melting points of imidazolium halides, which are not room-temperature ILs.[14] It is surprising, therefore, that tetraalkylphosphonium ILs, which are stable under highly basic conditions, commercially available at high levels of purity, less sensitive to moisture and oxygen than their imidazolium counterparts, and largely present as liquids at room temperature even when combined with highly coordinating anions such as halides, have not been investigated more extensively as potential replacements for imidazolium ILs in catalytic reactions of industrial and environmental importance.[15-17] Several groups, including our own, have shown that NP dispersions of catalytically active precious metals in tetraalkylphosphonium ILs are

effective and recyclable catalysts for diverse classes of reactions such as oxidations,[18] selective hydrogenations,[19,20] and C-C cross coupling reactions.[21,22]

One class of reactions that have remained relatively unexplored in the context of metal NP/tetraalkylphosphonium IL composite catalysts is deep hydrogenations, or hydrogenations of aromatic compounds.[23] This is a key reaction in processes such as hydro-refining of heavy oil, production of petrochemicals, synthesis of pharmaceutical products, and generation of biofuel from non-edible lignin.[24] Synthesis of biofuels from lignin includes both hydrogenation as well as hydrogenolysis steps,[25-27] and it is expected that under suitably tuned reaction conditions, a metal NP/IL composite catalyst can perform both reactions simultaneously. NPs of precious metals such as Ir, Rh and Ru have the advantage of high activity for the hydrogenation of aromatic compounds under mild reaction conditions, and their dispersions in functionalized imidazolium ILs have been used in several studies for hydrogenation of mononuclear aromatic species.[4,28-30] Dyson and co-workers, notably, have applied these systems as catalysts in reactions such as hydrodeoxygenation (HDO) of phenol to cyclohexane, and regioselective hydrogenation of toluene to methyl cyclohexene in imidazolium ILs.[31-33] Other protocols also exist for similar conversions, using metal or metal oxide catalysts in different IL media, but to the best of our knowledge, tetraalkylphosphonium ILs have not been used for metal NP-catalysed aromatic hydrogenations, despite their NP-stabilizing abilities and chemical inertness to a variety of reagents.[34,35]

In this work, we show the synthesis and stabilization of catalytically active precious metal NPs in a variety of tetraalkylphosphonium ILs. Initial studies concerning the correlation between structural aspects of the ILs (such as polarizability of anions, lengths of alkyl substituents, etc.) and their NP-stabilizing abilities show that trihexyl(tetradecyl)phosphonium chloride (P[6,6,6,14]Cl and bis(triflimide) ($P[6,6,6,14]NTf_2$) were promising candidates for catalytic NP/IL nanocomposite fabrication when compared to 'short-chain' (P[4,4,4,4]Cl), 'medium-chain' (P[8,8,8,8]Br), and poorly-coordinating-anion-containing ($P[6,6,6,14]N(CN)_2$) ILs. Ru, Rh, Pt, and RhPt NPs in P[6,6,6,14]Cl were active catalysts for simple hydrogenations of allylic alcohols. However, the Ru NP/P[6,6,6,14]Cl IL composite proved to be the most effective system for deep hydrogenations of aromatic compounds such as toluene and phenol (a lignin-analogue) at elevated temperatures and high hydrogen pressures. Interestingly, significant conversion of phenol to the HDO products was seen even in the absence of an added Lewis acid. Further investigations showed the presence of residual borates in the reaction medium (by-products from the initial BH_4^- reduction) facilitated the conversion of phenol to C_6-hydrocarbons.[36,37] This study shows that metal NP/IL composites hold promise for the potential conversion of lignin to C_6-alkanes.

6.3 Experimental

6.3.1 Materials

All chemicals except for the ones listed below were purchased from Sigma Aldrich and used as received. Tetrachloroauric acid, $HAuCl_4.4H_2O$ and potassium tetrachloropalladate, K_2PdCl_4, (both 99.9%, metals basis) were all obtained from Alfa Aesar. Other metal precursors, such as rhodium acetylacetonate ($[CH_3COCH=C(O-)CH_3]_3Rh$), ruthenium chloride ($RuCl_3.xH_2O$), sodium hexachlororhodate (Na_3RhCl_6), platinum acetylacetonate ($[CH_3COCHCOCH_3]_2Pt$), and rhodium acetate ($[Rh(CH_3COO)_2]_2{\cdot}2H_2O$) were purchased from Sigma Aldrich and used without purification. All metal salts were stored under vacuum and flushed with nitrogen after every use. Commercial samples of all the tetraalkylphosphonium ILs mentioned in this work were generously supplied by Cytec Industries Ltd. Commercial samples of liquid ILs were dried under vacuum at 70^{o}C for 5-6 hours with stirring before use. P[4,4,4,14]Cl, which was a solid at room-temperature, was melted via heating, and used without preceding purification steps, while P[4,4,4,4]Cl, which was obtained as a solution in toluene, was heated under vacuum for 6 hours at 70^{0}C for solvent removal. Deuterated solvents were purchased from Cambridge Isotope Laboratories. 18 MΩcm Milli-Q water (Millipore, Bedford, MA) was used throughout.

6.3.2 Synthesis of NPs in IL

In a representative synthesis of 5 mM Au NPs in IL, 20 mg of $HAuCl_4$ was added to a 10 mL sample of the trinbutyl(noctyl)phosphonium chloride (P[4,4,4,8]Cl) IL at 60°C,

and vigorously stirred. To this solution, a stoichiometric excess of $LiBH_4$ reagent (1.0 mL, 2.0 M in THF) was injected drop-wise over a period of five minutes. A brisk effervescence followed, and the entire solution turned wine-red, indicating NP formation. After the addition of $LiBH_4$, volatile impurities were removed by vacuum-stripping the system at 70°C. The Au NP solution thus obtained was stored under nitrogen in a capped vial until use. For the synthesis of Pt and Ru NPs, platinum acetylacetonate and ruthenium chloride, respectively, were used as precursors. Rh NPs, on the other hand, were difficult to synthesize, possibly owing to the limited solubility of most of our Rh precursors of choice. Rhodium acetate had a very high degree of solubility in our ILs, and subsequently, we used that as our precursor of choice. For the synthesis of co-reduced Pt-Rh bimetallic NPs, both precursors were simultaneously dissolved in the IL, and reduced at the same time. Generally, after NP synthesis, excess $LiBH_4$ was quenched with acetone, and volatiles were subsequently removed by vacuum-stripping at 70°C.

6.3.3 Stability Tests for NP/IL composites

As mentioned previously, the NPs were subjected to conditions similar to those they would experience during the course of reactions in order to evaluate their stability under such conditions. Briefly, Au NPs formed in short-alkyl-chained, medium-alkyl-chained, and long-alkyl-chained ILs were examined by UV-Vis spectroscopy (after dilution with MeOH to ~0.1 mM) directly after synthesis, after 3 days of storage, and after being heated to ~ 100°C under nitrogen for a period of 15 minutes to a half-hour.

Rh and Pt NPs, similarly, were heated under hydrogen at 150°C for 12 hours, and their TEM images recorded before and after the heat treatment. The results from these experiments assisted us in selecting an optimal metal NP/IL catalytic composite for high pressure hydrogenations.

6.3.4 General Procedure for Hydrogenation and Hydrodeoxygenation Reactions

These reactions were carried out in hermetically sealed stainless-steel Parr high-pressure reactors. For the hydrogenations of 2-methylbut-3-en-2-ol and toluene (except for one experiment; see Table 6.2), a Parr 4790 high-pressure static reactor (without stirring facilities) was used. For phenol HDO, a dynamic Parr reactor equipped with a temperature control system, a mechanical stirrer, and a pressure meter (Parr 4560) was selected. In a general procedure, 10 mL of the NP solution in IL was mixed with the precursor, transferred to the reaction chamber inside the reactor, flushed with hydrogen at moderate pressures to ensure removal of dissolved oxygen, and heated to the requisite temperature under a high pressure of hydrogen inside the sealed reactor (typically, 20-25 bar). After reaction, the mixture was allowed to cool to ambient temperatures, the hydrogen pressure was released, and the reaction mixture was transferred to a Schlenk flask and vacuum stripped to remove any products formed and/or unreacted starting materials. The products extracted were subsequently characterized by ^{1}H NMR, ^{13}C NMR, and GC-FID. Conversion and selectivity were obtained from GC-FID. For GC-FID analysis, 100 µL of a neat extract was mixed with enough ethyl acetate to make a final volume of 10 mL. 1mL of this solution was then

taken in a GC-vial, and subjected to analysis. The percentage conversion and product selectivities were calculated from two identical measurements, using the GC-FID peak areas and calibration curves for each species. To ensure reproducibility, each reaction was performed at least twice; the yields, etc., were found to vary by no more than ±2-3% between replicate experiments. The only exception to this was the HDO of phenol, where the product selectivities seemed to vary somewhat from experiment to experiment (Table 6.3). We are not sure as to why this variation is observed.

6.3.5 Characterization Techniques.

UV-Vis spectra were obtained using a Varian Cary 50 Bio UV-Vis spectrophotometer with a scan range of 200-800 nm and an optical path length of 1.0 cm. ^{1}H and ^{13}C NMR spectra were obtained using a Bruker 500 MHz Avance NMR spectrometer; chemical shifts were referenced to the residual protons of the deuterated solvent. TEM analyses of the NPs in IL were conducted using a Philips 410 microscope operating at 100 kV. The samples in IL were prepared by ultrasonication of a 5% solution of the NP/IL solution in THF followed by drop-wise addition onto a carbon-coated copper TEM grid (Electron Microscopy Sciences, Hatfield, PA). To determine average particle diameters, a minimum of 100 particles from each sample were measured from several TEM images using the ImageJ program. Conversion and selectivity for the catalytic reactions were obtained by gas- chromatography (GC) using a flame ionization detector (FID, Agilent Technologies 7890A) and a HP-Innowax capillary column.

6.4 Results and Discussion

6.4.1 Au NPs in different tetraalkylphosphonium ILs: UV-Vis and TEM studies

Au NPs were synthesized by reducing $HAuCl_4$ by $LiBH_4$ in a variety of ILs. Following the synthesis, the stability of the Au NPs over time and after heating under nitrogen at 150°C for an hour was monitored by UV-Vis spectroscopy, as shown in Figure 6.1. Other than the Au NP/P[4,4,4,4]Cl IL system, all systems show an initial Au plasmon band in the 520-600 nm range. It is evident that the Au NPs show maximum resistance to coalescence in P[6,6,6,14]Cl and P[4,4,4,14]Cl, given the absence of any tremendous shifts in the plasmon band. Au NPs were unstable to aggregation over 3 days in P[4,4,4,4]Cl, P[4,4,4,8]Cl, and P[8,8,8,8]Br ILs; this is seen by the shift and dampening of the plasmon band to much higher wavelengths, which is typically due to dipole-dipole interactions between aggregated particles.[38] This observation is in line with previous literature: namely, longer alkyl chains in a tetraalkylphosphonium IL bestow upon it greater NP stabilizing abilities and the presence of one alkyl chain longer than the other three (and the resultant asymmetry in the molecular structure of the IL) is crucial for the stability of the NPs in the ILs.[4,18-21] The presence of coordinating anions are necessary for the IL to be a good NP stabilizer.[20] It is evident, therefore, that P[6,6,6,14]Cl (and to a smaller extent, P[4,4,4,14]Cl) satisfy the criteria for being efficient NP-stabilizers, and could potentially be used in catalytic nanocomposites for hydrogenations. TEM images (Figure 6.2) support these conclusions: in P[4,4,4,14]Cl before heat treatment, the average particle size is 4.5± 0.6 nm; after heat treatment, there is an average particle

size growth of ~ 7 nm, with an average final particle size of 11.3 ± 7.1 nm. Similarly, in P[6,6,6,14]Cl, before heat-treatment, the average particle size is 4.1 ± 0.6 nm; after heat-treatment, a bimodal distribution of particle sizes is observed, with mean particle diameters of 3.5 ± 0.6 nm (which corresponds to the as-synthesized particle sizes) and 12.2 ± 3.5 nm (which corresponds to the sintered NP sizes). Although even the longer-chained, asymmetric ILs failed to protect Au NPs completely from heat-induced sintering (as indicated by a blue shift of the Au NP plasmon bands after heating), it was noted that no visible NP precipitation occurred in any of these systems.

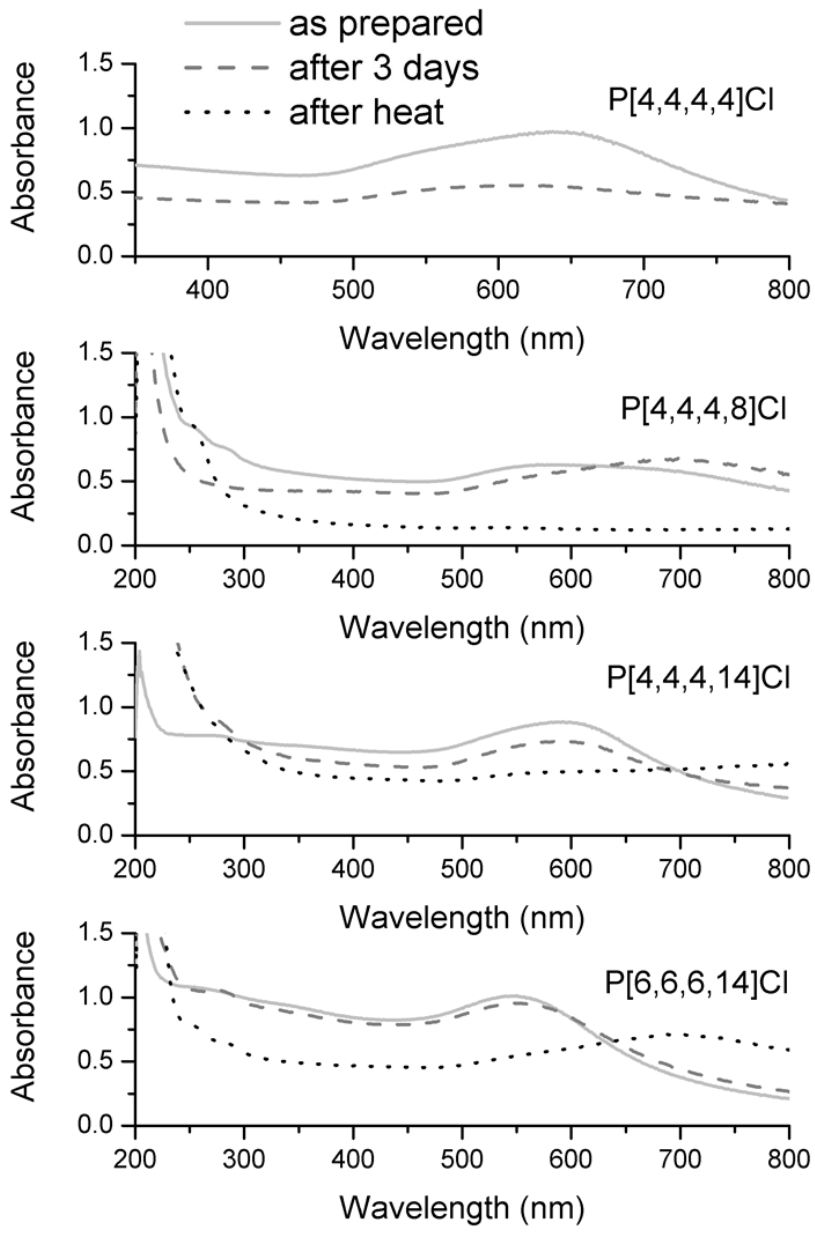

Figure 6.1 UV-Visible spectra of Au NPs in various representative ILs recorded immediately after synthesis (light grey solid line), after three days (deep grey dashed line), and after heating under N_2 at 150°C for 1 h (black dotted line).

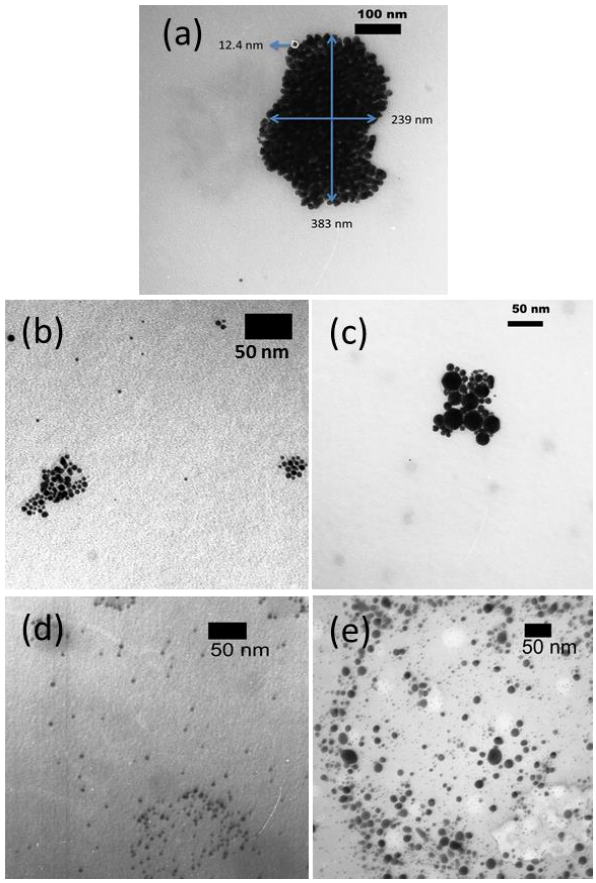

Figure 6.2 TEM images of Au NPs in representative ILs: (a) in P[8,8,8,8]Br after heat treatment- the individual particles (~12 nm average diameter) coalesce to form µm-sized aggregates; (b) in P[4,4,4,14]Cl before heat treatment, with an average particle size of 4.5± 0.6 nm; (c) in P[4,4,4,14]Cl after heat treatment- there is an average particle size growth of ~ 7 nm, with an average final particle size of 11.3 ± 7.1 nm ; (d) in P[6,6,6,14]Cl before heat-treatment, with an average particle size of 4.1 ± 0.6 nm; and (e) in P[6,6,6,14]Cl after heat-treatment- we now see a bimodal distribution of particle sizes, with mean particle diameters of 3.5 ± 0.6 nm (which corresponds to the as-synthesized particle sizes) and 12.2 ± 3.5 nm (which corresponds to the sintered NP sizes).

6.4.2 Pt NPs in ILs after hydrogen treatment

It is known that presence of hydrogen at elevated temperatures can lead to the formation of surface metal hydrides in Pt NPs. This could potentially destabilize the NPs, leading to their agglomeration and precipitation as other stabilizing species get displaced. Thus it was essential for us to study the a system under hydrogenation reaction conditions in the absence of substrates.[39,40] Pt NPs were synthesized in the ILs and exposed to 1 atm hydrogen at 150°C for 12 h to study their stability. TEM images of Pt NPs in P[4,4,4,8]Cl and P[6,6,6,14]Cl before and after hydrogen treatment are shown in Figure 6.3.

The Pt NPs grew in size from 4.7 ± 1.2 nm to 12.2 ± 6.1 nm upon heating under hydrogen in P[4,4,4,8]Cl. On the other hand, in P[6,6,6,14]Cl, both the initial size of the Pt NPs and the increase in Pt NP size was much smaller (<2 nm). The only non-halide IL tested, P[6,6,6,14]NTf_2, showed a moderate increase in particle size upon exposure to hydrogen under heat (from 5.2 ± 1.2 nm to 9.2 ± 2.1 nm). Other non-halide ILs such as P[6,6,6,14]$N(CN)_2$ showed spontaneous NP aggregation and precipitation at much lower temperatures (*ca.* 80°C). On the basis of these observations, we selected P[6,6,6,14]Cl (as a representative halide IL) and P[6,6,6,14]NTf_2 (as a representative non-halide IL) for subsequent experiments.

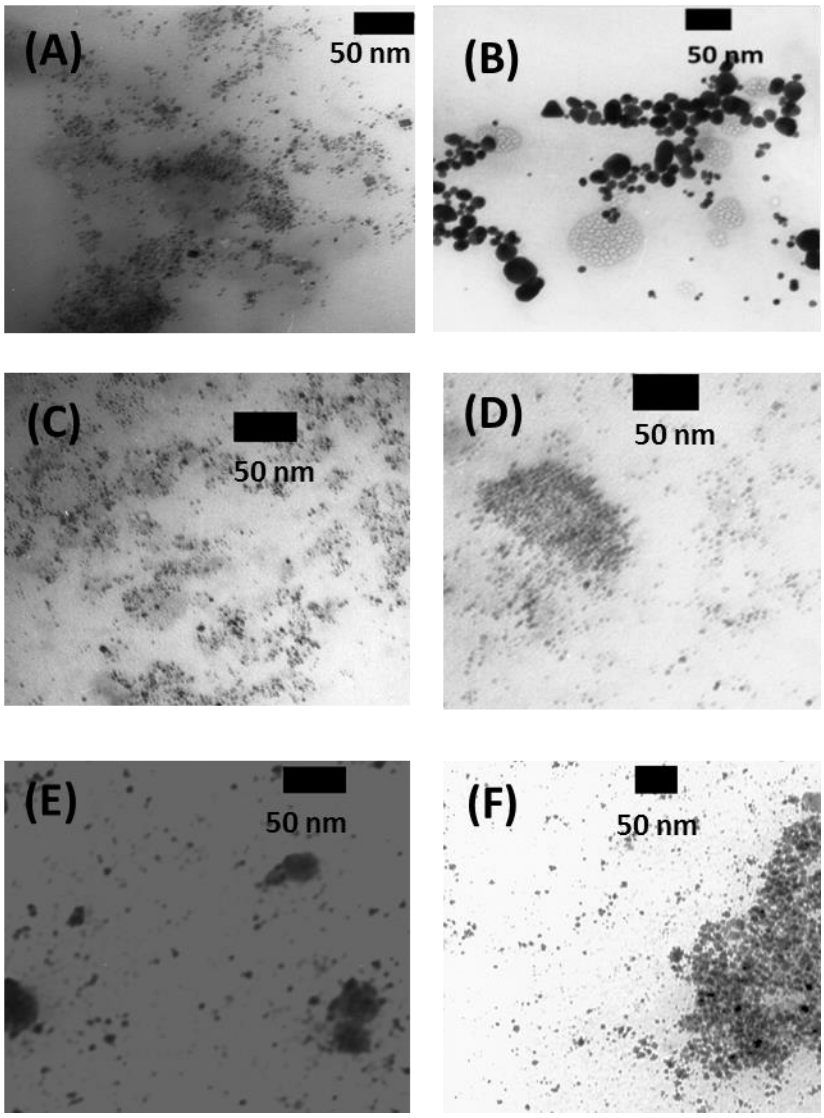

Figure 6.3 TEM images of Pt NPs in P[4,4,4,8]Cl (before heating: A, after heating: B), P[6,6,6,14]Cl (before heating: C, after heating: D), and P[6,6,6,14]NTf_2 (before heating: E, after heating: F). Average sizes of NPs are as follows: (A): 4.7 ± 1.2 nm, (B): 12.2 ± 6.1 nm, (C): 2.1 ± 0.4 nm, (D): 3.8 ± 0.9 nm, (E): 5.2 ± 1.2 nm, and (F): 9.2 ± 2.1 nm. Heating was performed under 1 atm hydrogen at 150°C for 12 h.

6.4.3 Hydrogenation of 2-methylbut-3-en-2-ol by NP/IL composites

The hydrogenation of 2-methylbut-3-en-2-ol to 2-methylbutan-2-ol was selected as an initial test reaction, using Pt, Ru, Rh, and Pt/Rh bimetallic NPs. At 30 bar hydrogen pressure and at moderately elevated temperatures (> 60°C), high conversions were the norm with almost all the NPs under investigation, with conversions ranging from 88-97% (Table 1). Both P[6,6,6,14]Cl and P[6,6,6,14]NTf_2 proved to be capable of metal NP stabilization under reaction conditions. Table 6.1 summarizes the results.

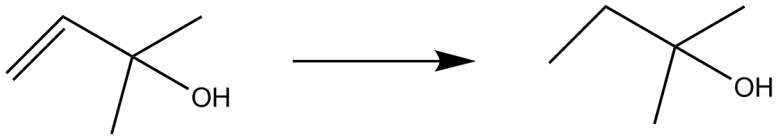

Entry[a]	IL	NP system	Conversion[b]
1	P[6,6,6,14]Cl	Pt	92%
2	P[6,6,6,14]Cl	Pt/Rh	90%
3	P[6,6,6,14]Cl	Ru	97%
4	P[6,6,6,14]NTf_2	Rh	90%
5	P[6,6,6,14]NTf_2	Pt	88%

[a] Conditions: substrate:catalyst = 215; 30 bar Hydrogen; 70°C; 24 h.

[b] % conversion derived from GC-FID analysis (see Experimental).

Table 6.1 Hydrogenation of 2-methylbut-3-en-2-ol catalyzed by 10 mM NP/IL composites

6.4.4 Deep hydrogenation of toluene by NP/IL composites

The deep hydrogenation of toluene to methylcyclohexane requires a high pressure of hydrogen and an efficient catalyst to go to completion, owing to the aromatic stability of the benzene ring.[41] It is, therefore, a suitable trial reaction for testing the efficacy of metal NP/IL nanocomposite hydrogenation catalysts. The results obtained during the course of these trials have been summarized in Table 6.2, for one halide-containing and one halide-free IL. It can be seen that Pt NPs and Pt-Rh NPs were unsuccessful in catalysing this reaction. When $Rh_2(OAc)_6$ was used as a precursor for the Rh NPs, poor conversions were obtained; use of Ru NPs led to higher yields and TONs of *ca.* 70. In all cases, methylcyclohexane was the only product; no partially hydrogenated products could be detected. This is in agreement with previous work by Dupont and co-workers, who used Ru NPs in ILs such as 1-butyl-3-methylimidazolium and 1-decyl-3-methylimidazolium N-bis(triflimides) (-NTf_2) and tetrafluoroborates to give TONs of *ca.* 170 after 18 hours of reaction.[42] Similarly, a Ru-cluster catalyst, used by Welton and co-workers for hydrogenation of toluene in 1-butyl-3-methylimidazolium tetrafluoroborate, gave an average TON of 240.[43] It has also been suggested that the presence of halides, which are known to inhibit catalytic activities of nanoparticles via active-site blocking, could be responsible for reduced yields; Finke and colleagues, for instance, observed that Ir nanoclusters were poisoned by Cl^- for benzene hydrogenation, but remained active for hydrogenation of simple olefinic moieties. However, this would not explain why Ru NPs in P[6,6,6,14]NTf_2 (a non-halide IL) show similarly modest catalytic activities.

It is also noted that MNP/IL composite systems are inherently complicated in nature, possibly containing several different species (larger metal nanoparticles, smaller metal 'nanoclusters', as well as different aggregates of the previous two, such as micrometer-sized particles) in equilibrium. Even for a single class of reaction (such as hydrogenation) catalysed by a single type of nanocluster, different substrate-specific reaction sites exist, which show selective participation in catalysis. Without a detailed study of the individual constituents of MNP/IL composite systems and their reaction sites, it would be impossible to determine the reasons behind enhanced or reduced catalytic activities of certain types of nanoparticle catalysts for specific reactions.

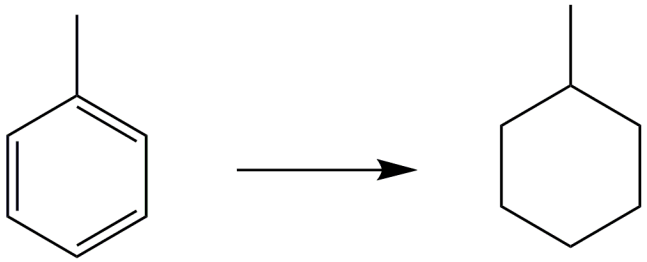

Entry[a]	IL	NP system	Conversion
1	P[6,6,6,14]NTf_2	Ru	22%
2	P[6,6,6,14]NTf_2	Pt	~2%
3	P[6,6,6,14]NTf_2	Rh	5%
4	P[6,6,6,14]Cl	Ru	34%
5	P[6,6,6,14]Cl	Pt	~2%
6	P[6,6,6,14]Cl	Pt/Rh	4%
7[b]	P[6,6,6,14]Cl	Ru	30%

[a] Conditions: substrate:catalyst = 188; 30 bar Hydrogen; 120°C; 24 h.

[b] Reaction performed in a Parr reactor equipped with a mechanical stirrer.

Table 6.2 Hydrogenation of toluene catalysed by 10 mM NP/IL composites

6.4.5 HDO of phenol by NP/IL composites

We selected 10 mM Ru NP/P[6,6,6,14]Cl as our composite catalyst of choice for the deep hydrogenation of phenol under elevated hydrogen pressures. From the TEM image of this system (Figure 6.4), the average particle size was determined to be 2.9 ±

1.2 nm. The hydrogenation of phenol and substituted phenols have been carried out over group VIII metals by others; hydrogenation of phenol produces two important compounds, cyclohexanone and cyclohexanol, both of which are utilized in the manufacture of a large number of industrial products.[44-49] A tentative pathway for phenol HDO has been depicted in Scheme 6.1.

Phenol was found to be highly soluble in the NP/IL composite solution, and showed moderate conversions under specified reaction conditions. Conversions, product distributions, etc. of various trials have been summarized in Table 6.3; ^{1}H and ^{13}C NMR spectra can be found Figure 6.5 (A-C). Higher temperatures and greater H_2 pressures led to a greater degree of conversion of phenol. Cyclohexanone was not present in any of our product isolates, indicating that it is rapidly converted to cyclohexanol; this is similar to results obtained by some researchers, while others have identified it as a key intermediate, possibly indicating that the nature of the catalyst determines the relative rates of the various steps.[50-52] It was surprising, however, that instead of cyclohexanol, the expected hydrogenation product of phenol, a mixture of cyclohexanol, cyclohexene and cyclohexane was isolated. In the presence of a Lewis Acid that had been added deliberately to the reaction mixture to catalyse the dehydration of the alcohol, this would be in accordance with previous reports: in fact, steps leading to each of these products has been summarised in Scheme 6.1.[53-55] However, our system did not contain any intentionally-added Lewis Acids. In the following section, we identify the species responsible for this serendipitous dehydration.

In a representative experiment, the TON for the phenol hydrogenation/HDO was ~65 after 24 h at 120°C under 25 bar hydrogen. This TON is modest compared to those reported by Yan *et al.* in their polymeric IL systems, as well as in the Lewis Acid-functionalized ILs,[31, 32, 50, 56] (TONs of the order of 200-500) but comparable with the TONs reported for other systems such as Pt nanowires in water (TON= 50), Pd/C/lanthanide triflates in dichloromethane and ILs (TON= 10) and Rh NPs in ILs (TON= 100).[57-59] The involvement of the hydroxyl group attached to the ring in the reaction mechanism has previously been found to diminish catalytic activity via active-site blocking,[60-62] which might account for reduced TONs. Heat-induced particle sintering under high H_2 pressures during the course of the reaction could also account for incomplete conversion of cyclohexene to cyclohexane. Two back-to-back catalytic cycles were carried out in order to investigate the recyclability of the system; it was seen that the conversion dropped slightly, with cyclohexene becoming the major product. TEM images of Ru NPs in P[6,6,6,14]Cl (Figure 6.4) after two catalytic cycles indicates a bimodal distribution of particle sizes, with primary particles (average size: 2.9 ± 1.2 nm) showing a slight growth, and secondary particles (average size: 14.6 ± 6.4 nm), presumably formed by coalescence of the primary particles.

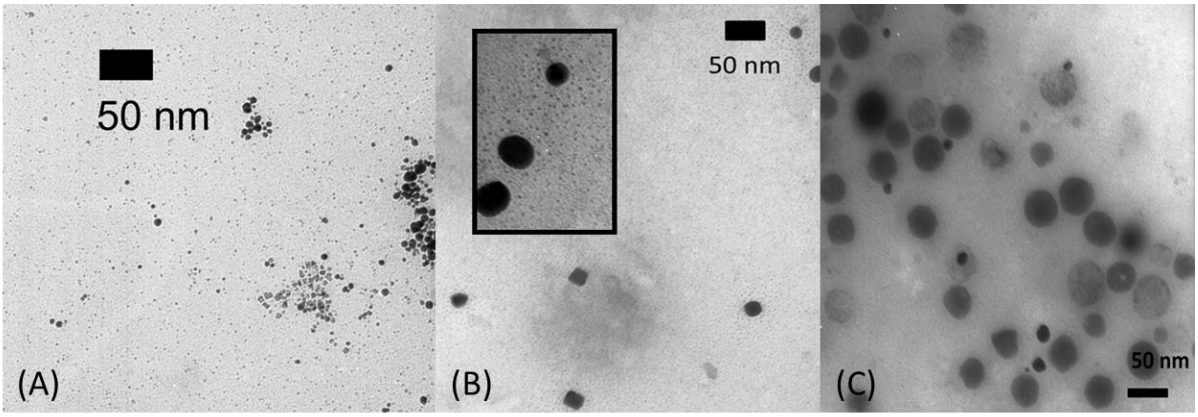

Figure 6.4 (A) TEM images of as-synthesized 10 mM Ru NPs in P[6,6,6,14]Cl. Average particle size is 2.9 ± 1.2 nm. (B,C) TEM images of 10 mM Ru NPs in P[6,6,6,14]Cl after one phenol HDO cycle. Average particle size is 14.6 ± 6.4 nm (ignoring the lighter blobs, which could be droplets of the ionic liquid). The inset in (B) shows two large Ru NPs surrounded by smaller Ru NPs, presumably during the process of particle coalescence.

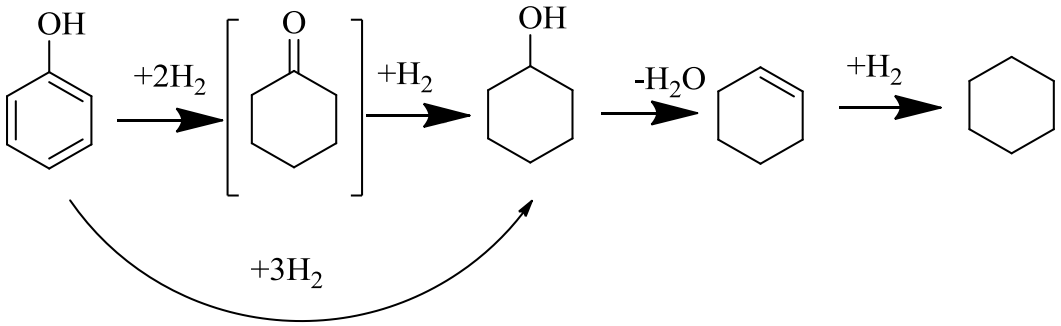

Scheme 6.1 Reaction pathways for phenol HDO by Ru NP in IL**.**

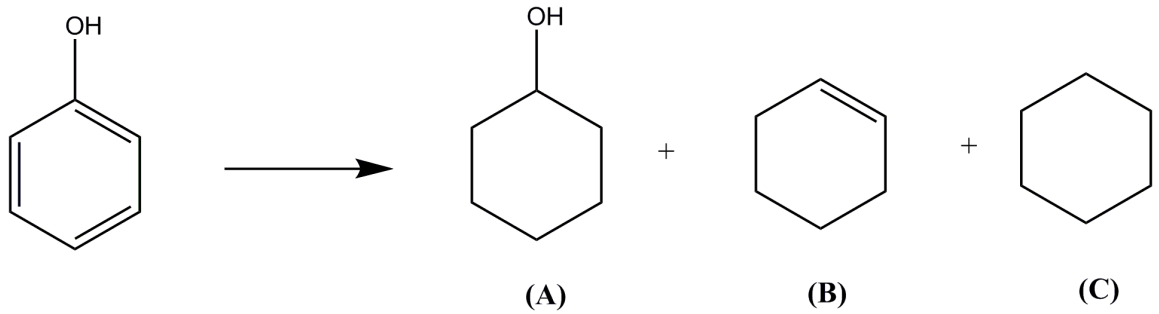

Entry[a]	T (°C)	P (bar)	Conversion[c]	A	B	C
1	120	25	23%	27%	52%	21%
2	120	25	28%	38%	48%	14%
3	110	22	20%	60%	3%	37%
4	135	25	20%	62%	20%	18%
5	65	20	10%	77%	11%	12%
6[b]	110	25	18%	41%	44%	15%

[a] Conditions: substrate:catalyst = 230; 24 h; all reactions performed in a Parr reactor equipped with a mechanical stirrer.

[b] Recyclability test: RuNP/IL composite recovered after removal of reactants and products via vacuum stripping used for a second catalytic cycle.

[c] % conversion and selectivities of A, B, and C derived from GC-FID analysis (see Experimental).

Table 6.3 HDO of phenol catalysed by 10mM RuNP/IL composites

(A)

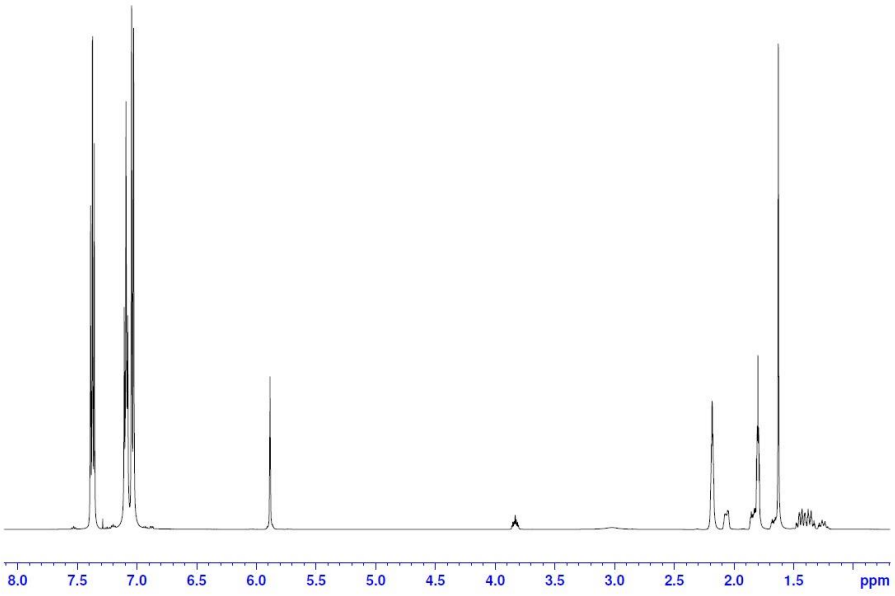
8.0
7.5
7.0
6.5
6.0
5.5
5.0
4.5
4.0
3.5
3.0
2.5
2.0
1.5
ppm

(B)

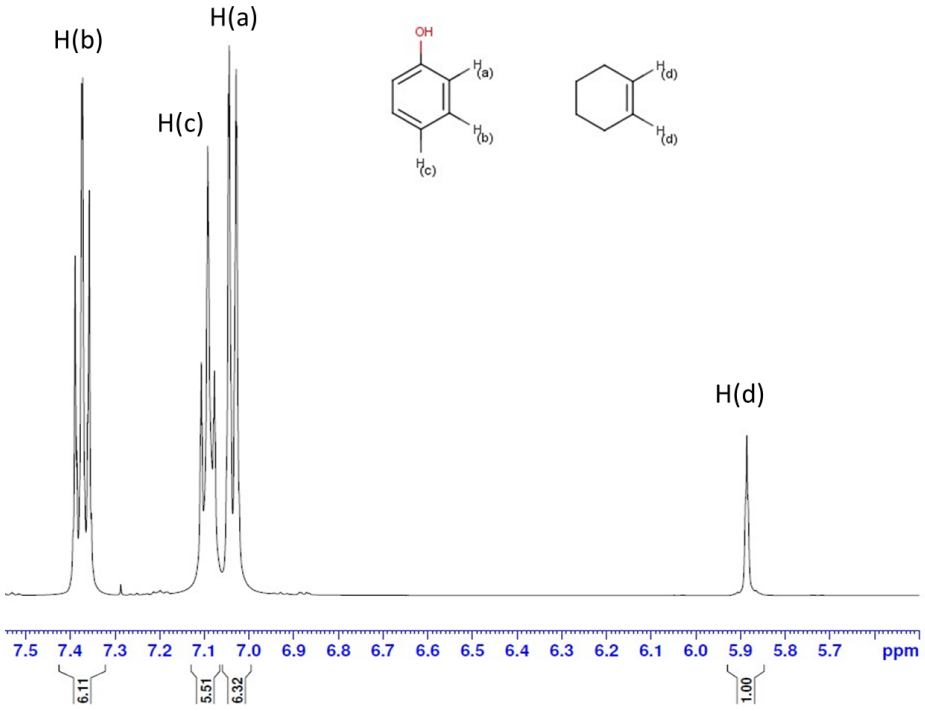
H(b)
H(a)
H(c)
H(d)
OH
H(a)
H(b)
H(c)
H(d)
H(d)
7.5
7.4
7.3
7.2
7.1
7.0
6.9
6.8
6.7
6.6
6.5
6.4
6.3
6.2
6.1
6.0
5.9
5.8
5.7
ppm
6.11
5.51
6.32
1.00

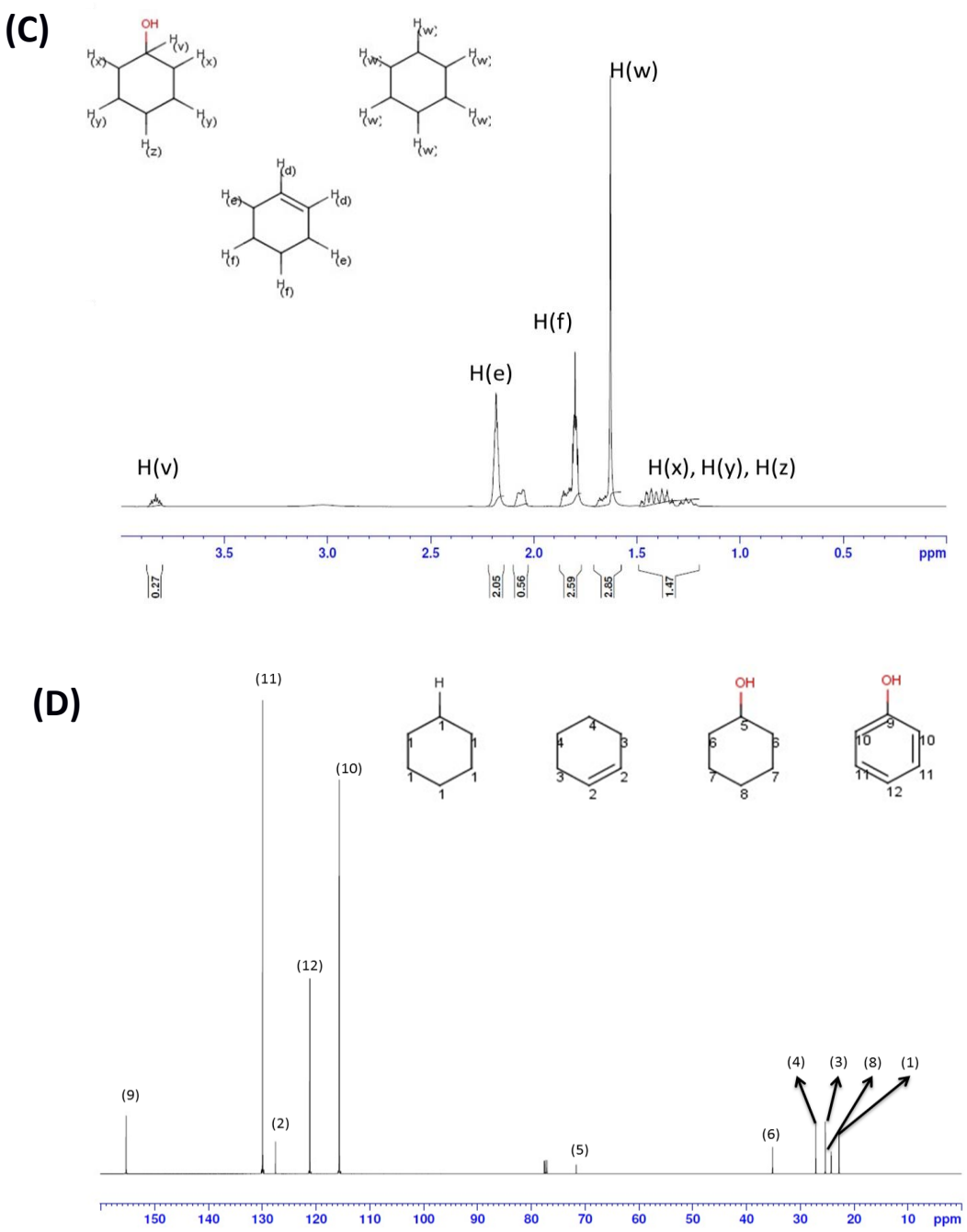

Figure 6.5 (A) ^{1}H NMR spectrum of neat reaction extract (in $CDCl_3$) after phenol HDO. For individual peak assignments, see (B) and (C). (D) ^{13}C NMR spectrum of neat reaction extract (in $CDCl_3$) after phenol HDO.

6.4.6 HDO of phenol by MNP/IL composites: role of borates

The generation of cyclohexane and cyclohexene products suggested that the initially generated cyclohexanol underwent dehydration promoted by a Lewis Acid entity present in the reaction mixture. A similar observation was made in the past by Kobayashi and coworkers using polymer-stabilized AuPd catalysts in water, who showed that advantageous borate species in the reaction medium were Lewis Acid catalysts.[69] Similarly, Riisager and co-workers showed that boric acid, in the presence of salts such as NaCl, is an efficient catalyst for the dehydration of fructose to 5-hydroxymethylfurfural.[70] Boric acid, being cheap, non-toxic, and less corrosive than traditional dehydrating agents (such as concentrated sulphuric acid), is a more benign option for acid-catalysed dehydrations.[71] Others have demonstrated the conversion of chitin into a nitrogen-containing furan derivative under optimized conditions by using boric acid as a dehydrating agent.[72] However, it was still essential for us to rule out other species present in the reaction mixture as possible catalysts. Therefore, control experiments were devised to eliminate the IL itself as the Lewis acid responsible for the dehydration. Details of these control experiments have been summarized in Scheme 6.2. The IL itself showed no dehydration activity (control experiment A in Figure 6.7), while Ru NPs generated in the IL by hydrazine reduction also did not convert cyclohexanol to C_6 hydrocarbons (control experiment B). Ru NPs prepared by borohydride reduction converted cyclohexanol to cyclohexane and cyclohexene (control experiment C). Addition of sodium tetraborate (100 mM) to the IL generated ca. 15% C_6 hydrocarbons from cyclohexanol. Higher conversions (*ca.* 35%) for the dehydration of

cyclohexanol were seen when lithium borohydride was added to a neat IL sample, followed by exposure to air and quenching, thereby generating a soluble borate species (control experiment D). An additional control experiment, in which the NP/IL composite was used in the absence of H_2 to estimate the effect of unreacted borohydride on the product distribution pattern, led to less than 1% conversion, with traces of the alkene as the only identifiable product. Further confirmation of the presence of borate species was obtained by ^{11}B NMR spectroscopy (Figure 6.6), which indicated the presence of unreacted borohydride in a freshly prepared unquenched Ru NP/IL composite. Upon being quenched with acidified methanol or by prolonged exposure to air, the borohydride peak vanished, and a new peak appeared, which could be assigned to a borate species.[73,74] Thus, one of the advantages of synthesizing metal NPs in ILs via borohydride reduction is the generation of Lewis Acidic borate by-products in the reaction mixture that can catalyze subsequent reaction steps in a tandem fashion.

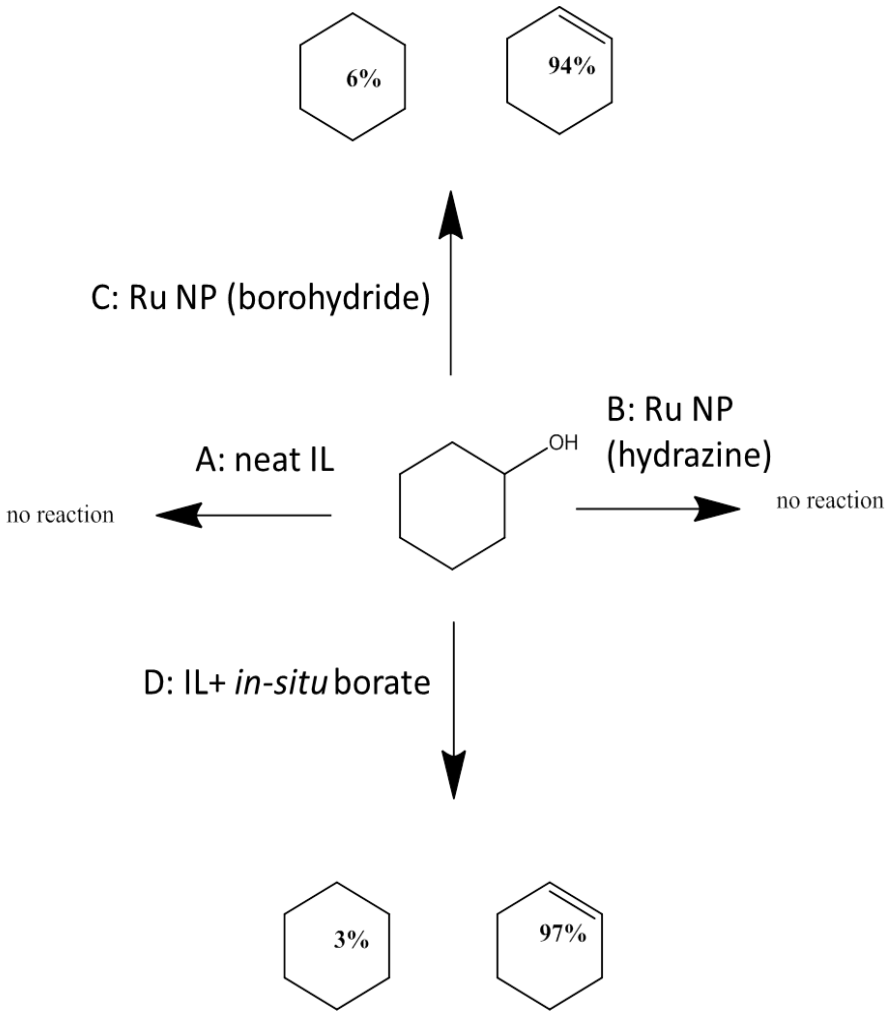

Scheme 6.2 Summary of control experiments performed to evaluate the role of borohydride side products present within the composite catalyst matrix in phenol HDO product distribution. Reaction conditions common to all reactions were as follows: 24 bar Hydrogen pressure; IL P[6,6,6,14]Cl; 120^{0}C, 24 hours. A: in neat P[6,6,6,14]Cl, B: in P[6,6,6,14]Cl containing 10mM Ru NPs synthesized via hydrazine reduction; C: in P[6,6,6,14]Cl containing 10mM Ru NPs synthesized via borohydride reduction; D: in P[6,6,6,14]Cl containing ca. 150 mM soluble borate generated from lithium borohydride.

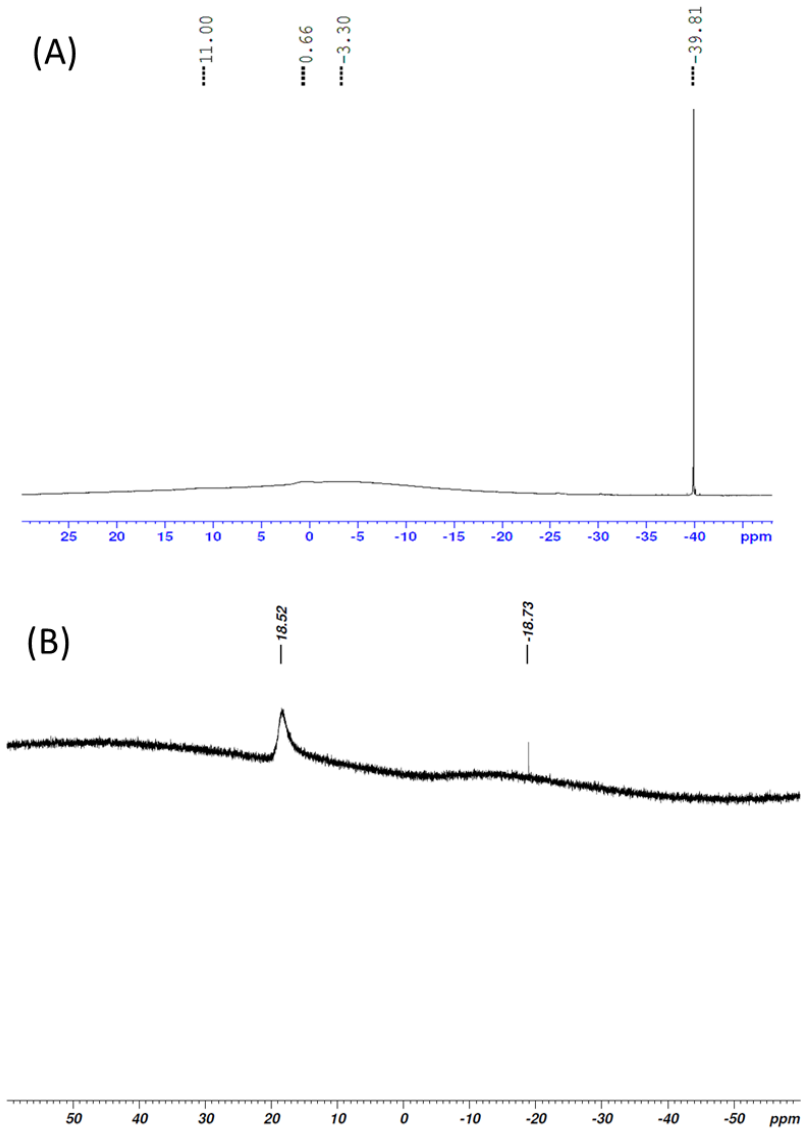

Figure 6.6 ^{11}B proton-decoupled NMR spectrum of P[6,6,6,14]Cl/Ru NP system: (A) ~30 minutes synthesis of NPs via borohydride addition; and (B)~24 hours after borohydride addition and quenching. NMR solvent is THF-D_8. The peak at δ = -40 could be assigned to a borohydride boron, and the one at δ = 18.5 could be assigned to a borate boron.

6.5 Conclusions

A new composite system, transition metal NPs dispersed in tetraalkylphosphonium ILs, was investigated for hydrogenation and phenol HDO catalysis at elevated temperatures and pressures. The following conclusions were drawn from the study:

1. Tetraalkylphosphonium ILs bearing three medium-to-long alkyl chains (such as hexyl) along with one long alkyl chain (such as tetradecyl) in the cation, along with a highly coordinating anion (such as halides, or to a smaller extent, bis-triflimides) are able to offer maximum stabilization for metal NPs.

2. Ru NPs in P[6,6,6,14]Cl and P[6,6,6,14]NTf_2 can catalyse the hydrogenation of aliphatic as well as aromatic molecules at high temperatures under high hydrogen pressures; yields and TONs are higher for the aliphatic substrate.

3. Ru NPs in P[6,6,6,14]Cl can catalyse the HDO of phenol at 110-125^{0}C under 20-25 bar hydrogen pressures, with moderate yields.

4. The product distribution pattern for the nanocomposite catalysed phenol HDO indicates that the residual borates present within the catalyst as a by-product of the borohydride reduction step actually serve as a Lewis acid catalyst leading to dehydration of cyclohexanol, thus generating C_6-hydrocarbons.

It is expected that further research into metal NP/IL nanocomposites, with or without co-catalytic additives, would offer greater insight into the chemistry of these promising catalytic materials.

Acknowledgements

The authors acknowledge financial assistance from the National Sciences and Engineering Research Council of Canada (NSERC) in the form of an NSERC Engage grant. In addition, we thank Al Robertson and Jeffrey Dyck (Cytec Industries, Inc.) for providing samples of the ILs surveyed as well as providing valuable input into the project design.

6.6 References

[1] Ali, M.; Gual, A.; Ebeling, G.; Dupont, J. *ChemCatChem*, **2014**, *6,* 2224-2228.

[2] Dupont, J.; Meneghetti, M.R. *Curr. Opin. Colloid Interface Sci.*, **2013,** *18*, 54-60.

[3] Fonseca, G.S.; Umpierre, A.P.; Fichtner, P.F.; Teixeira, S.R.; Dupont, J. *Chem. Eur. J.*, **2003**, *9*, 3263-3269.

[4] Banerjee, A.; Theron, R.; Scott, R.W.J. *Chem. Commun.*, **2013**, *49*, 3227-3229.

[5] Migowski, P; Dupont, J. *Chem. Eur. J.*, **2007**, *13*, 32-39.

[6] Dash, P.; Dehm, N.A.; Scott, R.W.J. *J. Mol. Catal. A: Chem.*, **2008**, *286*, 114-119.

[7] Dash, P.; Scott, R. W. J. *Chem. Commun.* **2009**, 812-814.

[8] Kessler, M.T.; Hentschel, M.K.; Heinrichs, C.; Roitsch, S.; Prechtl, M.H. *RSC Adv.*, **2014**, *4*, 14149-14156.

[9] Foppa, L.; Dupont J.; Scheeren, C.W. *RSC Adv*., **2014**, *4*, 16583-16588.

[10] Luza, L.; Gual, A.; Rambor, C.P.; Eberhardt, D.; Teixeira, S.R.; Bernardi, F.; Baptista, D.L.; Dupont, J. *Phys. Chem. Chem. Phys***.,** **2014**, *16*, 18088-18091.

[11] Ott, L. S.; Cline, M. L.; Deetlefs, M.; Seddon, K. R.; Finke, R. G. *J. Am. Chem. Soc.* **2005**, *127*, 5758-5759.

[12] Swatloski, R. P.; Holbrey, J. D.; Rogers, R. D. *Green Chem.* **2003**, *5*, 361-363.

[13] Lazarus, L. L.; Riche, C. T.; Malmstadt, N.; Brutchey, R. L. *Langmuir* **2012**, *28*, 15987-15993.

[14] Atilhan, M.; Jacquemin, J.; Rooney, D.; Khraisheh, M.; Aparicio, S. *Ind. Eng. Chem. Res.* **2013**, *52*, 16774-16785.

[15] Del Sesto, R. E.; Corley, C.; Robertson, A.; Wilkes, J. S. *J. Organomet. Chem.* **2005**, *690*, 2536-2542.

[16] Fraser, K. J.; MacFarlane, D. R. *Aust. J. Chem.* **2009**, *62*, 309-321.

[17] Bradaric, C. J.; Downard, A.; Kennedy, C.; Robertson, A. J.; Zhou, Y. *Green Chem.* **2003**, *5*, 143-152.

[18] Maclennan, A.; Banerjee, A.; Scott, R. W. *Catal. Today* **2013**, *207*, 170-179.

[19] Luska, K. L.; Moores, A. *Green Chemistry* **2012**, *14*, 1736-1742.

[20] Banerjee, A.; Theron, R.; Scott, R. W. J. *ChemSusChem* **2012**, *5*, 109-116.

[21] Kalviri, H. A.; Kerton, F. M. *Green Chem.* **2011**, *13*, 681-686.

[22] Ermolaev, V.; Arkhipova, D.; Nigmatullina, L. S.; Rizvanov, I. K.; Milyukov, V.; Sinyashin, O. *Russ. Chem. Bull.* **2013**, *62*, 657-660.

[23] Qi, S.-C.; Zhang, L.; Wei, X.-Y.; Hayashi, J.-i.; Zong, Z.-M.; Guo, L.-L. *R. Soc. Chem. Adv.* **2014**, *4*, 17105-17109.

[24] Srivastava, S. P., Hancsók, J. *Fuels and Fuel-Additives*; John Wiley and Sons: Hoboken, New Jersey, 2014.

[25] Hu, T. Q.; Lee, C.-L.; James, B. R.; Rettig, S. J. *Can. J. Chem.* **1997**, *75*, 1234-1239.

[26] Furimsky, E. *Appl. Cat. A: Gen.* **2000**, *199*, 147-190.

[27] Eachus, S. W.; Dence, C. W. *Holzforschung* **1975**, *29*, 41-48.

[28] Zhong, J.; Chen, J; Chen, L. *Catal. Sci. Technol.,* **2014**, *4*, 3555-3569.

[29] Mu, X.-D.; Meng, J.-Q.; Li, Z.-C.; Kou, Y. *J. Am. Chem. Soc*., **2005**, *127*, 9694-9695.

[30] Umpierre, A. P.; Machado, G.; Fecher, G. H.; Morais, J.; Dupont, J. *Adv. Synth. Catal.* **2005**, *347*, 1404-1412.

[31] Chen, J.; Huang, J.; Chen, L.; Ma, L.; Wang, T.; Zakai, U. I. *ChemCatChem* **2013**, *5*, 1598-1605.

[32] Yan, N.; Yuan, Y.; Dykeman, R.; Kou, Y.; Dyson, P. J. *Angew. Chem. Int. Ed.* **2010**, *49*, 5549-5553.

[33] Schwab, F.; Lucas, M.; Claus, P. *Angew. Chem. Int. Ed.* **2011**, *50*, 10453-10456.

[34] Ramnial, T.; Ino, D. D.; Clyburne, J. A. C. *Chem. Commun.* **2005**, 325-327.

[35] Ramnial, T.; Taylor, S. A.; Bender, M. L.; Gorodetsky, B.; Lee, P. T. K.; Dickie, D. A.; McCollum, B. M.; Pye, C. C.; Walsby, C. J.; Clyburne, J. A. C. *J. Org. Chem.* **2008**, *73*, 801-812.

[36] Ståhlberg, T.; Rodriguez-Rodriguez, S.; Fristrup, P.; Riisager, A. *Chemistry – A European Journal* **2011**, *17*, 1369-1369.

[37] Khokhlova, E. A.; Kachala, V. V.; Ananikov, V. P. *ChemSusChem* **2012**, *5*, 783-789.

[38] Link, S.; El-Sayed, M. A. *J. Phys. Chem. B* **1999**, *103*, 4212-4217.

[39] Kishore, S.; Nelson, J.A.; Adair, J.H.; Eklund, P.C. *J. Alloys Compd*., **2005**, *389*, 234-242.

[40] Hawa, T.; Zachariah, M. *J. Chem. Phys.* **2004**, *121*, 9043-9049.

[41] Rautanen, P. A.; Aittamaa, J. R.; Krause, A. O. I. *Ind. Eng. Chem. Res.* **2000**, *39*, 4032-4039.

[42] Prechtl, M.H.G.; Scariot, M.; Scholten, J.D.; Machado, G.; Teixeira, S.R.; Dupont, J. *Inorg. Chem.,* **2008**, *47*, 8995-9001.

[43] Dyson, P.; Ellis, D.; Parker, D. *Chem. Commun*., **1999**, 25-26.

[44] Bayram, E.; Zahmakıran, M.; Özkar, S.; Finke, R.G. *Langmuir*, **2010**, 26, 12455-12464.

[45] Finney, E.E.; Finke, R.G. *Inorg. Chim. Acta.*, **2006**, *359*, 2879-2887.

[46] Xia, Y.; Xiong, Y.; Lim, B.; Skrabalak, S.E. *Angew. Chem. Int. Ed.*, **2009,** *48*, 60-103.

[47] Tao, A.R.; Habas, S.; Yang, P. *Small*, **2008**, *4*, 310-325.

[33] Zhao, C.; Kou, Y.; Lemonidou, A. A.; Li, X.; Lercher, J. A. *Angew. Chem.* **2009**, *121*, 4047-4050.

[48] Mahata, N.; Raghavan, K.; Vishwanathan, V.; Park, C.; Keane, M. *Phys. Chem. Chem. Phys.* **2001**, *3*, 2712-2719.

[49] Zhu, J.-F.; Tao, G.-H.; Liu, H.-Y.; He, L.; Sun, Q.-H.; Liu, H.-C. *Green Chem.* **2014**, *16*, 2664-2669.

[50] Wang, Y.; Yao, J.; Li, H.; Su, D.; Antonietti, M. *J. Am. Chem. Soc.* **2011**, *133*, 2362-2365.

[51] Liu, H.; Jiang, T.; Han, B.; Liang, S.; Zhou, Y. *Science* **2009**, *326*, 1250-1252.

[52] Chen, A.; Li, Y.; Chen, J.; Zhao, G.; Ma, L.; Yu, Y. *ChemPlusChem* **2013**, *78*, 1370-1378.

[53] Xu, H.; Wang, K.; Zhang, H.; Hao, L.; Xu, J.; Liu, Z. *Catalysis Science & Technology* **2014**.

[54] Ohta, H.; Kobayashi, H.; Hara, K.; Fukuoka, A. *Chem. Commun.* **2011**, *47*, 12209-12211.

[55] Zhao, C.; Lercher, J. A. *ChemCatChem* **2012**, *4*, 64-68.

[56] Jongerius, A. L.; Jastrzebski, R.; Bruijnincx, P. C.; Weckhuysen, B. M. *J. Catal.* **2012**, *285*, 315-323.

[57] Yan, N.; Zhao, C.; Dyson, P.J.; Wang, C.; Liu, L.-T.; Kou, Y. *ChemSusChem*, **2008**, *1*, 626-629.

[58] Zhao, C; Kou, Y.; Lemonidou, A.A.; Li, X.; Lercher, J.A. *Chem. Commun*., **2010**, *46*, 412-414.

[59] Zhao, C; Kou, Y.; Lemonidou, A.A.; Li, X.; Lercher, J.A. *Angew. Chem. Int. Ed.,* **2009**, *48*, 3987-3990.

[60] Guo, Z.; Hu, L.; Yu, H.-h.; Cao, X.; Gu, H. *RSC Adv.* **2012**, *2*, 3477-3480.

[61] Yu, T.; Wang, J.; Li, X.; Cao, X.; Gu, H. *ChemCatChem* **2013**, *5*, 2852-2855.

[62] Maksimov, A. L.; Kuklin, S. N.; Kardasheva, Y. S.; Karakhanov, E. A. *Petrol. Chem.* **2013**, *53*, 157-163.

[63] Shin, J.Y.; Jung, D.J.; Lee, S.-g. *ACS Catal.*, **2013,** *3*, 525-528.

[64] Lee, D. K.; Ahn, S. J.; Kim, D. S. In *9th International Symposium on Catalyst Deactivation*; J.J. Spivey, G. W. R., B.H. Davis, Ed.; Elsevier: Lexington, KY, USA, 2001; Vol. 139, pp 69-76.

[65] Popov, A.; Kondratieva, E.; Mariey, L.; Goupil, J. M.; El Fallah, J.; Gilson, J.-P.; Travert, A.; Maugé, F. *J. Catal.* **2013**, *297*, 176-186.

[66] Furimsky, E. *Catalysis Reviews* **1983**, *25*, 421-458.

[69] Yoo, W.-J.; Miyamura, H.; Kobayashi, S. *J. Am. Chem. Soc.* **2011**, *133*, 3095-3103.

[70] Ståhlberg, T.; Rodriguez-Rodriguez, S.; Fristrup, P.; Riisager, A. *Chem. Eur. J.* **2011**, *17*, 1456-1464.

[71] Walia, M.; Sharma, U.; Agnihotri, V. K.; Singh, B. *R. Soc. Chem. Adv.* **2014**, *4*, 14414-14418.

[72] Chen, X.; Chew, S.L.; Kerton, F.M.; Yan, N. *Green Chem.*, **2014**, *16*, 2204-2212.

[73] Onak, T.P; Landesman, H.; Williams, R.E. *J. Phys. Chem.* **1959**, *63*, 1533-1535.

[74] Good, C.D.; Ritter, D.M. *J. Am. Chem. Soc.,* **1962**, 84, 1162-1166.

7 Synthesis, Characterization, and Evaluation of Iron Nanoparticles as Hydrogenation Catalysts in Tetraalkylphosphonium Ionic Liquids

Inspired by several recent publications that extolled the virtues of earth-abundant metal NPs in catalysis, the catalytic ability of earth-abundant 3d transition metals in IL media was investigated. There have been a number of studies on Fe/Fe_xO_y NPs as hydrogenation catalysts which showed remarkable catalytic abilities, but these studies were mostly conducted in water, alcohols, or other organic solvents. We wanted to explore the chemistry of bare Fe NPs in tetraalkylphosphonium ILs as a counterpoint to the existing studies on their catalytic behavior in protic solvents. It is expected that this chapter would form part of a collaborative publication with Yali Yao, who is presently studying hydrogenations in alcoholic media using PVP-protected oxide-coated Fe NPs as catalysts.

Synthesis, Characterization, and Evaluation of Iron Nanoparticles as Hydrogenation Catalysts in Tetraalkylphosphonium Ionic Liquids

7.1 ABSTRACT

The use of solvent-dispersed iron nanoparticles (Fe NPs) as catalysts has proliferated extensively within the last decade, especially for hydrogenations of unsaturated organic functionalities. Much of this work, however, has been done in solvents such as water and alcohols; very little is known about the fate of Fe NPs in other classes of solvents, such as ILs. In this study, Fe NPs synthesized in tetraalkylphosphonium ILs via a one-pot chemical reduction strategy are tested for their catalytic activities in the hydrogenation of simple olefins. It was observed that these NPs could catalyze the conversion of 2-norbornene to norbornane in good yields under moderately high hydrogen pressures. However, reduced conversions were observed upon recycling. A marked tendency for Fe NPs in these systems to undergo oxidative degradation was noted, which limits their utility in catalysis unless rigorous anhydrous and anoxic conditions are maintained. Finally, *in situ* X-ray Absorption Spectroscopy was applied to determine the fate of Fe in these systems upon catalysis and exposure to air. It could be concluded from the results of this survey that the formation of higher oxidation states of Fe from Fe NPs in anoxic solvents preclude the possibility of the protection offered by an iron oxide coating on

the NP surfaces, thereby allowing their oxidative decay to proceed more rapidly. The addition of a secondary stabilizer improved the longevity and reactivity of Fe NPs dispersed in ILs Fe NPs in ILs with strongly coordinating anions are not particularly stable to oxidation, while those in IL with non-coordinating anions agglomerate during catalysis, thus making these systems less useful for catalysis.

7.2 Introduction

Catalysis with transition metal NPs has been studied extensively in the last few decades owing to the inherent advantages associated with nanocatalysis, such as recyclability, robustness, and an unprecedented degree of control over reactivity and selectivity via controlled changes in NP shapes, sizes, and their surrounding environments.[1,2] While initial research on catalysis with NPs primarily focused on NPs of precious metals such as Pt, Au, Ru, Pd, in recent years, the focus has shifted to earth-abundant metal nanoparticles such as Fe, Ni and Cu, for obvious reasons such as cost-effectiveness, abundance, lower toxicity, and smaller environmental impact.[3] Fe, in particular, has emerged as a potential candidate for several catalytic reactions of industrial and scientific interest, such as hydrogenations, hydrosilylations, oxidations, and hydroaminations, owing to certain inherent advantages associated with the use of Fe, such as negligible bio-, cyto-, and environmental toxicity, lower cost, greater abundance in Earth's crust, and potential for facile magnetic recovery of the catalyst from the reaction medium.[4] Heterogeneous catalytic processes using Fe catalysts, such

as the Haber-Bosch and the Fischer-Tropsch reactions, are already well-known for their industrial applications.[5-7] Fe NPs are also noted for their role in environmental remediation as catalysts for oxidative or reductive degradation of contaminants such as dyes, halogenated organic species, malodorous sulfides, and toxic heterocycles.[8]

Some of the most remarkable recent developments in homogeneous catalysis using Fe complexes have been reported by Morris and coworkers, who have developed hydrogenation and transfer hydrogenation protocols using Fe complexes, with unprecedented catalytic activities and stereoselectivities.[9-11] However, often it is not necessary to use pre-synthesized organometallic complexes of Fe at all for hydrogenations: Thomas and co-workers, for instance, have reported *in-situ* Fe-catalyzed, hydride-mediated reductions of mono-, di-, and tri-substituted olefins, using 25 mol% $Fe(OTf)_2$ or $FeCl_2$ as a bench-stable iron precatalysts, $LiBEt_3H$ as the hydride source, and 1 mol% N-methylpyrrolidinone.[12,13] The reaction was believed to proceed through a radical mechanism, involving a homogeneous active catalyst. A combination of homogeneous and NP-catalyzed mechanistic regime was confirmed by Gieshoff *et al.* in their reported protocol for Fe-catalyzed hydrogenation of alkenes and alkynes at 1 bar hydrogen pressure.[14]

One of the first catalytic studies that utilized pre-formed (as opposed to formed *in situ*) Fe NPs was conducted by De Vries *et al*., who have demonstrated that ~2.5 nm Fe NPs generated by the reduction of ferrous or ferric salts in different solvents, using metal alkyls (such as R_3Al, RMgCl, or RLi) as reductants, can catalyze the hydrogenation

of alkenes and alkynes at >10 atm H_2 pressures. Chloride anions and donor solvents such as THF were thought to have stabilized the Fe NPs against agglomeration; it was also noted that even 1% water in the reaction medium could strongly reduce the catalytic efficiencies of the Fe NP systems for olefin hydrogenations.[15,16] Similar results have been noted by Chaudret and colleagues, who used well-defined, ultra-small Fe NPs, synthesized via the decomposition of $Fe\{(N[SiMe_3]_2)_2\}_2$ at 150°C under dihydrogen, for the hydrogenation of various alkenes and alkynes. They also quantified the hydride adsorption onto the Fe NP surfaces, arriving at a value of 0.4 to 0.6 hydrides per surface iron atom in 1.5 nm Fe NP dispersions.[17] Some of the first reports of Fe-NP-catalyzed hydrogenations in the presence of water and air came from the research group of Moores, who published several seminal studies on catalytic hydrogenations and oxidations using Fe/Fe-oxide core shell nanoparticles dispersed in solvents such as water and ethanol, both in conventional reactors, and under flow conditions.[18-20] Others involved in the study of catalytic properties of Fe have revealed that Fe-based catalysts can be effective for hydrogenation of substrates as diverse as alkenes, alkynes, imines, carbonates, and carbonyl functionalities, often with remarkably high yields and notable degrees off catalytic recyclability.[21] It is surprising, however, that the application of Fe NPs in alternative solvents such as ILs has not been explored in any great detail, despite an abundance of synthetic protocols for the fabrication of Fe NPs in ILs.[22-24] To the best of our knowledge, there is only one such study in the literature, where nitrile-functionalized bis(triflimide) imidazolium ILs, with a methyl substituent on the

imidazolium C_2 to prevent proton abstraction by the Grignard reagent used for reduction of the Fe precursor, was used as a solvent as well as a NP-stabilizer, for Fe NP catalyzed hydrogenations.[14] These Fe NPs could selectively generate *Z*-alkenes from alkynes. However, not only does this protocol necessitate the use of a task-specific IL, but also needs heptane as a co-solvent, as well as strict anaerobic conditions. There are certain obvious reasons why the fabrication of Fe NPs in solvents other than water or volatile organics merits a detailed investigation. While Fe oxide NPs in water are cheap and easy to make, they also suffer from challenges such as larger overall sizes and inhomogeneous size distributions. In addition, speciation studies performed on these catalytic systems are most commonly of the *ex situ* variety, such as XRD and XPS of isolated catalytic samples. These studies are incapable of monitoring changes in the oxidation states of Fe atoms on the NP surfaces, in real time, in the reaction medium.[25,26] It is to be noted that the behavior of metal NPs in ILs can differ significantly when compared to water and other protic solvents; it was recently shown by us that Ni nanoparticles in tetraalkylphosphonium halide ILs upon exposure to oxygen form a chloronickellate complex rather than a nickel oxide coating on the nanoparticle surfaces, which has been previously reported to happen in other solvents.[27,28] Similarly, Kessler *et al.* reported that adjustment of reaction parameters, such as temperature, time and heating methods, have a profound influence on the oxidation state of the metal in metal NPs generated via the heating of metal salts in tetraalkylphosphonium acetates.[29] It is important, therefore, to use techniques such as X-ray absorption spectroscopy (XAS)

which can give us valuable information about the composition and structure of species in solution having short range order. Since the recyclability of Fe NP catalysts in alternative solvents depend on their interactions with said solvent under reaction conditions, it is imperative for us to explore these interactions in order to have a better understanding of the catalytic process as a whole.

In this study, we synthesized Fe NPs in two tetraalkylphosphonium ionic liquids: tri(hexyl)tetradecylphosphonium chloride, P[6,6,6,14]Cl, a representative halide IL that has proved to be an excellent 'solvent-cum-stabilizer' for catalytically active Pd and Ru NPs, and tri(hexyl)tetradecylphosphonium bis(tiflimide), P[6,6,6,14]NTf_2, a halide-free IL, in which Ru NPs have been shown to remain highly active hydrogenation catalysts for eight consecutive reaction cycles by Luska *et al*.[30,31] These ILs possess what is referred to as 'intrinsic nanoparticle stabilizing ability', unlike solvents such as ethanol, where PVP must be used as an external stabilizer. These nanoparticles were then examined as catalysts in the hydrogenation of a representative alkene (2-norbornene) with molecular hydrogen as a cheap and atom-economic reducing agent. It was noticed that Fe NPs in P[6,6,6,14]Cl were difficult to synthesize and prone to oxidation, especially during the catalytic hydrogenation reactions, despite our best attempts to exclude air and moisture from these systems. In P[6,6,6,14]NTf_2, Fe NPs could be readily generated using lithium aluminum hydride, a stronger reductant than $LiBH_4$. These NPs were seen to be stable to oxidative degeneration under anaerobic conditions, and were able to catalyze the high pressure hydrogenation of alkenes, but were prone to post-catalytic aggregation in the

absence of a secondary stabilizer, such as PVP. XAS of Fe NPs samples in various solvents under a variety of conditions enabled us to explain these observations in terms of the stability and reactivity of the NPs in these solvents. In anoxic solvents such as the ILs, oxidative degeneration of Fe NPs occurs via a mechanism that does not involve the formation of a protective oxide coating on the nanoparticle surfaces. This might limit their use as stabilizing solvents far catalytically active Fe NPs. Finally, XANES spectra of these systems were used to gain insight into the fate of Fe NPs in alternative solvents at various stages of their life cycle.

7.2 Experimental

7.2.1 Materials

Unless otherwise mentioned, all chemicals were used as received. Iron(III) chloride and Iron(III) acetylacetonate were purchased from Fisher Scientific. $LiAlH_4$ (2.0 M in THF) was purchased from Sigma Aldrich. The tri(hexyl)tetradecylphosphonium (P[6,6,6,14]X; X= -Cl or -NTf_2) ILs were purchased from Cytec Industries Ltd., and were dried under vacuum at 70^oC for 10-12 hours with stirring before use. 2-norbornene and norbornane were purchased from Sigma Aldrich, and used as received.

7.2.2 Procedure for synthesis of Fe NPs in PVP-free IL.

In a representative synthesis of Fe NPs in P[6,6,6,14]Cl, 12 mg of $Fe(acac)_3$ (0.2 mmol with respect to Fe) was added under nitrogen to a 10 mL sample of the IL at 80^oC in a Schlenk flask, and vigorously stirred. The solution was cooled to 50^oC, and a stoichiometric excess of $LiAlH_4$ reagent (2 mL, 2.0 M in THF) was injected drop-wise into

it over a period of 2 to 3 minutes. A brisk effervescence followed, and the deep red solution turned black, which is indicative of NP formation. After the addition of $LiAlH_4$, volatile impurities were removed by vacuum-stripping the system at 80°C. The Fe NP-IL composites thus obtained were directly transferred to the glass reactor vessel for hydrogenation.

7.2.3 Procedure for synthesis of Fe NPs in P[6,6,6,14]NTf_2 containing PVP.

This procedure was identical to the previous one, except for the addition of 1 g of PVP (average molecular weight of 55,000; [PVP]/[Fe] ~ 0.1) to the IL prior to the addition of the $Fe(acac)_3$.

7.2.4 Procedure for Fe NP catalyzed hydrogenations.

Hydrogenations were carried out in a dynamic Parr reactor equipped with a temperature control system, a mechanical stirrer, and a pressure meter (Parr 4560). In a general procedure, 10 mL of the NP solution in IL was mixed with 10 mmol alkene, transferred under nitrogen to the reaction chamber inside the reactor, flushed with hydrogen at moderate pressures, and heated to the requisite temperature under a high pressure of hydrogen inside the sealed reactor (typically, 25 bar). After reaction, the mixture was allowed to cool to ambient temperatures, the hydrogen pressure was released, and the reaction mixture was transferred to a Schlenk flask and vacuum stripped to remove any products formed and/or unreacted starting materials. The products were removed from the IL/Fe-NP dispersion under vacuum, and were subsequently characterized by ^{1}H NMR, ^{13}C NMR, and GC-FID. Conversion and

selectivity were obtained from GC-FID. For GC-FID analysis, 250 µL of a neat extract was mixed with enough cyclohexane to make a final volume of 5 mL. 1 mL of this solution was then taken in a GC-vial, and subjected to analysis. The percentage conversion and product selectivities were calculated from two identical measurements, using the GC-FID peak areas and calibration curves for each species. To ensure reproducibility, each reaction was performed at least twice; the yields, etc., were found to vary by no more than ±1-2% between replicate experiments.

7.2.5 Characterization Techniques.

Unless otherwise stated, all reactions were performed using standard Schlenk techniques, with nitrogen used to provide an inert atmosphere, in oven-dried Schlenk glassware. A Varian Cary 50 Bio UV-Visible spectrophotometer with a scan range of λ=200–800 nm and quartz cuvettes with optical path lengths of 0.4 cm or 1 cm were used for ambient temperature UV-Vis spectra. TEM analyses of the NPs in ILs were conducted using a Hitachi HT7700 microscope equipped with a LaB_6 filament operating at 100 kV. The TEM samples were prepared by ultrasonication of ~5% solution of the Fe NPs in their respective matrices dissolved in THF followed by drop-wise addition onto a carbon-coated copper TEM grid (Electron Microscopy Sciences, Hatfield, PA). To determine particle diameters, a minimum of 100 particles from each sample from several TEM images were manually measured by using the ImageJ program. An Agilent 7890A Gas Chromatograph fitted with a HP-5 column was used for the detection of norbornene and norbornane. Karl Fischer titration of the ILs was carried out after the

dissolution of 0.5 g of each in 10 mL volumetric flasks containing clean, dry dichloromethane; A Mettler Toledo C20 Coulometric Karl Fischer titration apparatus was used. Three readings were taken per sample, and the reading for neat dichloromethane was subtracted from the resulting values to obtain the water content of the ILs in ppm.

Fe K-edge XANES spectroscopy was carried out on the SXRMB Beamline (06B1-1) at the Canadian Light Source (CLS). The beamline was equipped with InSb(111) and Si(111) crystals, and has an energy range of 1700 - 10000 eV with a resolution of 1×10^{-4} $\Delta E/E$. XANES spectra were obtained in fluorescence mode. The setup for liquid XANES work was similar to previous investigations; solution samples were placed in SPEX CertiPrep Disposable XRF X-Cell sample cups fitted with polypropylene inserts and sealed with an X-ray transparent film (Ultralene film, 4 µm thick, purchased from Fisher Scientific, Ottawa, ON). The sample solution cell was placed on the sample holder that faces the incident beam at 45° angle. The software package IFEFFIT was used for data processing.

7.3 Results and discussion

7.3.1 Characterization of Fe NPs in P[6,6,6,14]Cl and P[6,6,6,14]NTf_2

The synthesis of Fe NPs in tetraalkylphosphonium ILs was motivated by the possibility of formation of bare Fe NPs (i.e., without oxide shells) in these solvents, since oxidation of Fe(0) in P[6,6,6,14]Cl preferentially forms $FeCl_6^{3-}$ rather than Fe_xO_y.[32-35] The stability of Fe NPs (generated via reduction with $LiAlH_4$) in this IL, however, was very limited. Exposure to ambient moisture and oxygen readily led to degradation of the NPs,

turning the black dispersion to pale yellow, possibly indicating the oxidation of Fe(0) to higher oxidation states; this is in accordance with the observations of de Vries and co-workers, who recorded rapid oxidative degradation of their Fe NPs by 2 eq. of acetic acid, leading to a similar change in color.[15] Their stability issues make them poor candidates for catalysis.

In the P[6,6,6,14]NTf_2 IL, however, Fe NPs showed greater stability, possibly owing to the presence of the bis(triflimide) rather than chloride anions. Figure 7.1 shows the UV-Vis spectra of the $Fe(acac)_3$ precursor in P[6,6,6,14]NTf_2, as well as that of the as-synthesized Fe NPs. The UV-Vis spectrum of $Fe(acac)_3$ is identical to the ones mentioned in previous studies, with two maxima at 351 nm and 432 nm.[36] Similarly, for Fe NPs, the spectral features do not deviate from the ones noted in relevant literature; there is a broad peak at ~350 nm, believed to be due to the remnants of collective oscillation of the surface plasmons.[37]

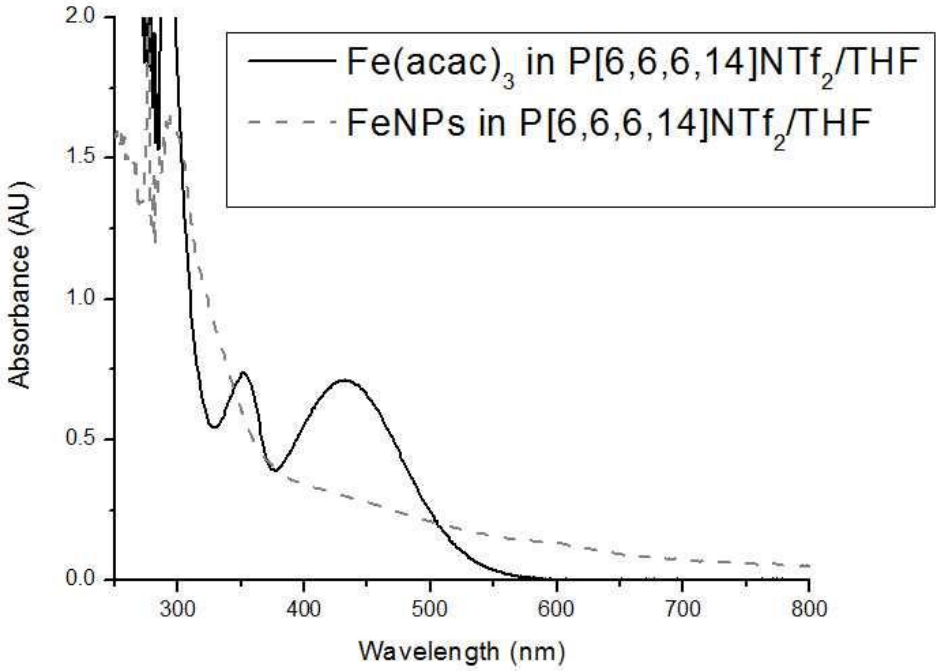

Figure 7.1 UV-Visible spectra of $Fe(acac)_3$ and Fe NPs in $P[6,6,6,14]NTf_2$, diluted with THF.

Figure 7.2 shows TEM images of the Fe NPs in $P[6,6,6,14]NTf_2$. Figure 7.2(A) shows the presence of Fe NPs synthesized in $P[6,6,6,14]NTf_2$ under anaerobic conditions via reduction with $LiAlH_4$; these are small in size (6.1 ± 1.9 nm), and resemble the Fe NPs generated by Gieshoff *et al.* in a nitrile-functionalized IL.[14] Fe NPs generated in the 'task-specific' ILs were found to be approximately 4–5 nm in diameter, and it was observed that they grow during the catalytic reactions, forming 8–20 nm NPs after 24 h under hydrogenation reaction conditions. This is in accordance with our own observations concerning the fate of Fe NPs after catalysis. Figure 7.2(B) depicts Fe NPs synthesized in $P[6,6,6,14]NTf_2$ in the presence of PVP. These are of an average size of 3.8 ± 1.1 nm, and are less polydisperse than the Fe NPs synthesized in the neat IL. Figure 7.2(C) shows Fe

NPs in P[6,6,6,14]NTf_2 after one cycle of norbornene hydrogenation; it is evident from the image that the systems has become more polydisperse, with larger aggregates (26.3 ± 5.5 nm) as well as smaller Fe NPs (7.1 ± 2.2 nm). We are not sure if this polydispersity is induced merely by NP coalescence induced by heat and hydrogen pressure, or by some incidental Ostwald ripening. Similar post-reaction changes in particle size and dispersity are noticed even in the presence of PVP, after one [Figure 7.2(D)] and five [Figure 7.2(E)] catalytic cycles. After five catalytic cycles in the absence of PVP, individual NPs or even NP clusters could no longer be identified [Figure 7.2(F)]; instead, large, micrometer sized domains or aggregates were noticed in the TEM images.

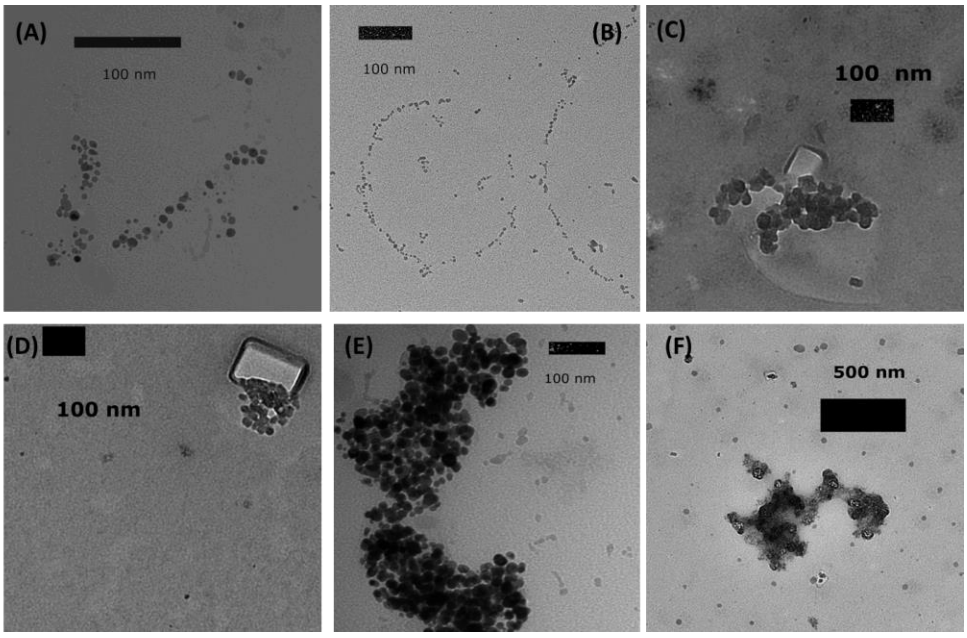

Figure 7.2 TEM images of Fe NPs formed in P[6,6,6,14]NTf_2 (A): as-synthesized; (B): as-synthesized in the presence of PVP; (C): after one catalytic cycle in the absence of PVP; (D): PVP-containing sample after one catalytic cycle; (E): PVP-containing sample after five catalytic cycles; (F): after five catalytic cycles in the absence of PVP.

7.3.2 2-norbornene hydrogenation catalyzed by FeNPs in ILs.

Table 7.1 documents our attempts to optimize the Fe-NP/IL catalyzed hydrogenation of 2-norbornene. Fe-NP/P[6,6,6,14]Cl composites when used as hydrogenation catalysts at $P(H_2)$ = 1 atm did not lead to any conversions; instead, Fe NP degradation over time was observed, with the solution turning bright yellow. At higher hydrogen pressures [$P(H_2)$= 25 bar], less than 5% conversion was observed in the P[6,6,6,14]Cl IL under standard conditions (entry 9, Table 7.1). Since these reactions were not performed in a glove-box, which is a fairly common practice for Fe-NP-catalyzed processes, it was likely that small amounts of air and/or adventitious moisture in the IL may be contributing to catalyst deactivation. A routine Karl Fischer titration indicated the presence of 133 ppm of water in P[6,6,6,14]Cl, and 48 ppm of water for P[6,6,6,14]NTf_2, thereby ensuring that inevitability of oxidation of some of the as-synthesized Fe(0) to higher oxidation states.

Much higher conversions were seen when P[6,6,6,14]NTf_2/Fe-NP composites were used as catalysts for the hydrogenation of 2-norbornene. At a substrate:catalyst ratio of 50, excellent conversions were recorded (entries 1 and 2, Table 7.1). Upon increasing the substrate:catalyst ratio to 200, however, the yield went down (entry 3, Table 7.1). A number of control experiments were performed in order to ensure that unreacted $LiAlH_4$ was not performing the actual hydrogenation; P[6,6,6,14]NTf_2/Fe-NP composites in the absence of hydrogen gas produced very small amounts of the alkane, possibly owing to the presence of some hydrogen dissolved in the system owing to hydrogen

evolution by the unreacted $LiAlH_4$ (entry 10, Table 7.1). Similarly, $P[6,6,6,14]NTf_2$ itself, in the absence of Fe NPs, did not convert 2-norbornene to norbornane under standard conditions in the presence of excess LAH (entry 8, Table 7.1).

Since recyclability is one of the key issues that needs to be addressed in processes carried out in alternative solvents, the Fe-NP/$P[6,6,6,14]NTf_2$ mixtures were reused again after vacuum extraction of the product and the unreacted norbornene (if any). It was seen that the yields decreased progressively after each catalytic run (entries 3 and 4, Table 7.1); after the fifth run, no appreciable conversion could be detected. TEM images of Fe-NPs in the IL after three consecutive catalytic cycles [Figure 7.2(E)] show large, micrometer-sized Fe aggregates, which would explain the catalyst deactivation. Visible precipitation of a black powder in the glass liner of the Parr reactor was also noticed after four catalytic runs. Clearly, the less coordinating $-NTf_2$ anion lacks the ability to prevent extensive NP growth, especially after repeated exposure to high hydrogen pressures at elevated temperatures.

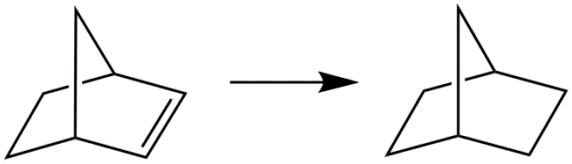

Experiment	Deviation from standard conditions[a]	Conversion (%)
1	-	85
2	-	83
3	[substrate]/[Fe]=200	17
4	Fe NP/IL recycled after first cycle	58
5	Fe NP/IL recycled after second cycle	25
6	PVP present in system[b]	91
7	PVP present in system; FeNP/IL/PVP recycled after first cycle[b]	80
8	No Fe present in system; LAH added to neat IL	<1%
9	IL used is P[6,6,6,14]Cl	3%
10	Reaction performed in the absence of hydrogen gas	5%

[a]Standard conditions: 10mL P[6,6,6,14]NTf_2; [norbornene]/[Fe]=50; 25 bar H_2; 75^0C; 20 h.

[b]molar ratio of PVP:Fe is ~0.1.

Table 7.1 Performance of Fe NP/IL composites in the catalytic hydrogenation of norbornene

Since von Wangelin and colleagues used a cyanide-bearing pendant arm attached to the imidazolium ring in their NP-stabilizing task-specific IL, we assumed that the presence of a secondary stabilizer might enhance the stability of Fe NPs in P[6,6,6,14]NTf_2.[14] To that end, we used poly(vinylpyrrolidone), an inexpensive polymer used by us[38] and others[39] for stabilizing Fe NPs in protic solvents, as an additional NP-stabilizer. Hydrogenation of 2-norbornene with PVP-FeNP/P[6,6,6,14]NTf_2 showed higher yields and TONs as their PVP-free counterparts; moreover, in the second run, greater conversions were seen in PVP-containing systems compared to the ones without PVP (entry 6 vs. entries 1 and 2, Table 7.1). However, the overall trend – namely, progressively reduced conversions for each consecutive catalytic run – remained unchanged, thereby indicating that PVP slows down rather than prevents NP growth and aggregation. TEM images of PVP-protected Fe NPs in P[6,6,6,14]NTf_2 before catalysis [Figure 7.2(B)] and after five catalytic cycles [Figure 7.2(E)] seem to corroborate this hypothesis.

7.3.3 Speciation of Fe in solvated Fe NP catalytic systems using XANES.

Insights into the behavior of solvent-stabilized Fe NPs were obtained via X-ray Absorption Spectroscopy (XAS). The XANES region, especially, was selected, in order to monitor changes in the oxidation state of the Fe NPs in the ILs under a variety of conditions relevant to their catalytic functions. Fe NPs of similar sizes have already been studied by de Vries and von Wangelin in order to determine the nature and composition of the catalytically active species; however, these studies were conducted in organic

solvents.[40,41] Initially, we attempted to identify the nature of the catalytic species via XANES. Figure 7.3 (A) compares the Fe NPs in P[6,6,6,14]NTf2 with bulk Fe foil. Close inspection of the spectral features, such as the white line position and intensity, indicates that Fe(0) is the *dominant* but not the *sole* species present in the sample under scrutiny. Upon comparison with a standard spectrum of Fe(II) in P[6,6,6,14]Cl, [shown in Figure 7.3(D)] a small but definite contribution from Fe(II) can be identified. This is not surprising in the light of previous studies carried out by our group, which revealed that small Fe NPs in neat methanol are, in fact, more oxidized, and contain a higher % of Fe(II) on the surface, than larger NPs synthesized in a water/methanol mixture.[38] It has already been shown via Karl Fischer titrations that our ILs, despite being subjected to a rigorous drying protocol, still contain some residual moisture. Other differences in the white line shapes between bulk metal samples and NPs can be explained on the basis of literature precedents; studies by Bazin and Rehr indicated, for instance, that the sharp features present in the K-edge XANES of Cu foil were dulled considerably in the analogous spectra for nanometer-sized metallic Cu particles.[42] These two factors, when taken into account, explain why our Fe NP sample spectrum is not identical to the spectrum of the sample iron foil, despite the two sharing (to a large extent) the same oxidation state.

Figure 7.3 (B) shows the XANES spectra of $Fe(acac)_3$ (in THF and in $P[6,6,6,14]NTf_2$), as-synthesized $LiAlH_4$-reduced Fe NPs in $P[6,6,6,14]NTf_2$, and Fe NPs in $P[6,6,6,14]NTf_2$ after one catalytic cycle and subsequent exposure to ambient air. The spectra for

$Fe(acac)_3$ in THF and in the IL are very similar, thereby indicating that $Fe(acac)_3$ upon dissolution in the IL does not undergo any drastic coordination changes (which would be expected if it were dissolved in P[6,6,6,14]Cl, where it has been known to form $FeCl_6^{3-}$). In the spectrum of the Fe NPs in the IL, the lower edge position (as compared to Fe^{3+} in IL) and the conversion of the sharp pre-peak at *ca.* 7113 eV to a broad shoulder is attributed to the formation of the electronic band structure in Fe NPs.[41] Moreover, after one catalytic cycle and subsequent exposure to air, Fe NPs are re-oxidized to form the Fe(III) species, which is evident from the changes in the white-line shape and edge energy of the corresponding spectrum.

The oxidative degeneration of Fe NPs in P[6,6,6,14]Cl upon exposure to air could also be followed in real time via XANES.[38] Figure 7.3 (C) depicts this reaction. It is observed that with longer exposure times, there is a gradual shift in the absorption edge towards higher energies. It is well-known that this is one of the definitive markers of a gradual increase in oxidation state. Furthermore, it must also be noted that the situation in halide ILs is somewhat different from that in water or organic solvents, where a large percentage of the oxidized $Fe^{2+}/^{3+}$ would be present on the surface of the NP, possibly as iron oxides or hydroxides, while a small fraction would go into solution. At elevated halide concentrations, the oxidized iron is stripped from the NP surface and enters the solution phase almost immediately, leading to rapid dissolution of the NPs; halides, in fact, have been used for decades for etching metal NPs. This is somewhat of an inverted scenario compared to the one published by von Wanglein and co-workers, who

recorded the XANES spectra of $FeCl_3$ in THF both before and after the addition of two and six equivalents of EtMgCl (a strong reductant, which is supposed to reduce Fe^{3+} and generate Fe NPs in situ).[41] Our observations follow the same (albeit, inverted) pattern: with increase in time, more and more of the Fe(0) undergoes oxidation, aided by adventitious moisture and air, and leaves the NP surface to enter into the IL medium. This changes the shape of the white-line (the first resonance after the edge), which begins to resemble the edges recorded for the higher oxidations states of Fe in the chloroferrate anions. In fact, after 4 h, the XANES for the Fe NPs was virtually indistinguishable from that of $P[6,6,6,14]_3FeCl_6$, as shown in Figure 7.3 (D).

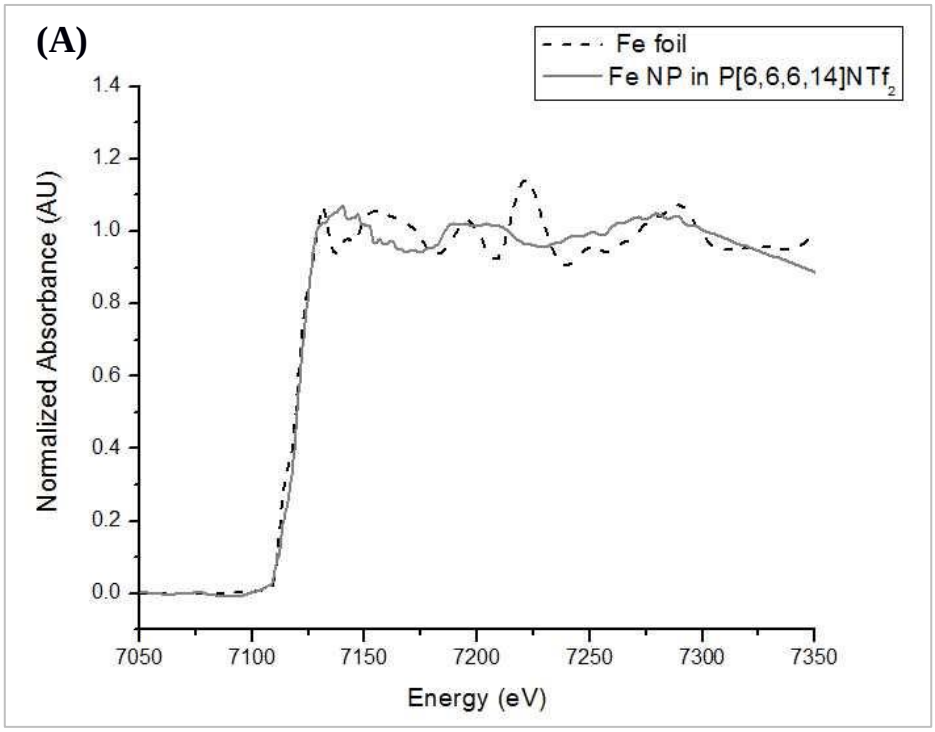
(A)
Fe foil
Fe NP in P[6,6,6,14]NTf2
Normalized Absorbance (AU)
Energy (eV)
0.0
0.2
0.4
0.6
0.8
1.0
1.2
1.4
7050
7100
7150
7200
7250
7300
7350

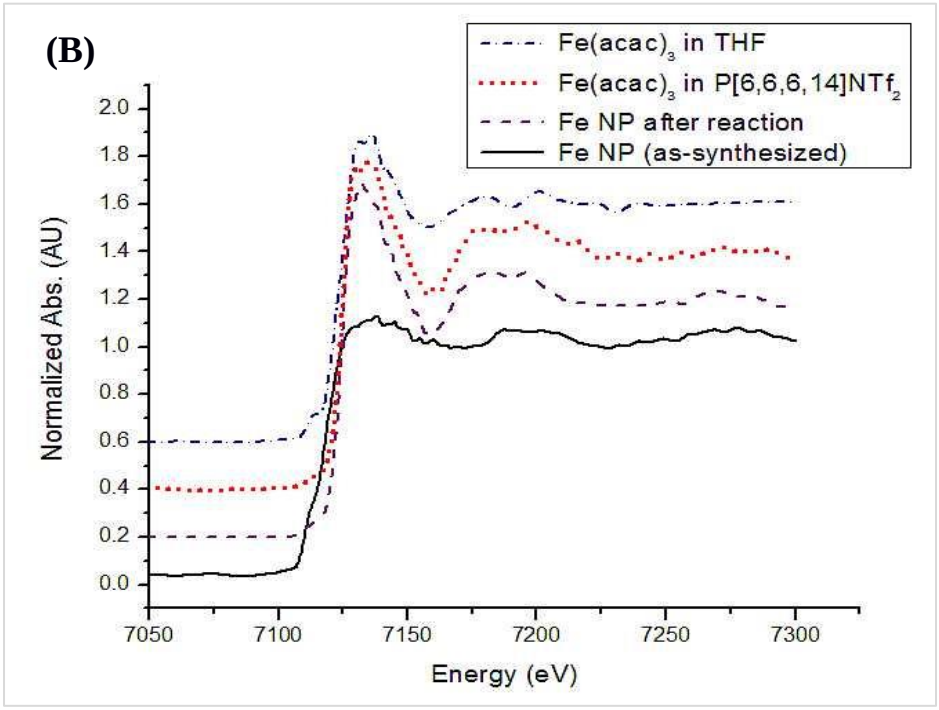
(B)
Fe(acac)3 in THF
Fe(acac)3 in P[6,6,6,14]NTf2
Fe NP after reaction
Fe NP (as-synthesized)
Normalized Abs. (AU)
Energy (eV)
0.0
0.2
0.4
0.6
0.8
1.0
1.2
1.4
1.6
1.8
2.0
7050
7100
7150
7200
7250
7300

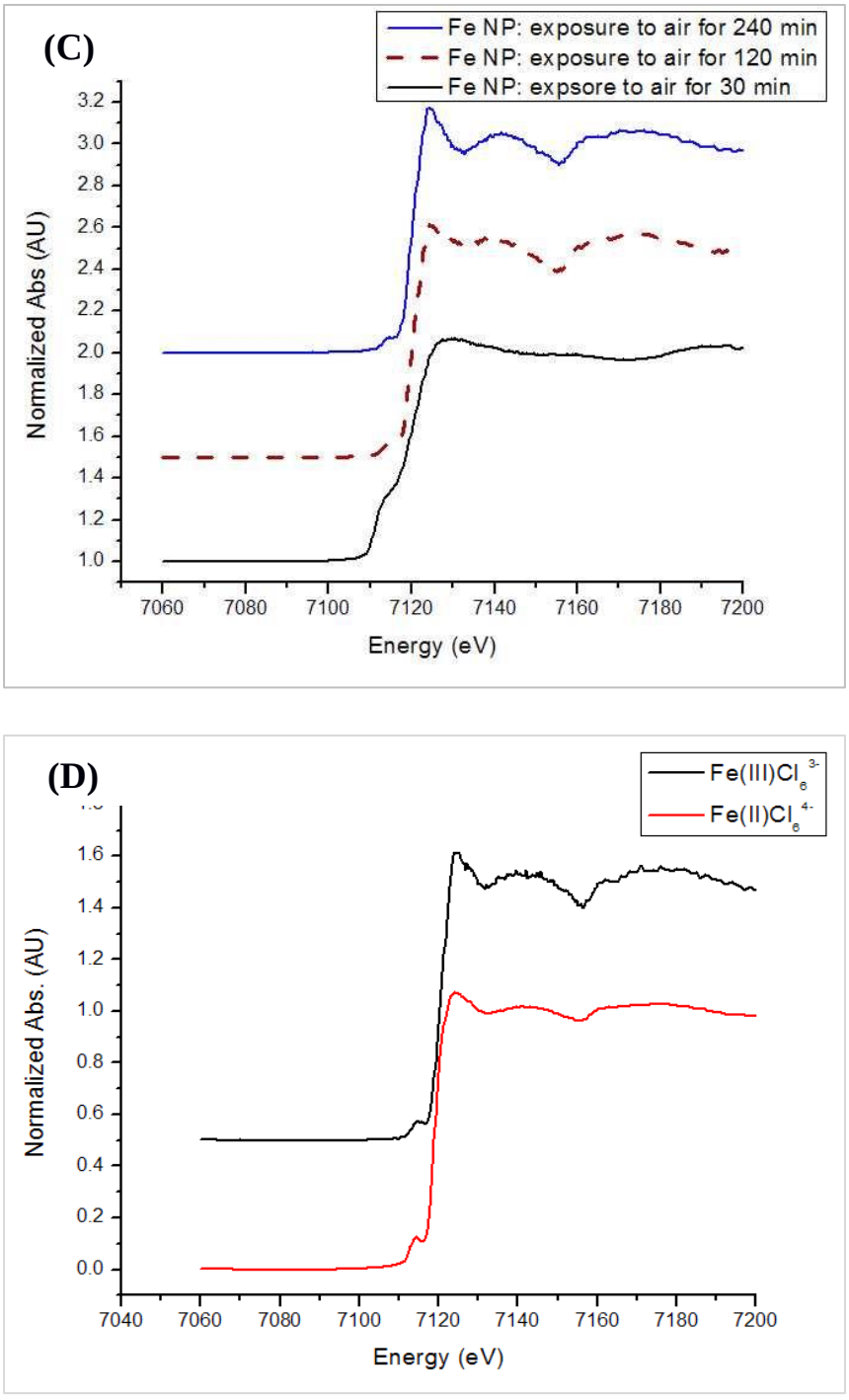

Figure 7.3 Fe K edge solution phase XANES spectra: (A) comparing Fe NPs and Fe foil; (B) comparing $Fe(acac)_3$ in THF, $Fe(acac)_3$ in $P[6,6,14]NTf_2$, as-synthesized Fe NPs in $P[6,6,6,14]NTf_2$, and the Fe NPs after hydrogenation; (C) Fe NPs in P[6,6,6,14]Cl showing oxidation of Fe(0) in air; and (D) comparing Fe(II) and Fe(III) in P[6,6,6,14]Cl.

7.4 Conclusions

The present results are from a study of the stability and catalytic behavior of Fe NPs in tetraalkylphosphonium ILs with or without halide anions. Key findings regarding the nature of these systems can be summarized as follows:

(i) Fe NPs generated in P[6,6,6,14]Cl ILs via a bottom-up strategy using $LiAlH_4$ as a reductant were stable to aggregation, but prone to oxidative degradation upon exposure to air and/or moisture. They were also catalytically inactive towards the hydrogenation of 2-norbornene.

(ii) Fe NPs generated in P[6,6,6,14]NTf_2 showed greater resistance to oxidative etching, and could catalyze the hydrogenation of 2-norbornene to norbornane in good yields at relatively high temperatures and hydrogen pressures.

(iii) Catalytic activity of FeNP/P[6,6,6,14]NTf_2 composites went down upon recycling, possibly owing to particle growth and/or aggregation, as evidenced by TEM images.

(iv) The addition of a secondary stabilizer allowed for more monodisperse Fe NP sizes and improved conversions, but did not completely prevent reduction in catalytic activity over multiple catalytic cycles.

(v) XANES spectroscopy of the Fe NPs in ILs allowed us to follow the oxidative etching of Fe NPs in real time, indicating progressive increase in the oxidation state of Fe over time.

While Fe NPs have emerged as promising catalysts in aqueous and alcoholic systems owing to the formation of a protective oxide coating on their surfaces, naked FeNPs in ILs can only be used under strict anaerobic conditions, thus restricting their applications outside the laboratory. However, the presence of secondary stabilizers and/or NP-stabilizing functionalities built into the IL structures might address these issues, and increase the longevity of these catalysts.

Acknowledgements

The authors acknowledge financial assistance from the National Sciences and Engineering Research Council of Canada (NSERC). A.B. was a recipient of the Gerhard Herzberg Thesis Acceleration Award, and expresses his gratitude for being selected for it. The authors would like to thank Dr. Yongfeng Hu and Aimee Maclennan of the SXRMB beamline at the Canadian Light Source for their help during data collection. XANES experiments described in this paper were performed at the Canadian Light Source, which is supported by the Natural Sciences and Engineering Research Council of Canada, the National Research Council Canada, the Canadian Institutes of Health Research, the Province of Saskatchewan, Western Economic Diversification Canada, and the University of Saskatchewan.

7.5 References

[1] Astruc, D. In *Nanoparticles and Catalysis*; Wiley-VCH Verlag GmbH: Berlin, 2008, pp 1-48.

[2] Polshettiwar, V.; Asefa, T. In *Nanocatalysis Synthesis and Applications*; John Wiley & Sons, Inc.: New York, 2013, pp 1-9.

[3] Albrecht, M.; Bedford, R.; Plietker, B. *Organometallics* **2014**, *33*, 5619-5621.

[4] Bauer, I.; Knölker, H.-J. *Chem. Rev.* **2015**.

[5] Park, J.-Y.; Lee, Y.-J.; Khanna, P. K.; Jun, K.-W.; Bae, J. W.; Kim, Y. H. *J. Mol. Catal. A: Chem.* **2010**, *323*, 84-90.

[6] Fan, X.-B.; Tao, Z.-Y.; Xiao, C.-X.; Liu, F.; Kou, Y. *Green Chem.* **2010**, *12*, 795-797.

[7] Kandemir, T.; Schuster, M. E.; Senyshyn, A.; Behrens, M.; Schlögl, R. *Angew. Chem. Int. Ed.* **2013**, *52*, 12723-12726.

[8] Kharisov, B. I.; Rasika Dias, H. V.; Kharissova, O. V.; Manuel Jimenez-Perez, V.; Olvera Perez, B.; Munoz Flores, B. *RSC Adv.* **2012**, *2*, 9325-9358.

[9] Sonnenberg, J. F.; Coombs, N.; Dube, P. A.; Morris, R. H. *J. Am. Chem. Soc.* **2012**, *134*, 5893-5899.

[10] Sonnenberg, J.; Pichugin, D.; Coombs, N.; Morris, R. *Top Catal* **2013**, *56*, 1199-1207.

[11] Sonnenberg, J. F.; Morris, R. H. *Catal. Sci. Technol.* **2014**, *4*, 3426-3438.

[12] Le Bailly, B. A. F.; Greenhalgh, M. D.; Thomas, S. P. *Chem. Commun.* **2012**, *48*, 1580-1582.

[13] Frank, D. J.; Guiet, L.; Kaslin, A.; Murphy, E.; Thomas, S. P. *RSC Adv.* **2013**, *3*, 25698-25701.

[14] Gieshoff, T. N.; Welther, A.; Kessler, M. T.; Prechtl, M. H. G.; Jacobi von Wangelin, A. *Chem. Commun.* **2014**, *50*, 2261-2264.

[15] Phua, P.-H.; Lefort, L.; Boogers, J. A. F.; Tristany, M.; de Vries, J. G. *Chem. Commun.* **2009**, 3747-3749.

[16] Rangheard, C.; de Julian Fernandez, C.; Phua, P.-H.; Hoorn, J.; Lefort, L.; de Vries, J. G. *Dalton Trans.* **2010**, *39*, 8464-8471.

[17] Kelsen, V.; Wendt, B.; Werkmeister, S.; Junge, K.; Beller, M.; Chaudret, B. *Chem. Commun.* **2013**, *49*, 3416-3418.

[18] Hudson, R.; Feng, Y.; Varma, R. S.; Moores, A. *Green Chem.* **2014**, *16*, 4493-4505.

[19] Hudson, R.; Hamasaka, G.; Osako, T.; Yamada, Y. M. A.; Li, C.-J.; Uozumi, Y.; Moores, A. *Green Chem.* **2013**, *15*, 2141-2148.

[20] Rak, M. J.; Lerro, M.; Moores, A. *Chem. Commun.* **2014**, *50*, 12482-12485.

[21] Li, Y.; Yu, S.; Wu, X.; Xiao, J.; Shen, W.; Dong, Z.; Gao, J. *J. Am. Chem. Soc.* **2014**, *136*, 4031-4039.

[22] Lartigue, L.; Long, J.; Dumail, X.; Nikitenko, S.; Cau, C.; Guari, Y.; Stievano, L.; Sougrati, M.; Guérin, C.; Sangregorio, C.; Larionova, J. *J Nanopart Res* **2013**, *15*, 1-13.

[23] Krämer, J.; Redel, E.; Thomann, R.; Janiak, C. *Organometallics* **2008**, *27*, 1976-1978.

[24] Zhu, Y.-L.; Katayama, Y.; Miura, T. *Electrochem. Solid-State Lett*. **2011**, *14*, 110-115.

[25] Beale, A. M.; Hofmann, J. P.; Sankar, M.; Schrojenstein Lantman, E. M.; Weckhuysen, B. M. In *Heterogeneous Catalysts for Clean Technology*; Wiley-VCH Verlag GmbH: Berlin, 2013, pp 365-411.

[26] Topsøe, H. *J. Catal.* **2003**, *216*, 155-164.

[27] Banerjee, A.; Theron, R.; Scott, R. W. J. *Chem. Commun.* **2013**, *49*, 3227-3229.

[28] Kumar, A.; Saxena, A.; De, A.; Shankar, R.; Mozumdar, S. *Adv. Nat. Sci. Nanosci. Nanotechnol.* **2013**, *4*, 025009-025015.

[29] Kessler, M. T.; Hentschel, M. K.; Heinrichs, C.; Roitsch, S.; Prechtl, M. H. G. *RSC Adv.* **2014**, *4*, 14149-14156.

[30] Banerjee, A.; Theron, R.; Scott, R. W. J. *ChemSusChem* **2012**, *5*, 109-116.

[31] Luska, K. L.; Moores, A. *Green Chem.* **2012**, *14*, 1736-1742.

[32] Sasaki, T.; Zhong, C.; Tada, M.; Iwasawa, Y. *Chem. Commun.* **2005**, 2506-2508.

[33] Taylor, A. W.; Qiu, F.; Villar-Garcia, I. J.; Licence, P. *Chem. Commun.* **2009**, 5817-5819.

[34] Nguyen, M. D.; Nguyen, L. V.; Jeon, E. H.; Kim, J. H.; Cheong, M.; Kim, H. S.; Lee, J. S. *J. Catal.* **2008**, *258*, 5-13.

[35] Yang, S.; Liu, Z.; Meng, X.; Xu, C. *Energ. Fuel.* **2009**, *23*, 70-73.

[36] Bhattacharjee, C. R.; Goswami, P.; Pramanik, H. A. R.; Paul, P. C.; Mondal, P. *Spectrochim. Acta Mol. Biomol. Spectrosc.* **2011**, *78*, 1408-1415.

[37] Siwach, O. P.; Sen, P. *Mater. Sci. Eng.,B* **2008**, *149*, 99-104.

[38] Yao, Y.; Hu, Y.; Scott, R. W. J. *J. Phys. Chem. C* **2014**, *118*, 22317-22324.

[39] Lee, H.-Y.; Lee, S.-H.; Xu, C.; Xie, J.; Lee, J.-H.; Wu, B.; Koh, A. L.; Wang, X.; Sinclair, R.; Wang, S. X.; Nishimura, D. G.; Biswal, S.; Sun, S.; Cho, S. H.; Chen, X. *Nanotechnology* **2008**, *19*, 165101.

[40] Welther, A.; Jacobi von Wangelin, A. *Curr. Org. Chem.* **2013**, *17*, 326-335.

[41] Welther, A.; Bauer, M.; Mayer, M.; Jacobi von Wangelin, A. *ChemCatChem* **2012**, *4*, 1088-1093.

[42] Bazin, D.; Rehr, J. J. *J. Phys. Chem. B* **2003**, *107*, 12398-12402.

8 Conclusions and Future Work

8.1 Synopsis

This dissertation examined the tetraalkylphosphonium family of ILs as novel solvents for reactions catalyzed by stable metal NPs in the IL phase. The use of tetraalkylphosphonium ILs as green(er) media for the genesis and stabilization of transition metal NP catalysts is favored by the various physico-chemical properties of the aforementioned class of ILs. The dependence of the catalytic efficiencies of these NP/IL composites on the structural aspects of the ILs (such as the number and length of the alkyl chains on the central phosphorus, and the nature of the anion) can be compared to the commonly-investigated interactions between NPs and supporting matrices in heterogeneous catalysts. The observed trends in the catalytic activities of these systems were explained on the basis of the properties of the ILs. In particular, the mode of stability, recyclability, and possible avenues for catalyst regeneration were explored in the context of these systems.

In **Chapter 2**, the synthesis of the tetraalkylphosphonium ILs themselves, as well as the generation of stable metal NPs within these IL matrices, was presented. It was found that there was no significant change in particle size for Au NPs in tetraalkylphosphonium ILs when stored under an inert atmosphere over a period of months. The catalytic behavior of IL-phase Pd NPs was explored, and it was observed that these are excellent catalysts for ambient-pressure hydrogenations. The catalytic activity of these systems was comparable to that of Pd NPs in imidazolium-based room-temperature ILs. The negligible volatility and high thermal stability of these ILs can allow

experimental conditions not accessible by conventional solvents, such as facile recycling of the catalyst phase via removal of unreacted substrates and/or products from the IL-phase under reduced pressure. The catalyst solution could be reused for over five cycles with small changes in catalytic activity. However, the use of these systems for catalytic oxidations proved to be challenging despite improved catalytic yields (in comparison to aqueous-phase oxidation catalyzed by Pd and AuPd bimetallic NPs) owing to rapid oxidative stripping of Pd shells (for AuPd bimetallic NPs) and Ostwald ripening (for Pd NPs) in tetraalkylphosphonium halide ILs. **Chapter 3** elaborates on this comparative study of metallic and bimetallic NP-catalyzed oxidations in water vis-a-vis tetraalkylphosphonium halide ILs.

Since the justification for using NP/IL catalytic systems depended on their recyclability, which was seen to be limited by NP growth and/or aggregation in tetraalkylphosphonium ILs, it was necessary to find a protocol for the redispersion of sintered NPs. We devised a two-step protocol where larger metal aggregates in tetraalkylphosphonium halide ILs were oxidized via the introduction of an oxidant in the system; the halometallate species were then re-reduced, thereby regenerating smaller NPs. The generality of this strategy was examined in **Chapter 4**. In **Chapter 5**, Ag NPs in P[6,6,6,14]X (X= Cl, Br) were seen to catalyze the borohydride-induced reductive degeneration of Eosin Y; however, heat-induced agglomeration depleted their catalytic activities. Upon subjecting these NPs to our regeneration protocol, they regained not only their initial sizes but also their catalytic activities. XANES analysis indicated that

oxidative degeneration of large Ag NPs in P[6,6,6,14]Cl produced a $AgCl_y^{(y-1)-}$ intermediate species.

The "deep" hydrogenation of aromatic substrates is an interesting catalytic reaction in the context of the evaluation of catalyst robustness, since these reactions are often conducted at higher temperatures in pressurized reactors. In **Chapter 6**, we attempted to study the stability of our tetraalkylphosphonium IL/NP systems under these conditions. An attempt was made to identify an optimal tetraalkylphosphonium IL/NP system which would be able to catalyze these reactions without significant aggregation under the reaction conditions. After preliminary experiments, Ru NPs in P[6,6,6,14]Cl and in P[6,6,6,14]NTf_2 were selected as the catalytic systems of choice. Surprisingly, while conducting the catalytic hydrogenation of phenol with these systems, we identified cyclohexane, cyclohexene, and cyclohexanol in the product mixture. After a series of control experiments, it was determined that a borate species produced in the IL as a by-product of the borohydride reduction step behaved as a Lewis Acid and catalyzed the dehydration of cyclohexanol to cyclohexene.

Finally, encouraged by reports of FeNP-catalyzed hydrogenations in various solvents, we evaluated tetraalkylphosphonium ILs as reaction media for these reactions (**Chapter 7**). While small FeNPs could be synthesized in tetraalkylphosphonium ILs via the use of stronger reductants, these NPs were seen to have limited stability in the presence of IL anions such as chlorides. An *in situ* XANES study showed the aerial oxidation of Fe NPs to higher oxidation states of Fe in P[6,6,6,14]Cl. In a chloride-free IL,

P[6,6,6,14]NTf_2, catalytically active Fe NPs could be generated under anaerobic conditions, and these could catalyze the hydrogenation of norbornene to norbornane in good yields. However, the yields went down progressively upon recycling, possibly owing to NP aggregation, which was confirmed by TEM. The use of a secondary stabilizer, PVP, slowed down, but did not prevent, NP aggregation. It was concluded that catalysis with 3d-transition metal NPs in tetraalkylphosphonium ILs was challenging owing to the absence of a protective oxide shell formation, which have been shown to stabilize these NPs, and help them retain their catalytic activities, in oxygenated solvents such as water.

In addition to our exploration of tetraalkylphosphonium ILs as novel "solvent-cum-stabilizers" for catalytically active metal NPs, there have been numerous other reports of catalysis and material synthesis using these ILs. In 2011, Kerton and Kalviri fabricated well-structured and monodisperse Pd NPs in tetraalkylphosphonium ILs with surfactant-like anions in the absence of external reducing agents, and used these to catalyse Suzuki cross-coupling reactions.[1] Moores and colleagues compared the catalytic activities of Ru NPs in imidazolium and tetraalkylphosphonium ILs for cyclohexene hydrogenation.[2] IL ionicity was identified as an important metric which provided insight into the dependence of NP stability and activity on the IL structure. Within the series of phosphonium and imidazolium ILs investigated, the IL with the lowest ionicity provided the most stable and catalytically active NPs. Similarly, Ermolaev *et al.* found that tetraalkylphosphonium IL-stabilized Pd NPs were active catalysts for C – C cross-coupling

reactions,[3] and Kessler *et al.* synthesized Cu, Ag, ZnO, and NiO NPs in tetraalkylphosphonium acetate ILs via microwave heating.[4] Exceptional stability of Au NPs in ILs were also noted by Ghandi and co-workers.[5] On the theoretical front, Aleksandrov and colleagues analyzed the IR spectra of Pd NPs confined in tetraalkylphosphonium ILs, and concluded that both IL cations and anions interact strongly with the NP surfaces. A simulation involving a Pd_6 cluster produced anion(IL)-Pd(0) binding energies ranging from ~6 to ~27 kcal/mol, with PF_6^-, the least coordinating anion, showing the weakest binding to the cluster, while Br^- and trifluoroacetate (TFA^-) showed high affinities for ligation to the Pd_6 surface. It was also noted that Pd NPs were kinetically rather than thermodynamically stabilized in tetraalkylphosphonium ILs.[6]

While the use of tetraalkylphosphonium ILs as novel media for NP synthesis has distinct advantages, there are some obvious challenges, too. For example, the solubility of H_2 in ILs is low compared to traditional organic solvents such as alcohols and ethers, which can lead to the necessity of biphasic conditions for NP/IL catalyzed hydrogenations.[7] Tetraalkylphosphonium ILs are available commercially in moderate to high degrees of purity, but the cost associated with their manufacture is much greater compared to traditional organic solvents. Recyclability, which is often a selling point of NP/IL catalytic systems, can be difficult to achieve in practice, owing to NP sintering, aggregation, or oxidation under reaction conditions. Even our best redispersion strategies still will lead to the build-up of reduction by-products within the catalyst matrix after every regeneration cycle. While this may be beneficial for certain reactions,

it could potentially limit the utility of these catalytic systems for others. However, a comparison of TONs in the hydrogenation of olefinic double bonds, at ambient hydrogen pressure, catalyzed by transition metal NPs, shows that tetraalkylphosphonium ILs in their role as solvents lead to TONs comparable to other representative systems, especially those in which a secondary stabilizer is not present (Table 8.1). It is to be noted that an exhaustive survey of metal NP catalyzed hydrogenations in IL media is beyond the scope of this thesis, but even a cursory inspection of the relevant literature reveals that in the absence of IL functionalization, incorporation of polymeric moieties within the structure of the IL, and other such elegant modifications, most IL/NP systems when applied as hydrogenation catalysts typically show TONs and TOFs which are quite comparable to the ones recorded in this thesis.

It is also note-worthy that catalysis with earth-abundant metal NPs is challenging in tetraalkylphosphonium ILs, owing to facile oxidative degeneration of metal NPs forming soluble cationic species rather than oxide-shell-protected NPs, which is customary in solvents such as water or alcohols. In conclusion, the tetraalkylphosphonium IL family has many unique properties that have not been explored with vigor by the scientific community. This dissertation provides a case study of their potential to enhance the “greenness” of catalytic processes involving ILs.

Solvent Type	Metal	External Stabilizer	T(°C)	TOF (h^{-1})	Number of Cycles	Reference
Water	Pd	PVP	40	284	2	8
Iso-octane/water (reverse micelles)	Pd	docusate sodium	30	156	--	9
BMIM-PF_6	Pd	PVP	40	266	2	8
BMMDPA-PF_6	Pd	--	35	90	3	10
P[6,6,6,14]Cl	Pd	--	75	612	5	Chapter 2 (this thesis)
P[4,4,4,14]NTf_2	Ru	--	75	335	8	2

Table 8.1 Comparison of the catalytic activities of transition metal NPs in ambient pressure hydrogenations in different solvents. [BMMDPA-PF_6 = 2,3-dimethyl-1-{3-N,N-bis(2-pyridyl)-propylamido} imidazolium hexafluorophosphate].

8.2 Future work

Tetraalkylphosphonium ILs, with their unique set of properties, could potentially be used in several chemical transformations of scientific and industrial significance. Three of these have been identified and discussed in some detail in the following sections.

8.2.1 CO_2 processing in tetraalkylphosphonium ILs

The need for affordable post-combustion CO_2 capture processes is becoming increasingly important as concerns over greenhouse gas emissions continue to receive worldwide attention, and this, in turn, has fueled numerous studies on CO_2 capture and processing.[11-14] A variety of ILs have been investigated as potential candidates for the sequestration of carbon dioxide from post-combustion flue gas, including amino-functionalized ILs, ILs bearing amino acid-based and heterocyclic anions, superbase-derived protic ionic liquids, and substituted phenolates of tetraalkylphosphonium cations.[15-19] However, concerns such as drastic increase in viscosity of IL after CO_2 capture, gelation, low efficiency and irreversibility of CO_2 sorption, and slow CO_2 capture kinetics have not yet been resolved, leading to continued research in this field. We carried out some preliminary investigations on the use of tetraalkylphosphonium ILs coupled with anions derived from organic bases (such as imidazolate) for reversible CO_2 sequestration, followed by reduction of the captured CO_2 by homogeneous ($LiBH_4$ or $NH_3.BH_3$) or quasi-homogeneous (NP/H_2) methods. The establishment of such a protocol for the conversion of a pollutant to value-added commodity chemicals is likely to be of immense scientific and commercial interest. The 'tailored-anion' ILs, described by Dai, Brenneke, and others, could be readily synthesized according to a well-established procedure, where P[6,6,6,14]OH in ethanol, prepared from P[6,6,6,14]Br using an anion-exchange resin, reacted with weak proton donors such as imidazole, thereby generating the IL with a functional anion, which could then be dried in vacuo (Scheme 8.1).

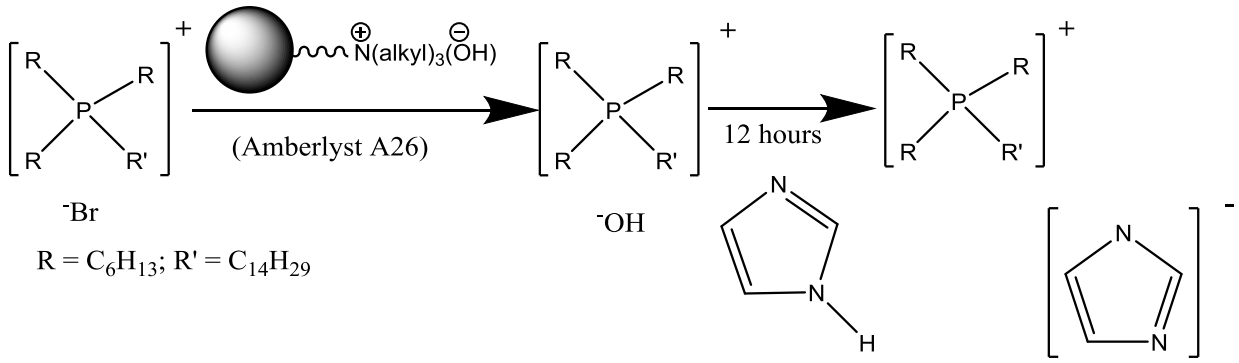

Scheme 8.1 Synthesis of 'tailored-anion' tetraalkylphosphonium ILs.

The CO_2-sorption properties of these ILs were subsequently investigated, and it was observed that the as-synthesized P[6,6,6,14]Im (Im= imidazolate) could absorb CO_2 continuously until it reaches saturation. ^{13}C NMR spectroscopy was applied to confirm the incorporation of CO_2 into the IL; the appearance of a new carbon peak at 163.1 ppm, due to the carbamate carbon, was an indication of CO_2 incorporation (Scheme 8.2).

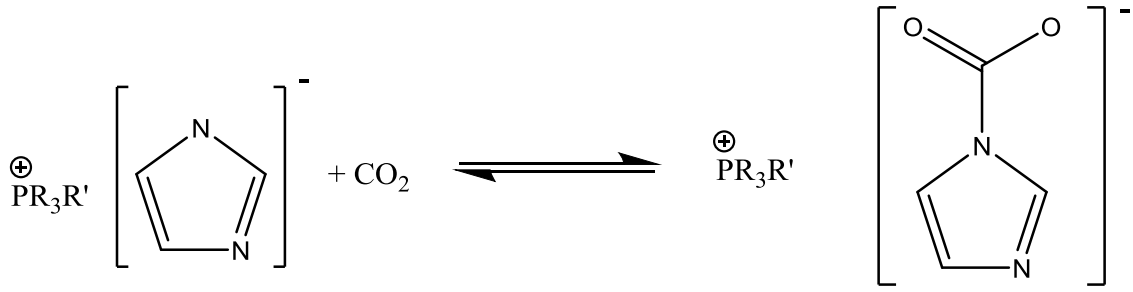

Scheme 8.2 CO_2 harvesting by 'tailored-anion' tetraalkylphosphonium ILs.

We also attempted to incorporate NPs in these anion-functionalized ILs, but it was noted that PVP-protected Pd NPs precipitated rapidly when dispersed in the

P[6,6,6,14]Im IL via a phase-transfer strategy from an organic solvent; while Pd NPs generated directly in P[6,6,6,14]Im were unstable and formed visible precipitates within a few days. Finally, Pd NPs were successfully synthesized in P[6,6,6,14]Im by simultaneous dissolution of K_2PdCl_4 and poly(ethyleneglycol) (PEG-1500) in P[6,6,6,14]Im under nitrogen at 29^0C, with the PEG:Pd molar ratio being 10:1. The Pd(II) precursor was then reduced to PEG-protected Pd NPs by a stoichiometric excess of $LiBH_4$ added drop-wise to the IL. The PEG-protected Pd NPs (Figure 8.1) were seen to be stable under nitrogen for weeks in P[6,6,6,14]Im. Three different reduction strategies were applied to the IL-bound CO_2: (i) homogeneous reduction by addition of $LiBH_4$; (ii) reduction using $BH_3.NH_3$ followed by quenching with heavy water; and (iii) NP-catalyzed reduction under high hydrogen pressures at ambient temperatures. The results for the borohydride reduction were inconclusive and irreproducible, although NMR data indicated formate and bicarbonate. No product formation was noticed for strategies (ii) and (iii). It was noted, however, that use of a Parr reactor with stirring capabilities might lead to improved results. Electrochemical reductions might also prove to be a valuable strategy for the conversion of CO_2 in tetraalkylphosphonium IL media.

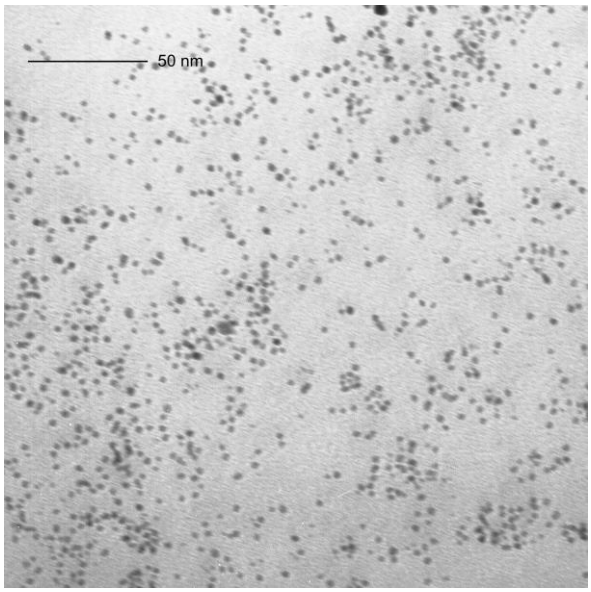

Figure 8.1 PEG-Pd NPs in P[6,6,6,14]Im with an average particle size of 2.5 ± 0.5 nm.

8.2.2 Metallurgy of gold in tetraalkylphosphonium halides

The interaction of metals and ionic liquids is being studied intensively by scientists, primarily owing to novel solvation properties of the ILs that make them extremely useful for applications such as extractive metallurgy, separation of metals, and electrodeposition.[20-22] Even in case of applications not directly concerned with metallurgy (such as catalysis), speciation of metals within these novel liquid matrices directly influences the reactivity of the metal ions.[23-25] It is well-known, for instance, that the presence of highly toxic cyanide ions renders metallic Au soluble in water owing to the formation of cyanoaurate complexes; however, it remains to be seen if similar redox behavior might be induced by ILs containing more benign species such as halide ions.[26-28] An extensive literature survey reveals that there are few speciation studies performed

on metals in tetraalkylphosphonium ILs, despite the fact that these are stable at high temperature, not prone to facile deprotonation, and occur as room-temperature ILs even when coupled with highly coordinating anions such as halides (alkylimidazolium halides, by comparison, are solids at room temperature).

While many analytical procedures have been applied for the speciation of metals in various systems, X-ray absorption spectroscopy remains the accepted standard for such characterization techniques, especially when performed at a synchrotron facility. Preliminary studies at the Canadian Light Source led to several interesting observations regarding the speciation of Au in tetraalkylphosphonium ILs. XANES provides useful structural information such as the oxidation states, site symmetry, and covalent bond strength, and therefore finds application in deterministic analyses of local structure around the central atom. XANES spectra were obtained for Au species in P[6,6,6,14]Cl, and P[6,6,6,14]NTf_2. It was evident that $HAuCl_4$ in P[6,6,6,14]NTf_2, upon exposure to the probing X-rays, underwent reduction to generate colloidal Au. This could be seen from visual inspection of the sample, as well as from their spectra [Figure 8.2(a), (b)]. A similar observation has recently been made by Xu *et al.*, who reported that [C_4mim][$AuCl_4$], upon exposure to X-ray radiation, generated Au(0).[24,25] In our other samples, however, no evidence of beam-damage or beam induced reduction could be seen, irrespective of the nature of the solvent (water, acetonitrile, acetonitrile in the presence of P[6,6,6,14]Cl, and neat P[6,6,6,14]Cl). The dissolution of Au in a solvent involves oxidation of Au into an ionic species, followed by complexation to stabilize the

gold ion in solution. Therefore, in the presence of a complexing agent such as Cl^-, the oxidation of Au(0) to Au(III) becomes thermodynamically favored. In fact, dissolution of Au using chlorine or chloride ions has been known from several centuries.[29] Also, at high concentrations of chloride anions, $AuCl_4^-$ becomes stable at lower potentials, and $AuCl_2^-$ can be stabilized.[26,29] Thus, photoreduction of Au is not observed in P[6,6,6,14]Cl, whereas in P[6,6,6,14]NTf_2, the anion is incapable of preventing the photoreduction of Au(III) to Au(I) and subsequently to Au(0). Au NPs in both the ILs showed identical XANES features.[30-33]

A detailed examination of the changes in the oxidation state of Au when Au particles in the nanometer or micrometer size regime dispersed in ILs are subjected to an etching routine might have tremendous consequences when it comes to the metallurgy of gold. It is expected that detailed studies in this direction would enable the scientific community to design a process involving a halide-containing IL/oxidant combination for the extraction of Au from its ore, in lieu of the highly toxic cyanide etching process that still remains prevalent in the hydrometallurgy of Au.

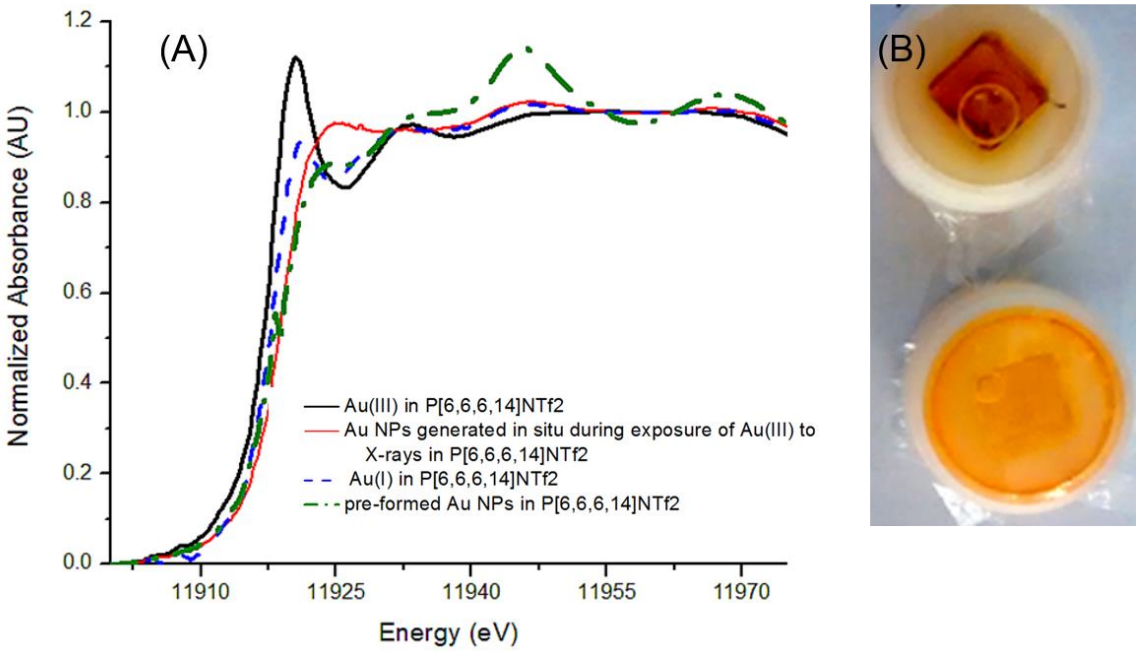

Figure 8.2 (a) XANES spectra of Au(III) in P[6,6,6,14]NTf_2 after the initial scan (blue) and after two consecutive scans (red), showing changes in speciation; (b) 10mM Au(III) in P[6,6,6,14]NTf_2: before (bottom) and after (top) exposure to synchrotron X-rays. Au(I) and pre-formed Au NPs in P[6,6,6,14]NTf2 have also been shown for comparison purposes.

8.2.3 Enantioselective catalytic hydrogenations in tetraalkylphosphonium ILs

While NP/IL composite catalysts have been used extensively in hydrogenations of various unsaturated groups, there are fewer examples of their use in stereoselective hydrogenations. There are several examples of asymmetric catalysis mediated by NPs with chiral surfaces in water or volatile organic solvents; some of these use the NPs as

structural scaffolds, with the active catalytic centers affixed onto the NP periphery via ligands, while others use chiral ligands such as BINAP, xylofuranoside diphosphate, or alkaloids.[34-38] In 2012, Baiker and colleagues synthesized 2-3 nm Pt NPs in BMIM-PF_6 in the presence of cinchonidine and used the resulting NPs as stereoselective hydrogenation catalysts; these were seen to act as active catalysts for the hydrogenation of ethyl pyruvate, generating (R)-methyl mandelate with a TOF of *ca.* 1700 h^{-1} and an *ee* of 78%.[37]

Chiral moieties built into the IL structure have been explored for imidazolium but not for tetraalkylphosphonium ILs, which is surprising, since there are two possible sites in these ILs where chirality might be induced. Tetraalkylphosphonium ILs of the type $P[R_1,R_2,R_3,R_4]X$, with four non-identical alkyl substituents on the central phosphorus, could in theory be synthesized, since protocols for the synthesis of trialkylphosphines with three different alkyl groups exist in literature.[39] Another avenue would be to incorporate a chiral anion (such as lactate or citrate) into the IL via ion-exchange; however, care must be taken to avoid racemization during the anion-exchange procedure.[39,40] Finally, the influence of an external chiral additive such as BINAP on NPs in a tetraalkylphosphonium IL with a weakly coordinating anion such as PF_6^- or BF_4^- could be studied in the context of catalytic hydrogenation of a prochiral substrate such as acetophenone or 2-methylindole.

8.3 Concluding remarks

"Water and air, the two essential fluids on which all life depends, have become global garbage cans", lamented Jacques-Yves Cousteau in the closing years of the last century.[41] As we approach the second decade of the new millennium, we have done much to prevent the gaping maw of pollution from engulfing our planet. However, there is much more to be done, and with every new advancement in sustainable chemical processes, with every stoichiometric process that is replaced by a catalytic process, and with every breakthrough in nanocatalysis, we are approaching our final goal of living in harmony with our environment even as we keep improving the quality of human life and experience during our brief sojourn on this planet.

8.4 References

[1] Kalviri, H. A.; Kerton, F. M. *Green Chem.* **2011**, *13*, 681-686.

[2] Luska, K. L.; Moores, A. *Green Chem.* **2012**, *14*, 1736-1742.

[3] Ermolaev, V. V.; Arkhipova, D. M.; Nigmatullina, L. S.; Rizvanov, I. K.; Milyukov, V. A.; Sinyashin, O. G. *Russ. Chem. Bull.* **2013**, *62*, 657-660.

[4] Kessler, M. T.; Hentschel, M. K.; Heinrichs, C.; Roitsch, S.; Prechtl, M. H. G. *RSC Adv.* **2014**, *4*, 14149-14156.

[5] Farren-Dai, M.; Awoonor-Williams, E.; MacNeil, C. S.; Mahimwalla, Z.; Ghandi, K. *Chem. Phys. Lett.* **2014**, *610–611*, 331-334.

[6] Zvereva, E. E.; Grimme, S.; Katsyuba, S. A.; Ermolaev, V. V.; Arkhipova, D. A.; Yan, N.; Miluykov, V. A.; Sinyashin, O. G.; Aleksandrov, A. *Phys. Chem. Chem. Phys.* **2014**, *16*, 20672-20680.

[7] Hasib-ur-Rahman, M.; Siaj, M.; Larachi, F. *Chem. Eng. Process. Process Intensif.* **2010**, *49*, 313-322.

[8] Dash, P.; Dehm, N.A.; Scott, R.W.J. *J. Mol. Catal. A. Chem.* **2008**, *286*, 114-119.

[9] Sato, H.; Ohtsu, T.; Komasawa, I. *J. Chem. Eng. Jpn*., **2002**, *35*, 255-260.

[10] Hua, Y.; Yang, H.; Zhanga, Y.; Houa, Z.; Wanga, X.; Qiaoa, Y.; Lia, H.; Fenga, B.; Huanga, Q. *Catal. Commun.,* **2009**, *10*, 1903-1907.

[11] Sun, X.; Huang, C.; Xue, Z.; Mu, T. *Energy Fuels*, **2015**, *29*, 1923–1930.

[12] Torralba-Calleja, E.; Skinner, J.; Gutierrez-Tauste, D. *J. Chem.* **2013**, *2013*, 16.

[13] Zhang, X.; Zhang, X.; Dong, H.; Zhao, Z.; Zhang, S.; Huang, Y. *Energy Environ. Sci.* **2012**, *5*, 6668-6681.

[14] Li, A.; Tian, Z.; Yan, T.; Jiang, D.-e.; Dai, S. *J. Phys. Chem. B* **2014**, *118*, 14880-14887.

[15] Wang, C.; Luo, H.; Li, H.; Zhu, X.; Yu, B.; Dai, S. *Chem. Eur. J.* **2012**, *18*, 2153-2160.

[16] Wang, C.; Luo, X.; Luo, H.; Jiang, D.-e.; Li, H.; Dai, S. *Angew. Chem. Int. Ed.* **2011**, *123*, 5020-5024.

[17] Zhang, Y.; Wu, Z.; Chen, S.; Yu, P.; Luo, Y. *Ind. Eng. Chem. Res.* **2013**, *52*, 6069-6075.

[18] Zhang, Y.; Zhang, S.; Lu, X.; Zhou, Q.; Fan, W.; Zhang, X. *Chem.Eur. J.* **2009**, *15*, 3003-3011.

[19] Abbott, A. P.; Frisch, G.; Hartley, J.; Ryder, K. S. *Green Chem.* **2011**, *13*, 471-481.

[20] Abbott, A. P.; McKenzie, K. J. *Phys. Chem. Chem. Phys.* **2006**, *8*, 4265-4279.

[21] Hoogerstraete, T. V.; Onghena, B.; Binnemans, K. *J. Phys. Chem. Lett.* **2013**, *4*, 1659-1663.

[22] Estager, J.; Holbrey, J. D.; Swadzba-Kwasny, M. *Chem. Soc. Rev.* **2014**, *43*, 847-886.

[23] Hartley, J. M.; Ip, C.-M.; Forrest, G. C. H.; Singh, K.; Gurman, S. J.; Ryder, K. S.; Abbott, A. P.; Frisch, G. *Inorg. Chem.* **2014**, *53*, 6280-6288.

[24] Hubbard, C. D.; Illner, P.; van Eldik, R. *Chem. Soc. Rev.* **2011**, *40*, 272-290.

[25] Billy, E.; Chainet, E.; Tedjar, F. *Electrochim. Acta* **2011**, *56*, 10340-10346.

[26] Kissner, R. *J. Electroanal. Chem.* **1995**, *385*, 71-75.

[27] Whitehead, J. A.; Lawrance, G. A.; McCluskey, A. *Green Chem.* **2004**, *6*, 313-315.

[28] Ma, J.; Zou, Y.; Jiang, Z.; Huang, W.; Li, J.; Wu, G.; Huang, Y.; Xu, H. *Phys. Chem. Chem. Phys.* **2013**, *15*, 11904-11908.

[29] Chang, S.-Y.; Uehara, A.; Booth, S. G.; Ignatyev, K.; Mosselmans, J. F. W.; Dryfe, R. A. W.; Schroeder, S. L. M. *RSC Adv.* **2015**, *5*, 6912-6918.

[30] Geoffroy, N.; Cardarelli, F. *J. Min. Mat. Met. Soc*. **2005**, *57*, 47-50.

[31] Gammons, C. H.; Yu, Y.; Williams-Jones, A. E. *Geochim. Cosmochim. Acta* **1997**, *61*, 1971-1983.

[32] Mori, K.; Kondo, Y.; Yamashita, H. *Phys. Chem. Chem. Phys.* **2009**, *11*, 8949-8954.

[33] Reimann, S.; Urakawa, A.; Baiker, A. *J. Phys. Chem. C* **2010**, *114*, 17836-17844.

[34] Roy, S.; Pericas, M. A. *J. Org. Biomol. Chem.* **2009**, *7*, 2669-2677.

[35] Son, S. U.; Jang, Y.; Yoon, K. Y.; Kang, E.; Hyeon, T. *Nano Lett.* **2004**, *4*, 1147-1151.

[36] Studer, M.; Blaser, H.-U.; Exner, C. *Adv. Synth. Catal.* **2003**, *345*, 45-65.

[37] Beier, M. J.; Andanson, J.-M.; Mallat, T.; Krumeich, F.; Baiker, A. *ACS Catal.* **2012**, *2*, 337-340.

[38] Fleckenstein, C. A.; Plenio, H. *Chem. Soc. Rev.* **2010**, *39*, 694-711.

[39] Dinares, I.; Garcia de Miguel, C.; Ibanez, A.; Mesquida, N.; Alcalde, E. *Green Chem.* **2009**, *11*, 1507-1510.

[40] Alcalde, E.; Dinarès, I.; Ibáñez, A.; Mesquida, N. *Molecules* **2012**, *17*, 4007-4027.

[41] Dell, P. *Protecting the Planet: Environmental Activism;* Compass Point Books: Mankato, MN, 2010; p 21.